EPIDEMIC DYNAMICS MODELLING AND ANALYSIS FOR THE RESPIRATORY INFECTIOUS DISEASES : CONTROL, PREVENTION AND TREATMENT

MOHAMMED ALTHUBYANI

A DISSERTATION SUBMITTED TO THE FACULTY OF GRADUATE STUDIES
IN PARTIAL FULFILMENT OF THE REQUIREMENTS
FOR THE DEGREE OF
DOCTOR OF PHILOSOPHY

GRADUATE PROGRAM IN MATHEMATICS AND STATISTICS
YORK UNIVERSITY
TORONTO, ONTARIO

SEPTEMBER 2021

Abstract

The goal of this thesis is to develop and analyze mathematical models of respiratory infection diseases, particularly MERS-CoV and influenza, that affect the Middle East daily, and through the Hajj Mass Gathering, to aid in understanding of how these diseases can be spread, and how they may be controlled through public health mitigation. The thesis work employs deterministic and stochastic models of disease transmission between humans and between animals and humans in different settings. We also include analysis of disease spread in a network, and using metapopulation models. We concentrate on the creation and use of models either as criteria for evaluation or as a way of understanding the epidemiological processes with theoretical findings using the following considerations:

1) Developing and checking hypotheses; evaluating quantitative assumptions; measuring sensitivity to changes in model parameters; assessing process conditions from data.

2) Evaluating and contrasting the efficacy of different public health interventions.

3) Interpreting mathematical results to the biological questions.

4) Evaluating the basic reproduction number R_0 to provide the early estimates of epidemiological thresholds.

5) Investigating the local and global stability for the equilibrium points.

Dedication

I am sure my father would have been proud of this great milestone and accomplishment, but unfortunately, he passed away before this achievement.

Acknowledgements

Firstly, I would like to express my sincere gratitude to my supervisor, Dr. Jane Heffernan for the never ending support, motivation, consultation, and guidance during my Ph.D studies and subsequent research. Dr. Jane insightful input provided me with the opportunity to enhance perceptions and implementation.

Secondly, I would like to extend my appreciation to the advisory committee: Dr. Neal Madras, and Dr. Seyed Moghadas for providing invaluable guidance that has proved crucial to conceiving and establishing research questions and methodology.

Furthermore, I would like to thank my colleagues for entertaining and stimulating my thought process and ideas.

Correspondingly, I am grateful for the prayers of my mom and her unlimited love and support, as well as my family for their wise counsel and sympathetic ears which proved instrumental to cultivate the courage and effort in working towards the accomplishment of my Ph.D.

Finally, I would like to convey my gratefulness to the Ministry of Higher Education in Saudi Arabia and Al-Baha University for sponsoring, and funding this study.

Table of Contents

List of Tables

List of Figures

Chapter 1

Introduction

Our scope of study is on infectious disease models that will aid in understanding disease spread and infection risk in the Middle East. Specifically, we will focus the thesis on models to study Middle East Respiratory Syndrome (MERS-COV), and to study respiratory infection spread during the Hajj mass gathering that can affect exportation risks for different countries.

Middle East Respiratory Syndrome coronavirus (MERS-COV) is a severe respiratory disease that has caused great burden in Kingdom of Saudi Arabia (KSA), among other countries, since 2012. Clinical reports have indicated human-to-human transmission of this virus. Dromedary camels are a significant reservoir for MERS-CoV and an animal vector of infection in humans as seen in the Figure 1.1. In this thesis, we develop mathematical models of MERS-COV spread in KSA including the human-camel interface to study the transmission and persistence of the virus. The models involve animal-animal, animal-environment, human-animal, and human-human disease transmission studies on different mathematical frameworks, from systems of ordinary differential equations, to stochastic models, and network models using pairwise approximations. Global stability analysis on the disease-free and endemic steady states will be conducted in some of our studies. Our models will be used to quantify the number of human and animal cases of MERS-COV, and will be used to inform public

health on MERS-COV public health education programs.

Respiratory diseases can be spread during mass gatherings, including the Hajj gathering. Many individuals from many different countries travel to the Hajj each year. The gathering, which is limited in space for the large number of people, a considerable length of time, can pose risk for transmission of respiratory diseases existing in the pilgrimage population. As such, the gathering includes importation risk of diseases, transmission spread, potential stress on the healthcare system of the host country, and the risk of exportation to pilgrim countries. In this study, we develop a metapopulatoin model to study these considerations. While the framework will be applicable to many diseases, we will focus our work on 2009 H1N1. The models dedication be based on extended SIR models to a metapopulation model by country. Stochastic and deterministic determination be used to study the mean and variance of infections, including importation and exportation of infected individuals.

1.1 Middle East Respiratory Syndrome Coronavirus (MERS-CoV)

The Middle East Respiratory Syndrome Coronavirus (MERS-CoV) is an RNA virus belonging to a family of Coronaviruses that attack the human respiratory system. MERS-CoV can cause lethal acute and severe respiratory disease in humans. Dipeptidyl peptidase 4 (DPP4, CD26), a type II transmembrane ectopeptidase, is the receptor for the Middle Eastern respiratory syndrome coronavirus (MERS-CoV), which allows the virus to infect cells of humans. This receptor is present in the epithelia and endothelia of the systemic vasculature, lung, kidney, small intestine and heart [1, 2]. The appearance of the Middle East respiratory syndrome-coronavirus (MERS-CoV), in 2017 Ahmed [3], created a $STIR$ in the global population, worrying about the next pandemic. This disease however has been largely contained in the

Middle East [4]. It has been reported that MERS-CoV originated from camels, with bats functioning as an intermediate and secondary host [5]. The interaction frequency between bats and humans is highly restricted in the Arabian Peninsula, we thus focus our studies on camels and humans only. The process of transmission of MERS-CoV is shown in Figure 1.1.

There are three routes for the transmission of MERS-CoV as seen in Figure 1.2: animals to animals, animals to humans, and humans to humans [6]. It has been suggested that human population mixing and population movement during religious events, closing and reopening of camel markets, camel racing events, as well as climatic factors, could influence the transmission of MERS-CoV between camels, from camels to humans and between humans [1, 7]. Moreover, it has been suggested that patients might be unprotected to MERS-CoV by ingestion of raw camel products like milk and meat etc. [6]. Meanwhile, human-to-human transmission occurs in hospital settings and wider society, with the virus being transmitted among humans during close human-to-human contact by the precipitations and droplets of respiratory secretions.

There is no effective vaccine or medication for MERS-COV, and it shows high mortality rate up to 40% [8, 9]. MERS-CoV vaccines are only at the pre-clinical phase, but by enhancing our consideration of its knowledge and epidemic potential of MERS-CoV a population might be able to achieve better preparation for forthcoming epidemics [6].

1.1.1 Transmission from camels to humans

The transmission of MERS-CoV from camels to humans has been established by viral RNA sequencing of samples acquired from asymptomatic or symptomatic patients after exposure to infected animals. A study of animal mass that are accompanying patients with MERS-CoV infection found that the nasal swabs of 75 out of 584 dromedary camels were positive for MERS-CoV for about two weeks [11, 12]. However, the nasal swabs were negative for MERS-

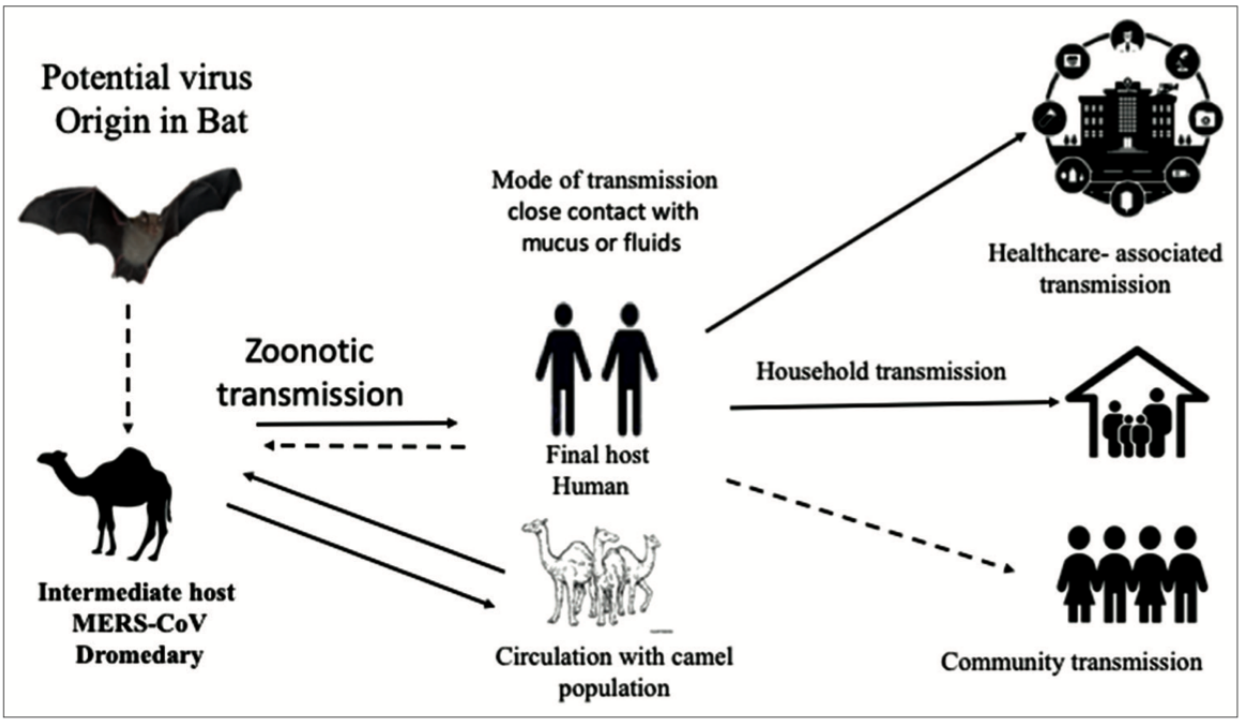

Figure 1.1: Middle East Respiratory Syndrome-A briefing of the coronavirus transmission pathway. The solid line specifies the identified transmission path, and the dotted line specifies the possible transmission path with incomplete or unrestricted support information [10].

CoV in different animals such as cattle, sheep and goats. Notably, more than 70% of camels were linked with the individuals having MERS-CoV infections and they also had MERS-CoV anti-bodies as evaluated by ELISA assays. Furthermore, the full genome sequencing recognized ten MERS-CoV camels that were identified from their corresponding patients. Although dromedary camels are a well-known host for MERS-CoV, researchers have revealed that long term evolution of MERS-CoV occurs entirely in camels, while human beings serve as a transient host [13]. The same study showed that human outbreaks of MERS-CoV were driven by varying zoonotic transfer (seasonally) of the viruses from camels.

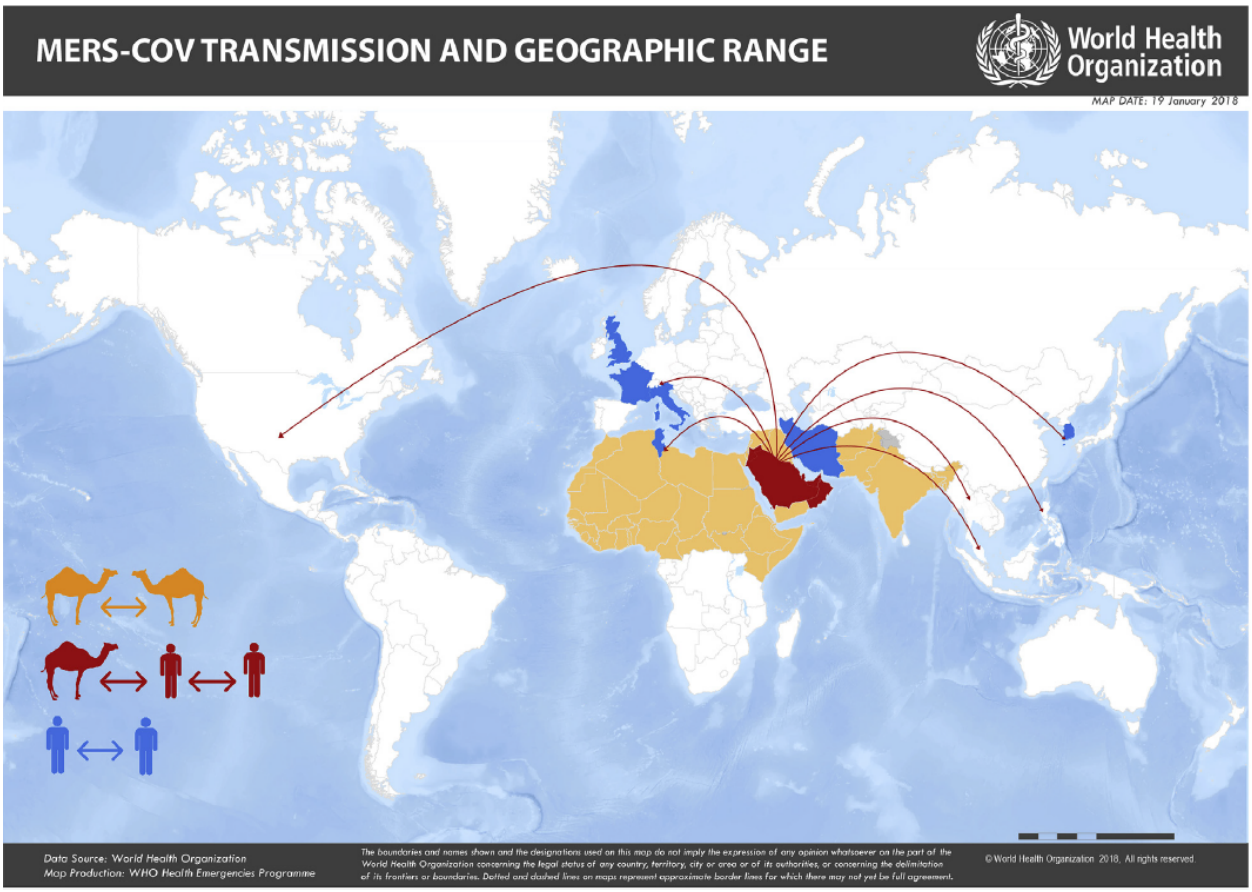

Figure 1.2: The geographic range of MERS-CoV in dromedary camels is indicated by the countries highlighted in red and orange. Spillover (camel-to-human) transmission with subsequent human-to-human transmission has been documented in those in red. Human-to-human transmission has been recorded in the countries highlighted in blue [7].(Source: WHO).

1.1.2 Transmission between humans

The primary source of MERS-CoV infection rises in humans is infection acquired in the community [14], between individuals. Infection can also be transmitted in the hospital setting. It is reported that the risk of transmission of the MERS-CoV virus in humans is determined by characteristics including the close contact with the patients, such as touching the respiratory secretions of patients, sleeping in the same room as patients, or removing and cleaning of the patients' waste including sputum, urine and stool with sub-clinical infection [15].

Before MERS-CoV was identified, the virus was transmitted at health-care facilities in numerous countries, including from patients to health-care workers and inside a health-care environment. Since symptoms and other clinical characteristics are often nonspecific, it is not always easy to identify individuals with MERS-CoV upfront or without testing. Infection prevention and control strategies are important to preventing the spread of MERSCoV in healthcare settings. Facilities that care for patients who are identified or consistently demonstrated to be infected with MERSCoV shall implement necessary precautions to reduce the risk of the virus spreading from an infected patient to other patients, healthcare staff, or visitors [16].

In South Korea, on May 20, 2015, the first confirmed case of MERS-CoV was reported in a man, who had a history of travel through the Middle East. Consequently, there was an outbreak in South Korea following importation from the Middle East region [17].

The total number of laboratory-confirmed MERS-CoV infection cases reported to WHO between 2012 and December 2020 is 2566, including 882 deaths, see Figure 1.3. The total number of laboratory-confirmed cases reported to WHO under the International Health Regulations (IHR 2005) to date is reflected in the global number [18].

1.1.3 Sustained outbreaks

Continual transmission for MERS-COV has been hard to prove. Studies have shown that there is no sustained outbreak of MERS-COV and that reseeding of infection in humans through interaction with the animal reservoir is needed. A substantial proportion of MERS-CoV cases have been part of clusters, in which non-sustained human-to-human transmission has ensued. This transmission has occurred in healthcare settings, in work places and in close family contacts. Persistent transmission in the community apart from these clusters would represent a major change and has not been observed in the epidemiology of MERS-CoV [19].

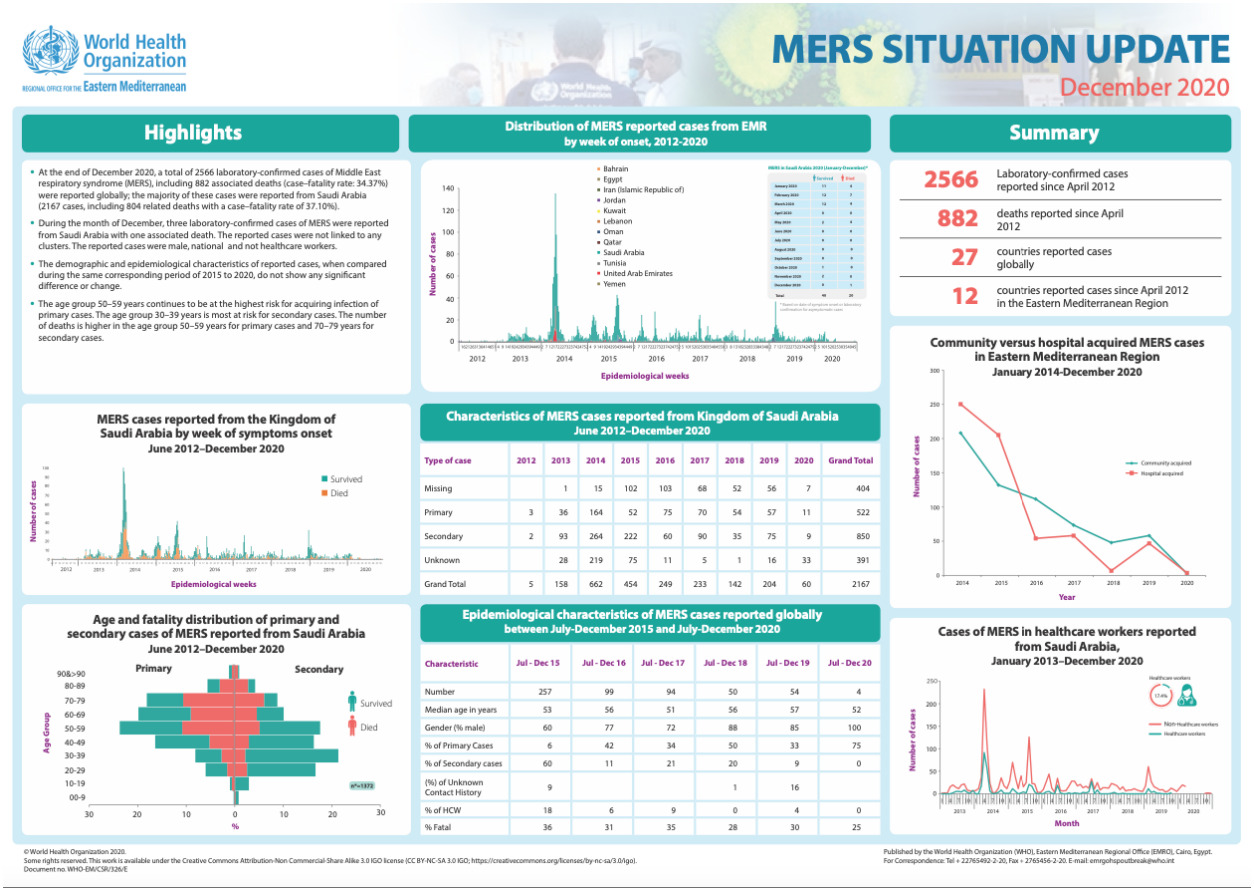

Figure 1.3: MERS situation update between 2012 and December 2020.(Source: WHO).

1.1.4 Public Health Education

Population awareness of an infectious disease can aid in mitigation and control. Awareness and diligence for control of MERS-CoV is not compulsory. Consequently, increases in death rates due to MERS-CoV have occurred [20]. According to one study, however, no suggestion was found for a link between the long time interval before reporting symptoms and patient outcomes [3]. However, the authors' findings were based on the time interval between symptom onset and hospital admission, rather than diagnosis. However, long-term spread of MERS-COV has not occurred in the Middle East. This could be due to increases in awareness

as case counts are reported during outbreaks [21, 22, 23].

1.1.5 Disease progression characteristics

The basic reproduction number R_0 is the average number of secondary cases created by infectious persons. MERS R_0 value was reported in several investigations. $R_0 < 1.0$ was found in four investigations that employed data from a variety of sources [13, 24, 25, 26]. $R_0 < 1.0$ was found to be 0.45-0.98 in studies employing Saudi Arabia or Middle East data [8, 19, 27, 28], however one study showed 1.9-3.9 [29]. Studies using South Korean data experienced significant values in the early stages, ranging from 2.5 to 8.09 [30, 31, 32, 33], and lower values in the later stages [33] or with prevention program [32].

The attack rate was measured in eight different investigations. Four of the studies looked at the general or secondary attack rate, while the other four looked at the attack rate of specific categories of activities. Secondary attack rates were found to be 0.42% [34] and 4% [35] in two investigations done in Saudi Arabia. Secondary attack rates in South Korea were 3.7% in one research [36] and 14.3-15.8% in another [37].

The attack rate among healthcare workers (HCWs) was reflected in different investigations. A 1.5 percent MERS infection rate among HCWs was found in one research in South Korea [33], while a 13.4-13.5% infection rate among HCWs was reported in another study combining various region data [24]. In one research, [38] the attacking rate among hospital patients was 4%, while in another [30], it was 22% in the early stages and 1% in the later time-frame.

The incubation period is the time between infection and the onset of symptoms. The incubation period of MERS was reported in a various of studies. Nine examined data from South Korea and found an incubation time of 6-7.8 days [17, 38, 39], [36, 37, 40, 41, 42, 43]. A 5.2-day incubation duration was reported in one research using data from Saudi Arabia [44], while a 5.5-day incubation time was reported in another study using data from several

places [13]. In a study comparing the incubation periods in the Middle East and South Korea, Sha et al.[45] found that they were 4.5-5 and 6 days, respectively [45].

The period between the start of symptoms in a main case and the beginning of symptoms in its subsequent cases is represented by the serial interval of an infected individual. Two investigations [37, 41], analysed data from South Korea and reported serial MERS intervals of 12.6 and 14.6 days, correspondingly.

Days from onset to confirmation reported in several studies. One research that looked at all cases in South Korea found that it took 5 days from earliest stages to confirmation [17]. For all instances, Park et al. reported 6.5 days, 9 for second generation, and 4 for third generation [43]. HCWs were given 6 days while non-HCWs have been afforded 10 days in a Taiwanese research [46]. From onset to confirmation, a Saudi Arabian study reported 4 days [3].

According to Centers for Disease Control and Prevention (CDC), secondary cases linked with limited human-to-human transmission have a median incubation time of around 5 days (range 2-14 days). The mean period from commencement of illness to hospitalization for MERS-CoV patients is around 4 days. The typical duration from onset to intensive care unit (ICU) admission in severely sick patients is around 5 days, and the median time from onset to death is roughly 12 days. The median duration of mechanical ventilation was 16 days, and the typical length of stay in the ICU was 30 days, with 58 percent death at 90 days in one group of 12 ICU patients.

The inconsistency in the incubation time period for contamination with Middle East Respiratory Syndrome coronavirus has been investigated. Early studies did not examine whether the time of the incubation in a person has any correlation with successive clinical consequences [40]. One study reviewed the available literature on EMBASE, Web of Science and MEDLINE that reported seroprevalence and prevalence of active Middle East infection in dromedary camels, from both longitudinal and cross-sectional studies. The review verified

that the chances of these syndromes may increase with age from 80 to 100% in adults by supporting geographical widespread. The endemicity of Middle East respiratory MERS-CoV in dromedaries in different countries which are exporting dromedaries (Africa) and the Arabian Peninsula the high incidence of active infection are also measured in juveniles. The dromedary populations are investigated [47].

Symptoms of the disease may appear at any time, usually within 2-14 days following infection. Fever, shortness of breath and cough are the main symptoms, but symptoms including vomiting, diarrhoea, and nausea and muscle pain (myalgia) can also occur. In some individuals, no symptoms or only slight cold-like symptoms are produced by infections. Yet in others, predominantly in persons with underlying medical conditions, infections can produce severe illness [48].

1.1.6 The seasonal trends in transmission and disease pattern

Seasonal variation in infectious disease transmission plays a significant role in defining when epidemics occur. It is important to understand the transmission of the virus, including any seasonal variation that has occurred in the transmission between animals and humans [49]. Based on early cases in April 2012, April to May 2013, and May 2014, it was concluded that there was a notable rise in MERS-CoV activity from March to May of each year. Early hospital outbreaks have also arisen in April 2012, April to May 2013, and April to May 2014. Therefore, it was assumed that MERS-CoV occurs mainly during the spring [50, 51]. Since sustained outbreaks of MERS-CoV have not occurred, and it is assumed that sporadic reseeding of outbreaks occurs, this suggests that seasonal transmission between humans and camels occurs. In this thesis, since sustained transmission does not occur, we have chosen to ignore seasonality in MERS-CoV thus far. Inclusion of seasonal effects is a course for future

work.

1.1.7 MERS-CoV immune protection

Antibodies against MERS-CoV have been found in past infected patients 1.5 years after initial infection. However, the duration of antibody responses beyond 1.5 years has not been reported [52]. Thus, it is not known what the long-term immune outcomes of infection are from MERS-CoV. In this thesis we do not consider sustained infection of MERS-CoV in the population. Additionally, since it is not clear what fraction of the affected populations in the Middle East have had MERS-CoV, we cannot assume that a large fraction has actually had this disease. We thus ignore the effects of long-term immunity in the population, as it is not clear if long-term immunity exists, and if it does, it is not clear that a significant fraction of the population has acquired it.

1.1.8 MERS-CoV evolutionary and mutational changes

In its evolutionary history, potential recombination events are common in MERS-CoV, particularly those in its receptor-binding domain, which have allowed for cross-species transmission from non-human hosts [53]. Since there is no evidence of sustained outbreaks of MERS-CoV because of human-to-human transmission, we assume that evolutionary changes in the virus to enhance fitness in human-to-human transmission are minimal. We thus ignore evolutionary changes of the virus in this thesis.

1.1.9 Pharmaceuticals and Vaccines

There are no FDA-approved treatments or vaccines for MERS-CoV. Only recently have there been vaccines developed against SARS-COV-2. The research on MERS-CoV immunization is in the primary stages [54, 55, 56]. However, initial intervention methods such as quarantine

(with patients in isolation) of suspected cases and fast diagnosis have proven to be the most effective and prominent control measures for quickly tackling a MERS epidemic. We ignore the effects of pharmaceuticals and vaccines in this study.

1.2 The Hajj

Mass gatherings (MG) are classified as any festival that gathers a large enough number of people with putting a burden on the town, city, or nation hosting the event's preparation and response resources [57]. MG are used for religious and political events, as well as music performances, festivals, and athletic contests. MG might have a small number of individuals or millions. They take happen during a short period of time and in a specific area. They might be pre-planned or unplanned. They may also be one-time events, like a royal wedding, or they can be repeated periodically at various sites, like the Olympics, or at the same venue, as the Hajj [57]. The Hajj is an annual mass gathering in Mecca, Saudi Arabia that has been taking place for almost 14 centuries [58]. It is a Muslim pilgrimage or spiritual journey that many Muslims undertake every year. It is the world's biggest, most diversified, and recurring mass gathering in existence today [59, 60]. The Hajj journey is required of all Muslims who are physically and financially capable of doing just that at least once in their lives; it's among the five pillars of the Muslim faith [61, 62, 63]. The Islamic calendar, which is based on the lunar year, determines the date of Hajj that changes every year as seen in the Figure 1.4.

Saudi Arabia is divided into 13 autonomous districts or provinces [65], with the cities in our research being in the Makkah and Medina provinces. Makkah province is Saudi Arabia's most largest province, and the city of Jeddah and Mecca (the province's headquarters) are the second and third populous cities in the country (after Riyadh, the capital) [65, 66].

For all applicants who applied to participate in Hajj recently, the Ministry of Health

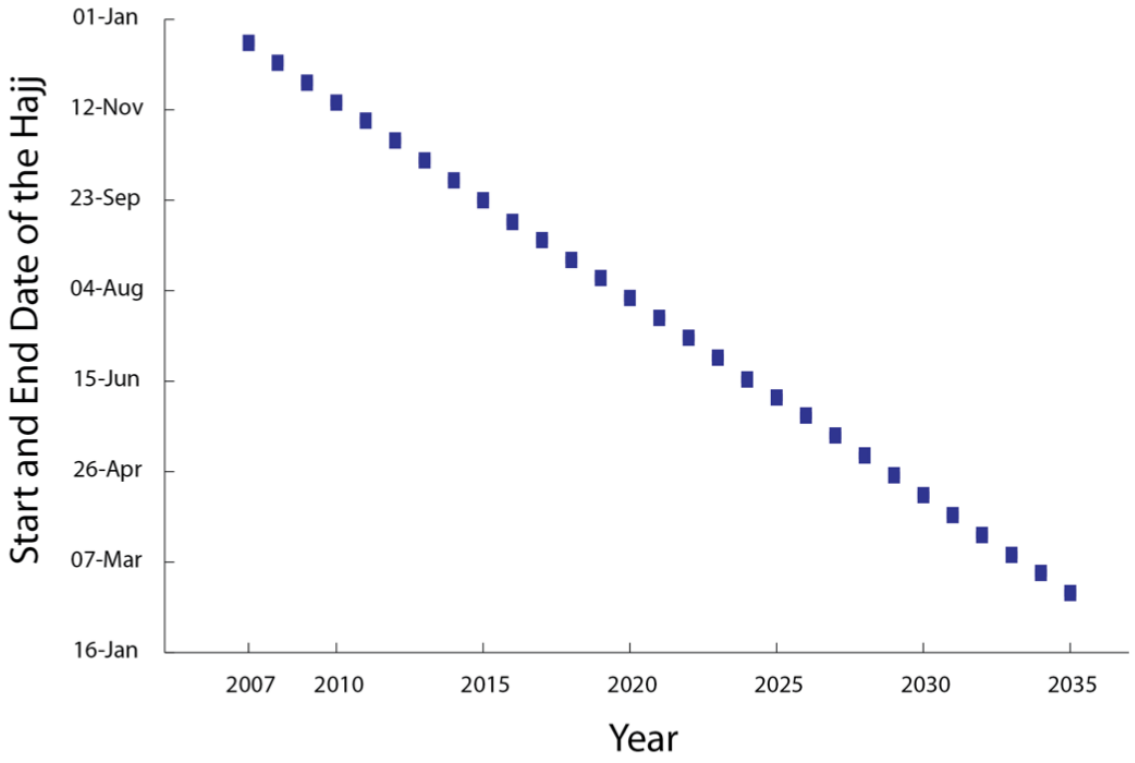

Figure 1.4: Dates of the Hajj, 2007 - 2035 [64].

created strict qualifying requirements. Participants had to meet the following criteria:

(1) be between the ages of 20 and 65 (with a warning for those over 50),

(2) not have specific high-risk chronic conditions,

(3) not be overweight,

(4) not be pregnant, and

(5) have a negative polymerase chain reaction in certain diseases; for example, (PCR) COVID-19 tests [67].

Pilgrims engage in religious practices in the holy cities of Mecca and Medina during the Hajj rites. Most pilgrims also visit Mina, where they remain in tents and spend the majority of their time reading the Quran. Pilgrims then proceed to Mount Arafat, where they stay in

tents and pray from sunrise to nightfall. After reaching Muzdalifah after nightfall, pilgrims gather stones for the Jamarat ritual, which involves throwing them at three stone pillars (symbols of the devil), before continuing on to Mecca as seen in the figure 1.5 and the studies that have been done by Memish et al., 2009, and 2014 [68, 69].

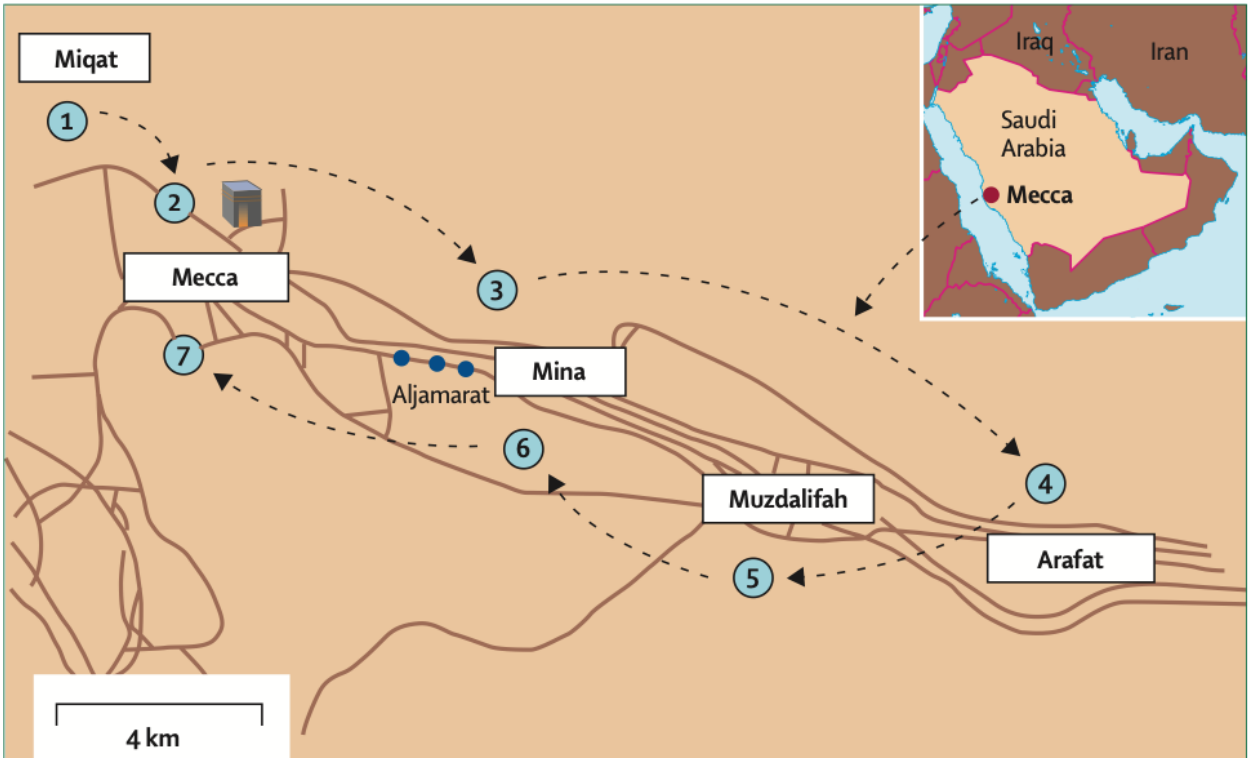

Figure 1.5: The Hajj Journey [61].

1.2.1 Respiratory disease transmission at the Hajj gathering

Acute respiratory tract infections are common during the Hajj season. Even though the Hajj gathering can occur in different times of the year, pilgrims can travel to the Hajj from all over the world, making it possible for any prevalent respiratory infections to be imported to the gathering, and transmitted. The close interactions between pilgrims during different stages of the Hajj, including times of extreme congestion, shared lodging, and excessive air emissions; for example dust storms, particulate matter and trace gases at a large scale and

vehicular emissions have a significant impact on the health of pilgrims.[70].

The 2009 H1N1 influenza strain caused a pandemic. The 2009 Hajj took place in November 2009, when the Northern Hemisphere was experiencing high levels of virus activity. There were therefore concerns that the Hajj gathering could become a hot spot for transmission, and contribute to global spread of the pandemic through the travelling pilgrims. In this thesis, I have chosen to focus my work on influenza infections. However, the work can be extended to other respiratory infection, including coronaviruses. An extension to a study of COVID-19 in the 2020 and 2021 Hajj gatherings is a course for future work.

Figure 1.6: comparing between Hajj in 2019 (left) and 2020 (right). A maximum of 1,000 pilgrims from 160 countries around the world residing in KSA were randomly assigned to undertake Hajj rites in 2020 since the outbreak of the COVID-19 pandemic began. [67].

comparing between Hajj in 2019 (right) and 2020 (left). A maximum of 1,000 pilgrims from 160 countries around the world residing in KSA were randomly assigned to undertake Hajj rites in 2020 since the outbreak of the COVID-19 pandemic began. [67].

1.2.2 Public health mitigation

Massive crowds of individuals challenge the public health abilities of the hosting communities and the areas of origin of travellers. The annual pilgrimage of Muslims to Saudi Arabia is one of the largest, most socially and geographically diverse mass meetings around the globe

as has been indicated in the Figure 1.7. In June 2009, the Saudi Ministry of Health (MoH) held a Risk Mitigation Committee meeting for the 2009 Pandemic Influenza A H1N1 and forthcoming Hajj. Specialists from global public health organisations worked with their Saudi colleagues in their authorized capacities. The goal of the MoH was to pool and exchange public health information on mass events and to evaluate the country's preparedness strategies, concentrating on the prevention and control of pandemic influenza. This review culminated in a variety of constructive suggestions [68], half of which were placed into effect before the beginning of Hajj and the majority during Hajj. Such disaster response strategies as shown in Figure 1.6 will ensure an adequate availability of health care for pilgrims to Saudi Arabia and a minimal spread of diseases upon their return home. In this thesis, we include public health mitigation strategies in our studies of respiratory infection spread at the Hajj gathering.

Mathematical models of disease transmission can be used to assess the effects of different public health mitigation strategies, and determine the potential for importation and exportation of infection diseases, as well as the burden of the disease in the host country during the pilgrimage season. In this thesis, we employ mathematical models to study such aspects of the Hajj gathering.

1.3 Mathematical Epidemiology

Infectious disease epidemiology has relied on mathematical interpretation and study of contagious diseases since the discipline's emergence more than a century ago. Due to advancements in computers, automated data storage, and the opportunity to exchange and deposit data over the internet, comprehensive electronic monitoring of infectious diseases has been popular in recent years.

An infectious disease is described as an infection caused by a pathogen or its lethal product that spreads from an infected human, infected animal, or contaminated inanimate item to a

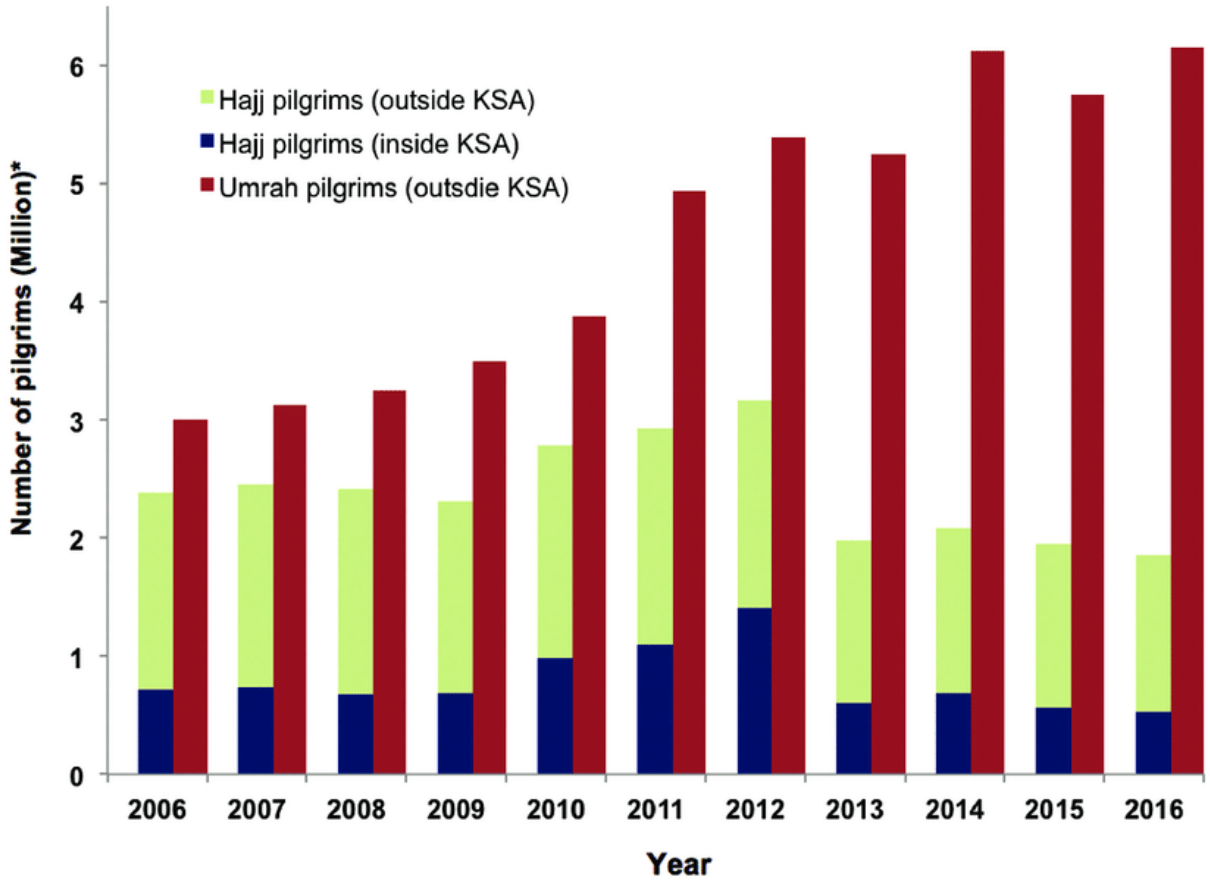

Figure 1.7: The number of Hajj and Umrah pilgrims 2006-2016 [71].

susceptible recipient. Infectious diseases cause a massive worldwide disease burden that has a widespread impact on the public health systems and economics [72].

Mathematical models have been shown to be powerful tools in elucidating key characteristics of infectious disease transmission that can inform public health mitigation, and pharmaceutical and vaccine intervention [73]. In this thesis, we have chosen to apply models in Mathematical Epidemiology to study disease spread and different public health mitigation strategies using a variety of mathematical frameworks. We now introduce the basic model of infectious disease dynamics, the SIR model, and introduce the mathematical frameworks employed here within.

1.3.1 The SIR model

The basic model of infectious disease spread was first developed by Kermack and McKendrick (1927) [74]. This model is called the SIR model as it tracks Susceptible, Infected, and Recovered (or immune) individuals in the population, which are assigned to susceptible, infected and recovered compartments of the population. The SIR model is thus called a compartmental model. Generally, a susceptible individual (S: no immunity to the disease) can be infected through contact with an infectious individual (I: already infected and therefore will spread the disease) and then the individual can recover (R: has acquired immunity) from the disease.

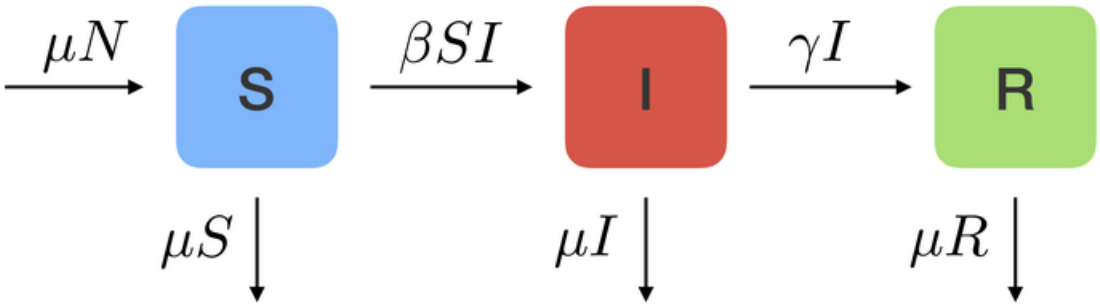

Figure 1.8: SIR Model; https://sineadmorris.github.io/post/the-sir-model/ .

Figure 1.8 shows a flow diagram of the basic SIR model. Extensions to the SIR model to includes other types of compartments are a plenty, including new classes of disease i.e., non-infectious periods, asymptomatic infections, different levels of immunity, and different sub-populations, delineating the population by, for example, age, sex, behaviour, or other population strata.

The SIR model and extensions can be studied using different types of modelling frameworks. In this thesis, we use five different modelling frameworks:

1- Deterministic Models:

Models are written as ordinary differential equations (ODEs) under the principle that population sizes can be determined with absolute confidence, and hence the solution of an ODE implements a predefined path or solution trajectory in state space. In many cases, a population's conduct is entirely defined by its history and the principles that characterize the model.

2- Stochastic Models:

Stochastic models are created using probability based frameworks to simulate population proportions, and therefore the behaviour of the population is not understood with certainty. A stochastic process solution path reflects only one realization of the process; each realization is different. The numerical analyses and simulations are based on the Gillespie's Direct Method [75].

3- Two-Species Models:

We incorporate connections between different species where we allow for susceptible, infectious and recovered individuals in each species that interact both directly and indirectly within a certain geographical region.

4- Network Models:

Networks provide a structured interpretation about both interactions between species or communities, and are particularly helpful since each individual has only a limited proportion of population in direct communication with [76, 77, 78, 79, 80].

5- Metapopulation Models:

Different geographic regions are connected. Subpopulations can move between geographic regions, and importation, transmission, and exportation can be tracked through time [81].

1.3.2 Deterministic Models:

Consider the SIR model shown in Figure 1.8. Let the maximum size of the population $N = S + I + R$ at a certain given time. The values S,I, and R are also known as the model's system variables. When N is sufficiently high, then S, I, and R can be interpreted as continuous variables, and the proposed framework can be used to predict the existence and time rates of independent members of the dominant population moving from one compartment to the other.

The classical SIR model satisfies the system of differential equations below:

$$\frac{dS}{dt} = b - \beta SI - \mu S, \tag{1.1}$$

$$\frac{dI}{dt} = \beta SI - \gamma I - \mu I, \tag{1.2}$$

$$\frac{dR}{dt} = \gamma I - \mu R. \tag{1.3}$$

The birth rate, $b = \mu N$, the natural death , μ, and the rate of infection recovery, γ, are the parameter values.

The SIR model has a disease free equilibrium $E^* = (S^*, I^*, R^*) = (b/\mu, 0, 0)$ and an infected equilibrium $\bar{E} = (\bar{S}, \bar{I}, \bar{R}) = (\frac{b^2}{\mu(\beta+b)}, \frac{\beta b}{(\beta+b)+(\mu+\gamma)}, \frac{\gamma\beta b}{\mu(\beta+b)(\mu+\gamma)})$. The stability condition of E^* depends on the basic reproduction number $R_0 = \beta N/(\mu + \gamma)$. If $R_0 < 1$, E^* is stable [82]. However, if $R_0 > 1$, the infected equilibrium $\bar{E}$ exists and is stable. Public health, pharmaceutical, and vaccine interventions can be implemented to reduce $R_0 < 1$ to prevent and/or eradicate a disease from the population. However, for various extensions for the SIR model, reducing $R_0 < 1$ may not always achieve eradication [83]. In this thesis, we derive the basic reproduction number for our employed models of study. Stability analysis (local and global stability analysis) is then pursued to determine existence and stability conditions of the model equilibrium points.

The SIR system is ideal for contagious diseases that grant lifetime immunity, such as measles [74, 84, 85, 86]. It is also a model that can be well-applied when studying short outbreaks whereby immunity gained provides protection from infection in the short term. In this case, demographics can be ignored, i.e., $b = \mu = 0$ [87, 88, 89] and disease free equilibria $(S^*, 0, R^*)$ only exist, where $S^* + R^*$ give the entire population.

Deterministic models in mathematical epidemiology are essential in that they provide for quantitative and qualitative understanding of the fundamental processes of infectious disease transmission. They can also suggest effective control strategies and enable simple methods for implementation in SIR models (and extensions). Finally, deterministic models can have complex non-linear dynamics, allow for analytical solutions, and allow for a simple and systematic study of the biological mechanisms.

We reiterate that, if demographics are included in the SIR model, an infected equilibrium $\bar{E}$ will always exist if $R_0 > 1$. However, the equilibrium level of infection can be very small, and unrealistic. In such cases, stochastic models (see next section) will allow for disease elimination.

The extension of the SIR model in term of study MERS-CoV has been done in various studies. For example, Lin et al. [90] developed a conceptual model that is based on the $SEIRS$ structure for camel-to-camel transmission. The model framework S, E,I, and R are the numbers of susceptible, exposed, infected, and recovered, respectively, while C is their number of weekly laboratory-based human confirmations. The main implications of there study were utilizing a simple epidemic model to analyze the prevalence of MERS-CoV in camels, and the estimations of biological justification.

Al-Asuoad et al. [91] conducted model predictions which are based on data from Riyadh (Saudi Arabia) outbreaks between 2013 and 2016. Model simulations show that MERS will eventually be contained in the city. However, the confinement time and severity of the outbreaks are highly dependent on the contact coefficients and the isolation rate constant.

The mathematical model developed in [92] is used in this study to investigate the dynamics of (MERS) in Saudi Arabia. It extends on the study that was conducted in the city of Riyadh [91], since preliminary data has become available after the paper's publication. The model describes the epidemic dynamics of five different population groups: susceptible $S(t)$, asymptomatic $E(t)$, symptomatic $I(t)$, isolated $J(t)$, and recovered $R(t)$, where t is expressed in days. The goals of this project are twofold. First, prove the (disease free equilibrium) DFE's local stability and the global stability of both the DFE and the (endemic equilibrium) EE using simply the effective reproduction number or stability control number R_c , which enhances the theoretical conclusions in [92]. The second and more essential goal is to model and anticipate a disease epidemic in Saudi Arabia during the following two years [91].

As of June 11, 2014, the Middle East respiratory syndrome coronavirus (MERS-CoV) epidemic had resulted in 209 fatalities and 699 laboratory-confirmed cases all across the Arabian Peninsula [19].

1.3.3 Stochastic Models:

A.G. McKendrick suggested an early stochastic disease model in 1926 [93], which predates his work with Kermack on deterministic models [93]. Greenwood suggested discrete time stochastic models in 1928 and 1931 [94]. Bartlett [95] investigated a continuous time stochastic SIR model. Bailey's [96] book discusses deterministic and stochastic disease models, as well as the estimation of the parameters [97].

Linda Allen has conducted comprehensive studies in this area, applying stochastic models in mathematical biology and epidemiology [98, 99, 100, 101].

The asymptotic dynamics of deterministic and stochastic disease models provide a significant difference between them. Even if the resulting deterministic solution converges to an endemic equilibrium, stochastic solutions can converge to the disease-free state. Rather than

focusing on the mean behaviour captured by deterministic models, stochastic models allow for the prediction of variance in model outcomes. Stochastic simulations can also be used to calculate the probability of an epidemic outbreak or the absence of a disease in a community given public health reduction strategies. The compartments used in deterministic ODEs are described as disease states in stochastic modelling. Individuals transition through one state to the next, with their motions dictated by current probabilities.

In a stochastic SIR model, the disease dynamics are identified by events affect the population size in each model compartment. For instance, in the dynamic described in the SIR system above, the events correspond to birth, death, disease transmission, and recovery. The transitions between the states are given in Table 1.1.

State transitions and rates for the CTMC		
Description	Rate	transitions
infection	βSI	$S \to S-1 \Rightarrow I \to I+1$
Recovery	γI	$I \to I-1 \Rightarrow R \to R+1$
Birth	bN	$S \to S+1$
Natural death of susceptible	dS	$S \to S-1$
Natural death of infected	dI	$I \to I-1$
Natural death of recoverd	dR	$R \to R-1$

Table 1.1: The Stochastic SIR Model

1.4 Two species model: MERS-COV

Lotka [102] and Volterra [103, 104] simultaneously constructed a two species prey-predator model in 1924 and 1926, concurrently, which is called the "Lotka-Volterra prey-predator model". As a result, there has been a substantial development of prey-predator models since

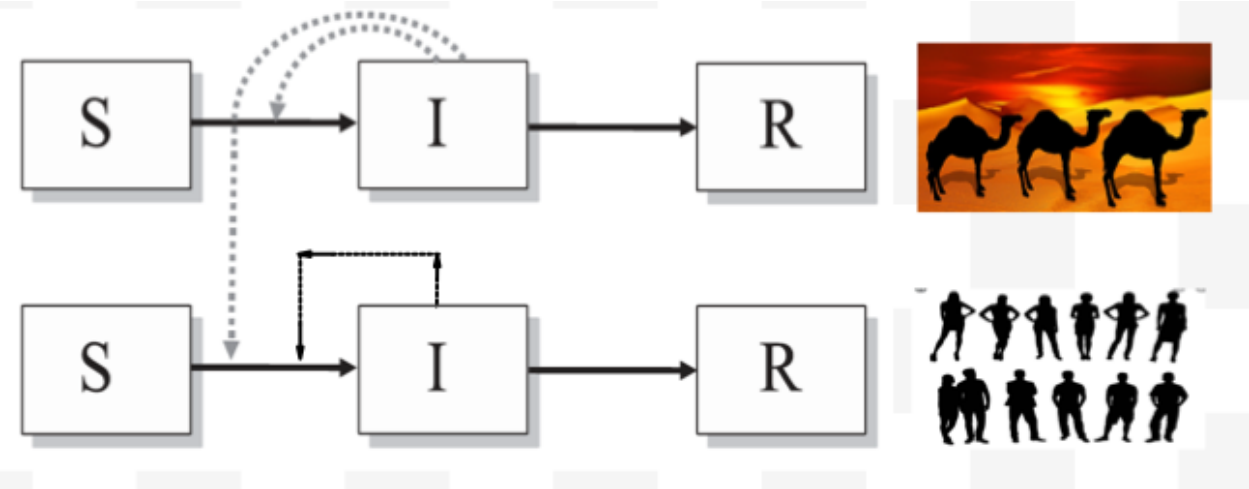

Figure 1.9: Two species MERS-COV model.

the pioneer works in the 1920s. Initially, some of these systems were developed in continuous time; in particular, see that the work of Rosenzweig and MacArthur 1963 [105] and Holling 1965 [106], as well as the investigation of Kolmogorov type equations introduced by Freedman and Waltman [107].

Predator-prey models provide a basis for two-species disease models. By combining disease compartments for each species, and coupling the species through transmission, we can study two-species disease models, and zoonoses. Zoonotic pathogens are those that could be transmitted from animals to humans. In specific, the animal host acts as the principal reservoir for the virus, with humans playing a minor impact on overall transmission. In the case of zoonotic pathogens, a two-species model can be used to study transmission between the two species, as well as, the transmission between individuals of the same species. Figure 1.9 shows a flow diagram of an SIR model involving two species, in particular, camels and humans, whereby camels can transmit the virus to humans and other camels, and humans can transmit the virus to other humans. It is interesting to note that when two species interact and the disease occurs in both, three different scenarios are possible:

(1) Both species are still afflicted with the disease.

(2) The disease remains in one species but is eradicated in the other.

(3) The disease is exterminated in all species.

1.4.1 Network Models

Networks are very effective methods for identifying the dissemination of infection in a population through social connections (for airborne infections), behavioural contacts (for other respiratory transmitted diseases) [108, 109].

The propagation of any disease can be interpreted as a network operation, with individuals representing nodes and epidemiologically related connections representing edges between nodes. Over the years, a variety of network-based methodologies to disease propagation have been created, varying in scale, functionality, and complexity. Numerous types of networks are widely used in epidemiological research (and by mathematical biologists); for instance, Random Networks [110, 111, 112, 113, 114, 115], Lattices [116, 117], Small World Networks [118, 119, 120, 121, 122], Spatial Networks [123, 124], Scale-Free Networks [125, 126, 127, 128]. In all network models, individuals are defined by nodes in network models of disease propagation, and the interaction pattern between them is described by network edges shown in the Figure 1.10. In this thesis, we assume static, unweighted networks that have an SIR disease that spreads across edges. The following node statuses are possible: susceptible S, infected I, and recovered R. The network's state is supplied at any given time t by the statuses of all N nodes. Therefore, in the case of an SIR model, there are 3^N states. In other words, the state space is made up of N triples of identifiers from the set $\{S, I\}$, or $\{S, I, R\}$. The condition varies over time, and the infection and recovery processes determine the rates at which the nodes' statuses adjust.

Networks offer a structured viewpoint about interaction between individuals or commu-

nities, which are highly beneficial where each individual is in direct contact with a small segment of the population. In addition, networks offer a reliable way of determining the individual existence of disease transmission. Two agents are connected if they have sufficient interaction to cause the infection to propagate between them. We will use network models to study MERS-COV in camel movement throughout different provinces of KSA.

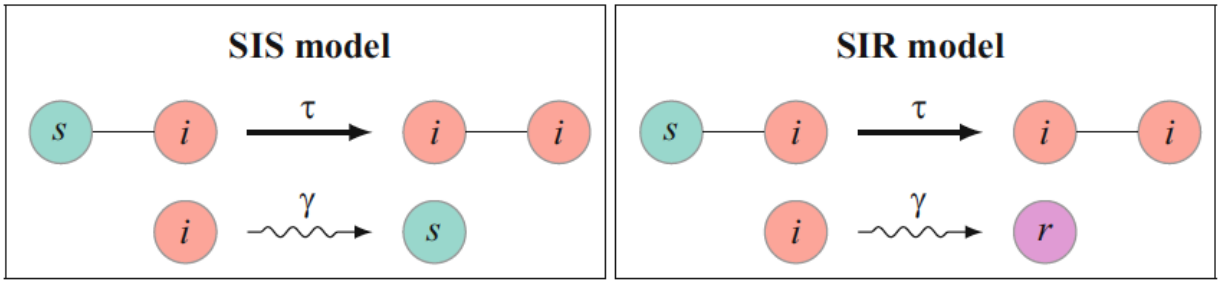

Figure 1.10: At a rate τ an infected node infects its susceptible neighbor. An infected node recovers at rate γ regardless of the state or number of contacts. Infected nodes are becoming susceptible after recovered in the SIS model, but immunity occurs in the SIR model [129].

Pairwise approximation Model

Given a network framework, a system of differential equations can be written describing the different types of states of different types of node connections. There is difficulty, however, in writing the models given that there smaller order network that will depend on larger order contact [116]. A way to simplify the model is to use Moment Closure techniques. Pairwise approximation methods have been shown to be effective in capturing network dynamics by approximating all higher order connections with pairs only [116, 130].

Figure 1.11 gives an example of a SIR model (and an SIS model) showing pairs in a network that can be used to approximate higher order connections. We observe that the variables in the SIR scheme are not independent due to the preservation relation $[S] + [I] + [R] = N$. The estimated number of S nodes ($[S]$) and I nodes ($[I]$); for instance, singles, dependent on the number of SI pairs ($[SI]$); thus, the scheme is dependent on pairs, for which additional

calculations are needed. Comparably, the number of pairs is related to the number of triples.

The numbers of SS pairs, for instance, reduces caused by infection from outside the pair, i.e. it varies proportionally to the number of SSI triples ($[SSI]$) with rate $2\tau[SSI]$ (recall the SS pair is counted twice). The infected node in a SI or IS pair will recover at rate γ; hence, in the case of a SIS outbreak, the number of $[SS]$ pairs increases at rate $\gamma([SI] + [IS])$. We will use $2\gamma[SI]$ because the quantity of $[SI]$ and $[IS]$ pairs is equal. We come to the following hypotheses by extending this basic methodology logic to $[SI]$ and $[II]$ pairs and accounting for all inside as well as outside transitions [129].

We can now conclude that the network is homogeneous, with each node having the same degree n. There are $[I]$ contaminated nodes, accounting for $\frac{[I]}{N}$ of the population. Assuming that infected nodes are uniformly distributed, a typical susceptible node has $\frac{n[I]}{N}$ infected neighbours. Since infected nodes are more likely to come into contact with all other infected nodes, this presumption allows the closed structure inexact. The approximation of the total number of SI edges can be given by

$$[SI] \approx \frac{n}{N}[S][I]. \tag{1.4}$$

The cumulative number of edges beginning with susceptible nodes is $n[S]$. Since the overall number of SI edges is $[SI]$, a proportion

$$\frac{[SI]}{n[S]},$$

of the edges beginning from susceptible nodes belong to infected nodes. Likewise, the edge to susceptible node ratio is

$$\frac{[SS]}{n[S]}.$$

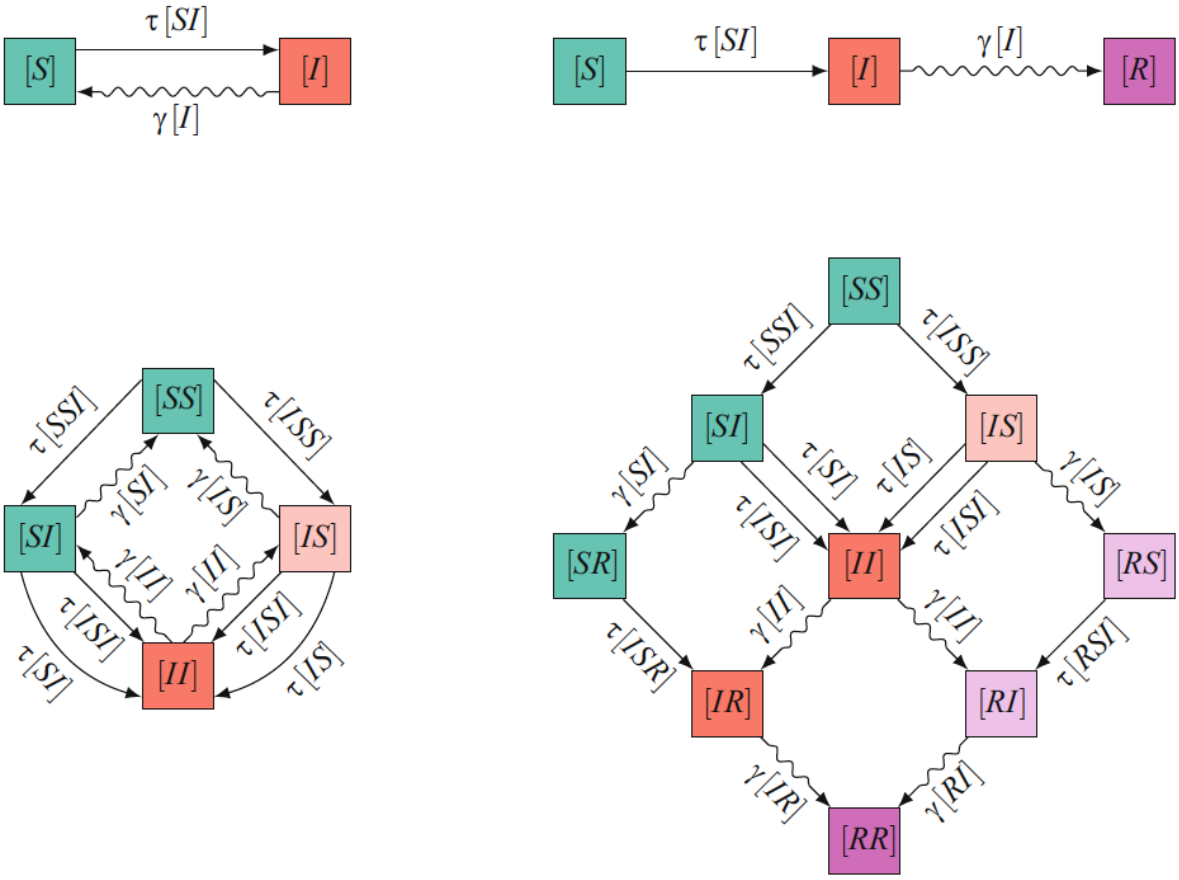

Figure 1.11: Graphs depicting the flux between singles compartments (top) and pairs compartments (bottom). The left case is showing the SIS model and the right case is representing the SIR model. In the compartments of pairs, hard lines indicate pathogens from inside the pair (with a rate dependent on the pair) or from outside the pair (with a rate dependent on the triple), and wiggle lines indicate recovery [129].

As a result, if we select a susceptible node$x$ and two neighbours y and z , the probability that y is susceptible while z is infected is

$$\frac{[SS][SI]}{n^2[S]^2}.$$

There are $n(n-1)$ ways to select y and z. As a result, the predicted number of SSI triples is

$$\frac{[S]n(n-1)[SS][SI]}{n^2[S]^2} = \frac{(n-1)[SS][SI]}{n[S]}. \tag{1.5}$$

Suppose that they are uniformly distributed, we can claim that

$$[SSI] \approx \frac{n-1}{n}\frac{[SS][SI]}{[S]}. \tag{1.6}$$

similarly,

$$[ISI] \approx \frac{n-1}{n}\frac{[SI]^2}{[S]} \tag{1.7}$$

From the graphs that show the flux between the compartments, the singles, pairs, and triple used to create a self contained structure will be considered using differential equations; such that the SIR model can be written as

$$\begin{aligned}
\frac{d[S]}{dt} &= -\tau[SI], && \text{(1.8a)}\\
\frac{d[I]}{dt} &= \tau[SI] - \gamma[I], && \text{(1.8b)}\\
\frac{d[R]}{dt} &= \gamma[I], && \text{(1.8c)}\\
\frac{d[SS]}{dt} &= -2\tau[SSI], && \text{(1.8d)}\\
\frac{d[SI]}{dt} &= \tau([SSI] - [ISI] - [SI]) - \gamma[SI], && \text{(1.8e)}\\
\frac{d[SR]}{dt} &= -\tau([ISR] + \gamma[SI]), && \text{(1.8f)}\\
\frac{d[II]}{dt} &= 2\tau([ISI] + [SI]) - 2\gamma[SI]), && \text{(1.8g)}\\
\frac{d[IR]}{dt} &= \tau([ISR] + [SI]) + \gamma([II] - [IR]), && \text{(1.8h)}
\end{aligned}$$

$$\frac{d[IR]}{dt} = 2\gamma[IR]. \tag{1.8i}$$

where τ is infection rate and γ is recovery rate [129].

We will apply pairwise approximations to simply the network models in our consideration. This allows for a study of a system using differential equations of individuals and pairs of individuals. Higher order connections (triples, etc.) are approximated using singles and pairs so that the system is computationally manageable.

1.4.2 Metapopulation Models

Models are used to track movements of individuals between geographic regions. Metapopulation models can be used to track the movement of susceptible, infectious and recovered individuals between regions. Figure 1.12 gives the general case of modelling the process of mobility among discrete geographical regions.

Consider N_{ij} as the number of individuals from country i who are present in country j at time t. Particularly, N_{ij} denotes the society remaining in the country of residence. The two parameters, σ_i and ρ_i, are specified as the mobility rate of residents in country i leaving their home country and the proportion of people attempting to return to their country of origin i from a foreign country j, respectively. Suppose that $N_{ii}(t)$ is the number of people currently in their home country i at time t, and $N_{ij}(t)$ is the number of individuals who are from country i and are in region j at time t. The following model represents the patterns of individuals among regions:

$$\frac{dN_{ii}}{dt} = \sum_{j=1} \rho_{ij} N_{ij} - \sigma_i N_{ii}, \tag{1.9}$$

$$\frac{dN_{ij}}{dt} = \sigma_i N_{ii} - \rho_{ij} N_{ij}. \tag{1.10}$$

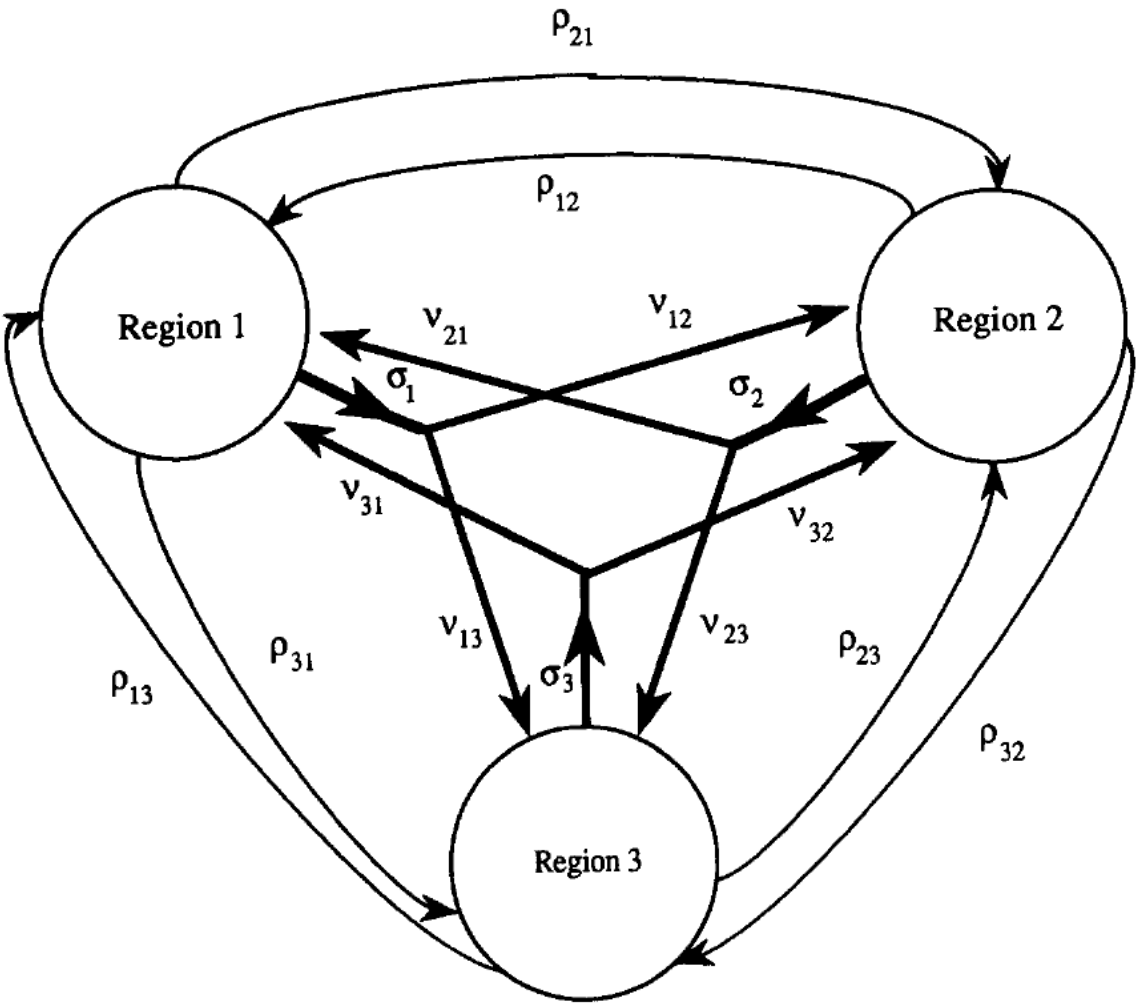

Figure 1.12: Diagram of the mobility mechanism connecting three geographic regions, where σ_i represents the rate at which people depart region i , ν_{ij} represents the probability that an individual who leaves region i moves to region j, and ρ_{ij} represents the rate of people from region i who visit region j return to region i [81].

The transmission of an infection in a population of individuals from different regions is defined by:

$$\sum_{j=1}^{n}\sum_{k=1}^{n}\tau_k\kappa_k\beta_{ijk}\frac{I_{jk}S_{ik}}{N_k^*} \tag{1.11}$$

where, τ_k is the probability of propagation per interaction in the area k, κ_k is the region's average number of contacts per person$k$, β_{ijk} is the fraction of interacts in region k among susceptible individuals from region i and Infected individuals from region j (S_{ik}), I_{jk} is the

number of infected people who are actually living in region k and are residents of region j [81].

Now, the number of people currently living in the region k is

$$N_k^* = \sum_m (S_{mk} + I_{mk} + R_{mk}), \tag{1.12}$$

People leaving area i to region k can be grouped by the overall population of region i so they are not comparable to those returning to region i. Susceptible people of area i who are currently present in that region are given by:

$$\frac{dS_{ii}}{dt} = \sum_k \rho_{ik} S_{ik} - \sigma_i S_{ii} - \sum_j \tau_k \kappa_i \beta_{iji} \frac{S_{ii} I_{ji}}{N_i^*}, \tag{1.13}$$

The change of susceptible citizens of area i who move to another region is defined by

$$\frac{dS_{ik}}{dt} = \sigma_i S_{ii} - \rho_{ik} S_{ik} - \sum_j \tau_k \kappa_k \beta_{ijk} \frac{S_{ik} I_{jk}}{N_k^*}. \tag{1.14}$$

The sum of these equations for all regions yields

$$\frac{dS_{ik}}{dt} = - \sum_j \tau_k \kappa_k \beta_{ijk} \frac{S_{ik} I_{jk}}{N_k^*}. \tag{1.15}$$

The last equation shows that the overall number of susceptibles in region i is changed solely as a result of disease transmission rather than a consequence of the mobility mechanism. This represents the fact that citizens should not adjust their home area index (they are selected to a certain region and do not change the assignment). As a result, while any system is included to implement adjustments in the index relating to a person's home area, the model would not include permanent migration. However, as the preceding study demonstrated, the mobility model does, at the limit of applicable parameters, provide similar findings with permanent

migration [81].

Differential equations for the number of I_{ik} and R_{ik} individuals in each region can also be derived. We are thus left with the following system of differential equations:

$$\frac{dS_{ii}}{dt} = \sum_k \rho_{ik} S_{ik} - \sigma_i S_{ii} - \sum_j \tau_k \kappa_i \beta_{iji} \frac{S_{ii} I_{ji}}{N_i^*}, \tag{1.16a}$$

$$\frac{dS_{ik}}{dt} = \sigma_i S_{ii} - \rho_{ik} S_{ik} - \sum_j \tau_k \kappa_k \beta_{ijk} \frac{S_{ik} I_{jk}}{N_k^*}, \tag{1.16b}$$

$$\frac{dI_{ii}}{dt} = \sum_k \rho_{ik} I_{ik} - \sigma_i I_{ii} + \sum_j \tau_k \kappa_i \beta_{iji} \frac{S_{ii} I_{ji}}{N_i^*} - \gamma I_{ii}, \tag{1.16c}$$

$$\frac{dI_{ik}}{dt} = \sigma_i I_{ii} - \rho_{ik} I_{ik} + \sum_j \tau_k \kappa_k \beta_{ijk} \frac{S_{ik} I_{jk}}{N_k^*} - \gamma I_{ik}, \tag{1.16d}$$

$$\frac{dR_{ii}}{dt} = \sum_k \rho_{ik} R_{ik} - \sigma_i R_{ii} + \gamma I_{ii}, \tag{1.16e}$$

$$\frac{dR_{ik}}{dt} = \sigma_i R_{ii} - \rho_{ik} R_{ik} + \gamma I_{ik}. \tag{1.16f}$$

Chapter 2

Two Species Population Model

2.1 Introduction

Many infectious diseases (including influenza) are caused by typical person-to-person interactions, and these people are considered homogeneous in terms of contact, and transmission behaviour [84]. The disease is spreading among heterogeneous populations in numerous cases [131]. In fact, due to prolonged contact with susceptible people, longer duration of contamination or precise services as food safety or quality assurance, some people are more likely to spread the more infectious disease [132]. SARS epidemic in 2003 highlighted as the high spreaders transmitted the disease to a large number of individuals [131, 133]. Some studies showed the impact of extensive of heterogeneity in infectiousness depending on large proportion infectious diseases such as SARS, measles, influenza, Ebola , and other diseases [134, 135]. Presently, there is no definite strategy to identify spread MERS-CoV within camels populations, and no control measures to reduce the spread of the disease to human [14]. However, infectious diseases that are related to certain cultural and wellbeing behaviors (like Ebola virus and Middle East Respiratory Syndrome) can be traced back to the mode of contact. In the present study, we will review these epidemic cases in order to describe the

insight into disease patterns. It is also useful in the course of intervention techniques for a wide range of population and management strategies for individuals [136].

MERS-CoV was first discovered in 2012, when it arose from an epidemic beginning in Saudi Arabia. The possible source of transmission has been recognized from dromedary camels. Though, in effect cases it is not due to human infection by camels, but human to human conveyance [137]. The interpersonal interactions intensify the outbreak of MERS among people. This case is mostly observed in medical institutions, where their health prevention and control measures are inadequate. South Korea's MERS virus was spread through three individuals, including a 68-year-old traditional male who took the virus from overseas visit and continue to travel, went to a number of clinics, and was transferred to a nursing home with 29 secondary infections. Out of 29 there were two cases that have been charged for the next infection of 106 cases. The people infected with MERS may have no symptoms, while others might have developed symptoms, such as: fever, cough, pneumonia and breath shortness. The fraction of cases resulting in death of MERS-CoV is 35% globally [14, 138]. So far there are no vaccines for the virus, but some strategies of treatment played big roles in terms of the reduction of the number of cases. It is highly recommended that individuals should maintain good hygiene and avoiding contact with sick animals.

Other prevention strategies include the intake of properly cooked and prepared animal products. Previous mathematical methods have been proposed to check the heterogeneity of transmission rate, which is exclusive to the environment using the compartmental modelling by applying various disease stages. These models allow us to better understand the impact of spreading dynamics of infectious. Presently, Lau et al. [139] combined spatial results to simulate the disease spread, and Nishiura et al. [26] developed a computational version to recognize the highly translatability characterize in multiple contacts that led to the outbreak of MERS.

In this study, mathematical methods are used to investigate the disease dynamics of the

MERS outbreak in KSA. We proposed a deterministic version based on ordinary differential equations, and improved it into a stochastic model, which was carried out as Markov linkage system. The analytical answers have been obtained and validated through model simulations, in order to anticipate the chance of extinction and epidemic by changing the initial susceptible individuals and model parameters. The main objective is to evaluate the characteristics of the disease dynamics which may affect the adaptability of the public health policy and vary with characteristics in the populations to help in the reduction of infections [91, 130].

2.1.1 Model Description and Formulation

The model divides the total human and camel populations at any time (t) into six compartments, see the flow chart for two species population Model 2.1. The total camels population represented by $N_1(t)$, is divided into compartments of Susceptible camel (S_1), Infectious camel (I_1), and Recovered camel(R_1). Therefore,

$$N_1(t) = S_1(t) + I_1(t) + R_1(t).$$

The human population represented by N_2, is divided into compartments of Susceptible humans (S_2), Infected humans (I_2), and Recovered humans (R_2). This gives,

$$N_2(t) = S_2(t) + I_2(t) + R_2(t).$$

The rate at which camels become infected is represented by $\beta_1 S_1 I_1$, and the natural death rate is μ_1. The death rate as a result of the disease is δ_1, and recovery rate is γ_1.

The recruitment rate of the human population is represented by π_2. Susceptible humans acquire disease through human-human contact or by camel-human is given by $\epsilon\beta_3 S_2 I_1 + \beta_2 S_2 I_2$.

Since it is challenging (as well as complex and time consuming) to assess infection in the animal population for many zoonoses, the emergence of human cases is often the prime index of severe epidemic within the animal population and an elevated risk to humans. The recovery rate of human from the disease at is γ_2. Humans who are infected die at a rate δ_2. The natural death rate of the human is μ_2.

The ordinary differential equations of two species population model is represented by,

$$\frac{dS_1}{dt} = \pi_1 - \beta_1 S_1 I_1 - \mu_1 S_1, \tag{2.1}$$

$$\frac{dI_1}{dt} = \beta_1 S_1 I_1 - (\mu_1 + \delta_1 + \gamma_1) I_1, \tag{2.2}$$

$$\frac{dR_1}{dt} = \gamma_1 I_1 - \mu_1 R_1, \tag{2.3}$$

$$\frac{dS_2}{dt} = \pi_2 - \epsilon\beta_3 S_2 I_1 - \beta_2 S_2 I_2 - \mu_2 S_2, \tag{2.4}$$

$$\frac{dI_2}{dt} = \epsilon\beta_3 S_2 I_1 + \beta_2 S_2 I_2 - (\mu_2 + \delta_2 + \gamma_2) I_2, \tag{2.5}$$

$$\frac{dR_2}{dt} = \gamma_2 I_2 - \mu_2 R_2. \tag{2.6}$$

Sufficient factual studies demonstrated that dromedary camels are the major carrier of the virus. 75 % of reported cases are due to human-to-human transmission, whereas the 25 % of reported cases are due to camel-to-human transmission [90]. Therefore,

$$\frac{\beta_2 S_2 I_2}{\epsilon\beta_3 S_2 I_1 + \beta_2 S_2 I_2} = 0.75, \tag{2.7}$$

or

$$\frac{\beta_1 S_1 I_1}{\epsilon\beta_3 S_2 I_1 + \beta_1 S_1 I_1} = 0.25. \tag{2.8}$$

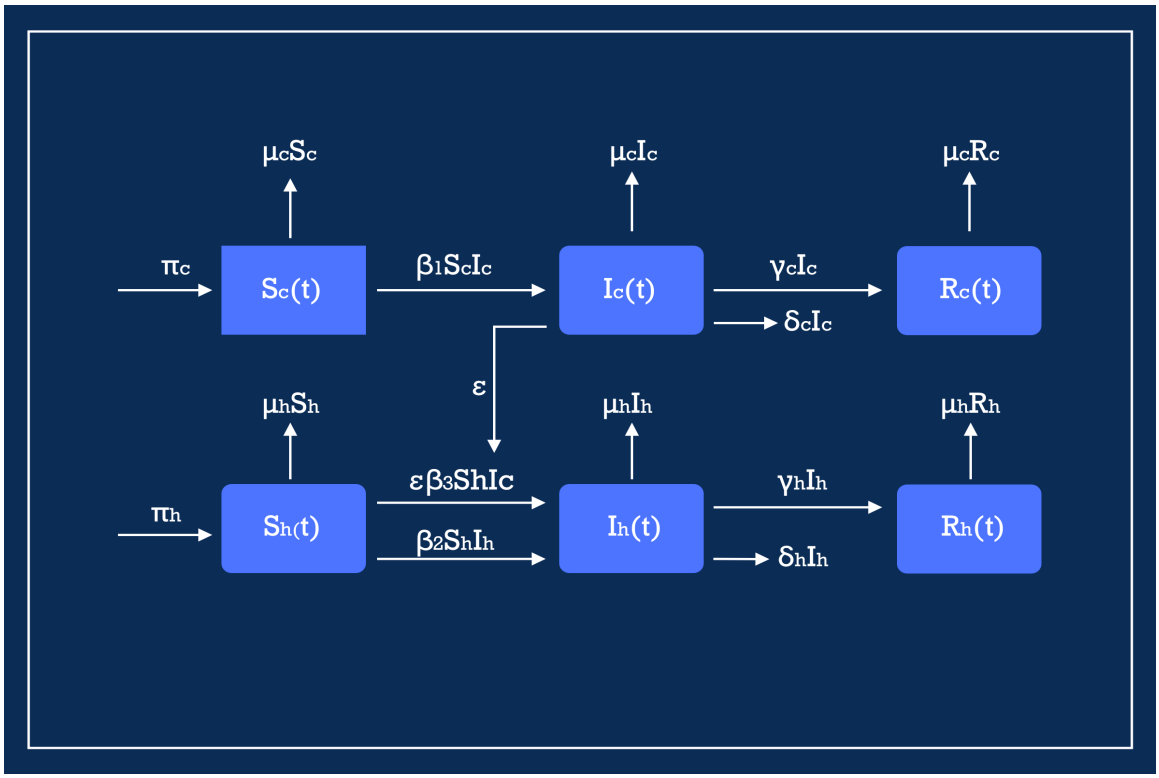

Figure 2.1: Flow chart for Two Species Population Model. The sub-letter c represents camel population [population(1)] and the sub-letter h represents human population [population(2)].

2.2 Analysis of the model

2.2.1 Positivity and Boundedness of Solutions

Theorem 2.2.1. *Let*

$$\Pi = \{(S_2(t), I_2(t), R_2(t), S_1(t), I_1(t), R_1(t)) \in \mathbb{R}_+^6 : (S_2(0), I_2(0), R_2(0), S_1(0), I_1(0), R_1(0)) > 0\}$$

then the solution of

$$\{(S_2(t), I_2(t), R_2(t), S_1(t), I_1(t), R_1(t)),\}$$

are non-negative for all time $t \geq 0$ *of the system 2.1 (i.e., if*

$$S_2(0), I_2(0), R_2(0), S_1(0), I_1(0), R_1(0)$$

are non-negative, then $S_2(t), I_2(t), R_2(t), S_1(t), I_1(t), R_1(t)$ *are also non-negative for all time* $t > 0$*).*

Proof. The total human population at any time (t) is given by,

$$N_2(t) = S_2(t) + I_2(t) + R_2(t),$$

and

$$\frac{dN_2}{dt} = \frac{dS_2}{dt} + \frac{dI_2}{dt} + \frac{dR_2}{dt}.$$

The above equation can be interpreted as,

$$\frac{dN_2}{dt} = \pi_2 - \mu_2 N_2 - \delta_2 I_2.$$

Absence of mortality due to disease gives,

$$\frac{dN_2}{dt} \leq \pi_2 - \mu_2 N_2. \tag{2.9}$$

Solving the differential equation 2.9 yields,

$$\pi_2 - \mu_2 N_2 \geq Ae^{-\mu_2 t},$$

where A is constant. Thus, applying the initial condition, $N_2(0) = N_{2(0)}$ can be used to show that,

$$\pi_2 - \mu_2 N_{2(0)} = A.$$

Therefore, $\pi_2 - \mu_2 N_2 \geq \left(\pi_2 - \mu_2 N_{2(0)}\right) e^{-\mu_2 t}$ and,

$$N_2 \leq \left(\frac{\pi_2 - \mu_2 N_{2(0)}}{\mu_2}\right) e^{-\mu_2 t}.$$

As $t \to \infty$, the population size, $N_2 \to \frac{\pi_2}{\mu_2}$. This implies that,

$$N_2(t) \leq \frac{\pi_2}{\mu_2}.$$

Also, if $N_{2(0)} \leq \frac{\pi_2}{\mu_2}$, then $N_2(t) \leq \frac{\pi_2}{\mu_2}$. So,

$$\Pi_2 = \left\{(S_2, I_2, R_2) \in \mathbb{R}^3_+ : S_2 + I_2 + R_2 \leq \frac{\pi_2}{\mu_2}\right\}.$$

The total camel population at any time (t) is given by,

$$N_1(t) = S_1(t) + I_1(t) + R_1(t),$$

and,

$$\frac{dN_1}{dt} = \frac{dS_1}{dt} + \frac{dI_1}{dt} + \frac{dR_1}{dt}.$$

We can rewrite the above equation as,

$$\frac{dN_1}{dt} = \pi_1 - \mu_1 N_1 - \delta_1 I_1.$$

Absence of mortality due to disease gives,

$$\frac{dN_1}{dt} \leq \pi_1 - \mu_1 N_1.$$

Solving the above differential equation gives $\pi_1 - \mu_1 N_1 \geq Ae^{-\mu_1 t}$, where A is constant.

Applying the initial condition yields

$$\pi_1 - \mu_1 N_1 \geq \left(\pi_1 - \mu_1 N_{1(0)}\right) e^{-\mu_1 t}. \tag{2.10}$$

Then,

$$N_1 \leq \left(\frac{\pi_1 - \mu_1 N_{1(0)}}{\mu_1}\right) e^{-\mu_1 t}.$$

As $t \to \infty$, the population size, $N_1 \to \frac{\pi_1}{\mu_1}$. This implies that, $N_1 \leq \frac{\pi_1}{\mu_1}$ and, $N_1(t) \leq \frac{\pi_1}{\mu_1}$ Also, if $N_{1(0)} \leq \frac{\pi_1}{\mu_1}$, then $N_1(t) \leq \frac{\pi_1}{\mu_1}$. So,

$$\Pi_1 = \left\{(S_1, I_1, R_1) \in \mathbb{R}^3_+ : S_1 + I_1 + R_1 \leq \frac{\pi_1}{\mu_1}\right\}. \tag{2.11}$$

The positively invariant region for the system of ordinary differential equations in 2.1 - 2.6 is given by,

$$\Pi = \Pi_1 \times \Pi_2 \subset= \mathbb{R}^3_+ \times \mathbb{R}^3_+, \tag{2.12}$$

where,

$$\Pi_1 = \left\{(S_1, I_1, R_1) \in \mathbb{R}^3_+ : S_1 + I_1 + R_1 \leq \frac{\pi_1}{\mu_1}\right\}, \tag{2.13}$$

$$\Pi_2 = \left\{(S_2, I_2, R_2) \in \mathbb{R}^3_+ : S_2 + I_2 + R_2 \leq \frac{\pi_2}{\mu_2}\right\}. \tag{2.14}$$

□

2.2.2 Disease-free equilibrium for the model

The disease-free equilibrium of the system yields

$$\xi_0 = (S_2^*, I_2^*, R_2^*, S_1^*, I_1^*, R_1^*).$$

At disease free equilibrium (DFE), there are no infected and recovered individuals in either species. So,

$$\left.\begin{array}{rcl} I_2^* &=& 0 \\ R_2^* &=& 0 \end{array}\right\} \quad \left.\begin{array}{rcl} I_1^* &=& 0 \\ R_1^* &=& 0 \end{array}\right\}.$$

The change in the human population is givin by:

$$\frac{dS_2}{dt} = \pi_2 - \epsilon\beta_3 S_2 I_1 - \beta_2 S_2 I_2 - \mu_2 S_2 = 0. \tag{2.15}$$

Therfore,

$$S_2^* = \frac{\pi_2}{\mu_2}.$$

Now considering the camels population:

$$\frac{dS_1}{dt} = \pi_1 - \beta_1 S_1 I_1 - \mu_1 S_1 = 0. \tag{2.16}$$

Thus,

$$S_1^* = \frac{\pi_1}{\mu_1}.$$

The disease-free equilibrium can be interpreted as,

$$\xi_0 = \left(\frac{\pi_2}{\mu_2}, 0, 0, \frac{\pi_1}{\mu_1}, 0, 0\right).$$

2.2.3 The Basic Reproductive Number

The next generation matrix is defined as, $K = FV^{-1}$ and $R_{12} = \rho\left(FV^{-1}\right)$,

where $\rho\left(FV^{-1}\right)$ represents the spectral radius of FV^{-1}.

The basic reproduction number R_{12} is known as the spectral radius of the next generation matrix.

Using the Next Generation Matrix, we consider only the infective classes in the system (2.1 - 2.6):

$$\frac{dI_1}{dt} = \beta_1 S_1 I_1 - (\mu_1 + \delta_1 + \gamma_1) I_1, \tag{2.17}$$

$$\frac{dI_2}{dt} = \epsilon\beta_3 S_2 I_1 + \beta_2 S_2 I_2 - (\mu_2 + \delta_2 + \gamma_2) I_2. \tag{2.18}$$

Thus,

$$f = \begin{bmatrix} \beta_1 S_1 I_1 \\ \epsilon\beta_3 S_2 I_1 + \beta_2 S_2 I_2 \end{bmatrix}, \; v = \begin{bmatrix} (\mu_1 + \delta_1 + \gamma_1) I_1 \\ (\mu_2 + \delta_2 + \gamma_2) I_2 \end{bmatrix},$$

where f is the number of potential new infections and v is the number of infections that leave the system either by death or by birth. The Jacobian matrix of f and v shall be obtained by F and V as observes:

$$F = \begin{bmatrix} \frac{\partial f_1}{\partial I_2} & \frac{\partial f_1}{\partial I_1} \\ \frac{\partial f_2}{\partial I_2} & \frac{\partial f_2}{\partial I_1} \end{bmatrix} = \begin{bmatrix} 0 & \beta_1 S_1 \\ \beta_2 S_2 & \epsilon\beta_3 S_2 \end{bmatrix}, \tag{2.19}$$

$$V = \begin{bmatrix} \frac{\partial v_1}{\partial I_2} & \frac{\partial v_1}{\partial I_1} \\ \frac{\partial v_2}{\partial I_2} & \frac{\partial v_2}{\partial I_1} \end{bmatrix} = \begin{bmatrix} 0 & \mu_1 + \delta_1 + \gamma_1 \\ \mu_2 + \delta_2 + \gamma_2 & 0 \end{bmatrix}. \tag{2.20}$$

By computing the product of FV^{-1},

$$FV^{-1} = \begin{bmatrix} 0 & \beta_1 S_1^* \\ \beta_2 S_2^* & \epsilon\beta_3 S_2^* \end{bmatrix} \begin{bmatrix} 0 & \frac{1}{\mu_2+\delta_2+\gamma_2} \\ \frac{1}{\mu_1+\delta_1+\gamma_1} & 0 \end{bmatrix},$$

$$FV^{-1} = \begin{bmatrix} \frac{\beta_1 S_1^*}{\mu_1+\delta_1+\gamma_1} & 0 \\ \frac{\epsilon\beta_3 S_2^*}{\mu_1+\delta_1+\gamma_1} & \frac{\beta_2 S_2^*}{\mu_2+\delta_2+\gamma_2} \end{bmatrix}. \tag{2.21}$$

Now, identify the dominant value of FV^{-1}. Let A be the eigenvalue of the matrix, such as

$$\begin{vmatrix} \frac{\beta_1 S_1^*}{\mu_1+\delta_1+\gamma_1} - A & 0 \\ \frac{\epsilon\beta_3 S_2^*}{\mu_1+\delta_1+\gamma_1} & \frac{\beta_2 S_2^*}{\mu_2+\delta_2+\gamma_2} - A \end{vmatrix} = 0. \tag{2.22}$$

Thus,

$$\left(\frac{\beta_1 S_1^*}{\mu_1+\delta_1+\gamma_1} - A\right)\left(\frac{\beta_2 S_2^*}{\mu_2+\delta_2+\gamma_2} - A\right) = 0. \tag{2.23}$$

Studies [1, 90] show that 75% of the cases were human-to-human transmission. Therefore, the largest eigenvalue is

$$A_1 = \frac{\beta_2 S_2^*}{\mu_2+\delta_2+\gamma_2}.$$

By substituting the above into the basic reproductive number R_{12}:

$$R_{12} = \frac{\beta_2 \pi_2}{\mu_2\left(\mu_2+\delta_2+\gamma_2\right)}.$$

Proposition 2.2.1. *The disease-free equilibrium (DFE) of model (2.1 - 2.6) is locally asymptotically stable if $R_{12} < 1$, and unstable if $R_{12} > 1$ [83].*

2.2.4 Global stability of the disease-free equilibrium

Theorem 2.2.2. *If $R_{12} \leq 1$, the disease-free equilibrium is globally asymptotically stable in the interior of* Π.

Proof. Considering the Lyapunov function below,

$$P(t) = (\mu_1 + \delta_1 + \gamma_1) I_2 + (\mu_2 + \delta_2 + \gamma_2) I_1. \tag{2.24}$$

By calculating the time derivative of$P$ along the system solutions (2.1-2.6), yields

$$\begin{aligned}
\frac{dP(t)}{dt} &= (\mu_1 + \delta_1 + \gamma_1) \frac{dI_2}{dt} + (\mu_2 + \delta_2 + \gamma_2) \frac{dI_1}{dt} = \\
&(\mu_1 + \delta_1 + \gamma_1) (\epsilon\beta_3 S_2 I_1 + \beta_2 S_2 I_2 - (\mu_2 + \delta_2 + \gamma_2) I_2) + \\
&(\mu_2 + \delta_2 + \gamma_2) (\beta_1 S_1 I_1 - (\mu_1 + \delta_1 + \gamma_1) I_1) \leq \\
&\leq \frac{\beta_1 I_1 \pi_1}{\mu_1} (\mu_2 + \delta_2 + \gamma_2) - (\mu_2 + \delta_2 + \gamma_2) (\mu_1 + \delta_1 + \gamma_1) I_1 + \\
&\frac{\epsilon\beta_3 I_1 \pi_2}{\mu_2} (\mu_1 + \delta_1 + \gamma_1) + \frac{\beta_2 I_2 \pi_2}{\mu_2} (\mu_1 + \delta_1 + \gamma_1) - \\
&(\mu_1 + \delta_1 + \gamma_1) (\mu_2 + \delta_2 + \gamma_2) I_2 \leq \\
&\leq -I_1 (\mu_1 + \delta_1 + \gamma_1) (\mu_2 + \delta_2 + \gamma_2) (1 - R_{12}) - \\
&I_2 (\mu_1 + \delta_1 + \gamma_1) (\mu_2 + \delta_2 + \gamma_2) (1 - R_{12}) = \\
&= - (I_1 + I_2) (\mu_1 + \delta_1 + \gamma_1) (\mu_2 + \delta_2 + \gamma_2) (1 - R_{12}).
\end{aligned} \tag{2.25}$$

Then, $\left(\frac{dP(t)}{dt}\right) \leq 0$, if and only if $R_{12} < 1$. Also, $\left(\frac{dP(t)}{dt}\right) = 0$, if and only if $I_1 + I_2 = 0$ or $R_{12} = 1$. Therefore, the largest compact invariant set in $S_2, I_2, I_1, \in \Pi; \left(\frac{dP(t)}{dt}\right) = 0$ if $R_{12} \leq 1$, is the singleton ξ_0. By LaSalle's invariant principle, ξ_0 is globally asymptotically stable in Π [140, 141]. □

2.2.5 Global stability of endemic equilibrium

The existence of the Endemic Disease Equilibrium (EDE) for two species population model exists when infected and recovered populations are not equal to zero:

$$\left.\begin{matrix} I_1^{**} \neq 0, \\ R_1^{**} \neq 0, \end{matrix}\right\} \qquad \left.\begin{matrix} I_2^{**} \neq 0, \\ R_2^{**} \neq 0, \end{matrix}\right\}.$$

Thus,

$$EDE = Eq_+ = (S_1^{**}, I_1^{**}, R_1^{**}, S_2^{**}, I_2^{**}, R_2^{**}).$$

Setting the system of ordinary differential equations (2.1 - 2.6) $= 0$ gives,

$$\begin{aligned} EDE =&(S_1^{**}, I_1^{**}, R_1^{**}, S_2^{**}, I_2^{**}, R_2^{**}) \\ =&(\frac{(\mu_1+\delta_1+\gamma_1)}{\beta_1}, \frac{\mu_1}{\beta_1}[R_{12}-1], \frac{\gamma_1}{\beta_1}[R_{12}-1], \\ &\frac{\pi_2(\mu_2+\delta_2+\gamma_2)[\varepsilon\gamma_2(R_{12}-1)+\mu_2]}{\mu_2}, \qquad (2.26) \\ &\frac{\pi_2\mu_2}{\beta_1[\mu_2+\delta_2+\gamma_2)[\varepsilon\gamma_1(R_{12}-1)+\mu_2]} - \frac{\varepsilon\mu_1}{\beta_1}[R_{12}-1] - \frac{\mu_2}{\beta_2}, \\ &\frac{\gamma_2}{\mu_2}[\frac{\pi_2\mu_2}{\beta_1(\mu_2+\delta_2+\gamma_2)[\varepsilon\gamma_1(R_{12}-1)+\mu_2]} - \frac{\varepsilon\mu_1}{\beta_1}[R_{12}-1] - \frac{\mu_2}{\beta_2}]). \qquad (2.27) \end{aligned}$$

Theorem 2.2.3. *The system of ordinary differential equations in (2.1-2.6) has an unique endemic equilibrium point if $R_{12} > 1$, and is globally asymptotically stable. The endemic equilibrium will only occur if and only if $R_{12} > 1$.*

Proof. Assume the function of Lyapunov is giving by,

$$L = S_2^{**}\left(\frac{S_2}{S_2^{**}} - \ln\frac{S_2}{S_2^{**}}\right) + I_2^{**}\left(\frac{I_2}{I_2^{**}} - \ln\frac{I_2}{I_2^{**}}\right) +$$

$$R_2^{**}\left(\frac{R_2}{R_2^{**}}-\ln\frac{R_2}{R_2^{**}}\right)+S_1^{**}\left(\frac{S_1}{S_1^{**}}-\ln\frac{S_1}{S_1^{**}}\right)+$$
$$I_1^{**}\left(\frac{I_1}{I_1^{**}}-\ln\frac{I_1}{I_1^{**}}\right)+R_1^{**}\left(\frac{R_1}{R_1^{**}}-\ln\frac{R_1}{R_1^{**}}\right).$$

When the above Lyapunov function is differentiated with respect to time; we obtain,

$$\begin{aligned}\frac{dL}{dt}=&\left(1-\frac{S_2^{**}}{S_2}\right)\frac{dS_2}{dt}+\left(1-\frac{I_2^{**}}{I_2}\right)\frac{dI_2}{dt}+\\&\left(1-\frac{R_2^{**}}{R_2}\right)\frac{dR_2}{dt}+\left(1-\frac{S_1^{**}}{S_1}\right)\frac{dS_1}{dt}+\\&\left(1-\frac{I_1^{**}}{I_1}\right)\frac{dI_1}{dt}+\left(1-\frac{R_1^{**}}{R_1}\right)\frac{dR_1}{dt}.\end{aligned}$$

$$\begin{aligned}\frac{dL}{dt}=&\left(1-\frac{S_2^{**}}{S_2}\right)\left(\pi_2-\epsilon\beta_3S_2I_1-\beta_2S_2I_2-\mu_2S_2-\pi_2+\epsilon\beta_3S_2^{**}I_1^{**}+\beta_2S_2^{**}I_2^{**}+\mu_2S_2^{**}\right)+\\&\left(1-\frac{I_2^{**}}{I_2}\right)\left(\epsilon\beta_3S_2I_1+\beta_2S_2I_2-f_2I_2\right)+\\&\left(1-\frac{R_2^{**}}{R_2}\right)\left(\gamma_2I_2-\mu_2R_2-\gamma_2I_2^{**}+\mu_2R_2^{**}\right)+\\&\left(1-\frac{S_1^{**}}{S_1}\right)\left(\pi_1-\beta_1S_1I_1-\mu_1S_1-\pi_1+\beta_1S_1^{**}I_1^{**}+\mu_1S_1^{**}\right)+\\&\left(1-\frac{I_1^{**}}{I_1}\right)\left(\beta_1S_1I_1-f_1I_1\right)+\\&\left(1-\frac{R_1^{**}}{R_1}\right)\left(\gamma_1I_1-\mu_1R_1-\gamma_1I_1^{**}+\mu_1R_1^{**}\right),\end{aligned}$$

where,

$$f_1=\left(\mu_1+\delta_1+\gamma_1\right),\ f_2=\left(\mu_2+\delta_2+\gamma_2\right).$$

Thus,

$$\begin{aligned}\frac{dL}{dt} =& \left(1-\frac{S_2^{**}}{S_2}\right)\left(-\epsilon\beta_3\left(S_2I_1-S_2^{**}I_1^{**}\right)+\beta_2\left(S_2^{**}I_2^{**}-S_2I_2\right)+\mu_2\left(S_2^{**}-S_2\right)\right)+\\ &\left(1-\frac{I_2^{**}}{I_2}\right)\left(\epsilon\beta_3S_2I_1+\beta_2S_2I_2-f_2I_2\right)+\\ &\left(1-\frac{R_2^{**}}{R_2}\right)\left(\gamma_2I_2-\mu_2R_2\right)+\\ &\left(1-\frac{S_1^{**}}{S_1}\right)\left(-\beta_1\left(S_1I_1-S_1^{**}I_1^{**}\right)+\mu_1\left(S_1^{**}-S_1\right)\right)+\\ &\left(1-\frac{I_1^{**}}{I_1}\right)\left(\beta_1S_1I_1\right)-\left(1-\frac{I_1^{**}}{I_1}\right)\left(f_1I_1\right)+\\ &\left(1-\frac{R_1^{**}}{R_1}\right)\left(\gamma_1I_1-\mu_1R_1\right).\end{aligned}$$

$$\begin{aligned}\frac{dL}{dt} =&\mu_1S_1^{**}\left(1-\frac{S_1^{**}}{S_1}\right)\left(1-\frac{S_1}{S_1^{**}}\right)+\\ &\beta_1\left(\left(1-\frac{S_1^{**}}{S_1}\right)\left(S_1^{**}I_1^{**}-S_1I_1\right)+S_1I_1\left(1-\frac{I_1^{**}}{I_1}\right)\right)+\\ &\mu_1R_1^{**}\left(1-\frac{R_1}{R_1^{**}}\right)+\gamma_1I_1\left(\left(1-\frac{R_1^{**}}{R_1}\right)-\frac{f_1}{\gamma_1}\left(1-\frac{I_1^{**}}{I_1}\right)\right)+\\ &\mu_2S_2^{**}\left(1-\frac{S_2^{**}}{S_2}\right)\left(1-\frac{S_2}{S_2^{**}}\right)+\\ &\epsilon\beta_3\left(\left(1-\frac{S_2^{**}}{S_2}\right)\left(S_2^{**}I_1^{**}-S_2I_1\right)+S_2I_1\left(1-\frac{I_2^{**}}{I_2}\right)\right)+\\ &\mu_2R_2\left(1-\frac{R_2^{**}}{R_2}\right)+\gamma_2I_2\left(\left(1-\frac{R_2^{**}}{R_2}\right)-\frac{f_2}{\gamma_2}\left(1-\frac{I_2^{**}}{I_2}\right)\right)+\\ &\beta_2\left(\left(1-\frac{S_2^{**}}{S_2}\right)\left(S_2^{**}I_2^{**}-S_2I_2+\right)+S_2I_2\left(1-\frac{I_2^{**}}{I_2}\right)\right).\end{aligned}$$

Then,

$$\frac{dL}{dt} =\mu_1S_1^{**}\left(1-\frac{S_1^{**}}{S_1}-\frac{S_1}{S_1^{**}}+1\right)+$$

$$\beta_1 S_1^{**} I_1^{**} \left(\left(1 - \frac{S_1^{**}}{S_1} \right) \left(1 - \frac{S_1}{S_1^{**}} \frac{I_1}{I_1^{**}} \right) + \frac{S_1}{S_1^{**}} \frac{I_1}{I_1^{**}} \left(1 - \frac{I_1^{**}}{I_1} \right) \right) +$$
$$\mu_1 R_1^{**} \left(1 - \frac{R_1}{R_1^{**}} \right) + \gamma_1 I_1^{**} \left(\frac{I_1}{I_1^{**}} \right) \left(\left(1 - \frac{R_1^{**}}{R_1} \right) - \frac{f_1}{\gamma_1} \left(1 - \frac{I_1^{**}}{I_1} \right) \right) +$$
$$\mu_2 S_2^{**} \left(1 - \frac{S_2^{**}}{S_2} - \frac{S_2}{S_2^{**}} + 1 \right) +$$
$$\epsilon \beta_3 \left(S_2^{**} I_1^{**} \right) \left(\left(1 - \frac{S_2^{**}}{S_2} \right) \left(1 - \frac{S_2}{S_2^{**}} \frac{I_1}{I_1^{**}} \right) + \frac{S_2}{S_2^{**}} \frac{I_1}{I_1^{**}} \left(1 - \frac{I_2^{**}}{I_2} \right) \right) +$$
$$\mu_2 R_2^{**} \left(1 - \frac{R_2}{R_2^{**}} \right) + \gamma_2 I_2^{**} \left(\frac{I_2}{I_2^{**}} \right) \left(\left(1 - \frac{R_2^{**}}{R_2} \right) + \frac{f_2}{\gamma_2} \left(\frac{I_2^{**}}{I_2} - 1 \right) \right) +$$
$$\beta_2 S_2^{**} I_2^{**} \left(\left(1 - \frac{S_2^{**}}{S_2} \right) \left(1 - \frac{S_2}{S_2^{**}} \frac{I_2}{I_2^{**}} \right) + \frac{S_2}{S_2^{**}} \frac{I_2}{I_2^{**}} \left(1 - \frac{I_2^{**}}{I_2} \right) \right).$$

$$\frac{dL}{dt} = \mu_1 S_1^{**} \left(1 - \frac{S_1^{**}}{S_1} - \frac{S_1}{S_1^{**}} + 1 \right) +$$
$$\beta_1 S_1^{**} I_1^{**} \left(\left(1 - \frac{S_1^{**}}{S_1} \right) \left(1 - \frac{S_1}{S_1^{**}} \frac{I_1}{I_1^{**}} \right) + \frac{S_1}{S_1^{**}} \frac{I_1}{I_1^{**}} \left(1 - \frac{I_1^{**}}{I_1} \right) \right) +$$
$$\mu_1 R_1^{**} \left(1 - \frac{R_1}{R_1^{**}} \right) + \gamma_1 I_1^{**} \left(\frac{I_1}{I_1^{**}} \right) \left(\left(1 - \frac{R_1^{**}}{R_1} \right) - \frac{f_1}{\gamma_1} \left(1 - \frac{I_1^{**}}{I_1} \right) \right) +$$
$$\mu_2 S_2^{**} \left(1 - \frac{S_2^{**}}{S_2} - \frac{S_2}{S_2^{**}} + 1 \right) +$$
$$\epsilon \beta_3 S_2^{**} I_1^{**} \left(\left(1 - \frac{S_2^{**}}{S_2} \right) \left(1 - \frac{S_2}{S_2^{**}} \frac{I_1}{I_1^{**}} \right) + \frac{S_2}{S_2^{**}} \frac{I_1}{I_1^{**}} \left(1 - \frac{I_2^{**}}{I_2} \right) \right) +$$
$$\mu_2 R_2^{**} \left(1 - \frac{R_2}{R_2^{**}} \right) + \gamma_2 I_2^{**} \left(\frac{I_2}{I_2^{**}} \right) \left(\left(1 - \frac{R_2^{**}}{R_2} \right) + \frac{f_2}{\gamma_2} \left(\frac{I_2^{**}}{I_2} - 1 \right) \right) +$$
$$\beta_2 S_2^{**} I_2^{**} \left(\left(1 - \frac{S_2^{**}}{S_2} \right) \left(1 - \frac{S_2}{S_2^{**}} \frac{I_2}{I_2^{**}} \right) \frac{S_2}{S_2^{**}} \frac{I_2}{I_2^{**}} \left(1 - \frac{I_2^{**}}{I_2} \right) \right).$$

$$\frac{dL}{dt} = \mu_1 S_1^{**} \left(2 - \frac{S_1^{**}}{S_1} - \frac{S_1}{S_1^{**}} \right) +$$
$$\beta_1 S_1^{**} I_1^{**} \left(1 - \frac{S_1^{**}}{S_1} + \frac{I_1}{I_1^{**}} - \frac{S_1}{S_1^{**}} \right) +$$

$$\mu_1 R_1^{**}\left(1-\frac{R_1}{R_1^{**}}\right)+\gamma_1 I_1^{**}\left(\frac{I_1}{I_1^{**}}-\frac{I_1}{I_1^{**}}\frac{R_1^{**}}{R_1}+\frac{f_1}{\gamma_1}-\frac{I_1}{I_1^{**}}\frac{f_1}{\gamma_1}\right)+$$
$$\mu_2 S_2^{**}\left(2-\frac{S_2^{**}}{S_2}-\frac{S_2}{S_2^{**}}\right)+$$
$$\epsilon\beta_3 S_2^{**} I_1^{**}\left(1-\frac{S_2^{**}}{S_2}+\frac{I_1}{I_1^{**}}-\frac{S_2}{S_2^{**}}\right)+$$
$$\mu_2 R_2^{**}\left(1-\frac{R_2}{R_2^{**}}\right)+\gamma_2 I_2^{**}\left(\frac{I_2}{I_2^{**}}-\frac{I_2}{I_2^{**}}\frac{R_2^{**}}{R_2}+\frac{f_2}{\gamma_2}-\frac{I_2}{I_2^{**}}\frac{f_2}{\gamma_2}\right)+$$
$$\beta_2 S_2^{**} I_2^{**}\left(1-\frac{S_2^{**}}{S_2}+\frac{I_2}{I_2^{**}}-\frac{S_2}{S_2^{**}}\right).$$

The arithmetic mean value exceeds the geometric mean [142]; as a result,

$$2-\frac{S_1^{**}}{S_1}-\frac{S_1}{S_1^{**}}\leq 0, \tag{2.28}$$
$$1-\frac{S_1^{**}}{S_1}+\frac{I_1}{I_1^{**}}-\frac{S_1}{S_1^{**}}\leq 0, \tag{2.29}$$
$$1-\frac{R_1}{R_1^{**}}\leq 0, \tag{2.30}$$
$$\frac{I_1}{I_1^{**}}\left(1-\frac{R_1^{**}}{R_1}-\frac{f_1}{\gamma_1}\right)+\frac{f_1}{\gamma_1}\leq 0, \tag{2.31}$$
$$2-\frac{S_2^{**}}{S_2}-\frac{S_2}{S_2^{**}}\leq 0, \tag{2.32}$$
$$1-\frac{S_2^{**}}{S_2}+\frac{I_1}{I_1^{**}}-\frac{S_2}{S_2^{**}}\leq 0, \tag{2.33}$$
$$1-\frac{R_2}{R_2^{**}}\leq 0, \tag{2.34}$$
$$\frac{I_2}{I_2^{**}}\left(1-\frac{R_2^{**}}{R_2}-\frac{f_2}{\gamma_2}\right)+\frac{f_2}{\gamma_2}\leq 0, \tag{2.35}$$
$$1-\frac{S_2^{**}}{S_2}+\frac{I_2}{I_2^{**}}-\frac{S_2}{S_2^{**}}\leq 0. \tag{2.36}$$

Based on the assumption that the parameters of the model are non-negative, it indicates that $\frac{dL}{dt}\leq 0$; if and only if the basic reproduction number of the system in equation (2.1 - 2.6)

is $R_{12} > 1$. As time t tends to infinity, according to LaSalle's Invariant Principle [143], all trajectorys of the model (2.1 - 2.6) approach the endemic equilibrium point if $R_{12} > 1$. □

2.2.6 Sensitivity Analysis

The goal of sensitivity analysis is to see how sensitive a model is to changes in parameter values. This is often done to aid in the identification of characteristics that have a significant influence on the basic reproduction number R_{12} with the statistical sensitivity measure partial rank correlation coefficient (PRCC), Latin hypercube sampling (LHS), initially introduced by McKay et al. [144], conducts a sensitivity analysis that investigates a specific parameter space of the model. In this epidemiological model, The quantity of the basic reproductive number influences the disease's or infection's opportunity to spread among the population. The decrease in disease-related infection was calculated by computing the sensitivity indices of the primary reproduction number R_{12} with regard to the parameter values in the model. The sensitivity indices serve as predictors of the importance of each parameter in diseases dynamics and prevalence. When such parameter is changed, they quantify the change in model variables. In this study, we will compute the sensitivity indices of R_{12} to parameter values for the model, which will be determined from accessible data or previously published articles in the literature, as shown in table 2.1. Taking into account the various parameters of the system of differential equations in the model (2.1 - 2.6), we can estimate the sensitivity of R_{12} to each of the parameters in the model. The sensitivity indices of the basic reproduction number of R_{12} with regard to each parameter of the system of differential equations in model (2.1 - 2.6) are shown in the table 2.2 below:

Parameter	Description	Sensitivity index(+ve/-ve)
π_1	camel's recruitment rate	+ve
π_2	human recruitment rate	+ve
μ_1	death rate of camel	-ve
μ_2	death rate of humans	-ve
δ_1	camel's death rate	-ve
δ_2	human death rate	-ve
β_1	the rate of the interaction between susceptible and infectious camel	+ve
β_2	the rate of the interaction between susceptible and infectious Human	+ve
β_3	the rate of the interaction between susceptible Human and infectious camel	+ve
γ_1	camel's recovery rate	-ve
γ_2	human rate of recovery	-ve

Table 2.1: Sensitivity indices of the parameters to R_{12}.

parameters List					
species 1	Baseline	References	species 2	Baseline	References
β_1	0.00025974	[90]	β_2	0.000034	[91]
			$\beta 3$	0.002304	Assumed
			ε	0.000576	Calculated
δ_1	0.00001	[90]	δ_2	0.0336	[91]
γ_1	1/14	[90]	γ_2	1/7	[91]
μ_1	$\frac{1}{(28.4)(365)}$	[90]	μ_2	$\frac{1}{(74.4)(365)}$	[91]

Table 2.2: Parameter values.

2.3 Stochastic Epidemic Models

The significance of host transmissibility of the Middle East respiratory syndrome virus (MERS-CoV) in disease emergence has been demonstrated in two species (camels and human) model. Infectious species are able to transmit the virus to a large number of susceptible class.

The chance of outbreaks, as well as disease impulsive mortality will increase with occurrence of spreaders within the populations. If a highly contagious disease happens quickly, there may be a biggest threat of transmitting communicable disease in the network. The greater numbers of initial large spreaders in the population, the earlier the outbreak is likely to occur.

2.3.1 Continuous Time Markov Chain

We numerically simulate the sample path to test the probability for an epidemic of MERS-CoV using the Continuous Time Markov Chain (CTMC) model by testing some properties such as (1) the number of deaths, (2) the time of an outbreak, (3) the time of peak infection, and

(4) the peak number of infected individuals.

The peak number of infected individuals indicates the maximum value of I_1 and I_2 and the peak time of infection corresponds to the time t at which this maximum occurs. Besides that, an outbreak implies that the cumulative number of I_1, and I_2 classes has nearly reached 50. In comparison, it is noted that for the $CTMC$ model, the criterion validity (for example, peak values, and time, also the number of deaths) is determined by the probability distribution and the trajectory of the sample generates one outcome of the distribution.

2.3.2 Markov chain model

If the number of hosts/pathogens is sufficiently small, an ODE model is not suitable. We use the $CTMC$ model which is continuous in time and discrete within the space. Table 2.3 summarizes the changes and the accompanying infinitesimal transition rates.

State transitions and rates for the CTMC					
species 1	Rate	transitions	species 2	Rate	transitions
infection	$\beta_1 S_1 I_1$	$S_1 \rightarrow S_1 - 1$ $I_1 \rightarrow I_1 + 1$	infection among species 2	$\beta_2 S_2 I_2$	$S_2 \rightarrow S_2 - 1$ $I_2 \rightarrow I_2 + 1$
			infection from species 1 to species 2	$\varepsilon\beta_3 S_2 I_1$	$S_2 \rightarrow S_2 - 1$ $I_2 \rightarrow I_2 + 1$
Recovery	$\gamma_1 I_1$	$I_1 \rightarrow I_1 - 1$ $R_1 \rightarrow R_1 + 1$	Recovery	$\gamma_2 I_2$	$I_2 \rightarrow I_2 - 1$ $R_2 \rightarrow R_2 + 1$
Birth	$\mu_1 N_1$	$S_1 \rightarrow S_1 + 1$	Birth	$\mu_2 N_2$	$S_2 \rightarrow S_2 + 1$
Death Susceptible	$\mu_1 S_1$	$S_1 \rightarrow S_1 - 1$	Death Susceptible	$\mu_2 S_2$	$S_2 \rightarrow S_2 - 1$
Death of Infected: Natural	$\mu_1 I_1$	$I_1 \rightarrow I_1 - 1$	Death of Infected: Natural	$\mu_2 I_2$	$I_2 \rightarrow I_2 - 1$
Death of Infected: by disease	$\delta_1 I_1$	$I_1 \rightarrow I_1 - 1$	Death of Infected: by disease	$\delta_2 I_2$	$I_2 \rightarrow I_2 - 1$
Death of Recoverd	$\mu_1 R_1$	$R_1 \rightarrow R_1 - 1$	Death of Recoverd	$\mu_2 R_2$	$R_2 \rightarrow R_2 - 1$

Table 2.3: State of transitions and rates in two species model.

2.3.3 Sample Paths

Example of pattern path as a result of stochastic model is given below. These sample trajectories are often closely matched with the population average response indicated by our ODE model. Nevertheless, the sample pathways of the CTMC model demonstrate the possible uncertainty in timing of the peak incidence of infection and the peak number of infections. Some sample paths are not presented since the infection is eradicated in those simulations. These simulations in (Fig. 2.2a and 2.2b) illustrate an epidemic for a total initial population of $N_1 = 1400$ and $N_2 = 2800$ with one initial infected individual ($I_1(0) = I_2(0) = 1$) and all individuals are susceptible.

2.3.4 Probability of Outbreak

Outbreak probability was measured by monitoring the numbers of individuals at infection classes for both species. The probability of an outbreak is determined by tracking the number of individuals in the I_1 and I_2 classes, and an outbreak is proclaimed when the total size of these compartments hits 50. Although 50 tends to be a significant extensive, it is reasonable considering that we are calculating the total number of individuals in all two species for a applicable size population of 4200. As predicted, the probability of an epidemic is related to the proportion of the populations that is initially infected, with the probabilities of an outbreak increasing as the number of initial affected individuals continues to grow.

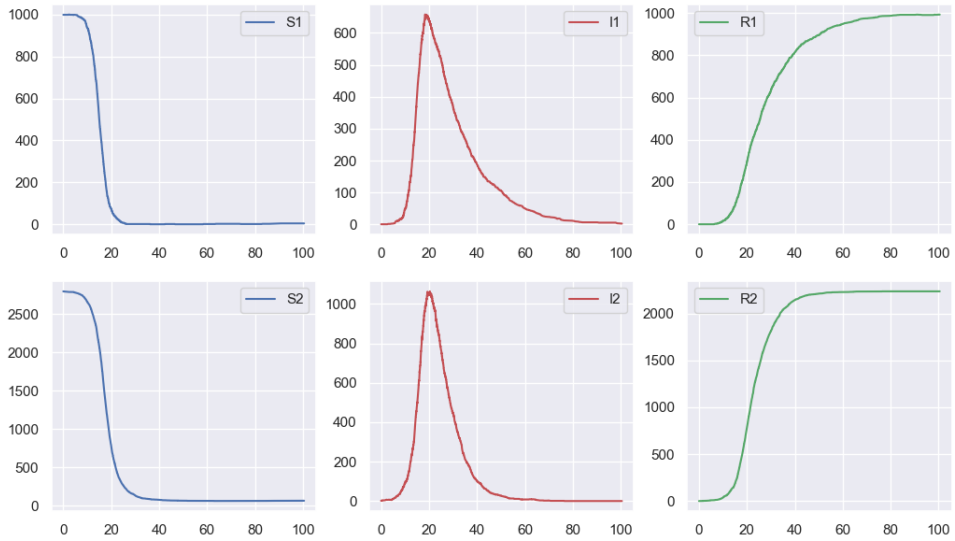

(a) Stochastic simulations of the model showing the sample paths.

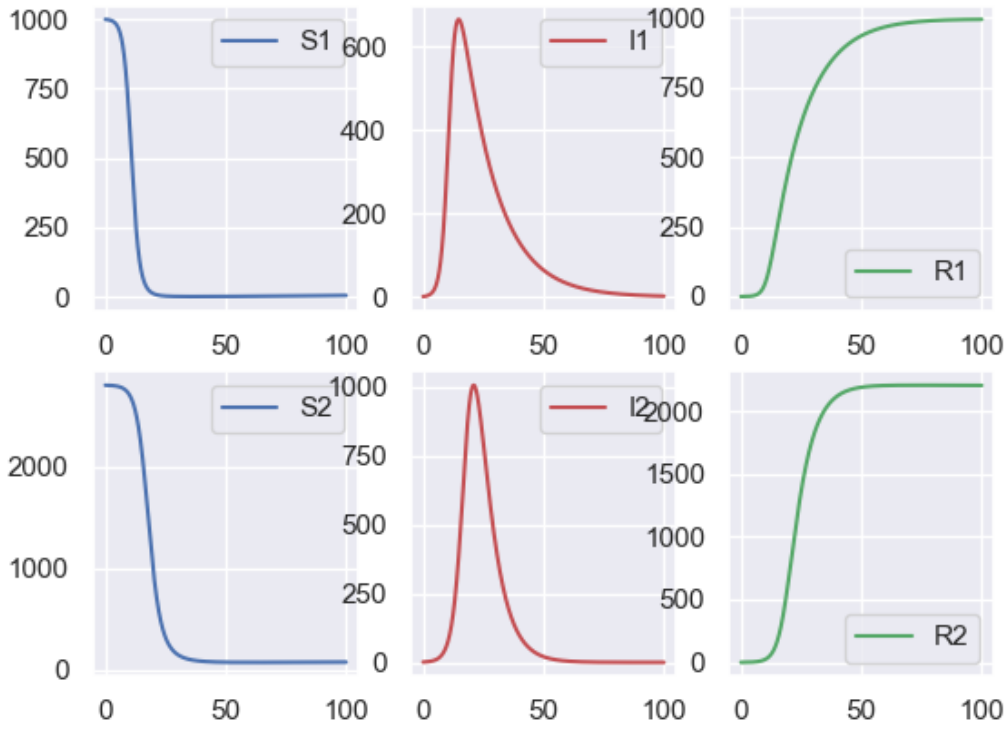

(b) Deterministic simulations of the model showing the sample path.

Figure 2.2: Stochastic and deterministic simulations of the model showing the sample path.

Fraction of population initially infected N_1	**Probability of outbreak**
0.0007	0.777
0.0014	0.961
0.0021	0.988
0.0028	0.998
0.0035	1.0
0.0042	1.0
0.005	1.0
0.0057	1.0
0.0064	1.0
0.0071	1.0
0.0078	1.0
0.0085	1.0
0.0092	1.0
0.01	1.0
0.0107	1.0
0.0114	1.0
0.0121	1.0
0.0128	1.0
0.0135	1.0

Table 2.4: Fraction of population initially infected N_1 with probability of outbreak

Fraction of Population Initially Infected N_2	**Probability of Outbreak**
0.0007	0.786
0.0014	0.961
0.0021	0.993
0.0028	0.998
0.0035	1.0
0.0042	1.0
0.005	1.0
0.0057	1.0
0.0064	1.0
0.0071	1.0
0.0078	1.0
0.0085	1.0
0.0092	1.0
0.01	1.0
0.0107	1.0
0.0114	1.0
0.0121	1.0
0.0128	1.0
0.0135	1.0

Table 2.5: Fraction of population initially infected N_2 with probability of outbreak.

2.3.5 Number of deaths

Apply stochastic version of MERS dynamics within a population of entity, we consequent required to examine whether or not the occurrence of individuals within the population

will be re-effected the severity of disease outbreak. We begin by examining the influence of susceptible camels and humans on the fatality rate that accumulate over a 150 day period following initial infection. The frequency rate of deaths has been increased as the size of susceptible class 25% , 50%, and 75% of the total populations see (Fig. 2.4 and 2.5). We observed a high frequency of outbreaks with reduce number of deaths whereas the small part of individuals at risk portion was reduced (not shown). For all subsequent simulations we start the population that comprised of 1400 susceptible camels and a 2800 susceptible human. Larger significantly, however; there has been a tenfold increase in the frequency of deaths projected even as the initial infected individuals as what have been shown in (Fig. 2.3a and 2.3b).

2.4 Time to outbreak

We observed that in a simulated MERS infection, the time to outbreak is decreased when the initial infected individual is minimized. These findings also show that as the proportion of susceptible increase time to outbreak rises. Each distribution in (Fig. 2.6a) is based on 10,000 sample pathways, whereas the time points in (Fig. 2.6b) are based on 1000 sample paths for each fraction initially infected.

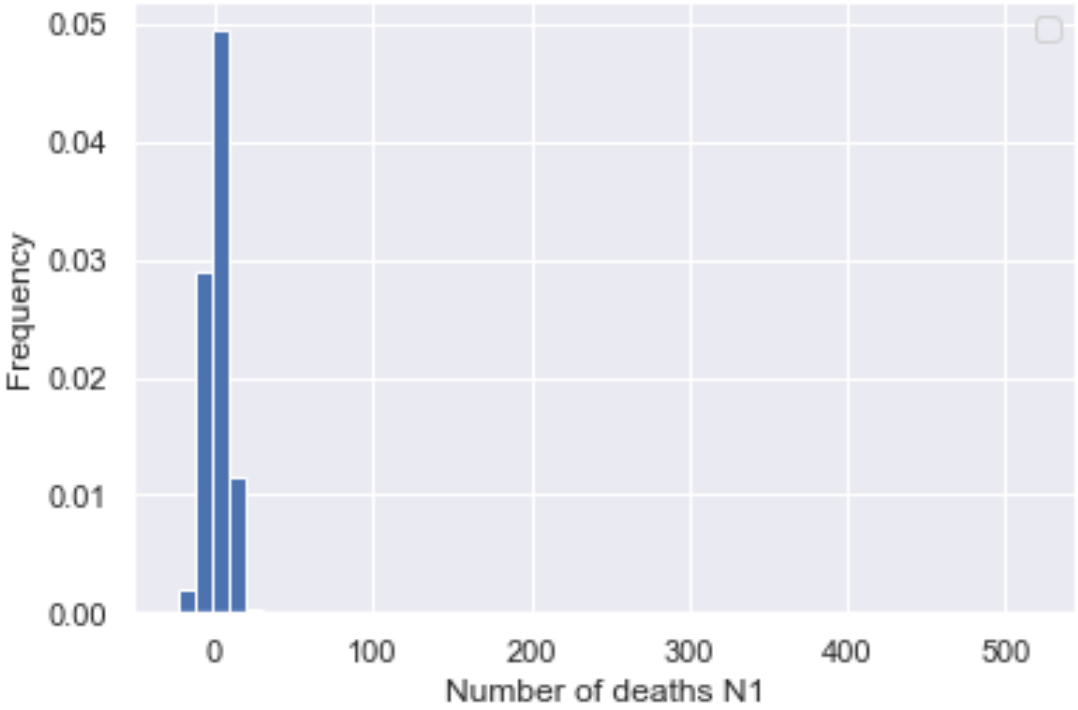

(a) Number of deaths N_1 vs frequency.

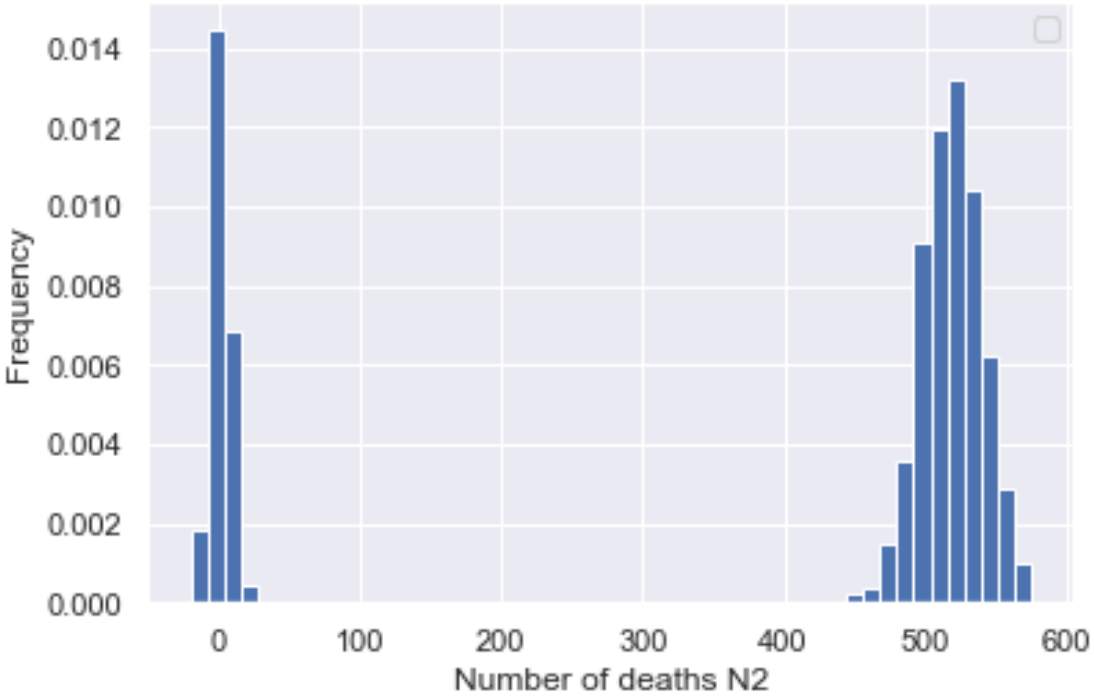

(b) Number of deaths N_2 vs frequency.

Figure 2.3: Number of deaths vs frequency.

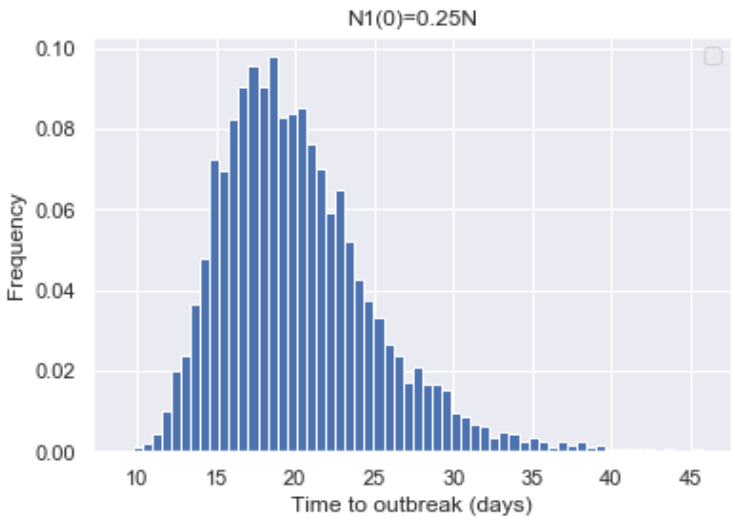

(a) Time to outbreak when $N_1 = 0.25N$, where $N = N_1 + N_2$

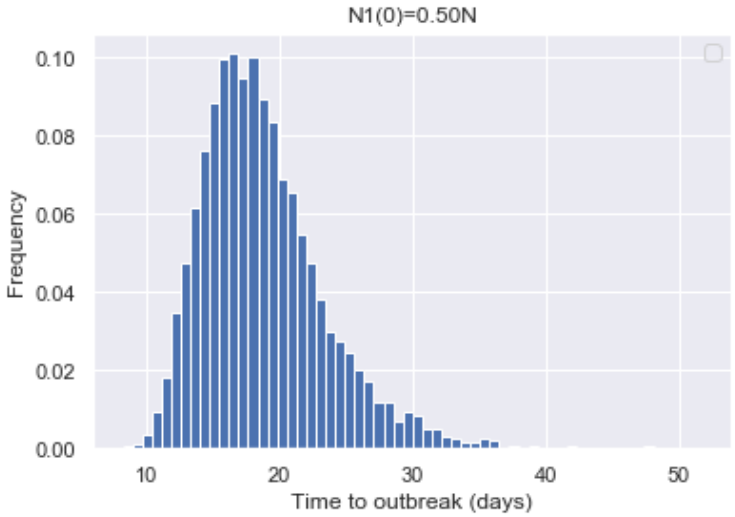

(b) Time to outbreak when $N_1 = 0.50N$, where $N = N_1 + N_2$

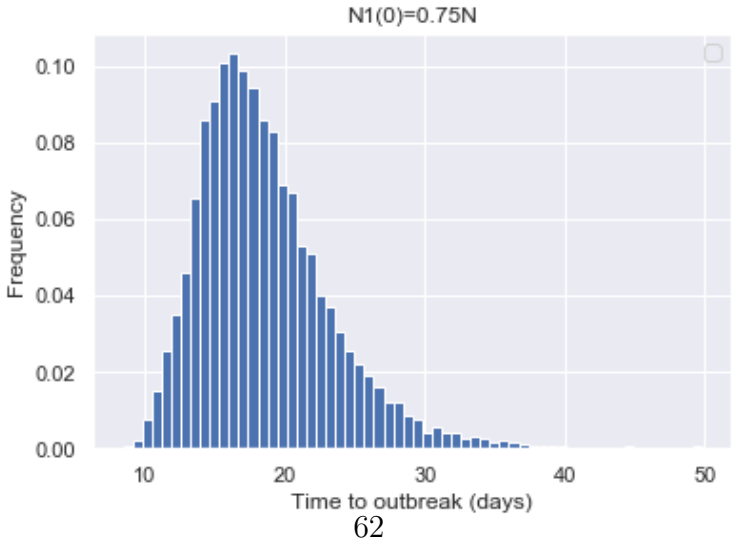

(c) Time to outbreak when $N_1 = 0.75N$, where $N = N_1 + N_2$

Figure 2.4: Time to outbreak for Camels population

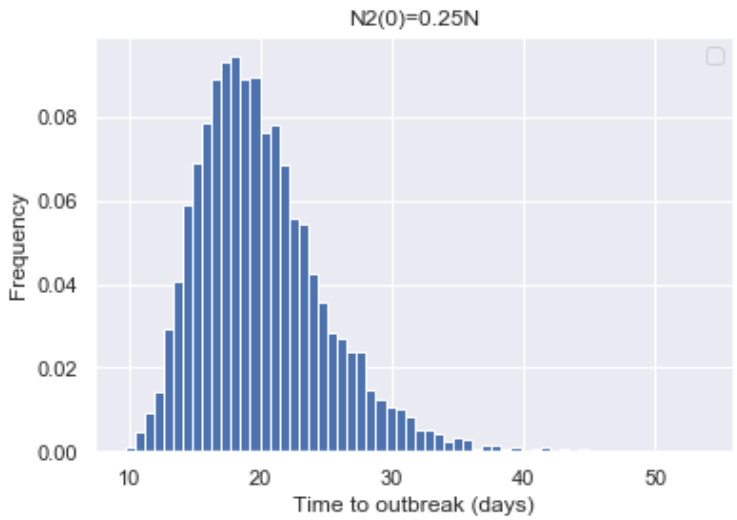

(a) Time to outbreak when $N_2 = 0.25N$, where $N = N_1 + N_2$

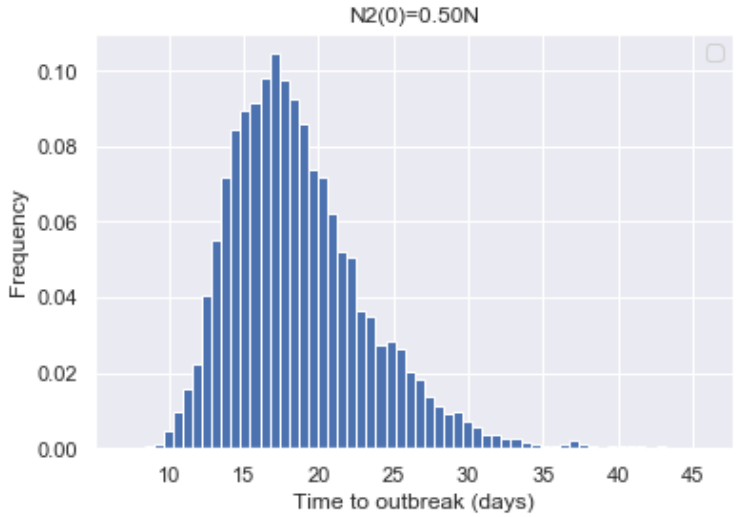

(b) Time to outbreak when $N_2 = 0.50N$, where $N = N_1 + N_2$

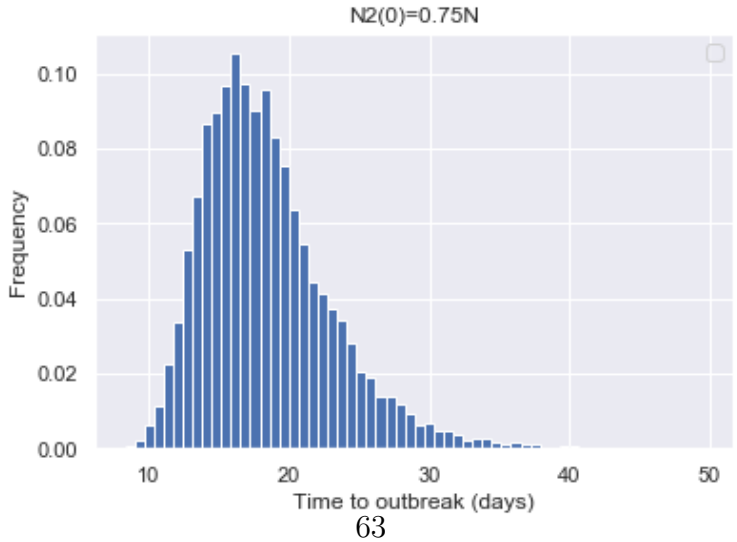

(c) Time to outbreak when $N_2 = 0.75N$, where $N = N_1 + N_2$

Figure 2.5: Time to outbreak for Human population

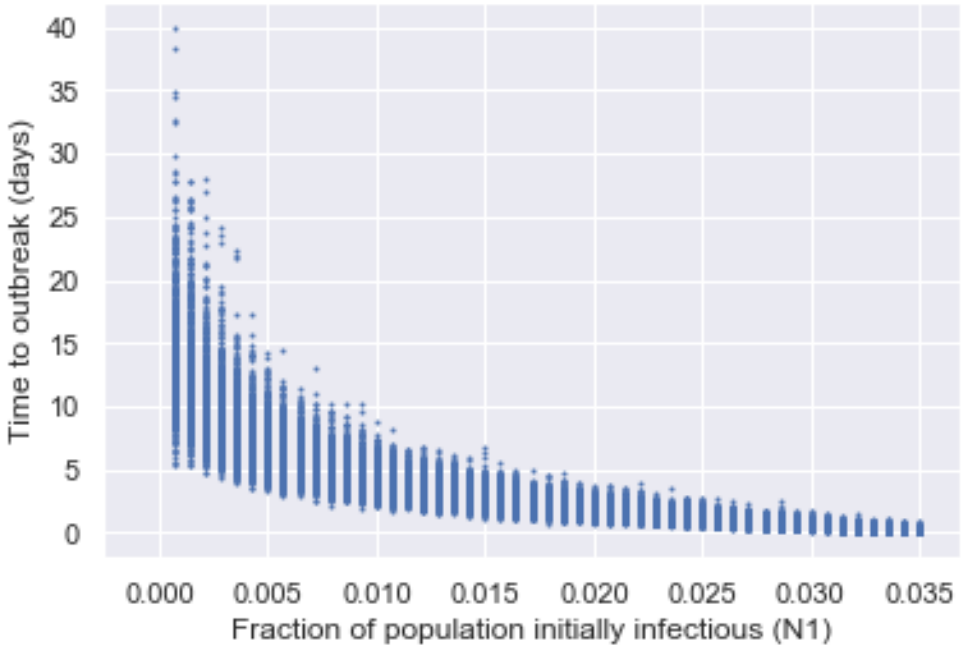

(a) Scatter plot for the time to outbreak with fraction of population initially infectious N_1.

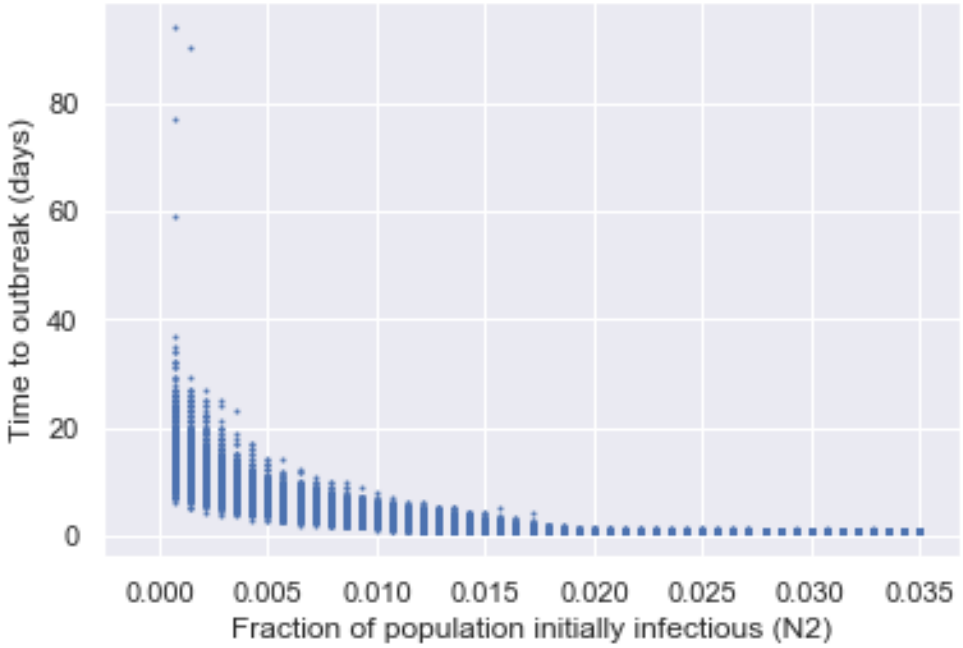

(b) Scatter plot for the time to outbreak with fraction of population initially infectious N_2.

Figure 2.6: Scatter plot for the time to outbreak with fraction of population initially infectious.

Chapter 3

Epidemic on Networks

3.1 Probabilistic Epidemic Model

Different network models of epidemics will be discussed in this chapter; for example, SI, SIS, and SIR. Looking at how these types of epizootic exist and propagate spreads on networks, and we will see what difference networks will make. When dealing with contagious diseases, we can write down certain equations by considering propagation within the populations, similar to agent based modelling.

The mathematical study of infectious diseases started at the beginning of the 20th century. The application of how epidemics spread on networks is still an active area of research. When dealing with networks, we investigate an adjacency matrix A that describes the network. Consider the networks to be undirected and matrix A to be symmetric, but in general, A is not necessarily symmetric. We have to split the population into different parts of infected and susceptible, and renormalize them to become fractions. The result of the simulation will be either susceptible, infected , which include the fractions of the population in (SI/SIS model); or susceptible, infected, and recovered which include fractions of the population in(SIR model). As we transition to a much more detailed model, we will introduce one

variable per node. Variables will carry an index i, which means its own node (node i); these will describe the node states. For the infected node, we will use x instead of i because i was used as an index. Furthermore, s and r represent those that are susceptible and recovered, respectively. The node could be in one of these three states. We purpose also using the same notations for infection and recovery rates (β and γ, respectively). When dealing with epidemics on networks, it is interesting when there is a connected component SI, SIS, or SIR. For example; two nodes s and x of a directed graph are connected if there is a trace from s to x and a trace from x to s. This relation called strongly connected components and weak components otherwise. If a network consists of connected components and there is an infected node in one of the components, the procedure of infected node is similar at any model ($SI/SIS/SIR$). In all real-world networks, there is always a gigantic connected component where most of the nodes are. Infection is assumed to be staged within the connected component [116].

Table 3.1: Some details of the probabilistic epidemic model.

Potential contacts (adjacency matrix $\mathbf{A}$) of network
probabilistic model (state of a node) $s_i(t)$ - probability of node i is susceptible at t . $x_i(t)$ - probability of node i is infected at t . $r_i(t)$ - probability of node i is recovered at t .
β - infection rate (geting infected by a contact in time δt)
γ - recovery rate (becomes recovered in a unit time δt)
from deterministic model to probabilistic description
connected graph means all nodes reachable

$$P_{inf} = s_i(t)\left(1 - \prod_{j\in\mathcal{N}(i)}(1-\beta x_j(t)\delta t)\right) \approx \beta s_i(t)\sum_{j\in\mathcal{N}(i)} x_j(t)\delta t \tag{3.1}$$

The equation implies that the probability of the central node becoming infected is proportional to the probability that it is not infected at this moment multiplied by the

probability that the infection comes from any other nodes. This linearization or simplification takes care of the fact that it can be infected from different nodes, and another process is the node of recovery. This process does not depend on the infection on the neighbouring nodes, but it is proportional to the recovery rate multiplied by the probability that the node is infected $x_i(t)$ and δt, because recovery rate or infection rate is in per unit time [145];

$$P_{rec} = \gamma x_i(t)\delta t. \tag{3.2}$$

Then, calculate the summation of the nearest neighbours. The sum of nearest neighbours can actually be replaced by the sum over all nodes in the graph. The adjacency matrix $\mathbf{A_{ij}}$ is zero everywhere except for the connections to the nearest node [146].

SI Model

At the beginning,we will start with SI model, and use the mathematical techniques for SIS and SIR models. s_i and x_i are probabilities and they sum up to 1, so

$$x_i(t) + s_i(t) = 1. \tag{3.3}$$

In the SI model, there is a one-way process (nodes can get infected). As a consequence, the probability that a node at time $t + \delta t$ is infected is equal to the probability of infection at the previous moment of time adding the probability that the node becomes infected from the neighbours. Thus,

$$x_i(t + \delta t) = x_i(t) + \beta s_i \sum_j A_{ij} x_j \delta t. \tag{3.4}$$

Similar to the non-network model, this equation can be immediately written as a differential equation. We simply take this expression, move $x_i(t)$ to the left-hand side, and divide the expression by dt to get our differential equation.

Together with the normalization equation $x_i + s_i = 1$, we have this simple system:

$$\frac{dx_i(t)}{dt} = \beta s_i(t) \sum_j A_{ij} x_j(t), \tag{3.5}$$

$$x_i(t) + s_i(t) = 1. \tag{3.6}$$

Accordingly, we express s_i as,

$$\frac{dx_i(t)}{dt} = \beta \left(1 - x_i(t)\right) \sum_j A_{ij} x_j. \tag{3.7}$$

We looked at this type of equation when we deal with the compartmental model or infections without network.

For every node, there is an equation, so we can find the solution of differential equations by using the solver for the systems of ODEs. We consider differential equations at early time and late time by considering what happens at the beginning of the evolution of the process and at the end of the process when the system stabilize and make certain approximations. Thus, the idea for early time approximation or when infection just started is that the probability for the nodes to be infected is much less than one. We have a few nodes infected, but for the majority of nodes, x_i is limited [146, 147],

$$\frac{dx_i(t)}{dt} = \beta \sum_j A_{ij} x_j. \tag{3.8}$$

This will result in a linear system that we can also express through the main matrix notation; such as,

$$\frac{d\mathbf{x}(t)}{dt} = \beta \mathbf{A}\mathbf{x}(t). \tag{3.9}$$

The generic way to solve the linear system is to look for the solution in terms of eigenvectors and eigenvalues of the matrix. The solution of the system $\mathbf{x}(\mathbf{t})$ will be a linear combination of basis vectors,

$$\mathbf{A}\mathbf{v}_k = \lambda_k \mathbf{v}_k, \tag{3.10}$$

$$\mathbf{x}(t) = \sum_k a_k(t)\mathbf{v}_k, \tag{3.11}$$

real eigenvalues and orthogonal eigenvectors will definitely form as a basis. ultimately, we substitute the expression for $\mathbf{x}$ into the equations. The results in an equation for time-dependent coefficients. Solve equation by separating variables to get the exponent. Using this traditional method, the initial condition is calculated as a dot product between eigenvectors and the original vector. The solution $\mathbf{x}$, which is a vector, is for every node. This is the linear combination over all eigenvectors of matrix $\mathbf{A}$. These eigenvectors are multiplied by this exponent and added together with the coefficients. Hence,

$$\sum_k \frac{da_k}{dt}\mathbf{v}_k = \beta \sum_k \mathbf{A}a_k(t)\mathbf{v}_k = \beta \sum_k a_k(t)\lambda_k \mathbf{v}_k, \tag{3.12}$$

$$\frac{da_k(t)}{dt} = \beta \lambda_k a_k(t), \tag{3.13}$$

$$a_k(t) = a_k(0)e^{\beta\lambda_k t}, \quad a_k(0) = \mathbf{v}_k^T \mathbf{x}(0), \tag{3.14}$$

$$\mathbf{x}(t) = \sum_k a_k(0)e^{\lambda_k \beta t}\mathbf{v}_k. \tag{3.15}$$

We now analyze at an early time by considering β; the infection rate, to be greater than

zero. The largest λ will be the dominating term when time goes to zero because we have a linear combination. We have different exponents and the fastest-growing exponent is the one that has the largest λ. Additionally, since we are only doing approximation, we will look at λ_1 which is the maximum λ. In consequence, λ_1 controls how fast the infection propagates. So, the growth rate of infection depends on λ_1. For this reason,

$$\mathbf{x}(t) = \mathbf{v}_1 e^{\lambda_1 \beta t} \qquad (t \to 0, \lambda_{max} = \lambda_1 > \lambda_k). \tag{3.16}$$

The rate of infection or the rate with which infection spreads depends on the β. This is the intensity of the probability of detection going from one node to another. The depends on the structure of the graph, λ_1 is an eigenvalue which encodes the structure of the network. That is how networks become involved. The larger λ, the faster growth of infections at the very beginning. The other narrative is at $\mathbf{x}(\mathbf{t})$, which is a vector, that depends strongly on the first eigenvector. If we have an undirected graph and we consider a random walk on the undirected graph, recall the values of the probability of a random walk being on a certain node. The node with the most connections will most likely become infected. If we consider flu propagation in a society, it is a socialite who will mostly get infected. The first eigenvector will be the largest element. The first eigenvector will correspond to the highest node degree [147]. We now look at the dynamics of infection at late times: $x \to \infty$,

$$\frac{dx_i(t)}{dt} = \beta \left(1 - x_i(t)\right) \sum_j A_{ij} x_j = 0, \tag{3.17}$$

$\mathbf{Ax} \neq 0$ since $\lambda_{min} \neq 0$, $1 - x_i(t) \approx 0$.

There are two solutions: either all $\mathbf{x}$ are equal to 1 or all $\mathbf{x}$'s are equal to zero. All $\mathbf{x}$'s being equal to zero means that there is no infection, where k denotes node degree of the node. Nodes with high degrees are getting infected faster rate with everything being equal.

SIS Model

The node in SIS model can be in susceptible mode, then be in infected mode, and then return to being in susceptible mode. The infection can actually persist for a long time. The change in infection in the probability of infection of the node comes either from the node becoming infected from the neighbour or from node recovery. For instance, if

$$\frac{dx_i(t)}{dt} = \beta s_i(t) \sum_j A_{ij} x_j(t) - \gamma x_i, \tag{3.18}$$

and,

$$x_i(t) + s_i(t) = 1, \tag{3.19}$$

the differential equation for the SIS model can be re-expressed as

$$\frac{dx_i(t)}{dt} = \beta \left(1 - x_i(t)\right) \sum_j A_{ij} x_j - \gamma x_i. \tag{3.20}$$

We consider the early time approximation: $x_i(t) \ll 1$. Using the same time of the same type of approximation, we look at times going to 0, where infection rate is low, and linearize the differential equation. δ_{ij} is a Kronecker symbol, where $\delta_{ij} x_j = x_i$, and rewrite the matrix form $\mathbf{A}$ δ_{ij} inside the summation . The Kronecker δ_{ij} is a diagonal matrix. Essentially, when

$$\frac{dx_i(t)}{dt} = \beta \sum_j A_{ij} x_j - \gamma x_i, \tag{3.21}$$

$$\frac{dx_i(t)}{dt} = \beta \sum_j \left(A_{ij} - \frac{\gamma}{\beta} \delta_{ij} \right) x_j, \tag{3.22}$$

$$\frac{d\mathbf{x}(t)}{dt} = \beta \left(\mathbf{A} - \left(\frac{\gamma}{\beta} \right) \mathbf{I} \right) \mathbf{x}(t), \tag{3.23}$$

and,

$$\frac{d\mathbf{x}(t)}{dt} = \beta \mathbf{M}\mathbf{x}(t), \quad \mathbf{M} = \mathbf{A} - \left(\frac{\gamma}{\beta}\right)\mathbf{I}. \tag{3.24}$$

Then, take the matrix $\mathbf{M}$, and determine the eigenvectors and eigenvalues. Since matrix $\mathbf{M}$ and matrix $\mathbf{A}$ differ on the diagonals, they will have the same eigenvectors the same as $\mathbf{A}$, but the eigenvalues will be shifted. Note that for matrices $\mathbf{A}$ and $\mathbf{M}$, we took the same matrix and we modified the diagonal and changed the diagonal by subtracting $\frac{\gamma}{\beta}$. Thus,

$$\mathbf{M}\mathbf{v}'_k = \lambda'_k \mathbf{v}'_k, \quad \mathbf{M} = \mathbf{A} - \left(\frac{\gamma}{\beta}\right)\mathbf{I}, \quad \mathbf{A}\mathbf{v}_k = \lambda_k \mathbf{v}_k, \tag{3.25}$$

and,

$$\mathbf{v}'_k = \mathbf{v}_k, \quad \lambda'_k = \lambda_k - \frac{\gamma}{\beta}, \tag{3.26}$$

we end up with a getting linear combination. Therefore,

$$\mathbf{x}(t) = \sum_k a_k(t)\mathbf{v}'_k = \sum_k a_k(0)\mathbf{v}'_k e^{\lambda'_k \beta t} = \sum_k a_k(0)\mathbf{v}_k e^{(\beta\lambda_k - \gamma)t}. \tag{3.27}$$

Previously, the exponent was $\beta\lambda t$, however, now the exponent is $(\beta\lambda - \gamma)t$. Depending on the values β, λ, and γ, the difference can be either greater than zero or less than zero. If the difference is greater than zero, then the solution will grow with time, otherwise, the solution will decrease, when the difference is less than zero. The critical point is when $\beta\lambda_1 = \gamma$. λ_1 is the largest eigenvector and has the largest contribution to the solution. If $\beta\lambda_1 > \gamma$, we will have growth, but if $\beta\lambda_1 < \gamma$, we have decay.

For $\lambda_1 \geq \lambda_k$, it is critical when $\beta\lambda_1 = \gamma$.Thus,

$$\text{if} \quad \beta\lambda_1 > \gamma, \quad \mathbf{x}(t) \to \mathbf{v}_1 e^{(\beta\lambda_1 - \gamma)t} \quad (growth). \tag{3.28}$$

and,

$$\text{if} \quad \beta\lambda_1 < \gamma, \quad \mathbf{x}(t) \to 0 \qquad (decay). \tag{3.29}$$

We consider the epidemic threshold $R_0 = \frac{\beta}{\gamma}$. If $\frac{\beta}{\gamma} < R_0$, infection dies over time, but if $\frac{\beta}{\gamma} > R_0$, infection survives and becomes epidemic. For the SIS model, the epidemic threshold is $\frac{1}{\lambda_1}$. Furthermore, $\mathbf{A}\mathbf{v}_1 = \lambda_1\mathbf{v}_1$. Now $\frac{\beta}{\gamma}$ is comparing to $\frac{1}{\lambda_1}$, where λ_1 encodes the structure of the graph. Taking a graph and calculate the eigenvalues and eigenvectors (λ_1, the largest eigenvalue) will control the propagation of infection in this model. If λ_1 is large, the barrier is very small, meaning that the epidemic threshold is small if λ_1 is large.

When we have an infection on a graph, and consider long time approximation; time goes to infinity and x_i becomes constant.

If we take the derivative $\frac{dx_i(t)}{dt}$:

$$\frac{dx_i(t)}{dt} = \beta\,(1 - x_i)\sum_j A_{ij}x_j - \gamma x_i = 0. \tag{3.30}$$

The solution is as follows,

$$x_i = \frac{\sum_j A_{ij}x_j}{\frac{\gamma}{\beta} + \sum_j A_{ij}x_j}. \tag{3.31}$$

Note that with ratios $\beta \gg \gamma$, x_i goes to 1, and if does not, β is in magnitude of γ. Furthermore, x_i becomes approximately as the first eigenvector.

In general, the epidemic threshold ($\beta/\gamma > R_0$): if $\beta \gg \gamma$, $x_i(t) \to 1$. If $\beta \sim \gamma$, $x_i\frac{\gamma}{\beta} = \sum_j A_{ij}x_j$, then $\lambda_1 = \frac{\gamma}{\beta}$, and $\quad x_i(t) \to (v_1)_i$.

SIR Model

The SIR model is differs only by the addition of the r_i component. We have three possible states: the node can be susceptible, infected, or recovered (removed), this means that it can no longer be infected. Assume,

$$x_i(t) + s_i(t) + r_i(t) = 1. \tag{3.32}$$

Then, the infection equations are given by,

$$\frac{dx_i}{dt} = \beta s_i \sum_j A_{ij} x_j - \gamma x_i, \tag{3.33}$$

and,

$$\frac{dr_i}{dt} = \gamma x_i. \tag{3.34}$$

As,

$$x_i(t) + s_i(t) + r_i(t) = 1, \tag{3.35}$$

we can be implemented,

$$\frac{dx_i(t)}{dt} = \beta \left(1 - r_i - x_i\right) \sum_j A_{ij} x_j - \gamma x_i. \tag{3.36}$$

When time goes to zero or at the very beginning of infection, very few nodes get infected and less nodes get recovered. As a result,

$$\frac{dx_i(t)}{dt} = \beta \left(1 - x_i\right) \sum_j A_{ij} x_j - \gamma x_i. \tag{3.37}$$

We have the same equation as we used for the SIS model; this means that we have the equivalent with the exponent. And as with SIS model, we also have the critical exponent where $\beta\lambda_1$ is equal to γ. Solutions can either be growing with time or decreasing, as we can observe in the following,

$$\mathbf{x}(t) \sim \mathbf{v}_1 e^{(\beta\lambda_1 - \gamma)t}. \tag{3.38}$$

Looking at the solutions, infections will happen per node, and the rates of infection and recovery depend on the node degree. We consider the probability that a node becomes infected, the probability that a node recovers, and the probability that a node is susceptible as a function of time. Nodes with higher degrees have higher probabilities and faster rates of infection. Infections propagate quickly for the nodes with high degrees depending on the ratio β. There may be a situation with a certain number of infected nodes and with time, everybody (or the majority of the population) becomes infected. The reason to look at the very beginning of an infection is twofold. First, this informs us whether progression will explode or die out. Second, we can look at the differential equations which give the probabilities per node as a function of time. However, to observe the process or changes, every node can be either in state S or in state I, and initialize a certain number of nodes to the state infected I. We consider a graph and take a few nodes to be initially infected. Now, at every time step, the infected node has a nonzero probability to infect its neighbours. The node stays infected for a certain period of time. Again, we go through several steps in time when the node stays infected and can infect its neighbouring nodes. It is an exponential distribution for time of infection. We can calculate the average for node infection, which is $\frac{1}{\gamma}$. The node stays infected for several time steps. For every time step, it can infect its neighbours with some probability. Assume that on one step each week, the node infected these other nodes but it recovered itself. Then, the node recovered and this state is now infected. With the SIS model, the node can be reinfected easily because there is no immunity. The two parameters that control the dynamics of infection are β and γ (or $\frac{\beta}{\gamma}$). Depending on the ratio of β to γ, the infection can quickly disappear or the infection can persist through the system for a long time [116].

To perform the SIR model, add the R state, which denotes the nodes that have been recovered or removed. For each time step, the node has a probability β to infect the neighbor,

Table 3.2: Some details of the SIS simulation.

1. The node is in the state S, or I at time t.
2. The node remain infected by $\tau_\gamma = \int_0^\infty \tau e^{-\tau\gamma} d\tau = 1/\gamma$ at each time steps
3. Each node I has a probability β to infect its nearest neighbors, $S \to I$ on each time step.
4. After certain time steps τ_γ , the node recovers: $I \to S$

then it stays infected for a while. After that, it recovers and goes to the state R; it cannot be infected anymore.

Table 3.3: Some details of the SIR simulation.

1. The node is in the state S, I, R at time t.
3. The node remain infected by $\tau_\gamma = 1/\gamma$ at each time steps
4. Each node I has a probability β to infect to infect its nearest neighbors, $S \to I$ on each time step.
5. After time steps τ_γ , the node recovers: $I \to R$
6. Nodes R do not participate in further infection propagation.

In the SIR model, the important parameters include the time when the node is infectious and the time when a recovered node stays recovered forever. When the infection dies out, there will be some nodes that were never infected. Thus, we can calculate how the fraction of recovered nodes changes over time. For every time step, the system must make a decision of whether or not to infect the neighbouring node.

Let us consider one interesting observation for the SIR model. If we are only interested in the final distribution of the infection, meaning we are interested in a late time or when the infection is already done, we want to know which nodes eventually get infected. The node can infect either node x or node v; the edge activates and propagates the infection. In the next moment of time, the two edges are activated, and at the final moment, notice that the nodes are infected; these are the activated edges. Only the nodes are on the connected

component through the activated edges with the originally infected nodes that will become infected. In summary, we flip the coin each time to go through the activation process. The idea is to flip all of the coins for every edge upfront, so as not to wait through iterations. At the very beginning, for every edge we will decide if it will get activated or not. We can look and see if there is an infected node in the path of active edges. If so, then all nodes in that connected component will eventually become infected. Instead of tracing every time step, we determine which edge will transmit the infection. We looked at the gigantic connected components and the connectivity in that random graph. In an Erdo's-Renyi graph, there are nodes and there is a probability that nodes are connected. A graph structure and the probability that the particular edge will actually be active. Thus, in this case, we will also get this gigantic connected component. In general case, different graphs have different thresholds depending on the graph structure. Keeling et al. (2005) tried applying epidemic models on different graph structures and looking for random graphs as lattice, a regular graph, and a small-world model [148]. There is a spatial graph where just put nodes on 2D space and connect the nearest nodes; and there is a traditional scale-free graph like the Barab'asi-Albert power-law graph. Keeling looked at how infection spreads on the graphs where the larger the diameter, the longer it takes to reach the edge of the graph. There will be a connection between the structure, which is the diameter or λ. For the infection to propagate successfully, if a node has a high degree, it is more likely to become infected. For example, this may occur if we get a set of nodes and there is one edge that connects [127, 129].

Now we can set up the probabilistic epidemic model for two species:

$$\frac{dS_{1i}}{dt} = \pi_1 - \beta_1 S_{1i} \sum_j A_{ij} I_{1j}(t) - \mu_1 S_{1i}, \tag{3.39a}$$

$$\frac{dI_{1i}}{dt} = \beta_1 S_{1i} \sum_j A_{ij} I_{1j}(t) - (\mu_1 + \delta_1 + \gamma_1) I_{1i}, \tag{3.39b}$$

$$\frac{dR_{1i}}{dt} = \gamma_1 I_{1i} - \mu_1 R_{1i}, \tag{3.39c}$$

$$\frac{dS_{2i}}{dt} = \pi_2 - \varepsilon\beta_3 S_{2i} \sum_j A_{ij} I_{1j}(t) - \beta_2 S_{2i} \sum_j A_{ij} I_{2j}(t) - \mu_2 S_{2i}, \tag{3.39d}$$

$$\frac{dI_{2i}}{dt} = \varepsilon\beta_3 S_{2i} \sum_j A_{ij} I_{1j}(t) + \beta_2 S_{2i} \sum_j A_{ij} I_{2j}(t) - (\mu_2 + \delta_2 + \gamma_2) I_{2i}, \tag{3.39e}$$

$$\frac{dR_{2i}}{dt} = \gamma_2 I_{2i} - \mu_2 R_{2i}. \tag{3.39f}$$

3.1.1 Parameters

π_1, π_2: recruitment rate of camel and human respectively.

β_1 : contact rate of camel.

β_2 : contact rate of human.

μ_1, μ_2: natural death of camel and human respectively.

δ_1, δ_2: disease death rate.

$\frac{1}{\gamma_1}$: the mean infectious period of infected camel for survivors.

$\frac{1}{\gamma_2}$: the mean duration for infected human for surivors.

ε : is generally small and measures the trickle of infection from the camel population into the human one.

$$A = \begin{bmatrix} 0 & 1 & 1 & 1 & 1 & 1 & 0 & 1 & 1 & 0 & 1 & 0 & 0 \\ 1 & 0 & 1 & 0 & 0 & 1 & 0 & 0 & 0 & 1 & 0 & 1 & 0 \\ 1 & 1 & 0 & 1 & 0 & 0 & 1 & 1 & 0 & 0 & 0 & 0 & 0 \\ 1 & 0 & 1 & 0 & 0 & 0 & 0 & 1 & 0 & 0 & 0 & 0 & 0 \\ 1 & 0 & 0 & 0 & 0 & 0 & 0 & 0 & 1 & 0 & 1 & 0 & 0 \\ 1 & 1 & 0 & 0 & 0 & 0 & 0 & 0 & 0 & 1 & 1 & 1 & 0 \\ 0 & 0 & 1 & 0 & 0 & 0 & 0 & 1 & 0 & 0 & 0 & 0 & 1 \\ 1 & 0 & 1 & 1 & 0 & 0 & 1 & 0 & 1 & 0 & 0 & 0 & 1 \\ 1 & 0 & 0 & 0 & 1 & 0 & 0 & 1 & 0 & 0 & 0 & 0 & 1 \\ 0 & 1 & 0 & 0 & 0 & 1 & 0 & 0 & 0 & 0 & 0 & 0 & 0 \\ 1 & 0 & 0 & 0 & 1 & 1 & 0 & 0 & 0 & 0 & 0 & 0 & 0 \\ 1 & 0 & 0 & 0 & 0 & 1 & 0 & 0 & 0 & 0 & 0 & 0 & 0 \\ 0 & 0 & 0 & 0 & 0 & 0 & 1 & 1 & 1 & 0 & 0 & 0 & 0 \end{bmatrix}$$

A is adjacency matrix of potential contacts in the probabilistic model.

$S_i(t)$: probability that at t node i is susceptible.

$I_i(t)$: probability that at t node i is infected.

$R_i(t)$: probability that at t node i is recovered.

β : infection rate (probably to get infected on a contact per unit time δt).

γ : recovery rate (probability to recover per unit time δt).

(Fig. 3.1) shows the simulations of the probabilistic model demonstrate the probability for all nodes (camel populations) by using the same parameter values in the previous chapter 2.2.

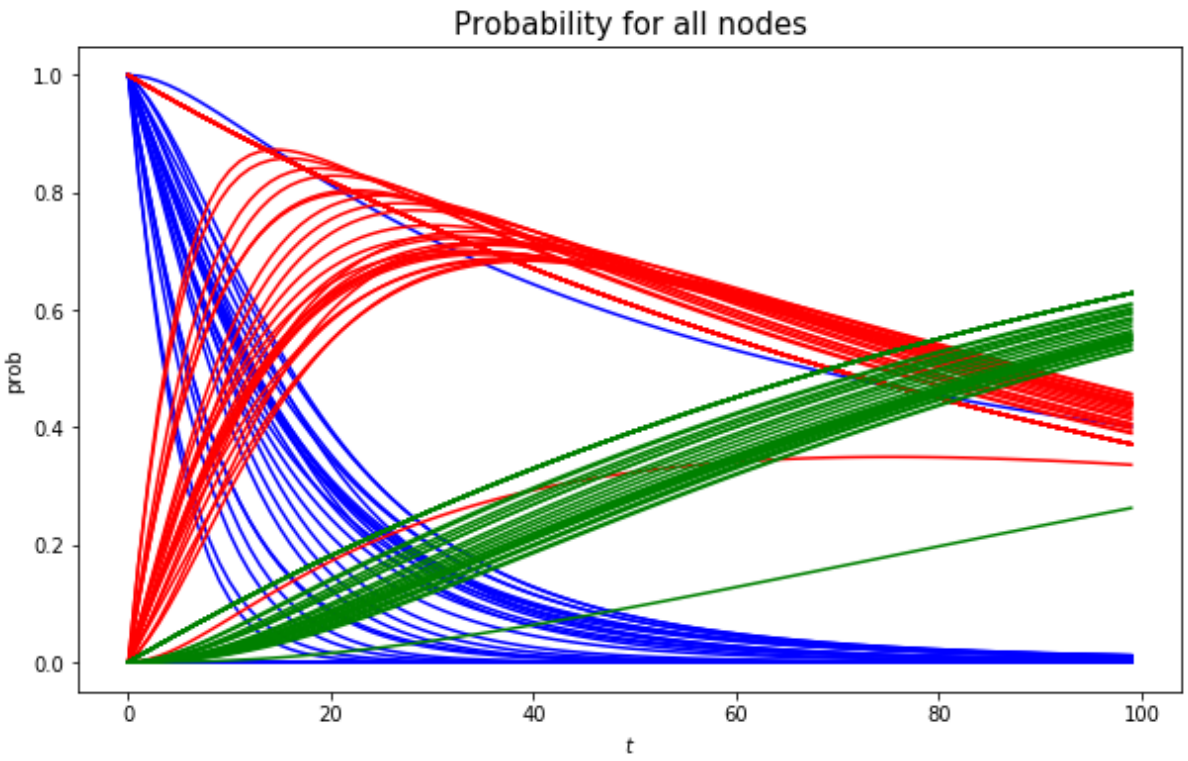

Figure 3.1: Simulations of the probabilistic model showing the probability for all nodes (camel populations); blue (susceptible), red (infected) and green (recovered).

3.2 Pairwise Approximation

We used the pairwise approximation model that has been studied by Keeling 2005 [116].

$$\frac{d[S_1]}{dt} = -\tau_1[S_1 I_1], \tag{3.40a}$$

$$\frac{d[I_1]}{dt} = \tau_1[S_1 I_1] - \sigma_1[I_1], \tag{3.40b}$$

$$\frac{d[R_1]}{dt} = \sigma_1[I_1], \tag{3.40c}$$

$$\frac{d[S_1 S_1]}{dt} = -2\tau_1[S_1 S_1 I_1], \tag{3.40d}$$

$$\frac{d[S_1 I_1]}{dt} = \tau_1([S_1 S_1 I_1] - [I_1 S_1 I_1] - [S_1 I_1]) - \sigma_1[S_1 I_1], \tag{3.40e}$$

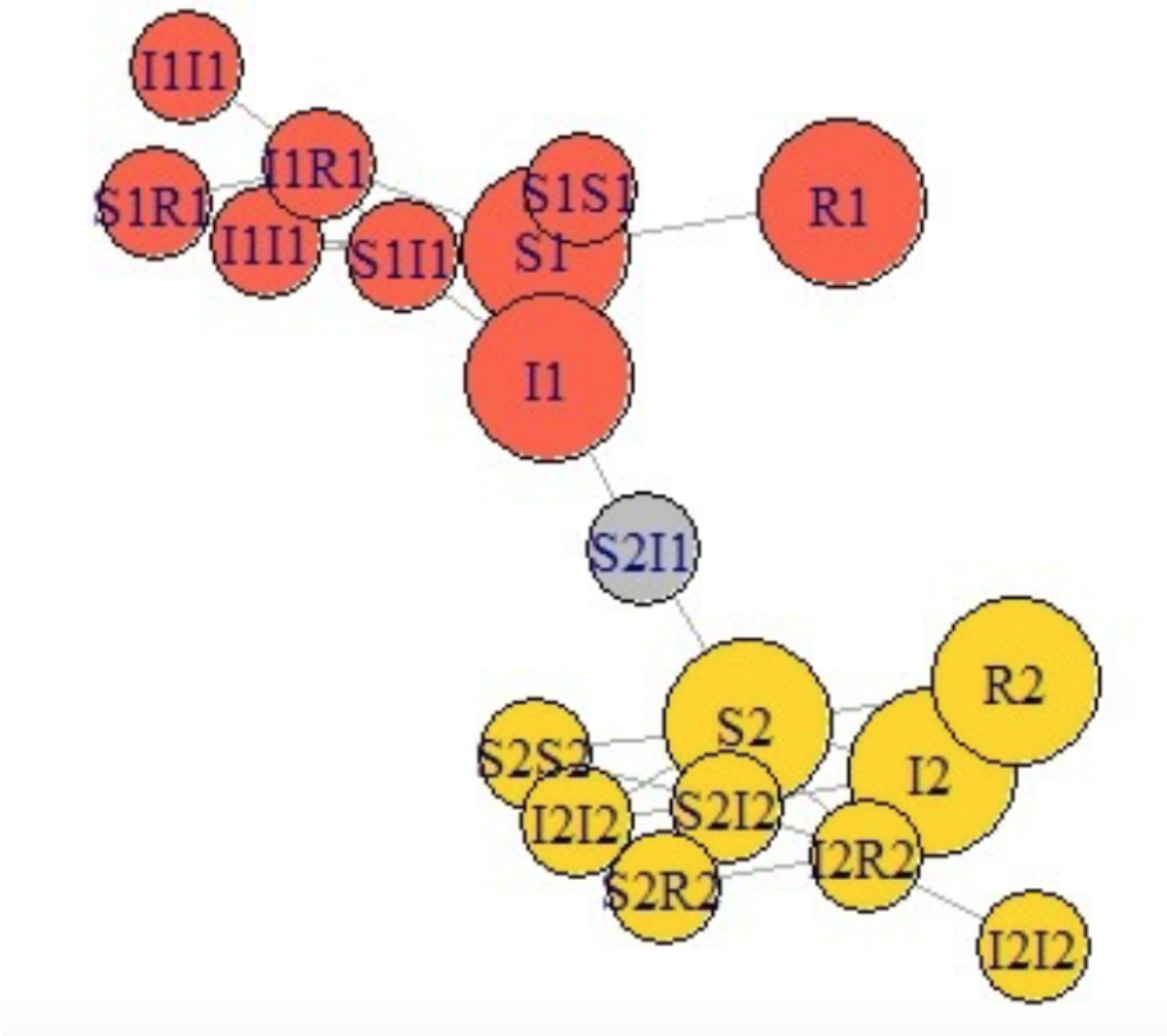

Figure 3.2: Scheme of the $SIR4$ pairwise approximation model with two populations.

$$\frac{d[S_1R_1]}{dt} = -\tau_1([I_1S_1R_1] + \sigma_1[S_1I_1), \tag{3.40f}$$

$$\frac{d[I_1I_1]}{dt} = 2\tau_1([I_1S_1I_1] + [S_1I_1]) - 2\sigma_1[S_1I_1), \tag{3.40g}$$

$$\frac{d[I_1R_1]}{dt} = \tau_1([I_1S_1R_1] + [S_1I]_1) + \sigma_1([I_1I_1] - [I_1R_1]), \tag{3.40h}$$

$$\frac{d[I_1R_1]}{dt} = 2\sigma_1[I_1R_1]. \tag{3.40i}$$

3.2.1 Parameters

β_1 : contact rate of camel.

β_2 : contact rate of human.

$\frac{1}{\gamma_1}$: the mean infectious period of infected camel for survivors.

$\frac{1}{\gamma_2}$: the mean duration for infected human for survivors.

ε : is generally small and measures the trickle of infection from the camel population into the human one.

Assume,

$N_{1i} := S_{1i} + I_{1i} + R_{1i} = 1$, and

$N_{2i} := S_{2i} + I_{2i} + R_{2i} = 1$.

The following results in (Fig. 3.3, and 3.4) show the prevalence of the camel population which match with results that have been shown by Kasem et al. 2018 [1] using the same parameter values of the previous chapter 2.2.

The two species model of pairwise approximation Fig. 3.2 can be written as

$$\frac{d[S_1]}{dt} = -\tau_1[S_1I_1], \tag{3.41a}$$
$$\frac{d[I_1]}{dt} = \tau_1[S_1I_1] - \sigma_1[I_1], \tag{3.41b}$$
$$\frac{d[R_1]}{dt} = \sigma_1[I_1], \tag{3.41c}$$
$$\frac{d[S_1S_1]}{dt} = -2\tau_1\phi_1[S_1S_1I_1], \tag{3.41d}$$
$$\frac{d[S_1I_1]}{dt} = \tau_1([S_1S_1I_1] - [I_1S_1I_1] - [S_1I_1]) - \sigma_1[S_1I_1], \tag{3.41e}$$
$$\frac{d[S_1R_1]}{dt} = -\tau_1([I_1S_1R_1] + \sigma_1[S_1I_1), \tag{3.41f}$$
$$\frac{d[I_1I_1]}{dt} = 2\tau_1([I_1S_1I_1] + [S_1I_1]) - 2\sigma_1[S_1I_1), \tag{3.41g}$$
$$\frac{d[I_1R_1]}{dt} = \tau_1([I_1S_1R_1] + [S_1I]_1) + \sigma_1([I_1I_1] - [I_1R_1]), \tag{3.41h}$$
$$\frac{d[R_1R_1]}{dt} = 2\sigma_2[I_2R_2]. \tag{3.41i}$$

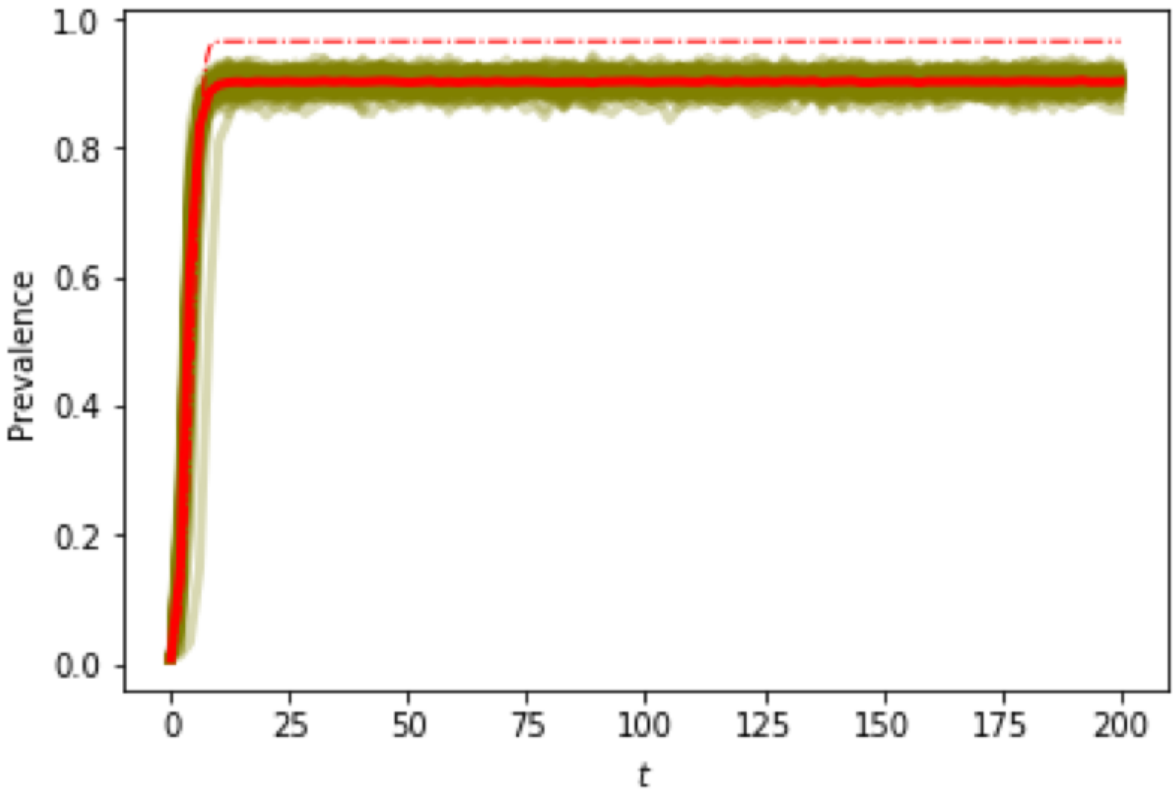

Figure 3.3: Prevalence SIR pairwise approximations (camel population).

$$\frac{d[S_2]}{dt} = -\tau_2[S_2I_2] - \varepsilon\tau_2[S_2I_1], \tag{3.41j}$$

$$\frac{d[I_2]}{dt} = \tau_2[S_2I_2] + \varepsilon\tau_2[S_1I_1] - \sigma_2[I_2], \tag{3.41k}$$

$$\frac{d[R_2]}{dt} = \sigma_2[I_2], \tag{3.41l}$$

$$\frac{d[S_2S_2]}{dt} = -2\tau_2[S_2S_2I_2] - 2\varepsilon\tau_2 f[S_2S_2I_1], \tag{3.41m}$$

$$\frac{d[S_2I_1]}{dt} = \tau_2\varepsilon([S_2S_2I_1] - [I_1S_2I_1] - [S_2I_1]) - \sigma_2[S_2I_1], \tag{3.41n}$$

$$\frac{d[S_2I_2]}{dt} = \varepsilon\tau_2(f[S_2S_2I_1] - [I_2S_2I_2] - [S_2I_2]) - \sigma_2[S_2I_2], \tag{3.41o}$$

$$\frac{d[S_2R_2]}{dt} = -\tau_2([I_2S_2R_2] + \sigma_2[S_2I_2), \tag{3.41p}$$

$$\frac{d[I_2I_2]}{dt} = 2\tau_2([I_2S_2I_2] + [S_2I_2]) - 2\sigma_2[S_2I_2), \tag{3.41q}$$

$$\frac{d[I_2R_2]}{dt} = \tau_2([I_2S_2R_2] + [S_2I_2) + \sigma_2([I_2I_2] - [I_2R_2]), \tag{3.41r}$$

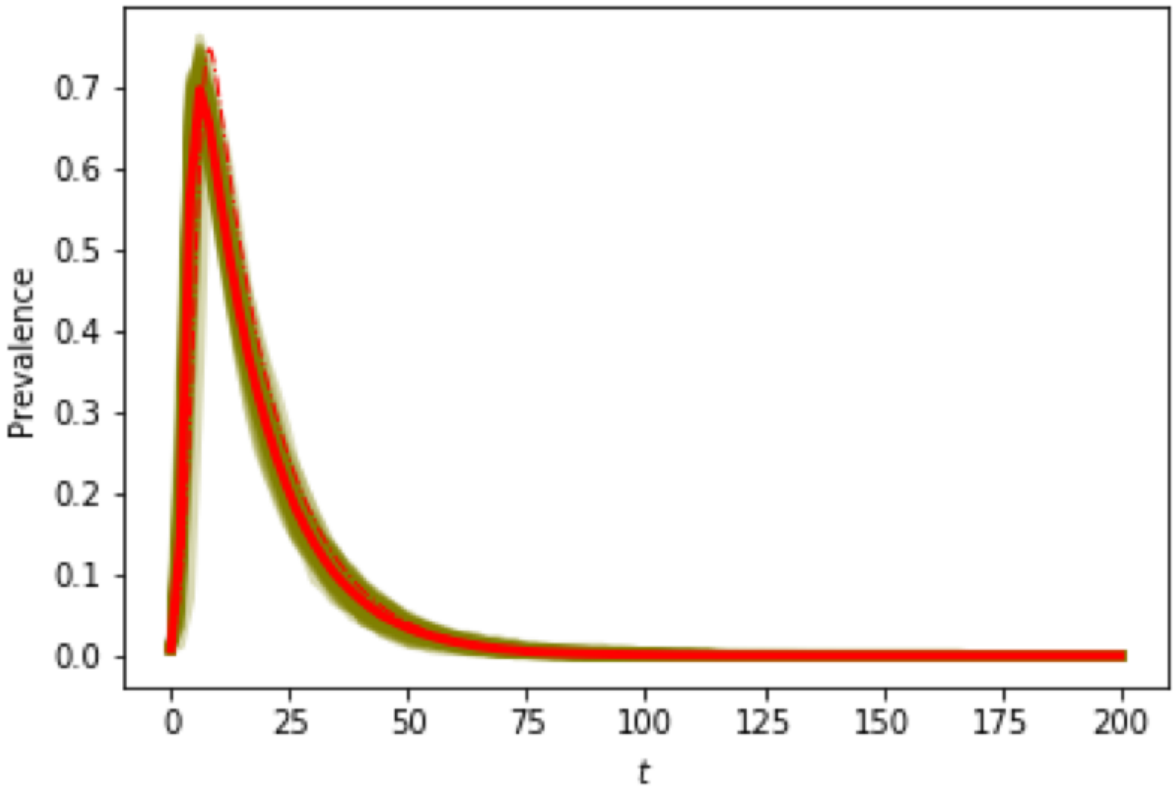

Figure 3.4: Prevalence SIR pairwise approximations (camel population).

$$\frac{d[R_2R_2]}{dt} = 2\sigma_2[I_2R_2], \tag{3.41s}$$

where $\phi_i = (n-1)/n$, $i = 1, 2$.

Consider the system 3.41, which defines modification of the generalized the SIR model with two populations. Each of these population consists of three groups susceptible, infectious and recovered compartments. Most of the relations between group sizes $[S_i], [I_i], [R_i], i = 1, 2$ are described by analogies equation 3.40. Notice, that this system describe evolution of the singletons, $[S_i], [I_i],[R_i],i = 1, 2$ and pairs $[S_iI_i],[S_iR_i],[I_iR_i],i = 1, 2$. First consider all relations between all subjects of the our system $[S_i],[I_i],[R_i],i = 1, 2$ and pairs $[S_iI_i],[S_iR_i],[I_iR_i], i = 1, 2$. Notice, that relation in each population (in the first population between $[S_1],[I_1],[R_1],[S_1I_1],[S_1R_1],[I_1R_1]$ and in the second population between

$[S_2]$,$[I_2]$,$[R_2]$,$[S_2I_2]$,$[S_2R_2]$,$[I_2R_2]$ is same as in the system 3.40. This model includes existing on the pairs $[XY]$ in the system, if the system consists of singleton $[X]$ and $[Y]$. In our case, we assume the existing relations between all singletons in each group. For vanish all triplets $[XYZ]$, we use the formula at [116]; such as,

$$[XYZ] = (n-1)/n[XY][YZ]/[Y], \tag{3.42}$$

where n is the average number of contacts per individual, which assumes conditional independence of the infection statuses of neighbours of a given number of individual. The main assumption is using Markovian property of the system state in time $t+1$ depend only from the state of the system in time t and do not depend on the state of the system in time when $s < t$. Now consider in detail relations between two groups, which define relations between two populations. For this aim we consider only one relation between two populations: between infected individuals from population 1 (camel population,I_1) and susceptible individuals from population 2 (human population, S_2). This new variable will generate new dependencies in population 2. Then number of the susceptible individuals in the human population decrease by $\varepsilon\tau_2[S_2I_1]$, number of the infected individuals in the human population increase by $\varepsilon\tau_2[S_2I_1]$. Notice, that this two additional terms do not change general number of the individuals in the human population: $d[S_2]/dt + d[I_2]/dt + d[R_2]/dt = (dN_2)/dt = 0$, where N_2 number of individuals in the second (human) population. So, new system consist three main parts [125]

1- Subsystem, which describe of the dynamic of the population 1 (camel population) variables $[S_1]$,$[I_1]$,$[R_1]$,$[S_1I_1]$,$[S_1R_1]$,$[I_1R_1]$;

2- Subsystem, which describe of the dynamic of the population 2 (human population) variables$[S_2]$,$[I_2]$,$[R_2]$,$[S_2I_2]$,$[S_2R_2]$,$[I_2R_2]$;

3- Subsystem, which describe dynamic of the numerical relations between two populations

variable $[S_2I_1]$.

This system is shown in (Fig. 3.2). As we can see, the proposed system with two populations contains two main subsystems and a third element (state S_2I_1), which connect these two populations.

Using all previous descriptions and results of the works [116, 148], we can define dynamic of the system with two populations as system of differential equations with 19 equations, by using formula 3.42 to write 3.41 as,

$$\frac{d[S_1]}{dt} = -\tau_1[S_1I_1], \tag{3.43a}$$

$$\frac{d[I_1]}{dt} = \tau_1[S_1I_1] - \sigma_1[I_1], \tag{3.43b}$$

$$\frac{d[R_1]}{dt} = \sigma_1[I_1], \tag{3.43c}$$

$$\frac{d[S_1S_1]}{dt} = -2\tau_1\phi_1\frac{[S_1S_1][S_1I_1]}{[S_1]}, \tag{3.43d}$$

$$\frac{d[S_1I_1]}{dt} = \tau_1(\phi_1\frac{[S_1S_1][S_1I_1]}{[S_1]} - \phi_1\frac{[S_1I_1]^2}{[S_1]} - [S_1I_1]) - \sigma_1[S_1I_1], \tag{3.43e}$$

$$\frac{d[S_1R_1]}{dt} = -\tau_1\phi_1\frac{[I_1S_1][S_1R_1]}{[S_1]} + \sigma_1[S_1I_1], \tag{3.43f}$$

$$\frac{d[I_1I_1]}{dt} = 2\tau_1(\phi_1\frac{[I_1S_1][S_1R_1]}{[S_1]} + [S_1I_1]) - 2\sigma_1[I_1I_1], \tag{3.43g}$$

$$\frac{d[I_1R_1]}{dt} = \tau_1\phi_1(\frac{[I_1S_1][S_1R_1]}{[S_1]} + \sigma_1([I_1I_1] - [I_1R_1])), \tag{3.43h}$$

$$\frac{d[R_1R_1]}{dt} = 2\sigma_1[I_1R_1], \tag{3.43i}$$

$$\frac{d[S_2]}{dt} = -\tau_2[S_2I_2] - \varepsilon\tau_2[S_2I_1], \tag{3.43j}$$

$$\frac{d[I_2]}{dt} = \tau_2[S_2I_2] + \varepsilon\tau_2[S_2I_1] - \sigma_2[I_2], \tag{3.43k}$$

$$\frac{d[R_2]}{dt} = \sigma_2[I_2], \tag{3.43l}$$

$$\frac{d[S_2S_2]}{dt} = -2\tau_2\phi_2\frac{[S_2S_2][S_2I_2]}{[S_2]} - 2\varepsilon\tau_2\phi_2\frac{[S_2S_2][S_2I_2]}{[S_2]}, \tag{3.43m}$$

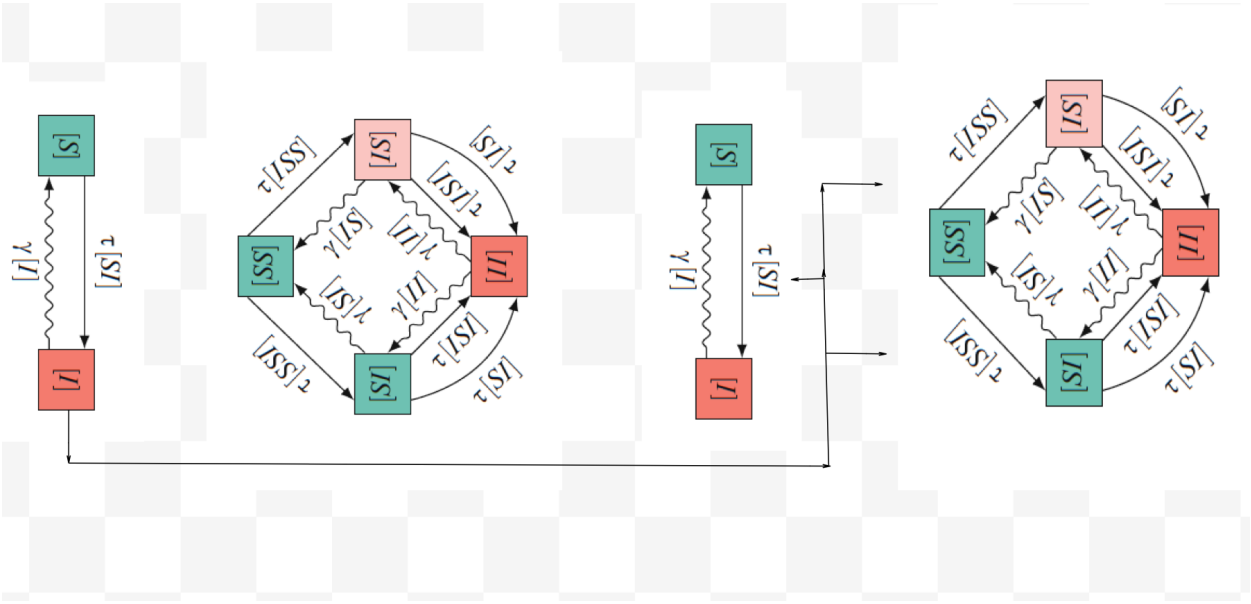

(a)

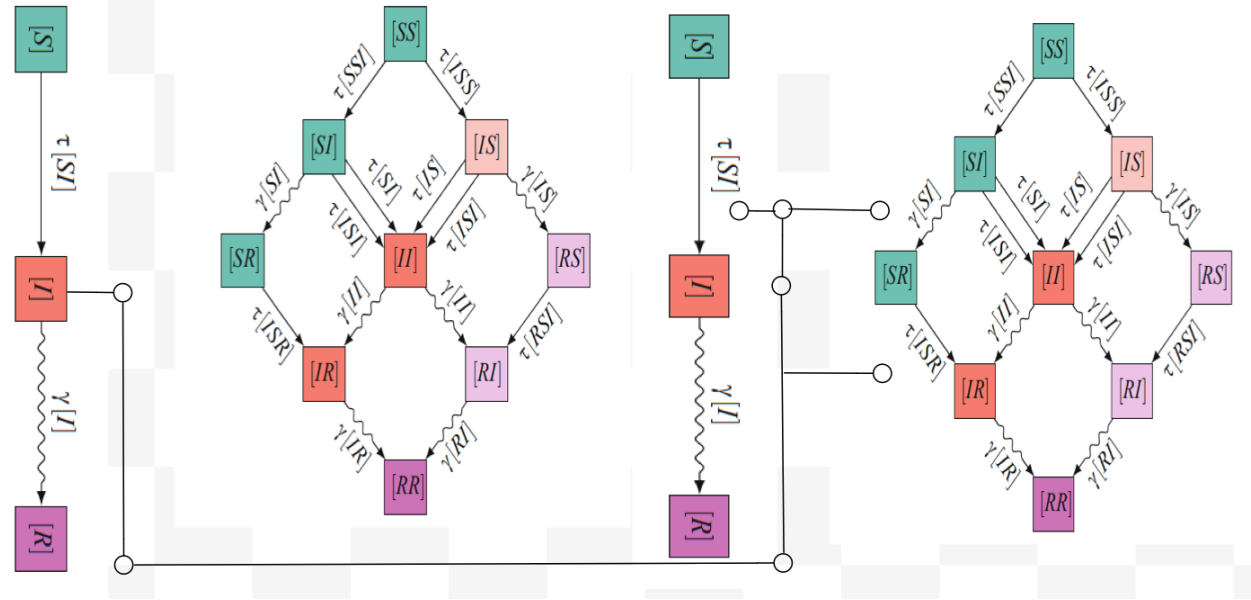

(b)

Flow diagrams illustrating the fluxes among singles compartments left and pairs compartments right, where the transmission of infection involve animal-animal, animal-human, and human-human. The SIS scenario is on the (top), while the SIR case is on the (bottom). In the compartments of pairs, solid lines represent infections from inside pair with a rate dependent on the pair or from outside of the pair with a rate dependent on the triple, while wiggly lines show recovery [129].

$$\frac{d[S_2I_1]}{dt} =\varepsilon\tau_2(\phi_2\frac{[S_2S_2][S_2I_1]}{[S_2]} - \phi_2\frac{[S_2I_1]^2}{[S_2]} - [S_2I_1]) - \sigma_2[S_2I_1], \tag{3.43n}$$

$$\frac{d[S_2I_2]}{dt} =\tau_2(\phi_2\frac{[S_2S_2][S_2I_1]}{[S_2]} - \phi_2\frac{[S_2I_2]}{[S_2]} - [S_2I_2]) - \sigma_2[S_2I_2], \tag{3.43o}$$

$$\frac{d[S_2R_2]}{dt} = -\tau_2\phi_2\frac{[I_2S_2][S_2R_2]}{[S_2]} + \sigma_2[S_2I_2], \tag{3.43p}$$

$$\frac{d[I_2I_2]}{dt} =2\tau_2(\phi_2\frac{[S_2I_2]^2}{[S_2]} + [S_2I_2]) - 2\sigma_2[I_2I_2], \tag{3.43q}$$

$$\frac{d[I_2R_2]}{dt} =\tau_2(\phi_2\frac{[I_2S_2][S_2R_2]}{[S_2]} + \sigma_2([I_2I_2] - [I_2R_2])), \tag{3.43r}$$

$$\frac{d[R_2R_2]}{dt} =2\sigma_2[I_2R_2], \tag{3.43s}$$

which describe the evolution of the singletons and pairs where $\phi_i = (n-1)/n$, $i = 1, 2$. If we use the assumptions of relations in the objects of $[S_i]$, $[I_i]$, $[R_i]$, $[S_iI_i]$, $[S_iR_i] + [I_iR_i]$,$i = 1, 2$, then the next conditions are in hold

$$\frac{d[S_i]}{dt} + \frac{d[I_i]}{dt} + \frac{d[R_i]}{dt} = 0, \qquad i = 1, 2 \tag{3.44a}$$

$$\sum_{i=1}^{2}(\frac{d[S_iS_i]}{dt}+\frac{d[S_iI_i]}{dt} + \frac{d[S_iR_i]}{dt} + \frac{d[I_iI_i]}{dt} + \frac{d[I_iR_i]}{dt} + \frac{d[R_iR_i]}{dt}) = 0. \tag{3.44b}$$

First condition in 3.44 means that number in the each population is constant and satisfy next relations

$$[S_1] + [I_1] + [R_1] = N_1, \tag{3.45a}$$

$$[S_2] + [I_2] + [R_2] = N_2, \tag{3.45b}$$

where $N_1$and N_2 – numbers of individuals in first and second population respectively. Second condition in 3.44 indicates that the number of pairs in the system 3.43 is constant

and satisfy the following:

$$\sum_{i=1}^{2} \left([S_i S_i] + [S_i I_i] + [S_i R_i] + [I_i I_i] + [I_i R_i] + [R_i R_i] \right) = n * (N_1 + N_2) \,, \tag{3.46a}$$

where n is the average number of contacts per individual.

The condition 3.44 is also true, so general assumption of the generalized SIR model for two populations holds. Lets rewrite system 3.43 in more simple form

$$\frac{dx}{dt} = f\left(x\right), \tag{3.47a}$$

where,

$$x = \begin{pmatrix} [S_1] \\ [I_1] \\ [R_1] \\ [S_1S_1] \\ [S_1I_1] \\ [S_1R_1] \\ [I_1I_1] \\ [I_1R_1] \\ [R_1R_1] \\ [S_2] \\ [I_2] \\ [R_2] \\ [S_2S_2] \\ [S_2I_2] \\ [S_2R_2] \\ [I_2I_2] \\ [I_2R_2] \\ [R_2R_2] \\ [S_2I_1] \end{pmatrix}.$$

f – function, which define right-hand side of the equation 3.43. Using relations 3.44, we can reduce the system 3.43 as

$$\frac{d[S_1]}{dt} = -\tau_1[S_1I_1], \tag{3.48a}$$

$$\frac{d[I_1]}{dt} = \tau_1[S_1I_1] - \sigma_1[I_1], \tag{3.48b}$$

$$\frac{d[S_1S_1]}{dt} = -2\tau_1\phi_1\frac{[S_1S_1][S_1I_1]}{[S_1]}, \tag{3.48c}$$

$$\frac{d[S_1I_1]}{dt} = \tau_1(\phi_1\frac{[S_1S_1][S_1I_1]}{[S_1]} - \phi_1\frac{[S_1I_1]^2}{[S_1]} - [S_1I_1]) - \sigma_1[S_1I_1], \tag{3.48d}$$

$$\frac{d[S_1R_1]}{dt} = -\tau_1\phi_1\frac{[I_1S_1][S_1R_1]}{[S_1]} + \sigma_1[S_1I_1], \tag{3.48e}$$

$$\frac{d[I_1I_1]}{dt} = 2\tau_1(\phi_1\frac{[I_1S_1][S_1R_1]}{[S_1]} + [S_1I_1]) - 2\sigma_1[I_1I_1], \tag{3.48f}$$

$$\frac{d[I_1R_1]}{dt} = \tau_1\phi_1(\frac{[I_1S_1][S_1R_1]}{[S_1]} + \sigma_1([I_1I_1] - [I_1R_1])), \tag{3.48g}$$

$$\frac{d[R_1R_1]}{dt} = 2\sigma_1[I_1R_1], \tag{3.48h}$$

$$\frac{d[S_2]}{dt} = -\tau_2[S_2I_2] - \varepsilon\tau_2[S_2I_1], \tag{3.48i}$$

$$\frac{d[I_2]}{dt} = \tau_2[S_2I_2] + \varepsilon\tau_2[S_2I_1] - \sigma_2[I_2], \tag{3.48j}$$

$$\frac{d[S_2S_2]}{dt} = -2\tau_2\phi_2\frac{[S_2S_2][S_2I_2]}{[S_2]} - 2\varepsilon\tau_2\phi_2\frac{[S_2S_2][S_2I_2]}{[S_2]}, \tag{3.48k}$$

$$\frac{d[S_2I_1]}{dt} = \varepsilon\tau_2(\phi_2\frac{[S_2S_2][S_2I_1]}{[S_2]} - \phi_2\frac{[S_2I_1]^2}{[S_2]} - [S_2I_1]) - \sigma_2[S_2I_1], \tag{3.48l}$$

$$\frac{d[S_2I_2]}{dt} = \tau_2(\phi_2\frac{[S_2S_2][S_2I_1]}{[S_2]} - \phi_2\frac{[S_2I_2]}{[S_2]} - [S_2I_2]) - \sigma_2[S_2I_2], \tag{3.48m}$$

$$\frac{d[S_2R_2]}{dt} = -\tau_2\phi_2\frac{[I_2S_2][S_2R_2]}{[S_2]} + \sigma_2[S_2I_2], \tag{3.48n}$$

$$\frac{d[I_2I_2]}{dt} = 2\tau_2(\phi_2\frac{[S_2I_2]^2}{[S_2]} + [S_2I_2]) - 2\sigma_2[I_2I_2], \tag{3.48o}$$

$$\frac{d[I_2R_2]}{dt} = \tau_2(\phi_2\frac{[I_2S_2][S_2R_2]}{[S_2]} + \sigma_2([I_2I_2] - [I_2R_2])), \tag{3.48p}$$

$$\tag{3.48q}$$

Elements $[R_1]$, $[R_2]$ and $[R_2R_2]$, we define from equations 3.44 and 3.45 as

$$[R_1] = N_1 - [S_1] - [I_1], \tag{3.49a}$$

$$[R_2] = N_2 - [S_2] - [I_2], \tag{3.49b}$$

$$[R_2R_2] = n * (N_1 + N_2) - (\sum_{i=1}^{2}([S_iS_i]+[S_iI_i] + [S_iR_i] + [I_iI_i] + [I_iR_i]) + [S_2I_1] + [R_1R_1]). \tag{3.49c}$$

Lets rewrite system 3.48 in the vector form:

$$\frac{dx}{dt} = g(x).$$

Observe that the functions $f\,(x)$ and $g(x)$ are non-linear by parameters x. This means that we must to use numerical methods for estimation for the solutions of the system,

$$g(x) = 0. \tag{3.50}$$

System 3.50 define all stationary points of the system 3.48. This means that stationary points depend from initial conditions:

$$x_{t=0} = x_0,$$

as what has been shown in the results at the following in (Fig. 3.6a and Fig. 3.6b).

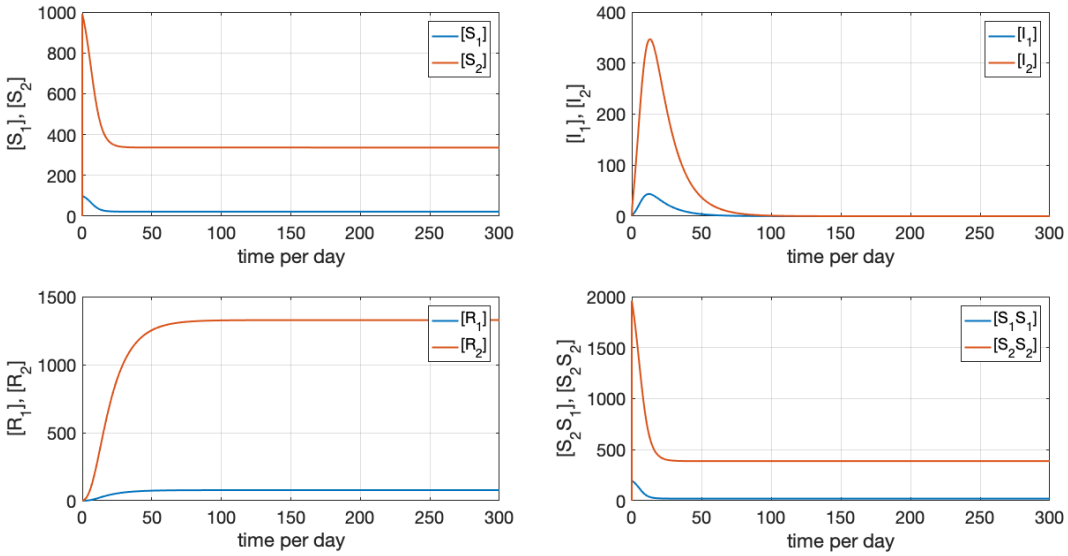

(a)

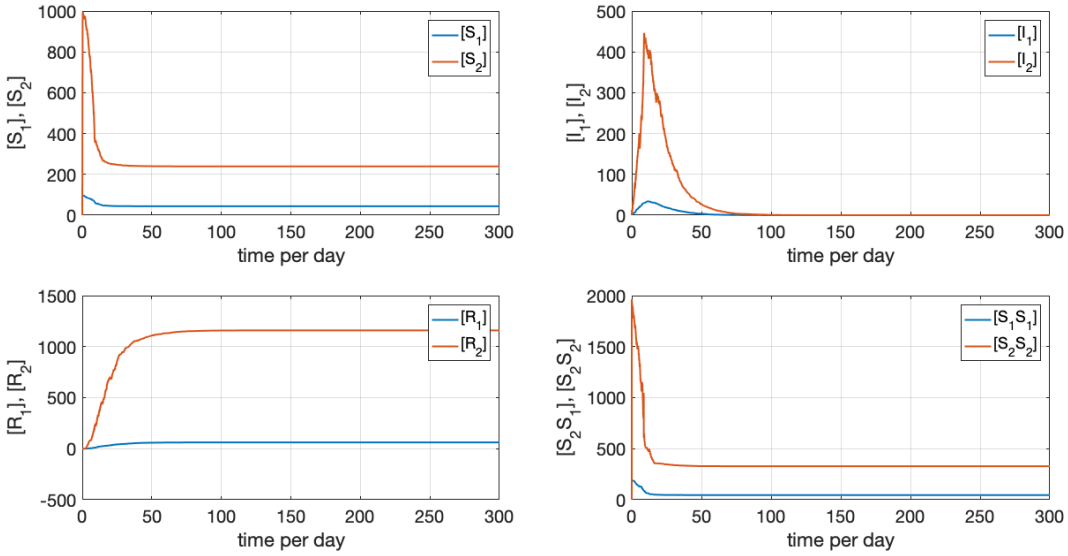

(b)

Figure 3.6: (a) Determinstic pairwise approximation, and (b) Stochasic pairwise approximation.

Chapter 4

Environmental Infection Transmission

4.1 Introduction

MERS-COV can be transmitted through a contaminated environment such as air, fumes, foodstuffs, hands, and fluids. In this chapter we study a model of virus transmission between hosts, and through the environment. The environmental communication mechanisms need more objectively comprehensive interaction network formulations than those focused on social interactions or physical closeness.

Physical and behavioral aspects obtained from empirical investigations as the creation of transmission parameters that can be independently tested in environmental field trials, along with the incidence of pathogens in the area, and the transmission factor from fomites to hands [149]. In addition, Brouwer et. al 2017 formulate a transmission pathways in a way that enables the estimation of possible environmental regulation consequences and the analysis of measures of environmental pathogens [150]. We develop an $SIRV$ model, where V stands for virus in the environment. Model results could be used to inform public health mitigation strategies at households, groceries and hospitals, including hand washing, and surface cleaning. Developing a mechanical theory of biological dependent transmission rates

determined by zoology factors that are easily calculated in the field.

4.2 Model Formulation

S: Susceptible, I: Infected, R: Recovered, V: Virus in the environment,

satisfies the below differential system:

$$\frac{dS}{dt} = \Lambda - \rho\pi SV - \beta SI - dS, \tag{4.1a}$$

$$\frac{dI}{dt} = \rho\pi SV + \beta SI - \gamma I - \delta I - dI, \tag{4.1b}$$

$$\frac{dR}{dt} = \gamma I - dR, \tag{4.1c}$$

$$\frac{dV}{dt} = \alpha I - V\left[(S + I + R)\rho + \mu + c\right], \tag{4.1d}$$

see the flow chart of environmental infection transmission model 4.1.

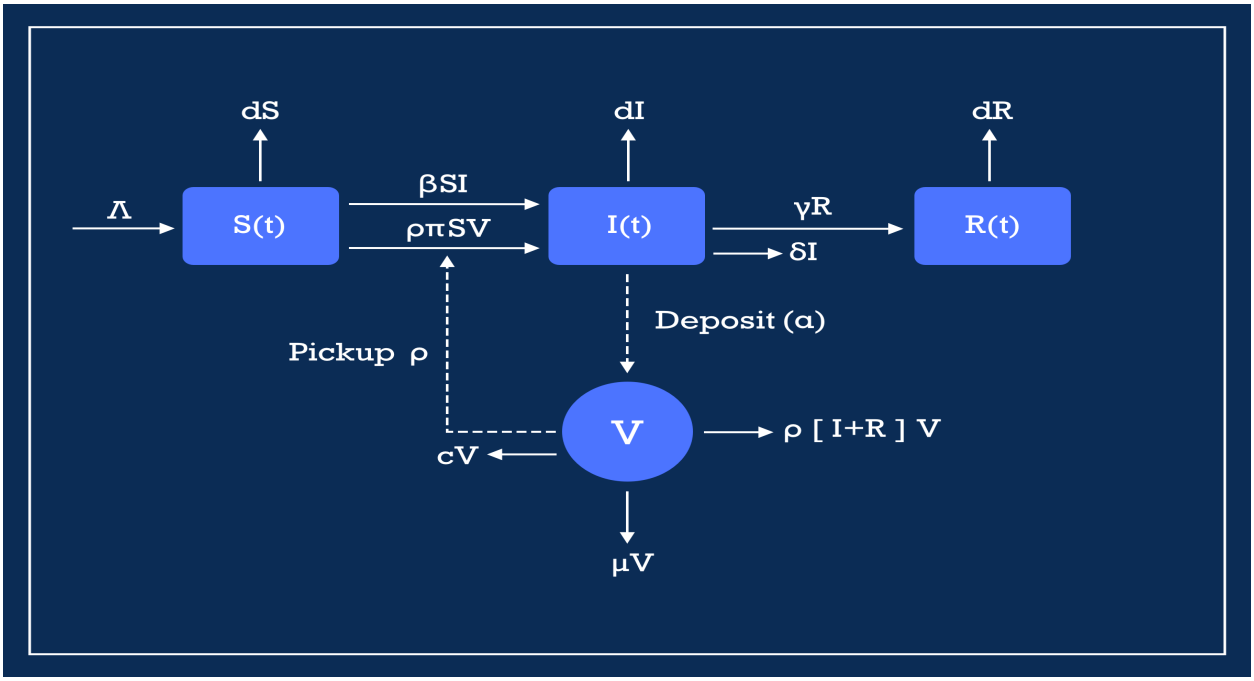

Figure 4.1: Flow chart for the environmental infection transmission model.

Parameters List	
Parameter	Description
Λ	recruitment rate of humans population.
d	natural death of humans .
δ	disease death rate of humans.
β	contact rate between susceptible individual and infectious individual.
ρ	the fraction of V picked up by each individual.
π	the probability of a susceptible turn into infectious per pathogen V picked up.
γ	the rate of recovery.
α	the number of pathogens that an infectious individual deposits into the environment.
μ	the rate of eliminated pathogens from the environment by naturally dying.
c	the rate of pathogens extracted to be degrade by decontamination or to be cleaned or otherwise eliminated from the environment.

Table 4.1: Parameters description for environmental infection transmission model.

Consider the following system

$$\begin{cases} \frac{dS}{dt} = \Lambda - \rho\pi SV - \beta SI - dS, \\ \frac{dI}{dt} = \rho\pi SV + \beta SI - \gamma I - \delta I - dI, \\ \frac{dR}{dt} = \gamma I - dR \\ \frac{dV}{dt} = \alpha I - V\left\{(I + R + S)\,\rho + \mu + c\right\}, \end{cases} \tag{4.2}$$

where the parameters are described in the table 4.1.

4.3 Nonnegativity:

4.3.1 Nonnegativity of $S(t)$:

Assume that,

$$\frac{dS}{dt} = \Lambda - \rho\pi SV - \beta SI - dS \ ,$$

$$\frac{dS}{dt} + (\rho\pi V + \beta I + d)\, S = \Lambda \ .$$

Since $\Lambda > 0$, then

$$\frac{dS}{dt} + (\rho\pi V + \beta I + d)\, S > 0 \ ,$$

$$\frac{dS}{dt} + \Phi_S(t)\, S > 0 \ , \tag{4.3}$$

where,

$$\Phi_S(t) = \rho\pi V + \beta I + d \ . \tag{4.4}$$

Then for $t > 0$ (4.3) can be written as,

$$\frac{dS}{dt} \exp\left\{\int_0^t \Phi_S(\tau)\, d\tau\right\} + \Phi_S(t)\, S \exp\left\{\int_0^t \Phi_S(\tau)\, d\tau\right\} > 0 \ ,$$

$$\frac{d}{dt}\left[S(t) \exp\left\{\int_0^t \Phi_S(\tau)\, d\tau\right\}\right] > 0 \ ,$$

$$S(t) \exp\left\{\int_0^t \Phi_S(\tau)\, d\tau\right\}\Bigg|_0^t > 0 \ ,$$

$$S(t) \exp\left\{\int_0^t \Phi_S(\tau)\, d\tau\right\} - S(0) > 0 \ ,$$

$$S(t) > S(0) \exp\left\{-\int_0^t \Phi_S(\tau)\, d\tau\right\} \ . \tag{4.5}$$

Hence, since $S(0) \geq 0$, then for any $t \geq 0$ we get that $S(t) \geq 0$.

4.3.2 Nonnegativity of $I(t)$ and $V(t)$

Consider the following statements,

$$\begin{cases} \frac{dI}{dt} = \rho\pi SV + \beta SI - \gamma I - \delta I - dI, \\ \frac{dV}{dt} = \alpha I - V\left\{(I+R+S)\,\rho + \mu + c\right\}, \end{cases} \tag{4.6}$$

we have

$$\frac{dI}{dt}V + I\frac{dV}{dt} = \rho\pi SV^2 + \alpha I^2 + \left\{\beta S - \gamma - \delta - d - (I+R+S)\,\rho - \mu - c\right\} IV \ ,$$

$$\frac{d}{dt}(IV) + \left\{\gamma + \delta + d + (I+R+S)\,\rho + \mu + c - \beta S\right\} IV = \rho\pi SV^2 + \alpha I^2 \ .$$

Since $S(t) \geq 0$, $\rho > 0$, $\pi > 0$ and $\alpha > 0$, then for any $t \geq 0$: $\rho\pi SV^2 + \alpha I^2 \geq 0$. Hence,

$$\frac{d}{dt}(IV) + \left\{\gamma + \delta + d + (I+R+S)\,\rho + \mu + c - \beta S\right\} IV \geq 0 \ ,$$

$$\frac{d}{dt}(IV) + \Phi_{IV}(t)\, IV \geq 0 \ , \tag{4.7}$$

where

$$\Phi_{IV}(t) = \gamma + \delta + d + (I+R+S)\,\rho + \mu + c - \beta S \ . \tag{4.8}$$

Then for $t > 0$ (4.7) can be written as

$$\frac{d}{dt}(IV)\exp\left\{\int_0^t \Phi_{IV}(\tau)\,d\tau\right\} + \Phi_{IV}(t)\, IV \exp\left\{\int_0^t \Phi_{IV}(\tau)\,d\tau\right\} \geq 0 \ ,$$

$$\frac{d}{dt}\left[I(t)V(t)\exp\left\{\int_0^t \Phi_{IV}(\tau)\,d\tau\right\}\right] \geq 0\ ,$$

$$I(t)V(t)\exp\left\{\int_0^t \Phi_{IV}(\tau)\,d\tau\right\}\Bigg|_0^t \geq 0\ ,$$

$$I(t)V(t)\exp\left\{\int_0^t \Phi_{IV}(\tau)\,d\tau\right\} - I(0)V(0) \geq 0\ ,$$

$$I(t)V(t) \geq I(0)V(0)\exp\left\{-\int_0^t \Phi_{IV}(\tau)\,d\tau\right\}\ . \tag{4.9}$$

Since $I(0) \geq 0$ and $V(0) \geq 0$, then for any $t \geq 0$ we get that $I(t)V(t) \geq 0$. It is also easy to detect for some $t > 0$ we have $I(t)V(t) = 0$, as a consequence this means that $I(t) \equiv 0$ and $V(t) \equiv 0$. Therefore, if $I(t) \neq 0$ and $V(t) \neq 0$ for $t > 0$: $I(t)V(t) > 0$, hence, $I(t) > 0$ and $V(t) > 0$ (the case $I(t) < 0$ and $V(t) < 0$ is impossible because $I(0) \geq 0$ and $V(0) \geq 0$). As a result, we have that if $I(0) \geq 0$ and $V(0) \geq 0$, then for any $t \geq 0$ we obtain $I(t) \geq 0$ and $V(t) \geq 0$.

4.3.3 Nonnegativity of $R(t)$

Looking at

$$\frac{dR}{dt} = \gamma I - dR\ ,$$

it takes the form

$$\frac{dR}{dt} + dR = \gamma I\ .$$

Since $I(t) \geq 0$ and $\gamma > 0$, then for any $t \geq 0$: $\gamma I \geq 0$. In this case, we write,

$$\frac{dR}{dt} + dR \geq 0\ . \tag{4.10}$$

Thus for $t > 0$ (4.10) could be generated as

$$\frac{dR}{dt}\exp\{dt\} + dR\exp\{dt\} \geq 0 \ ,$$

$$\frac{d}{dt}\left[R\left(t\right)\exp\{dt\}\right] \geq 0 \ ,$$

$$R\left(t\right)\exp\{dt\}|_0^t \geq 0 \ ,$$

$$R\left(t\right)\exp\{dt\} - R\left(0\right) \geq 0 \ ,$$

$$R\left(t\right) \geq R\left(0\right)\exp\{-dt\} \ . \tag{4.11}$$

Consequently $R(0) \geq 0$, then for any $t \geq 0$ we get that $R(t) \geq 0$.

4.4 Boundedness of $N(t)$

Effectuate the following

$$\begin{cases} \frac{dS}{dt} = \Lambda - \rho\pi SV - \beta SI - dS, \\ \frac{dI}{dt} = \rho\pi SV + \beta SI - \gamma I - \delta I - dI, \\ \frac{dR}{dt} = \gamma I - dR, \end{cases} \tag{4.12}$$

by adding equations (4.12), we obtain

$$\frac{dS}{dt} + \frac{dI}{dt} + \frac{dR}{dt} = \Lambda - \delta I - d\left(S + I + R\right) \ ,$$

$$\frac{d}{dt}\left(S + I + R\right) = \Lambda - \delta I - d\left(S + I + R\right) \ . \tag{4.13}$$

Since $N = S + I + R$, then (4.13) takes the form

$$\frac{dN}{dt} = \Lambda - \delta I - dN \ ,$$

$$\frac{dN}{dt} + dN - \Lambda = -\delta I \ . \tag{4.14}$$

Since I$(t) \geq 0$ and $\delta > 0$, then for any $t \geq 0$: $\delta I \geq 0$. Hence,

$$\frac{dN}{dt} + dN - \Lambda \leq 0 \ . \tag{4.15}$$

Then for $t > 0$ (4.15) can be written as

$$\frac{dN}{dt} \exp\{dt\} + dN \exp\{dt\} - \Lambda \exp\{dt\} \leq 0 \ ,$$

$$\frac{d}{dt}\left[\left(N(t) - \frac{\Lambda}{d}\right) \exp\{dt\}\right] \leq 0 \ ,$$

$$\left(N(t) - \frac{\Lambda}{d}\right) \exp\{dt\}\Big|_0^t \leq 0 \ ,$$

$$\left(N(t) - \frac{\Lambda}{d}\right) \exp\{dt\} - \left(N(0) - \frac{\Lambda}{d}\right) \leq 0 \ ,$$

$$\left(N(t) - \frac{\Lambda}{d}\right) \exp\{dt\} \leq N(0) - \frac{\Lambda}{d} \ ,$$

$$N(t) \leq \frac{\Lambda}{d} + \left(N(0) - \frac{\Lambda}{d}\right) \exp\{-dt\} \ . \tag{4.16}$$

Hence, if $N(0) \leq \frac{\Lambda}{d}$, then for any $t \geq 0$ we get that $N(t) \leq \frac{\Lambda}{d}$.

If $N(0) > \frac{\Lambda}{d}$, then it follows that $N(t) \leq N(0)$. Therefore, in the general case, we arrive at $N(t) \leq \max\left(N(0), \frac{\Lambda}{d}\right)$.

4.5 Derivation of R_0

Consider the system

$$\begin{cases} \frac{dS}{dt} = \Lambda - \rho\pi SV - \beta SI - dS, \\ \frac{dI}{dt} = \rho\pi SV + \beta SI - \gamma I - \delta I - dI, \\ \frac{dR}{dt} = \gamma I - dR, \\ \frac{dV}{dt} = \alpha I - V\left\{(I + R + S)\,\rho + \mu + c\right\}, \end{cases} \tag{4.17}$$

Let's transform the second equation of the system (4.17) as follows:

$$\frac{dI}{dt} = \rho\pi SV + \beta SI - \varepsilon I \ ,$$

$$\frac{dI}{dt} = \varepsilon I\left(\frac{\rho\pi SV}{\varepsilon I} + \frac{\beta S}{\varepsilon} - 1\right) \ , \tag{4.18}$$

where

$$\varepsilon = \gamma + \delta + d \ . \tag{4.19}$$

From the 4^{th} equation, in the system (4.17) subject to $\frac{dV}{dt} = 0$, we obtain

$$0 = \alpha I - V\left\{N\rho + \psi\right\} \ ,$$

$$V = \frac{\alpha I}{N\rho + \psi} \ , \tag{4.20}$$

where

$$N = I + R + S \ , \tag{4.21}$$

$$\psi = \mu + c \ . \tag{4.22}$$

Substituting (4.20) into (4.18), we attain

$$\frac{\rho\pi S(0)V}{\varepsilon I}+\frac{\beta S(0)}{\varepsilon}=\frac{\beta S(0)}{\varepsilon}\left(1+\frac{\rho\pi V}{\beta I}\right)=\frac{\beta S(0)}{\varepsilon}\left(1+\frac{\rho\pi\alpha}{\beta\left(N\rho+\psi\right)}\right)\ . \tag{4.23}$$

Assuming $S(0)=N$ in (4.23), we get

$$R_0=\frac{\beta N}{\varepsilon}\left(1+\frac{\rho\pi\alpha}{\beta\left(N\rho+\psi\right)}\right)\ . \tag{4.24}$$

Start with one infected person, we can have

$\frac{\beta N}{\varepsilon}$: direct transmission to susceptibles and viral shedding, which then infects susceptibles.

$\frac{\alpha}{\varepsilon}$: viral shedding from the host to the environment.

$\frac{\rho\pi\beta N}{\beta(N\rho+\psi)}$: infection of a susceptible from the environment.

It can be noted that if we substitute $N=\frac{\Lambda}{d}$ (or in other words, taking into account the parameter values for disease-free equilibrium ($S=\frac{\Lambda}{d}$, $I=R=V=0$) in (4.24), then we get the expression of R_0:

$$R_0\left(N=\frac{\Lambda}{d}\right)=\frac{\beta\Lambda}{\varepsilon d}\left(1+\frac{\rho\pi\alpha d}{\beta\left(\Lambda\rho+d\psi\right)}\right)\ . \tag{4.25}$$

4.5.1 Derivation of R_0 via next generation matrix

Let's rewrite the system of equations (4.1) in the following form (using the sequence I,V,R,S):

$$\begin{cases}\frac{dI}{dt}=\rho\pi SV+\beta SI-\varepsilon I,\\ \frac{dV}{dt}=\alpha I-V\left\{\left(I+R+S\right)\rho+\psi\right\},\\ \frac{dR}{dt}=\gamma I-dR,\\ \frac{dS}{dt}=\Lambda-\rho\pi SV-\beta SI-dS.\end{cases} \tag{4.26}$$

Consider the following matrices:

$$x = \begin{pmatrix} I \\ V \\ R \\ S \end{pmatrix}, \tag{4.27}$$

$$f = \begin{pmatrix} (\rho\pi V + \beta I) S \\ 0 \\ 0 \\ 0 \end{pmatrix}, \tag{4.28}$$

$$w = \begin{pmatrix} -\varepsilon I \\ \alpha I - V \{(I + R + S) \rho + \psi\} \\ \gamma I - dR \\ \Lambda - \rho\pi SV - \beta SI - dS \end{pmatrix}. \tag{4.29}$$

Further, considering only the variables (I, V), we construct the following matrices:

$$F = \left(\frac{\partial f_i}{\partial x_j}\right) = \begin{pmatrix} \beta S & \rho\pi S \\ 0 & 0 \end{pmatrix}, \tag{4.30}$$

$$W = \left(\frac{\partial w_i}{\partial x_j}\right) = \begin{pmatrix} -\varepsilon & 0 \\ \alpha - \rho V & -\{(I + R + S) \rho + \psi\} \end{pmatrix}, \tag{4.31}$$

where $i, j = 1, 2$, hence, $x_1 = I$, $x_2 = V$. Then

$$det\ W = \varepsilon \{(I + R + S) \rho + \psi\}, \tag{4.32}$$

and

$$W^{-1} = \frac{1}{det\ W} \begin{pmatrix} W_{22} & -W_{12} \\ -W_{21} & W_{11} \end{pmatrix} =$$

$$= \frac{1}{\varepsilon \left\{ (I+R+S)\,\rho + \psi \right\}} \begin{pmatrix} -\left\{ (I+R+S)\,\rho + \psi \right\} & 0 \\ -(\alpha - \rho V) & -\varepsilon \end{pmatrix} . \tag{4.33}$$

Accordingly,

$$FW^{-1} = \begin{pmatrix} -\frac{\beta S\{(I+R+S)\rho+\psi\}+\rho\pi S(\alpha-\rho V)}{\varepsilon\{(I+R+S)\rho+\psi\}} & -\frac{\rho\pi S}{(I+R+S)\rho+\psi} \\ 0 & 0 \end{pmatrix} . \tag{4.34}$$

Now let's find the eigenvalues of the matrix FW^{-1}:

$$\begin{vmatrix} -\frac{\beta S\{(I+R+S)\rho+\psi\}+\rho\pi S(\alpha-\rho V)}{\varepsilon\{(I+R+S)\rho+\psi\}} - \lambda & -\frac{\rho\pi S}{(I+R+S)\rho+\psi} \\ 0 & -\lambda \end{vmatrix} = 0 ,$$

$$\lambda \left(\lambda + \frac{\beta S \left\{ (I+R+S)\,\rho + \psi \right\} + \rho\pi S\,(\alpha - \rho V)}{\varepsilon \left\{ (I+R+S)\,\rho + \psi \right\}} \right) = 0 . \tag{4.35}$$

Subsequently, we have two solutions

$$\lambda_1 = 0 , \tag{4.36}$$

and

$$\lambda_2 = -\frac{\beta S}{\varepsilon} \left(1 + \frac{\rho\pi\,(\alpha - \rho V)}{\beta \left\{ (I+R+S)\,\rho + \psi \right\}} \right) , \tag{4.37}$$

Then, taking into account the parameter values for disease-free equilibrium ($S = \frac{\Lambda}{d}$, $I = R = V = 0$), we get

$$R_0 = |\lambda|_{max} = \frac{\beta\Lambda}{\varepsilon d} \left(1 + \frac{\rho\pi\alpha d}{\beta \left\{ \Lambda\rho + d\psi \right\}} \right) . \tag{4.38}$$

The basic reproduction number is the same at(4.38) as in the previous section in the form (4.25).

4.6 Stability Analysis:

4.6.1 Existence of the disease-free equilibrium

The equilibrium points are determined by the following system of equations

$$\begin{cases} \Lambda - \rho\pi SV - \beta SI - dS = 0 \\ \rho\pi SV + \beta SI - \gamma I - \delta I - dI = 0, \\ \gamma I - dR = 0 \\ \alpha I - V\left\{(I + R + S)\,\rho + \mu + c\right\} = 0. \end{cases} \tag{4.39}$$

Adding the 1^{st} and 2^{nd} equations in (4.39), we obtain

$$\Lambda - dS - (\gamma + \delta + d)\, I = 0 \ ,$$

$$S = \frac{\Lambda - (\gamma + \delta + d)\, I}{d} \ ,$$

$$S = \frac{\Lambda - \varepsilon I}{d} \ , \tag{4.40}$$

where

$$\varepsilon = \gamma + \delta + d \ . \tag{4.41}$$

From the 3^{rd} equation in the system (4.39) we have

$$R = \frac{\gamma}{d} I \ . \tag{4.42}$$

Substituting (4.40) and (4.42) in the 4^{th} equation (4.39), we obtain

$$\alpha I - V\left\{\left(I + \frac{\gamma}{d}I + \frac{\Lambda - \varepsilon I}{d}\right)\rho + \mu + c\right\} = 0 \ ,$$

$$\alpha I - V\left\{\frac{\Lambda - \delta I}{d}\rho + \mu + c\right\} = 0 \ ,$$

$$V = \frac{\alpha d I}{(\Lambda - \delta I)\,\rho + d\psi} \ , \tag{4.43}$$

where

$$\psi = \mu + c \ . \tag{4.44}$$

Then from the 2^{nd} equation (4.39) we obtain

$$(\rho\pi V + \beta I)\,S - \varepsilon I = 0 \ ,$$

$$\left(\rho\pi\frac{\alpha d I}{(\Lambda - \delta I)\,\rho + d\psi} + \beta I\right)\frac{\Lambda - \varepsilon I}{d} - \varepsilon I = 0 \ ,$$

or

$$I\left[\left(\frac{\alpha\pi\rho d}{(\Lambda - \delta I)\,\rho + d\psi} + \beta\right)\frac{\Lambda - \varepsilon I}{d} - \varepsilon\right] = 0 \ . \tag{4.45}$$

From equation (4.45) it follows that one of the roots is

$$I = 0 \ . \tag{4.46}$$

Then from (4.40), (4.42) and (4.43) we obtain

$$S = \frac{\Lambda}{d} \ , \tag{4.47}$$

$$R = 0 \ , \tag{4.48}$$

$$V = 0 \ . \tag{4.49}$$

Formulas (4.46), (4.47),(4.48), and (4.49) correspond to the disease-free equilibrium

$$(\frac{\Lambda}{d}, 0, 0, 0). \tag{4.50}$$

4.6.2 Local stability of the disease-free equilibrium

Let's consider the Jacobian of the system (4.39)

$$J = \begin{pmatrix} -\rho\pi V - \beta I - d & -\beta S & 0 & -\rho\pi S \\ \rho\pi V + \beta I & \beta S - \varepsilon & 0 & \rho\pi S \\ 0 & \gamma & -d & 0 \\ -\rho V & \alpha - \rho V & -\rho V & -\{(I + R + S)\,\rho + \psi\} \end{pmatrix}. \tag{4.51}$$

Substituting (4.50) into (4.51) yields

$$J_0 = \begin{pmatrix} -d & -\frac{\beta\Lambda}{d} & 0 & -\frac{\rho\pi\Lambda}{d} \\ 0 & \frac{\beta\Lambda}{d} - \varepsilon & 0 & \frac{\rho\pi\Lambda}{d} \\ 0 & \gamma & -d & 0 \\ 0 & \alpha & 0 & -\left(\frac{\Lambda\rho}{d} + \psi\right) \end{pmatrix}. \tag{4.52}$$

Next, we solve the characteristic equation

$$|J_0 - \lambda E| = 0 \ ,$$

$$\begin{vmatrix} -d-\lambda & -\frac{\beta\Lambda}{d} & 0 & -\frac{\rho\pi\Lambda}{d} \\ 0 & \frac{\beta\Lambda}{d}-\varepsilon-\lambda & 0 & \frac{\rho\pi\Lambda}{d} \\ 0 & \gamma & -d-\lambda & 0 \\ 0 & \alpha & 0 & -\left(\frac{\Lambda\rho}{d}+\psi\right)-\lambda \end{vmatrix} = 0,$$

or

$$(\lambda+d)^2\left[\lambda^2+\left\{\varepsilon+\psi+\frac{\Lambda}{d}(\rho-\beta)\right\}\lambda+\left(\varepsilon-\frac{\beta\Lambda}{d}\right)\left(\frac{\Lambda\rho}{d}+\psi\right)-\frac{\rho\pi\Lambda}{d}\alpha\right]=0. \tag{4.53}$$

Equation (4.53) has the following solutions

$$\lambda_1 = -d\ , \tag{4.54}$$

$$\lambda_2 = -d\ , \tag{4.55}$$

$$\lambda_3 = \frac{1}{2}\left[\frac{\Lambda}{d}(\beta-\rho)-\varepsilon-\psi+\sqrt{\left\{\varepsilon-\psi-\frac{\Lambda}{d}(\beta+\rho)\right\}^2+4\frac{\rho\pi\Lambda}{d}\alpha}\right]\ , \tag{4.56}$$

$$\lambda_4 = \frac{1}{2}\left[\frac{\Lambda}{d}(\beta-\rho)-\varepsilon-\psi-\sqrt{\left\{\varepsilon-\psi-\frac{\Lambda}{d}(\beta+\rho)\right\}^2+4\frac{\rho\pi\Lambda}{d}\alpha}\right]\ . \tag{4.57}$$

From (4.54), (4.55) and (4.57) it is clear that $\lambda_1 < 0$, $\lambda_2 < 0$, since $d > 0$.

Let's find when $\lambda_3 = 0$:

$$\frac{1}{2}\left[\frac{\Lambda}{d}(\beta-\rho)-\varepsilon-\psi+\sqrt{\left\{\varepsilon-\psi-\frac{\Lambda}{d}(\beta+\rho)\right\}^2+4\frac{\rho\pi\Lambda}{d}\alpha}\right]=0\ ,$$

$$\left\{\varepsilon-\psi-\frac{\Lambda}{d}(\beta+\rho)\right\}^2+4\frac{\rho\pi\Lambda}{d}\alpha=\left\{\varepsilon+\psi-\frac{\Lambda}{d}(\beta-\rho)\right\}^2\ ,$$

$$4\frac{\rho\pi\Lambda}{d}\alpha=4\left(\varepsilon-\frac{\beta\Lambda}{d}\right)\left(\frac{\Lambda\rho}{d}+\psi\right)\ ,$$

$$\frac{\rho\pi\alpha d}{\beta\left(\Lambda\rho + d\psi\right)} = \frac{\varepsilon d}{\Lambda\beta} - 1 \ ,$$

$$\frac{\beta\Lambda}{\varepsilon d}\left(1 + \frac{\rho\pi\alpha d}{\beta\left(\Lambda\rho + d\psi\right)}\right) = 1 \ ,$$

Then,

$$R_0 = \frac{\beta\Lambda}{\varepsilon d}\left(1 + \frac{\rho\pi\alpha d}{\beta\left(\Lambda\rho + d\psi\right)}\right) \ . \tag{4.58}$$

Hence, if $R_0 > 1$, then $\lambda_3 > 0$ and if $R_0 < 1$, thus $\lambda_3 < 0$. Therefore, the disease-free equilibrium (DFE) is locally asymptotically stable if $R_0 < 1$ and unstable if $R_0 > 1$.

Furthermore, the fact that $\lambda_4 < 0$ is seen from formula (4.57). There are two cases:

The first case - suppose that $\varepsilon - \psi - \frac{\Lambda}{d}\left(\beta + \rho\right) \geq 0$, then λ_4 can be written as:

$$\lambda_4 = \frac{1}{2}\left[-\left\{\varepsilon - \psi - \frac{\Lambda}{d}\left(\beta + \rho\right)\right\} - 2\frac{\Lambda}{d}\rho - 2\psi - \right.$$
$$\left. -\sqrt{\left\{\varepsilon - \psi - \frac{\Lambda}{d}\left(\beta + \rho\right)\right\}^2 + 4\frac{\rho\pi\Lambda}{d}\alpha}\right] \ .$$

The first term is ≤ 0, and the other three are < 0, so we can get that $\lambda_4 < 0$.

The second case - suppose that $\varepsilon - \psi - \frac{\Lambda}{d}\left(\beta + \rho\right) < 0$, then

$$\sqrt{\left\{\varepsilon - \psi - \frac{\Lambda}{d}\left(\beta + \rho\right)\right\}^2 + 4\frac{\rho\pi\Lambda}{d}\alpha} > \left|\varepsilon - \psi - \frac{\Lambda}{d}\left(\beta + \rho\right)\right| \ ,$$

that is,

$$\sqrt{\left\{\varepsilon - \psi - \frac{\Lambda}{d}\left(\beta + \rho\right)\right\}^2 + 4\frac{\rho\pi\Lambda}{d}\alpha} > -\varepsilon + \psi + \frac{\Lambda}{d}\left(\beta + \rho\right) \ .$$

Then, λ_4 can be written as:

$$\lambda_4 < \frac{1}{2}\left[\frac{\Lambda}{d}\left(\beta - \rho\right) - \varepsilon - \psi - \left(-\varepsilon + \psi + \frac{\Lambda}{d}\left(\beta + \rho\right)\right)\right] = -\psi - \frac{\Lambda}{d}\rho < 0 \ .$$

Hence, $\lambda_4 < 0$.

4.6.3 Global stability of the disease-free equilibrium

Assume that $\Gamma = \left\{(S, I, R, V) : S \geq 0, I \geq 0, R \geq 0, V \geq 0, N \leq \frac{\Lambda}{d}\right\}$. From item 4.6.2 we know that if $0 < R_0 < 1$, the DFE is locally asymptotically stable. According to Perko [151], any solution of model system (4.1) starting in Γ must approach either an equilibrium or a closed orbit in Γ. With reference to Kelley and Peterson [152], if the solution path approaches a closed orbit, then this closed orbit must enclose equilibrium. Since at $0 < R_0 < 1$, DFE (4.50) is located in the boundary of Γ, therefore there is no closed orbit in Γ. Hence, any solution of system (4.1) with initial condition in Γ must approach the point DFE as $t \to \infty$. Thus, the DFE is globally asymptotically stable in Γ when $0 < R_0 < 1$. When $R_0 > 1$ the DFE is globally asymptotically unstable.

4.6.4 Existence of the endemic disease equilibrium

In part 4.6.1, we considered one of the possible solutions to equation (4.45). Now consider the second solution, which is found from the equation

$$\left(\frac{\alpha\pi\rho d}{(\Lambda - \delta I)\,\rho + d\psi} + \beta\right)\frac{\Lambda - \varepsilon I}{d} - \varepsilon = 0\ . \tag{4.59}$$

Solving the equation (4.59), we obtain

$$\left[\alpha\pi\rho + \frac{\beta}{d}\left\{(\Lambda - \delta I)\,\rho + d\psi\right\}\right](\Lambda - \varepsilon I) - \varepsilon\left\{(\Lambda - \delta I)\,\rho + d\psi\right\} = 0\ ,$$

$$\beta\varepsilon\delta\rho I^2 + \left\{(\varepsilon d - \Lambda\beta)\,\delta\rho - \beta\varepsilon\,(\Lambda\rho + d\psi) - \alpha\pi\rho\varepsilon d\right\} I +$$

$$+\left\{(\Lambda\beta-\varepsilon d)(\Lambda\rho+d\psi)+\alpha\pi\rho\Lambda d\right\}=0\ . \quad (4.60)$$

We got the quadratic equation. The discriminant of the equation (4.60) has the form:

$$D=\left[(\varepsilon d-\Lambda\beta)\delta\rho-\beta\varepsilon(\Lambda\rho+d\psi)-\alpha\pi\rho\varepsilon d\right]^2-$$
$$-4\beta\varepsilon\delta\rho\left\{(\Lambda\beta-\varepsilon d)(\Lambda\rho+d\psi)+\alpha\pi\rho\Lambda d\right\}=$$

$$=\left[(\varepsilon d-\Lambda\beta)\delta\rho+\beta\varepsilon(\Lambda\rho+d\psi)-\alpha\pi\rho\varepsilon d\right]^2+$$
$$+4\beta\varepsilon\alpha\pi\rho d\left\{\Lambda\rho(\gamma+d)+\varepsilon d\psi\right\} \quad (4.61)$$

From the expression (4.61) it is clear that $D>0$, therefore, equation (4.60) has two solutions:

$$I=\frac{1}{2\beta\varepsilon\delta\rho}\left\{-\left[(\varepsilon d-\Lambda\beta)\delta\rho-\beta\varepsilon(\Lambda\rho+d\psi)-\alpha\pi\rho\varepsilon d\right]\pm\sqrt{D}\right\}\ . \quad (4.62)$$

Since we need $I>0$, $S>0$, $R>0$ and $V>0$, then in (4.62) we select the the negative root. As a result, we get a solution

$$I=-\sqrt{\left[\frac{\varepsilon d-\Lambda\beta}{2\beta\varepsilon}+\frac{\Lambda\rho+d\psi}{2\delta\rho}-\frac{\alpha\pi d}{2\beta\delta}\right]^2+\frac{\alpha\pi d}{\beta\varepsilon\delta^2\rho}\left\{\Lambda\rho(\gamma+d)+\varepsilon d\psi\right\}}+$$
$$+\left[\frac{\Lambda\rho+d\psi}{2\delta\rho}-\frac{\varepsilon d-\Lambda\beta}{2\beta\varepsilon}+\frac{\alpha\pi d}{2\beta\delta}\right]\ . \quad (4.63)$$

The remaining parameters S, R, V corresponding to the new equilibrium can be found by formulas (4.40), (4.42) and (4.43).

Then, endemic disease equilibrium can be written as

$$EDE=Eq^{+}=(S^{**},I^{**},R^{**},V^{**}).$$

Thus,

$$EDE = (\frac{\Lambda - \varepsilon(\frac{1}{2\beta\varepsilon\delta\rho}\left\{-\left[(\varepsilon d - \Lambda\beta)\,\delta\rho - \beta\varepsilon\,(\Lambda\rho + d\psi) - \alpha\pi\rho\varepsilon d\right] \pm \sqrt{D}\right\}\ )}{d},$$
$$\frac{1}{2\beta\varepsilon\delta\rho}\left\{-\left[(\varepsilon d - \Lambda\beta)\,\delta\rho - \beta\varepsilon\,(\Lambda\rho + d\psi) - \alpha\pi\rho\varepsilon d\right] \pm \sqrt{D}\right\},$$
$$\frac{\gamma}{d}[\frac{1}{2\beta\varepsilon\delta\rho}\left\{-\left[(\varepsilon d - \Lambda\beta)\,\delta\rho - \beta\varepsilon\,(\Lambda\rho + d\psi) - \alpha\pi\rho\varepsilon d\right] \pm \sqrt{D}\right\}],$$
$$\frac{\alpha d(\frac{1}{2\beta\varepsilon\delta\rho}\left\{-\left[(\varepsilon d - \Lambda\beta)\,\delta\rho - \beta\varepsilon\,(\Lambda\rho + d\psi) - \alpha\pi\rho\varepsilon d\right] \pm \sqrt{D}\right\})}{\left(\Lambda - \delta(\frac{1}{2\beta\varepsilon\delta\rho}\left\{-\left[(\varepsilon d - \Lambda\beta)\,\delta\rho - \beta\varepsilon\,(\Lambda\rho + d\psi) - \alpha\pi\rho\varepsilon d\right] \pm \sqrt{D}\right\})\right)\rho + d\psi}). \quad (4.64)$$

4.7 Conclusion

An environmental infection transmission system framework $SIRV$ has been analyzed to understand the impact of human interaction with pathogens in the environment. It is described as a step forward into enhanced evaluation of environmental intervention strategies, interpretation of active network, and improved utilisation environmental composites to investigate transmission.

The environment factors are the infection elimination rate, μ, the rate at which people pick up ρ, and deposit infectious agents, α. They show whether spread of the pathogens, is density dependent (orienting), frequency dependent (high proportion), or a combination of the two.

The increasing environmental proportion, $\frac{\alpha}{\gamma}$, indicates cumulative agent deposition for every infection and the probability of an epidemic, where γ is specified as the recovery rate. These findings give theoretical frameworks for investigating the role of the environment in disease transmission, as well as a methodology for interpreting environmental evidence to guide environmental interventions.

Chapter 5

Public Health Education Mathematical Model

5.1 Introduction

The aim of this study is demonstrating the successful public awareness campaigns which minimizing the incidence of infection. Making individuals aware of the preventative measures as early as necessary is an effective way of slowing the spread of the disease. We establish and analyze a mathematical model for the dynamics of the MERS-CoV infection, including public health education. The basic reproduction number R_E is derived and used to assess once the epidemic breaks out in the community which occurs in an endemic equilibrium or dies out of a disease-free state. Numerical analyses are provided to demonstrate our theoretical predictions. Analytical and empirical findings indicate that public health awareness is a very successful prevention mechanism for the eradication of a MERS-CoV infestation in large endemic populations. This study investigates the effectiveness of public health strategies on the dynamics of disease spread among a population.

In KSA, the public health used a variety of novel treatments including immunosuppressants

and antivirals for MERS-CoV patients. For example, many patients received broad-spectrum antibiotics and hydrocortisone , and others were treated with interferon beta or alpha, also another patients got treated by anti-viral combinations as mycophenolate mofetil, or extracorporeal membrane oxygenationc for those patients who required intensive care unit (ICU) care [153].

During 2014, the evaluation of this suggestion among a large cohort of MERS-CoV patients was assessed in the Jeddah region of KSA [154]. The researchers identified that, according to the responders, the most significant reproductive-disorder is uterine infection (60.2%) followed by obesity (22.3%) biological conditions adhesions (3.9%), hormonal disturbances (7.8%), and repeat breeders (2.9)%. Of the camel herders, 46% described cases in the last season between 2015 and 2016, while 78.6% reported that preceding occurrence of abortion in their herds and incidence of no history of absorption is 21.4% [155]. Therefore, applying health education strategies are very important to reduce the disease cases. Another study designated the medical and clinical features of all 186 patients with confirmed cases of MERS-CoV infection during the epidemic in the Republic of Korea. The researchers compared the medical features of the deceased and clinical characteristics of survivors for 28 days at the beginning of the epidemic. The intermediate ages of the patients were 55 years and male patients were predominant over female patients. The total patients had a co-existing medical condition including diabetes and solid organ malignancy [156] 39 patients (approximately 21.0%) were healthcare workers were most shared is 38.6% and these two cases approximately 1.1% were asymptomatic. The comparison with the deceased and survivors was more frequent and older had a co-existing medical conditions.

Researchers also reported involvement with (MERS-CoV) infection in Saudi Arabia at a single centre. Seventy successive patients were analysed, with patients mostly being older (having a median age of 62 years), while the male is 46, 65.7% that had the health-care achievement of infection of 39, and 55.7%. They included, the patient with dyspnea are 42,

60%, with cough 38, 54.3% and fever (43, 61.4%), and all these symptoms are concluded in the most common symptoms. The number who developed pneumonia is 63 (90%) and those that may require intensive care is 49 (70%). The infections occurred commonly in clusters. The liberated risk factors for severe infection that may demand intensive care (which included associated infections, including odds ratio (OR)) is 14.13, (95%) with low albumin (Odd Ratio-6.31, 95% confidence of interval 1.24 to 31.90; p = 0.026 and also has different confidence interval (CI) 1.58 to 126.09, p = 0.018). The mortality was high at 42, (60%), with an age of 65 years or older linked with greater mortality; The Odds Ratio is 4.39, 95% with the confidence of Interval 2.13-9.05; p = 0.001. By this, researchers conclude that the MERS-CoV can form the basis for severe infection that has high mortality and requires concentrated care. The low albumin and the related infections were established to be interpreters. The simple infection at the age of 65 years was the only forecaster of increased mortality [157]. The epidemiological studies recognized diabetes as the main comorbidity connected with lethal and severe MERS-CoV infection.

Public health initiatives are crucial in identifying health concerns because they operate as a key source of knowledge and impact changes in people's behaviour. As a result, it is important to investigate epidemic transmission and devise effective prevention, control, and containment measures. Individuals' reactions to a disease threat are primarily determined by risk perception, which is obtained essentially from information given to the public by the authorities, such as the number of infections, hospitalizations, and fatalities recorded by the public health department [158, 159]. The guidelines for infection prevention, control, and public health education program for (MERS-CoV) Infection was adopted from the ministry of health in KSA [160].

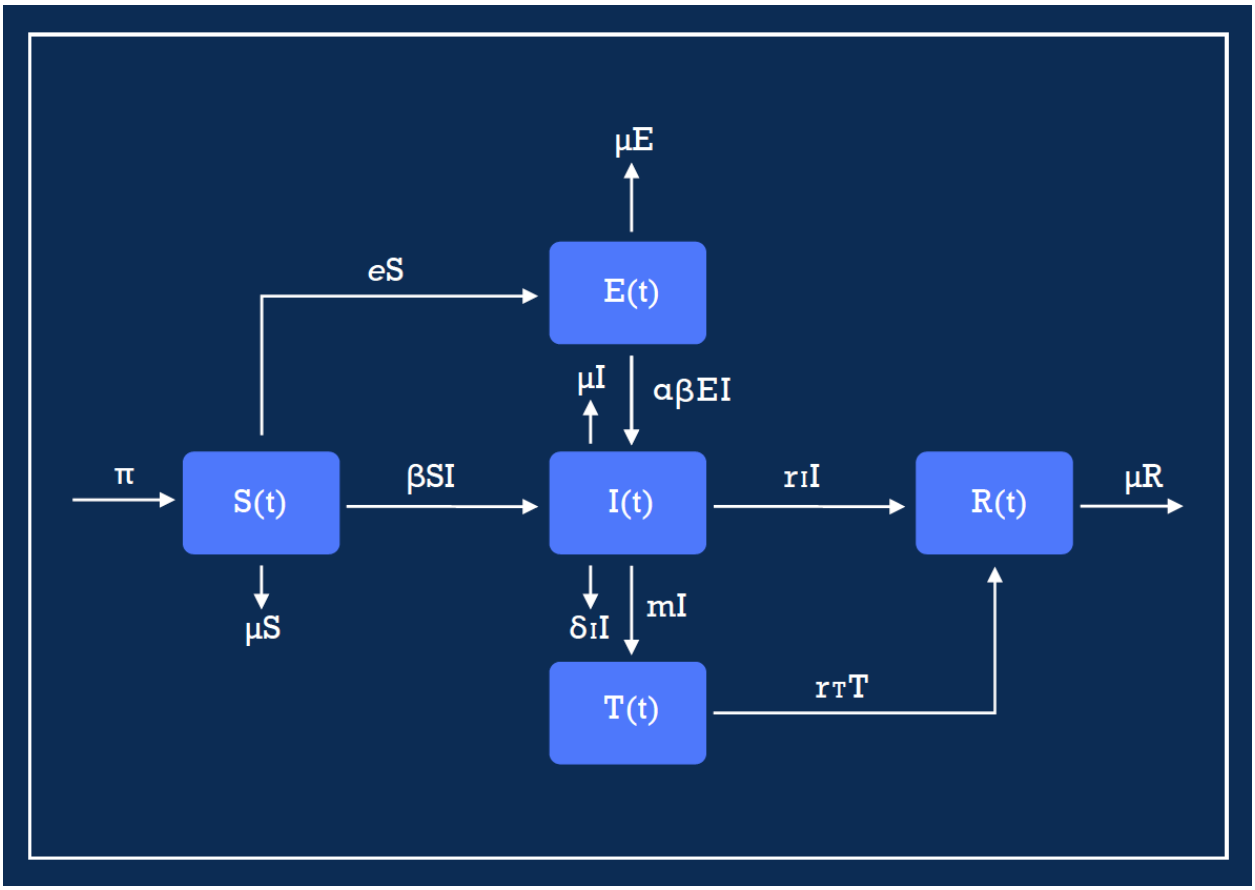

Figure 5.1: Flow chart for Public Health Education Mathematical Model.

5.2 Model Formulation

To model the dynamics of the population, we split the population into a number of distinct compartments. At time t each compartment is defined as $S(t)$: Susceptible, $E(t)$: Educated, $I(t)$: Infected, $T(t)$: Treated, and $R(t)$: Recovered. The population satisfies the system of differential equations

$$\left.\begin{aligned}
\frac{dS}{dt} &= \pi - \beta SI - (e+\mu)S\,, \\
\frac{dE}{dt} &= eS - \alpha\beta EI - \mu E\,, \\
\frac{dI}{dt} &= \beta SI + \alpha\beta EI - (m + d_I + r_I + \mu)I\,, \\
\frac{dT}{dt} &= mI - (d_T + r_T + \mu)T\,, \\
\frac{dR}{dt} &= r_I I + r_T T - \mu R\,.
\end{aligned}\right\} \tag{5.1}$$

The parameters be defined in the table 5.1 as

Parameters List	
Parameter	Description
π	Recruitment rate.
μ	The rate of the natural death.
e	Intervention program of public health and disseminate strategies education.
α	The effect of reducing the infection due to public health education.
β	Disease transmission contact rate.
m	The rate of movement from being infected to be in treated.
d_I	The death rate from infected individuals.
d_T	The death rate from treated individuals.
r_I	The recovery rate from infected individuals.
r_T	The recovery rate from treated individuals.

Table 5.1: Parameters description for public health education mathematical model

The awareness techniques of public health propagate to susceptible individuals is given by

the parameter e. As the may not be permanent or the techniques used may not be particularly successful, the experience of taking control measures slowly wears off, and so on through this process. The impact of instructional approaches will be decreased, and then informed people infected at a lower rate $\alpha\beta EI$, where $0 < \alpha < 1$. Community health awareness decreases individual infection by fraction α . So, in this work, $0 < \alpha < 1$ because $\alpha = 0$ means public health education is completely effective in preventing $MERS - CoV$ infection, and $\alpha = 1$ implies education is not sufficient [161].

where the total population is denoted as

$$N(t) = S(t) + E(t) + I(t) + T(t) + R(t). \tag{5.2}$$

In order to simplify some of the equations in the subsequent linear stability analysis, we define

$$\left.\begin{aligned} D_1 &= e + \mu, \\ D_2 &= m + d_I + r_I + \mu, \\ D_3 &= d_T + r_T + \mu\,, \end{aligned}\right\} \tag{5.3}$$

so that the model 5.1 can be written as

$$\left.\begin{aligned} \frac{dS}{dt} &= \pi - \beta SI - D_1 S, \\ \frac{dE}{dt} &= eS - \alpha\beta EI - \mu E, \\ \frac{dI}{dt} &= \beta SI + \alpha\beta EI - D_2 I, \\ \frac{dT}{dt} &= mI - D_3 T, \\ \frac{dR}{dt} &= r_I I + r_T T - \mu R\,. \end{aligned}\right\} \tag{5.4}$$

Since the system (5.4) demonstrate a human population, it is important that all its state

variables and associated parameters are non-negative for all time, t. Hence, the following non-negativity result holds for the state variables in the model (5.4).

5.3 Positivity and Boundedness

Theorem 5.3.1. *Let the initial conditions for the model (5.4) be $S(0) > 0$, $E(0) > 0$, $I(0) > 0$, $T(0) > 0$, and $R(0) > 0$. Solutions $(S(t), E(t), I(t), T(t), R(t))$ of the model (5.4), with positive initial conditions, will remain positive for all time $t > 0$.*

Proof. Let

$$t_1 = \sup\{t > 0 : S > 0, E > 0, I > 0, T > 0, R > 0\} > 0.$$

That is, since we are dealing with humans, all the sub populations must be non negative and the positivity must not fail in order to for the model to be realistic. The first equation of system (5.4) is

$$\frac{dS}{dt} = \pi - \beta SI - D_1 S\,,$$

which we rewrite it as

$$\frac{dS}{dt} + D_1 S + \phi S = \pi, \tag{5.5}$$

where $\phi = \beta I$. We solve equation (5.5) by using the integrating factor

$$\psi = \exp\left(D_1 t + \int_0^t \phi(\tau) d\tau\right). \tag{5.6}$$

Multiplying through by ψ, and after some simplification, we have

$$\frac{d}{dt}\left[S(t)exp\left(D_1t+\int_0^t\phi(\tau)d\tau\right)\right]=\pi\left[exp\left(D_1t+\int_0^t\phi(\tau)d\tau\right)\right]. \tag{5.7}$$

Therefor, integrating from $t=0$ to t_1 yields

$$\begin{aligned}S(t_1)=S(0)\exp\left(-D_1t_1-\int_0^{t_1}\phi(\tau)d\tau\right)\\ +\pi\exp\left(-D_1t_1-\int_0^{t_1}\phi(\tau)d\tau\right)\int_0^{t_1}\exp\left(D_1s+\int_0^s\phi(\tau)d\tau\right)ds>0.\end{aligned} \tag{5.8}$$

In particular, the trivial cases are expressed in the following:

$$\begin{aligned}\dot{E}(t)\geq-\mu E\Longrightarrow E(t)>0,\\ \dot{I}(t)\geq-D_2I\Longrightarrow I(t)>0,\\ \dot{T}(t)\geq-D_3T\Longrightarrow T(t)>0,\\ \dot{R}(t)\geq-\mu R\Longrightarrow R(t)>0,\end{aligned}$$

provided that the initial conditions $E(0)>0, I(0)>0, T(0)>, R(0)>0$. □

The dynamics of the model (5.4) are analyzed in the following invariant region:

$$\mathcal{D}_1=\left\{(S,E,I,T,R)\in\mathcal{R}_+^5:\left\{N\leq\frac{\pi}{\mu}\right\}\right\}. \tag{5.9}$$

We claim that

Lemma 5.3.1. *The domain $\mathcal{D}_1$ is positively invariant and an attractor of all positive solutions of the system (5.4).*

Proof. The total population N satisfies

$$\frac{dN}{dt} = \frac{dS}{dt} + \frac{dE}{dt} + \frac{dI}{dt} + \frac{dT}{dt} + \frac{dR}{dt}\,. \tag{5.10}$$

Substituting each term in (5.4) into (5.10), the rate of change of the total population, at (5.10) give

$$\begin{aligned}\frac{dN}{dt} &= \pi - \mu N - d_I I - d_T T,\\ &\leq \pi - \mu N.\end{aligned}$$

Since the right hand side of the above inequality is bounded by $\pi - \mu N$, a standard theorem (see, e.g., [162]) establishes that

$$\frac{dN}{dt} \leq \frac{\pi}{\mu} + \left(N_0 - \frac{\pi}{\mu}\right)\exp(-\mu t).$$

If $N(0) \leq \frac{\pi}{\mu}$, this implies that $N_H(t) \leq \frac{\pi}{\mu}$ for all time $t > 0$. Furthermore, if $N(0) > \frac{\pi}{\mu}$, then the solution will either enter the domain $\mathcal{D}_1$ in finite time, or $N(t) \to \frac{\pi}{\mu}$ as time t tends to infinity. Thus, $\mathcal{D}_1$ attracts all the solutions in $\mathcal{R}^5_+$. Since the domain $\mathcal{D}_1$ is positively-invariant, it is sufficient to consider the dynamics of model (5.4) in $\mathcal{D}_1$. In this region, the model (5.4) can be considered as being both epidemiologically and mathematically well posed [163]. □

5.4 Disease free equilibrium

In this section we establish the disease free dynamics of the system. This can be obtained by setting $d_I = d_T = 0$, and thus

$$\frac{dN}{dt} = \pi - \mu N, \tag{5.11}$$

which we rearrange, and multiple by the integrating factor $e^{\mu t}$ to yield

$$\frac{d}{dt}\left(Ne^{\mu t}\right) = \pi e^{\mu t}\,. \tag{5.12}$$

Setting the initial population to be $N(0) = N_0$, we integrate to an arbitrary positive time t to obtain the solution

$$N(t)e^{\mu t} - N(0)e^{\mu 0} = \frac{\pi}{\mu}\left(e^{\mu t} - e^{\mu 0}\right)\,. \tag{5.13}$$

Solving for $N(t)$, we get

$$N(t) = \frac{\pi}{\mu} + (N_0 - \frac{\pi}{\mu})e^{-\mu t}\,. \tag{5.14}$$

Taking the limit as $t \to \infty$, we see that

$$N \to \frac{\pi}{\mu}\,, \tag{5.15}$$

which is also known as the carrying capacity of the population. Indeed this may also be computed by setting $\frac{dN}{dt} = 0$ in (5.11) and solving for N.

Case 1: Since S is bounded by N (that is, $S \leq N$), then the DFE, E_0 (when $e = 0$), can be expressed as

$$E_0 : (S, E, I, T, R) = \left(\frac{\pi}{\mu}, 0, 0, 0, 0\right).$$

Case 2: Where $E^* \neq 0$ and $I^* = 0$. We do this by setting the equations in system (5.4) to zero.

$$0 = \pi - \beta S^* I^* - D_1 S^*, \tag{5.16}$$

$$0 = eS^* - \mu E^*, \tag{5.17}$$

$$0 = \beta S^* I^* - D_2 I^*, \tag{5.18}$$

$$0 = mI^* - D_3 T^*, \tag{5.19}$$

$$0 = r_I I^* + r_T T^* - \mu R^*. \tag{5.20}$$

Solving equations (5.16), (5.17), (5.18), and (5.20) in terms of I, we have

$$\left.\begin{aligned} S^* &= \frac{\pi}{\beta I^* + D_1}, \\ E^* &= \frac{\pi e}{(\beta I^* + D_1)\,\mu}, \\ T^* &= \frac{mI^*}{D_3}, \\ R^* &= \frac{D_3 r_I I^* + m r_T I^*}{\mu D_3}. \end{aligned}\right\} \tag{5.21}$$

When $I^* = 0$ in (5.21), we have

$$\left.\begin{aligned} S^* &= \frac{\pi}{D_1}, \\ E^* &= \frac{\pi e}{\mu D_1}, \\ I^* &= 0, \\ T^* &= 0, \\ R^* &= 0. \end{aligned}\right\} \tag{5.22}$$

Hence, the second case of the DFE, is given by

$$E_I : (S^*, E^*, I^*, T^*, R^*) = \left(\frac{\pi}{D_1}, \frac{\pi e}{\mu D_1}, 0, 0, 0\right). \tag{5.23}$$

5.5 Basic reproduction number

The basic reproduction number of the model, R_0, is determined using the next generation matrix approach of Driessche and Watmough [164] at the DFE, E_0 and E_I. This is given by

$$R_0 = \rho(FV^{-1}),$$

where $\rho(A)$ denotes the spectral radius of the matrix A. The basic reproduction number is the average number of infected individuals that contract infection from one infected individual during the period of infection in a susceptible population Driessche and Watmough [164]. From the system (5.4), we do the following computations. We then respectively find F, V

and V^{-1}:

$$\mathbb{F} = \begin{pmatrix} 0 \\ (\beta S + \alpha\beta E)I \\ mI \end{pmatrix}, \quad \mathbb{V} = \begin{pmatrix} \mu E \\ D_2 I \\ D_3 T \end{pmatrix}.$$

or,

$$F = \begin{pmatrix} 0 & 0 & 0 \\ \alpha\beta I & \beta S + \alpha\beta E & 0 \\ 0 & m & 0 \end{pmatrix}, \quad V = \begin{pmatrix} \mu & 0 & 0 \\ 0 & D_2 & 0 \\ 0 & 0 & D_3 \end{pmatrix}.$$

Thus,

$$V^{-1} = \begin{pmatrix} \frac{1}{\mu} & 0 & 0 \\ 0 & \frac{1}{D_2} & 0 \\ 0 & 0 & \frac{1}{D_3} \end{pmatrix}.$$

Finally we have,

$$FV^{-1} = \begin{pmatrix} 0 & 0 & 0 \\ \alpha\beta I & \frac{\beta S + \alpha\beta E}{D_2} & 0 \\ 0 & \frac{m}{D_2} & 0 \end{pmatrix}.$$

Thus, the basic reproduction number R_0 for the DFE, E_0, in the absence of education intervention or public health intervention is

$$R_0 = \frac{\pi\beta}{\mu D_2}. \tag{5.24}$$

While the basic reproduction number R_E for the DFE, E_I, in the presence of education intervention and public health intervention is

$$R_E = \frac{\beta\pi\left[\mu + \alpha e\right]}{\mu D_1 D_2}. \tag{5.25}$$

The threshold quantities, R_0 and R_E, are the effective reproduction number for the system (5.4). More importantly, R_0 measures the average number of newly recruited susceptible individuals into the infected classes generated by a single infected member in the population in the absence of education intervention or public health intervention, although R_E applies in the presence of education intervention and public health intervention.

5.6 Local stability of the DFE

In this section, the Jacobian matrix of the model described by (5.4) is given by

$$J = \begin{bmatrix} -\beta I - D_1 & 0 & -\beta S & 0 & 0 \\ e & -\alpha\beta I - \mu & -\alpha\beta E & 0 & 0 \\ \beta I & \alpha\beta I & \beta S + \alpha\beta E - D_2 & 0 & 0 \\ 0 & 0 & m & -D_3 & 0 \\ 0 & 0 & r_I & r_T & -\mu \end{bmatrix}. \tag{5.26}$$

Evaluating (5.26) at E_0, and expressing in the form $J(E_0)-\lambda I$, where I is the identity matrix yields

$$J(E_0)-\lambda I=\begin{bmatrix} -D_1-\lambda & 0 & -\frac{\pi\beta}{\mu} & 0 & 0 \\ e & -\mu-\lambda & 0 & 0 & 0 \\ 0 & 0 & -(D_2-\frac{\pi\beta}{\mu})-\lambda & 0 & 0 \\ 0 & 0 & m & -D_3-\lambda & 0 \\ 0 & 0 & r_I & r_T & -\mu-\lambda \end{bmatrix}. \tag{5.27}$$

We take the determinant of the system (5.27), expressed as $|J(E_0)-\lambda I|$ to yield

$$\begin{aligned} \mid J(E_0)-\lambda I \mid &= (-D_1-\lambda)(-\mu-\lambda)(-D_3-\lambda)(-\mu-\lambda)\left[-(D_2-\frac{\pi\beta}{\mu})-\lambda\right], \\ &= (D_1+\lambda)(\mu+\lambda)(D_3+\lambda)(\mu+\lambda)\left[D_2\left(1-\frac{\pi\beta}{\mu D_2}\right)+\lambda\right], \\ &= (D_1+\lambda)(\mu+\lambda)(D_3+\lambda)(\mu+\lambda)\left[D_2\left(1-R_0\right)+\lambda\right]. \end{aligned}$$

When $R_0<1$, then the eigenvalues values $\lambda_i<0$ for $i=1,2,3,4,5$. Hence, the model (5.4) at E_0 is locally asymptotically stable (LAS) when all the zeros of $\mid J(E_0)-\lambda I \mid$ have negative real parts, and this occurs if and only if $R_0<1$. Note also that if $R_0>1$, then exactly one of the zeros of $\mid J(E_0)-\lambda l \mid$ has positive real part. Similarly, evaluating (5.26) at E_I, and expressing in the form $J(E_I)-\lambda I$, we have

$$J=\begin{bmatrix} -D_1 & 0 & -\beta S & 0 & 0 \\ e & -\mu & -\alpha\beta E & 0 & 0 \\ 0 & 0 & \beta S+\alpha\beta E-D_2 & 0 & 0 \\ 0 & 0 & m & -D_3 & 0 \\ 0 & 0 & r_I & r_T & -\mu \end{bmatrix}. \tag{5.28}$$

$$
\begin{aligned}
\mid J(E_I) - \lambda I \mid &= (-D_1 - \lambda)(-\mu - \lambda)(-D_3 - \lambda)(-\mu - \lambda)\left[-(D_2 - \beta S^* - \alpha\beta E^*) - \lambda\right] \\
&= (D_1 + \lambda)(\mu + \lambda)(D_3 + \lambda)(\mu + \lambda)\left[D_2\left(1 - \frac{\beta S^* + \alpha\beta E^*}{D_2}\right) + \lambda\right] \\
&= (D_1 + \lambda)(\mu + \lambda)(D_3 + \lambda)(\mu + \lambda)\left[D_2\left(1 - R_E\right) + \lambda\right] .
\end{aligned}
$$

Hence, we claim the following:

Lemma 5.6.1. *The DFE, E_0 of the model (5.4) is locally asymptotically stable (LAS) if $R_0 < 1$ and unstable if $R_0 > 1$, when $e = 0$.*

Lemma 5.6.2. *The DFE, E_I of the model (5.4) is locally asymptotically stable (LAS) if $R_E < 1$ and unstable if $R_E > 1$.*

5.7 Global Stability of the DFE, E_0

Lemma 5.7.1. *The DFE, E_0, of the model is globally asymptotically stable (GAS) (with $e = \alpha = 0$) if $R_0 \leq 1$.*

Proof. We prove the global asymptotic stability of the DFE, E_0, with the special case $e = \alpha = 0$ by employing the approach of Castillo-Chavez *et al.* [87, 165, 166]. We set up an additional system derived from the model under consideration as

$$
\begin{aligned}
\dot{X}_1 &= F(X_1, X_2) \quad X_1 = (S) \in \mathcal{R}, \\
\dot{X}_2 &= G(X_1, X_2), \quad G(X_1, 0) = 0, \quad X_2 = (E, I, T, R) \in \mathcal{R}^4.
\end{aligned}
$$

Here, X_1 and X_2 are the uninfected individuals and corresponding infected individuals; we

then redefine $E_0 = (X_0, 0)$ as the DFE given by

$$(S, E(0), I(0), T(0), R(0)) = \left(\frac{\pi}{\mu}, 0, 0, 0, 0\right).$$

Hence, the equilibrium point E_0 of the model is GAS if the following conditions hold for $R_0 < 1$:

1. $\dot{X}_1 = F(X_1, 0), X_0$ is GAS,
2. $\widehat{G}(X_1, X_2) = D_{X_2} G(X_0, 0) X_2 - G(X_1, X_2)$ for $(X_0, 0) \in \mathcal{D}_1$.

We define another set

$$\mathcal{D}_2 = \{(S, E, I, T, R) \in \mathcal{D}_1 : S \leq S(0)\},$$

which is also positively invariant and attracts all solutions in $\mathcal{D}_1$ for all time $t \geq 0$. The uninfected system and infected systems are given by

$$\dot{X}_1 = F(X_1, X_2) = \left(\pi - \beta SI - \mu S \right), \tag{5.29}$$

and

$$\dot{X}_2 = G(X_1, X_2) = \begin{pmatrix} -\mu E \\ \beta SI - D_2 I \\ mI - D_3 T \\ r_I I + r_T T - \mu R \end{pmatrix}, \tag{5.30}$$

where $D_2 = m + d_I + r_I + \mu$, and $D_3 = d_T + r_T + \mu$. By rewriting (5.29) (at E_0, i.e., $I = 0$), we have

$$\frac{dS}{dt} - \mu S = \pi \tag{5.31}$$

Solving this by integration factor yields

$$S = S(0)\exp(-\mu t) + \frac{\pi}{\mu}\left(1 - \exp(-\mu t)\right), \tag{5.32}$$

at $S^0 = S(0)$, $t = 0$. Taking the limit of S in (5.32) as $t \to \infty$, ([noting E_0]), $S = \frac{\pi}{\mu}$. Hence, the condition number one has been satisfied as $S \to S(0), t \to \infty$, for $R_0 < 1$. Going further, we set up the system

$$D_{X_2}G(X_0, Z^0)\cdot X_2 = \begin{pmatrix} -\mu & 0 & 0 & 0 \\ 0 & \beta S(0) - D_2 & 0 & 0 \\ 0 & m & -D_3 & 0 \\ 0 & r_1 & r_T & -\mu \end{pmatrix} \cdot \begin{pmatrix} E(0) \\ I(0) \\ T(0) \\ R(0) \end{pmatrix} \tag{5.33}$$

$$= \begin{pmatrix} -\mu E(0) \\ \beta S(0)\cdot I(0) - D_2 I(0) \\ mI(0) - D_3 T(0) \\ r_I I(0) + r_T T(0) - \mu R(0) \end{pmatrix}. \tag{5.34}$$

Hence, the condition two is satisfied given that

$$\hat{\mathrm{G}}(X_1, X_2) = \begin{pmatrix} -\mu E(0) \\ \beta S(0) I(0) - D_2 I(0) \\ mI(0) - D_3 T(0) \\ r_I I(0) + r_T T(0) - \mu R(0) \end{pmatrix} - \begin{pmatrix} -\mu E \\ \beta S\cdot I - D_2 I \\ mI - D_3 T \\ r_I I + r_T T - \mu R \end{pmatrix}. \tag{5.35}$$

Since $S(0) \geq S \Longrightarrow S(0) - S \geq 0$, then $\hat{\mathrm{G}}(X_1, X_2) \geq 0$.

Thus, $(S, E, I, T, R) \to (S(0), E(0), I(0), T(0), R(0))$ as $t \to \infty$ for $R_0 < 1$ and this completes the proof. □

5.8 Existence of the DEE

Consider a special case of the disease endemic equilibrium (DEE), E_{II}, with $\alpha = 0$ (when the impact of the public health is ineffective). We then solve these equations with $\frac{dS}{dt} = \frac{dE}{dt} = \frac{dI}{dt} = \frac{dT}{dt} = \frac{dR}{dt} = 0$ for the endemic equilibrium solutions. We can proceed by setting the equations in system (5.4) to zero. We process this as

$$0 = \pi - \beta S^{**} I^{**} - D_1 S^{**}, \tag{5.36}$$

$$0 = eS^{**} - \mu E^{**}, \tag{5.37}$$

$$0 = \beta S^{**} I^{**} - D_2 I^{**}, \tag{5.38}$$

$$0 = mI^{**} - D_3 T^{**}, \tag{5.39}$$

$$0 = r_I I^{**} + r_T T^{**} - \mu R^{**}. \tag{5.40}$$

When $I^{**} > 0$ in (5.36), (5.37), (5.38), (5.39), and (5.40), we obtain the following

$$\left.\begin{aligned} S^{**} &= \frac{D_2}{\beta}, \\ E^{**} &= \frac{eD_2}{\mu\beta}, \\ I^{**} &= \frac{\pi\beta - D_1D_2}{\beta D_2}, \\ T^{**} &= \frac{mI^{**}}{D_3} \\ R^{**} &= \frac{eD_2r_T + \mu r_I\beta I^{**}}{\mu^2\beta}. \end{aligned}\right\} \tag{5.41}$$

The system (5.41) can be related to the reproduction number R_0 such that

$$\left.\begin{aligned} S^{**} &= \frac{D_2}{\beta}, \\ E^{**} &= \frac{eD_2}{\mu\beta}, \\ I^{**} &= \frac{D_1D_2\left[\frac{R_0}{D_1} - 1\right]}{\beta D_2}, \\ T^{**} &= \frac{mI^{**}}{D_3}, \\ R^{**} &= \frac{eD_2r_T + \mu r_I\beta I^{**}}{\mu^2\beta}. \end{aligned}\right\} \tag{5.42}$$

The positivity of I^{**} is ensured when $D_1 < R_0$ since $R_0 > 1$. Consequently, if $R_0 > 1$, then $I^{**} > 0$. Hence, there exists unique endemic equilibrium (E_{II}) point for the model (5.4) whenever $R_0 > 1$. Furthermore, we can consider the general case when the disease endemic equilibrium (DEE), E_{II}, when there is the presence of the impact of the public health intervention. We then solve these equations with $\frac{dS}{dt} = \frac{dE}{dt} = \frac{dI}{dt} = \frac{dT}{dt} = \frac{dR}{dt} = 0$ for the endemic equilibrium solutions. We do this by setting the equations in system (5.4) to zero.

Therfore,

$$\left.\begin{aligned} S^{**} &= \frac{\pi}{\beta I^{**} + D_1}, \\ E^{**} &= \frac{\pi e}{(\alpha\beta I^{**} + \mu)(\beta I^{**} + D_1)}, \\ T^{**} &= \frac{I^{**} m}{D_3}, \\ R^{**} &= \frac{D_3 I^{**} r_I + m I^{**} r_T}{\mu D_3}. \end{aligned}\right\} \tag{5.43}$$

So that when $I^{**} \neq 0$ (that is, $I^{**} > 0$) in (5.43), we obtain the following.

$$\begin{aligned} I^{**} =& \left[\alpha\beta E^{**} + \beta S^{**} - D_2\right], \\ =& D_2 \left[\frac{\alpha\beta E^{**} + \beta S^{**}}{D_2} - 1\right], \\ =& D_2 \left[\beta \left(\frac{\alpha \frac{\pi e}{\mu D_1} + \frac{1}{D_1}}{D_2}\right) - 1\right], \\ =& D_2 \left[\pi\beta \left(\frac{\alpha e + \mu}{\mu D_1 D_2}\right) - 1\right], \\ =& D_2[R_E - 1], \end{aligned}$$

where R_E is as defined in (5.25). The positivity of I^{**} is ensured since $R_E > 1$. Consequently, if $R_E > 1$, then $I^{**} > 0$. Hence, there exists a unique endemic equilibrium (E_{II}) point for the model (5.4) whenever $R_E > 1$.

5.9 Global Stability of the DEE

Let

$$\mathcal{D}_3 = \{(S, E, I, T, R) \in \mathcal{D}_1 : E = T = I = R = 0\}.$$

Lemma 5.9.1. *The DEE, E_{II}, of the model is globally asymptotically stable (GAS) in $\mathcal{D}_1|\mathcal{D}_3$ whenever $R_E > 1$.*

Proof. Consider model (5.4) with $R_E > 1$, so that the associated unique endemic equilibrium exists. Also, consider the nonlinear Lyapunov function of the Goh-Volterra type

$$\mathcal{F} = S - S^{**} - S^{**}ln\left(\frac{S}{S^{**}}\right) + E - E^{**} - E^{**}ln\left(\frac{E}{E^{**}}\right) + \left[I - I^{**} - I^{**}ln\left(\frac{I}{I^{**}}\right)\right]. \quad (5.44)$$

The Lyapunov equation (5.44) can be differentiated with respect to time as

$$\dot{\mathcal{F}} = \dot{S} - \left(\frac{S^{**}}{S}\right)\dot{S} + \dot{E} - \left(\frac{E^{**}}{E}\right)\dot{E} + \dot{I} - \left(\frac{I^{**}}{I}\right)\dot{I}. \quad (5.45)$$

Substituting the time derivatives of S, E and I in (5.4) into (5.45) gives

$$\left.\begin{aligned}\dot{\mathcal{F}} &= (\pi - \beta SI - D_1 S) - \left(\frac{S^{**}}{S}\right)(\pi - \beta SI - D_1 S) + (eS - \alpha\beta EI - \mu E) \\ - &\left(\frac{E^{**}}{E}\right)(eS - \alpha\beta EI - \mu E) + (\beta SI + \alpha\beta EI - D_2 I) - \left(\frac{I^{**}}{I}\right)(\beta SI + \alpha\beta EI - D_2 I)\end{aligned}\right\}. \quad (5.46)$$

At the steady state solution, we obtain the following

$$\left.\begin{aligned}\pi &= \beta I^{**} + D_1 S^{**}, \\ e &= \frac{\alpha\beta I^{**}E^{**} + \mu E^{**}}{S^{**}}, \\ D_2 &= \alpha\beta E^{**} + \beta S^{**}.\end{aligned}\right\} \quad (5.47)$$

Applying the steady state expression in (5.47), after several algebraic calculations, we have that

$$\left.\begin{aligned}\dot{\mathcal{F}} = \; & \mu S\left(2-\frac{S}{S^{**}}-\frac{S^{**}}{S}\right)+\frac{eES}{E^{**}}\left(1-\frac{E^{**}}{E}\right)\\ & +\mu E\left(1-\frac{E}{E^{**}}\right)+\frac{\beta I^2 S}{I^{**}}\left(1-\frac{S^{**}}{S}\right)\\ & +\beta I^{**}S\left(1-\frac{IS}{I^{**}S^{**}}\right)+\beta I\left(1-\frac{I^{**}}{I}\right)S^{**}\\ & +\alpha\beta I E^{**}\left(1-\frac{I}{I^{**}}\right)+\frac{\alpha\beta I^2 E}{I^{**}}\left(1-\frac{I^{**}E}{IE^{**}}\right)\end{aligned}\right\}. \tag{5.48}$$

The following inequalities from (5.48) hold:

$$2-\frac{S}{S^{**}}-\frac{S^{**}}{S}\leq 0;\quad 1-\frac{E^{**}}{E}\leq 0;\quad 1-\frac{E}{E^{**}}\leq 0;$$
$$1-\frac{S^{**}}{S}\leq 0;\quad 1-\frac{IS}{I^{**}S^{**}}\leq 0;\quad 1-\frac{I^{**}}{I}\leq 0;\quad 1-\frac{I}{I^{**}}\leq 0;\quad 1-\frac{I^{**}E}{IE^{**}}\leq 0,$$

when, $E\leq E^{**}$ and $I\leq I^{**}$. Thus, $\dot{\mathcal{F}}\leq 0$ for $R_E>1$. The classes T,R as $t\to\infty$ tends toward their respective endemic equilibrium points in E_{II}, i.e.,

$$T(t)\to T^{**}\quad \text{as } t\to\infty,$$
$$R(t)\to R^{**}\quad \text{as } t\to\infty.$$

Hence, $\dot{\mathcal{F}}$ is a Lyapunov function in $\mathcal{D}_1|\mathcal{D}_3$ and it follows from the LaSalle's invariance principle , that every solution to the equations of the model (5.4) approaches the associated unique endemic equilibria E_{II}, of the model (5.4) as $t\to\infty$ for $R_E>1$. □

5.10 Computational Analysis

Parameters List			
Parameters	Baseline	Range	References
α	$0 < \alpha < 1$	[0,1]	varies with scenario
e	$1.431 * 10^{-2}$	$1.231 * 10^{-2} - 1.631 * 10^{-2}$	[161]
β	0.0001	$0.00001 - 0.001$	[91]
m	0.6937	0.59-0.79	[91]
d_I	0.0191	$0.010 - 0.029$	[91]
d_T	0.1260	$0.1060 - 0.1360$	[91]
r_I	0.0336	0.02-0.04	[91]
r_T	0.2472	0.14-0.34	[91]
μ	$\frac{1}{(74.4)(365)}$	$\frac{1}{(64.56)(365)} - \frac{1}{(80.56)(365)}$	[91]

Table 5.2: Parameter values for public health education mathematical model.

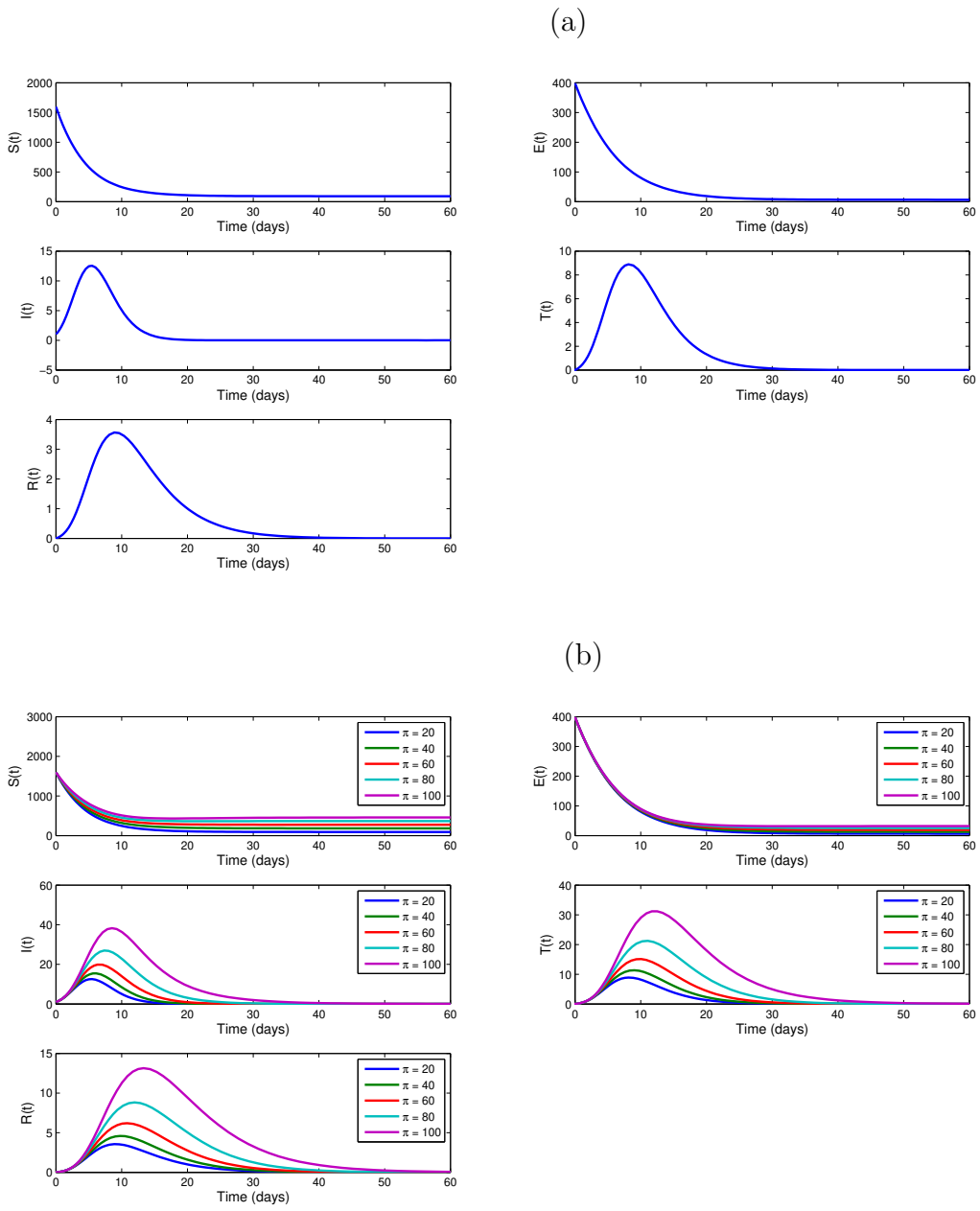

Figure 5.2: (a): population $S(t)$, $E(t)$, $I(t)$, $T(t)$ and $E(t)$, when $R_0 = 0.1612, R_E = 0.1654$; (b): population $S(t)$ and $E(t)$, and $I(t)$ with π varied, when $R_0 < 1, R_E < 1$.

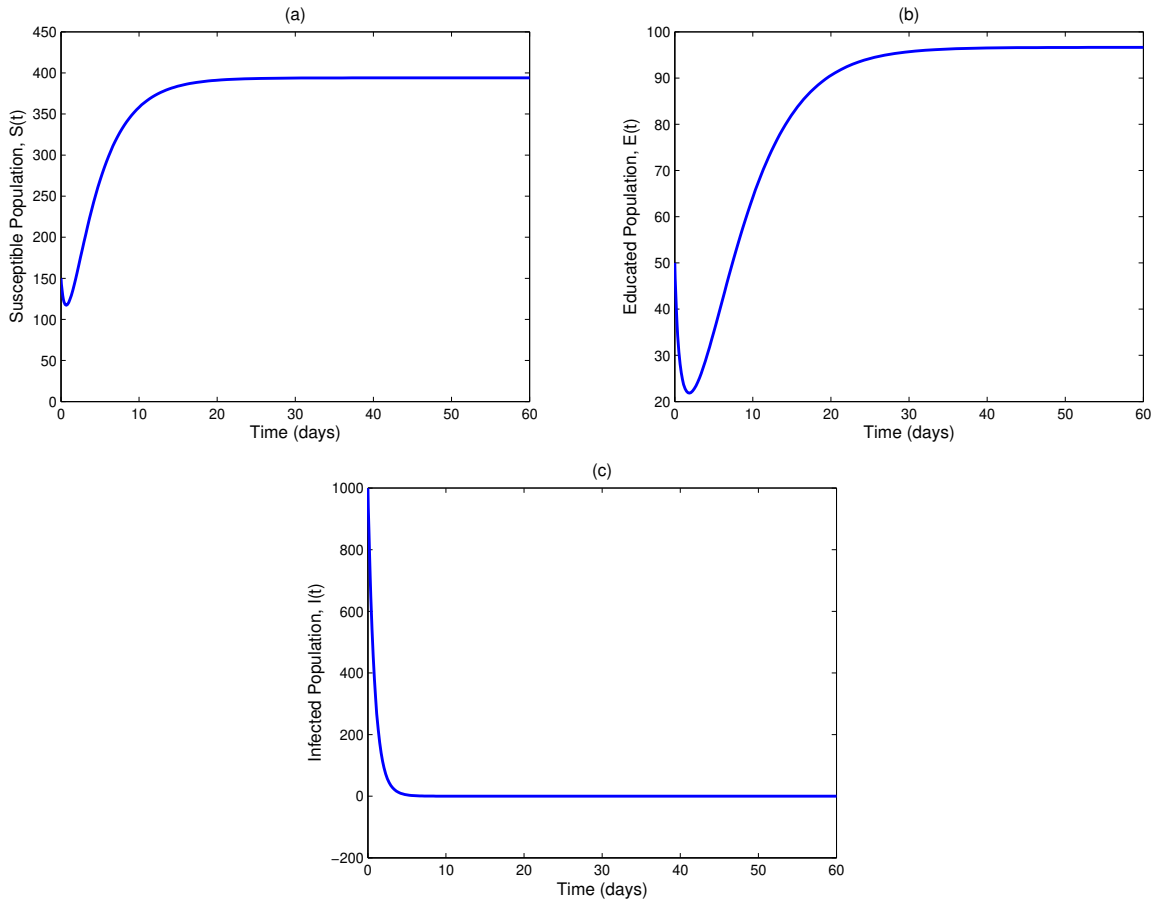

Figure 5.3: Population $S(t), E(t)$, and $I(t)$, $e = 0.0500$ when $R_E = 0.5526 < 1$.

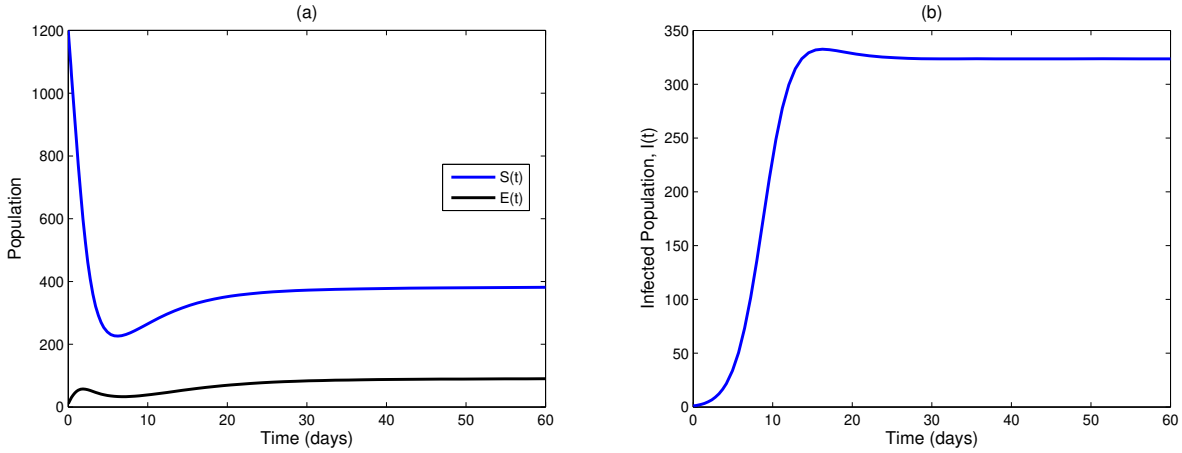

Figure 5.4: (a) Population $S(t)$ and $E(t)$, when $R_E = 1.2332 > 1$ and $I(t)$ (b) when $R_E = 1.7773 > 1$.

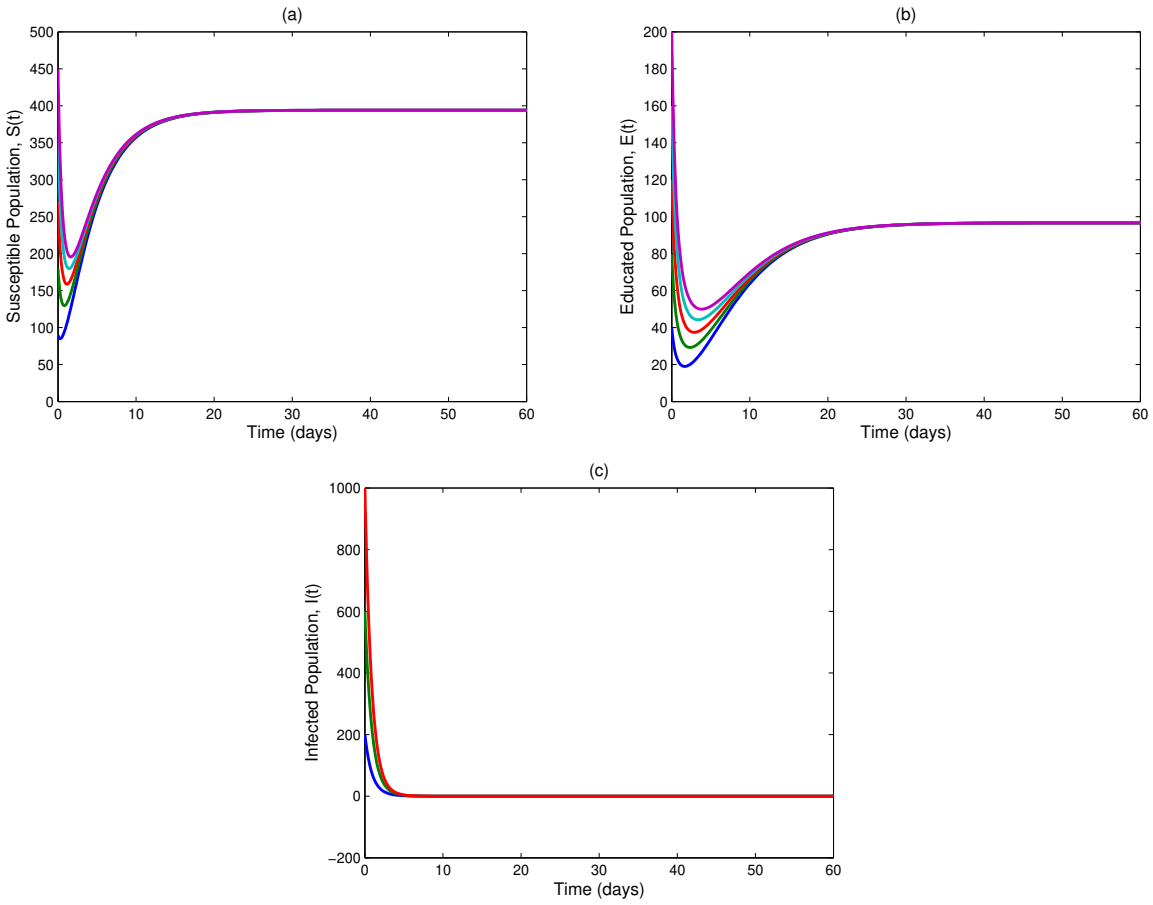

Figure 5.5: Population $S(t), E(t)$, and $I(t)$ with multiple initial conditions, $e = 0.0500$ when $R_E = 0.5526 < 1$.

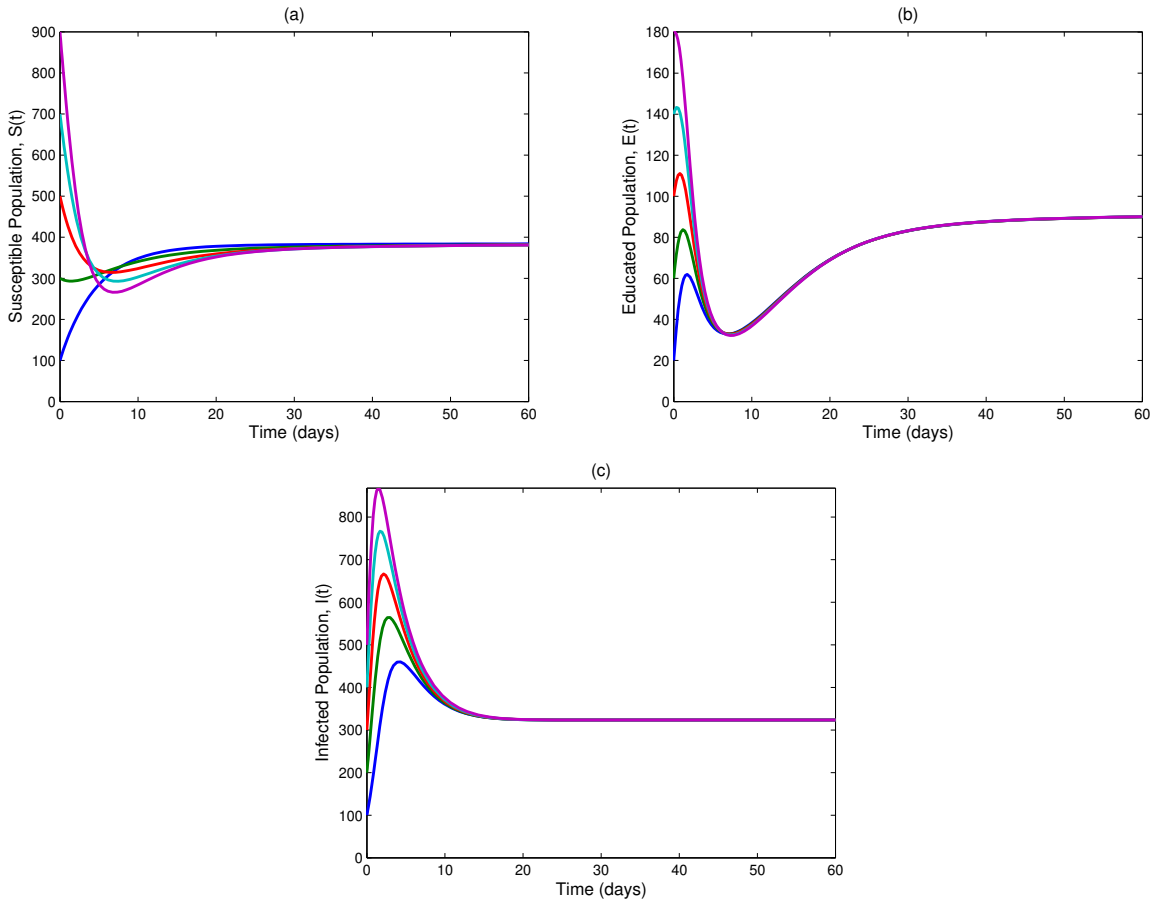

Figure 5.6: (a) and (b): population $S(t)$ and $E(t)$, when $R_E = 1.2332 > 1$, and (c): population $I(t)$ when $R_E = 3.5547 > 1$.

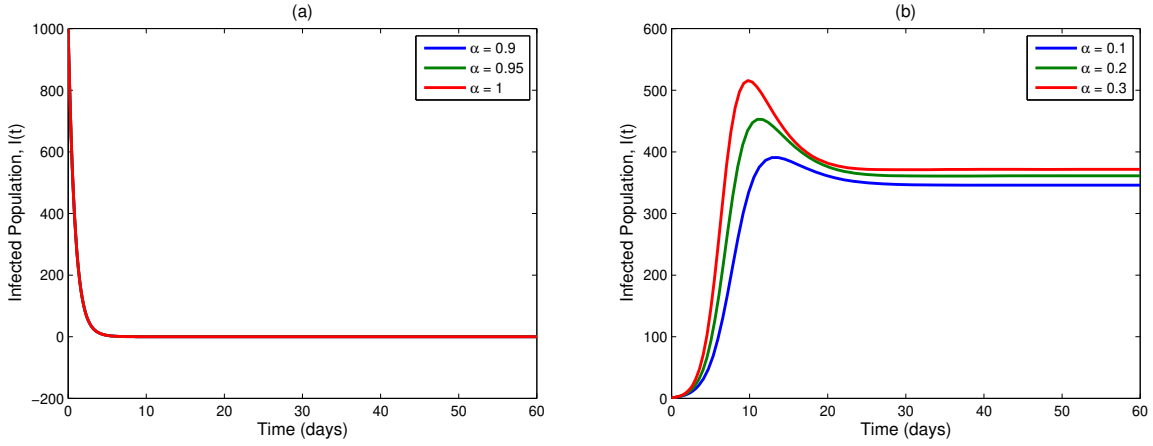

Figure 5.7: (a) Population $I(t)$, when $R_E < 1$, $\alpha = (0.90, 0.95, 1)$, and (b) $R_E > 1$, $\alpha = (0.1, 0.2, 0.3)$.

5.11 Discussion and Conclusion

The dynamics of susceptible (a), educated (b), and infected (c) populations in model system 5.1 shows in (Fig. 5.2) using parameter values in Table 5.2 when $R_0 < 1, R_E < 1$ with different values of π.

(Fig. 5.3) depicts the local stability of disease free equilibrium when $e = 0.0500$ and $R_E = 0.5526 < 1$ as $t \to \infty$ for susceptible (a), educated (b), and MERS-Cov infected (c) populations. We observe that the total number of educated individuals is less than the number of MERS-CoV susceptible individuals. This is possibly a product of illiteracy in public health caused by the education's nonessential nature due to the lack of infections in the population at the early stage of MERS-CoV propagation. We note that the population of MERS-Cov infected individuals declines drastically as the number of educated individuals grows. The theoretical and Computational finding indicate that public health education is a very competent regulatory measure.

When $R_E > 1$ as $t \to \infty$ (Fig. 5.4) illustrates that the disease endemic equilibrium is locally asymptotically stable for susceptible, educated (a), and infected populations (b). (Fig. 5.4) also displays a substantial growth in the number of infected individuals at the initial outbreak of infection before reaching stability. This considerable increase in infected individuals can be associated with the fall in the educated population and the increase in the number of susceptible individuals.

An increasing number of educated individuals leads to a decreasing number of susceptible individuals, therefore producing a decreased number of infected individuals see (Fig. 5.5) (a), (b), and (c). We also observed that MERS-CoV can be effectively removed from a population following a certain period through public health education, disregarding the initial number of infected individuals.

(Fig. 5.6) (a), (b), and (c), confirm when $R_E > 1$, the data obtained demonstrate that

model system 5.1 has one unique positive endemic equilibrium point. This indicates that there is no bifurcation, thus resulting in a continuation of disease spread through the population if control measures are not implemented.

We recognize when α approaches one, the disease spread rate approaches an equilibrium point at (Fig. 5.7). When $R_E > 1$, The edification of public health does not ultimately change the value of the epidemic threshold R_0, but reduces the final density of the number of MERS-CoV infected individuals. Due to this observation, we recommend measures are taken to reduce R_0 thus helping combat the spread of the disease.

This research is confirmation that extensive public health education is necessary for controlling the transmission of this disease. This also lends credence to our theoretical analysis, where we demonstrate that public health education significantly decreases the basic reproduction number of the model.

Chapter 6

KSA Human population Modeling

Healthcare associated infections contribute significant consequences to the health-care system and society, as well as avoidable suffering and deaths among patients. Therefore, the quality of care, treatment, and prevention against adverse occurrences all contribute in the hospitals to the patient safety, and the safety of healthcare workers. In this chapter, we devolved a mathematical model that is tailored to the extent of infection prevention to deal with the transmission dynamics of MERS-CoV infections. Emergency preparation in the work-place which provides existing knowledge on infection control as a foundation for establishing rules and practices to prevent hospital infections will also be induced in the study. It is reported that the risk of transmission of the MERS-CoV virus in humans is determined by characteristics including the close contact with the patients, such as touching the respiratory secretions of patients, sleeping in the same room as patients, or removing and cleaning of the patients' waste [167] with sub-clinical infection[168]. The positive PCR results of MERS-CoV have been prominent in some patients with having the negative viral cultures of MERS-CoV who are recovering from the infection. It has been recognized that healthcare workers could transmit the virus (MERS-CoV) to other health care workers, in spite of being asymptomatic [19].

The proposed study's goal is to give a systematic comprehensive research of a deterministic model for quarantine and isolation of the hospitalized individuals in order to get a better understanding of the effect of these control measures on the propagation of an arbitrary infection that is controlled through confinement and isolation. The model to be developed builds on some of the existing assessment scheme that have been published in the literature [169]. Furthermore, the commitment extends to a comprehensive qualitative analysis of a quarantine and isolation strategy.

Coherence and accordance with standard contact relating to airborne precautions are vital to reducing the risk of infection, and thus should be ensured. This following of rules is especially important in hospital settings, where rates of transmission are high. The following precautions contain practices and equipment to guarantee optimization of transmissions between hospital workers and patients with (or presumed to have) MERS-CoV. For example, one common practice is proper hand hygiene, which begins to become necessary as it should be done at all times in contact with the patients, and when putting on or removing personal protective equipment (PPE). Hand hygiene should not only be used by hospital staff but practically all within the hospital. Additionally, such hospital facilities for proper hand hygiene must corroborate within all personnel. Another procedure that must be ensured to follow is patient placement in which a patient who might be infected with MERS-CoV must be put in an Airborne Infection Isolation Room, also known as an AIIR. AIIRs should be strictly regulated to facilitate methods in combating transmission; these include negative pressure in comparison to the outside room and at least 6 air changes an hour. Furthermore, following OSHA's PPE standards, employers must provide the necessary PPEs for hospital workers, as well as provide the appropriate training on how to wear, use, and remove such equipment. After and between usage, all reusable PPE must be cleaned, sanitized, and maintained correctly. Different types of PPEs are also used in conjunction with one another

to maximize various transmission methods. These PPEs are the subsequent following: gloves, gowns, respiratory protections, and eye protections. Non-sterile gloves are to be worn and disposed of at the appropriate times such as upon entering the patient's room or when they become contaminated; these guidelines also apply to disposable gowns. Respiratory protections such as disposable N95 masks and respirators are to be used when visiting the patient's room. In addition, hospital workers should ensure that respiratory protections are the last part of a PPE uniform to be removed and follow the Occupational Safety and Health Administration (OSHA) guidelines for Respiratory Protection. Eye protections such as disposable face shields or reusable goggles should be removed when leaving the patient's room or, if reusable, should be sanitized and cleaned after use [170, 171].

6.1 Model Formulation

Let $N(t)$ denote the total population at time t which sub-divided into six compartments; susceptible $(S(t))$, exposed $(E(t))$, asymptomatic $(A(t))$, infectious $(I(t))$, hospitalized $(H(t))$ and recovered $(R(t))$ individuals, thus

$$N(t) = S(t) + E(t) + A(t) + I(t) + H(t) + R(t).$$

Recruitment individuals will increase the susceptible population by rate π. Susceptible people can get infected after making effective contact with infectious people at a rate of

$$\lambda = \beta \frac{(A + I + \zeta H)}{N}.$$

Now that, the $0 \leq \zeta < 1$ indicates the predicted decrease in disease transmission by hospitalized individuals relative to non-hospitalized infectious individuals in the I class. As a result, ζ tests the effectiveness of isolation or care provided to hospitalized association. The

number of susceptible is diminished by natural death (at a rate of μ). Then, the susceptible population is given by

$$\frac{dS}{dt} = \pi - (\lambda + \mu)\, S.$$

The number of persons exposed is caused by contamination of susceptible people (at a rate of λ). It is presumed that exposed persons (classes E) do not spread infection (i.e., only infected individuals capable of transmitting the disease to susceptible individuals) The population is diminished by the occurrence of disease signs (at a rate of κ) and natural mortality (at a rate of μ), so that

$$\frac{dE}{dt} = \lambda S - (\kappa + \mu)\, E.$$

Asymptomatic people are monitored at the rate of $(1-p)\kappa$. The symptomatic individuals is limited by the recovery rate of γ_1 and natural mortality (at the rate of μ). So,

$$\frac{dA}{dt} = (1-p)\, \kappa E - (\gamma_1 + \mu)\, A.$$

The infectious individuals are produced at a rate of $p\kappa$, recovered (at a rate of γ_2), and hospitalized (at a rate of Φ). The rate of mortality is μ) and disease-induced death (at a rate of δ_1). So,

$$\frac{dI}{dt} = p\kappa E - (\gamma_2 + \Phi + \mu + \delta_1)\, I.$$

The number of hospitalized individuals is created by the hospitalization of infected patients (at a rate of Φ). This number of people is limited by recovery (at the rate of γ_3), natural death (at the rate of μ) and disease-induced death (at the rate of δ_2). As a result, the rate of change in the population of hospitalized persons is determined by

Variable	Description
S	Susceptible
E	Exposed
A	Asymptomatic
I	Infected
H	Hospitalized
R	Recovered

Parameter	Description
π	Recruitment rate
μ	The rate of the natural death
β	Contact rate
κ	Rate of the growth from exposed to infectious.
Φ	Rate of symptomatic individuals proceed to hospitalization
γ_1	Recovery rate for asymptomatic infected person
γ_2	Rate of recovery for infection individuals
γ_3	Rate of recovery for hospitalized individuals
δ_1	Death rate for infectious individuals
δ_2	Death rate for hospitalized individuals
λ	$\beta\dfrac{(A+I+\zeta H)}{N}$

Table 6.1: The model variables and parameters for KSA human population modeling.

$$\frac{dH}{dt} = \Phi I - (\gamma_3 + \mu + \delta_2) H.$$

Ultimately, the number of recovered individuals is created by the recovery of asymptomatic, infected and hospitalized infectious members (γ_1, γ_2 and γ_3, respectively). The natural death is given by (the rate of μ), so that

$$\frac{dR}{dt} = \gamma_1 A + \gamma_2 I + \gamma_3 H - \mu R.$$

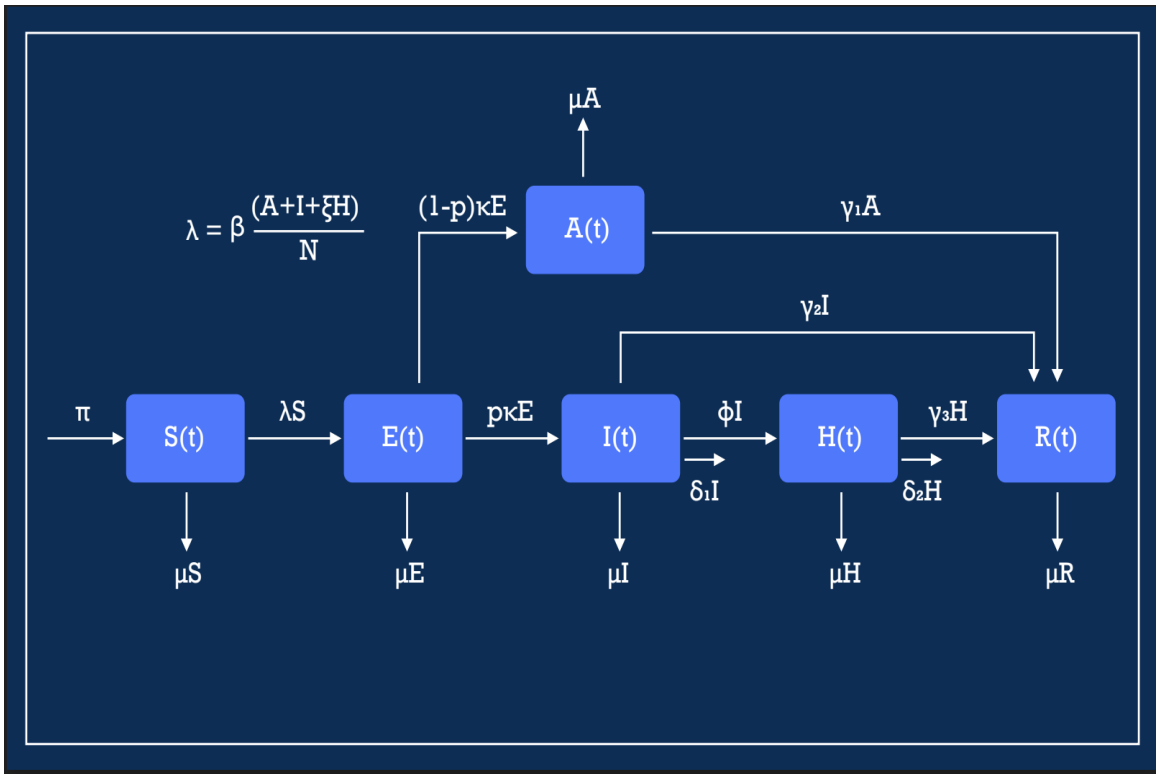

Figure 6.1: Flow chart for KSA Human Population Mathematical Model

Thus, the model equations are

$$\begin{aligned}
\frac{dS}{dt} &= \pi - (\lambda + \mu)\, S, \\
\frac{dE}{dt} &= \lambda S - (\kappa + \mu)\, E, \\
\frac{dA}{dt} &= (1-p)\, \kappa E - (\gamma_1 + \mu)\, A, \\
\frac{dI}{dt} &= p\kappa E - (\gamma_2 + \Phi + \mu + \delta_1)\, I, \\
\frac{dH}{dt} &= \Phi I - (\gamma_3 + \mu + \delta_2)\, H, \\
\frac{dR}{dt} &= \gamma_1 A + \gamma_2 I + \gamma_3 H - \mu R,
\end{aligned} \tag{6.1}$$

where

$$\lambda = \beta \frac{A + I + \zeta H}{N}.$$

We are going to apply a prominent control measure in the hospitalized compartment since the health care comprised 1/3 of all Saudi Middle East Respiratory Syndrome cases [172].

Here, we prove the following assertion following the theory and findings of Mohammad et al. [169].

Theorem 6.1.1. *With the positive initial data, the solutions of the model system (6.1) will remain positive for all* $t > 0$.

Proof. Let $t_1 = sup\{t > 0 : S > 0, E > 0, I > 0, A > 0, H > 0 \in [0, t]\}$; therefore, $t_1 > 0$. The first equation of the system 6.1 yeilds,

$$\frac{dS}{dt} = \pi - \lambda(t)S(t) - \mu S(t) \geqslant -(\lambda + \mu)S(t), \tag{6.2}$$

which can be re-written as,

$$\frac{d}{dt}\left[S(t)\exp\left\{\mu t + \int_0^t \lambda(\tau)d\tau\right\}\right] \geqslant \exp\left\{\mu t + \int_0^t \lambda(\tau)d\tau\right\}. \tag{6.3}$$

Accordingly,

$$S(t_1)\exp\left\{\mu t + \int_0^t \lambda(\tau)d\tau\right\} - S(0) \geqslant \int_0^{t_1} \exp\left\{\mu y + \int_0^y \lambda(\tau)d(\tau)\right\}dy. \tag{6.4}$$

Hence,

$$\begin{aligned} S(t) \geqslant & S(0)\exp\left\{-\mu t_1 - \int_0^{t_1} \lambda(\tau)d\tau\right\} \\ & \left[\exp\left\{-\mu t_1 - \int_0^{t_1} \lambda(\tau)d\tau\right\}\right]\int_0^{t_1} \exp\left\{\mu y + \int_0^y \lambda(\tau)d\tau\right\}dy > 0. \end{aligned}$$

Similarly, it can be shown that $E > 0$, $I > 0$, $A > 0$, $H > 0$ and $R > 0$ for all time $t > 0$. □

Lemma 6.1.1. *The closed set*

$$\mathcal{D} = \left\{ (S, E, A, I, H, R) \in \mathbb{R}_+^6 : S + E + A + I + H + R \leq \frac{\pi}{\mu} \right\}$$

is positively-invariant for the model (6.1).

Proof. Adding all the equations of the model (6.1) gives,

$$\frac{dN}{dt} = \pi - \mu N - (\delta_1 I + \delta_2 H) .$$

Because $dN/dt \leq \pi - \mu N$, it implies that $dN/dt \leq 0$ if $N \geq \pi/\mu$. The standard comparison theorem will also be used to illustrate that $N(t) \leq N(0)e^{-\mu t} + \pi/\mu\,(1 - e^{-\mu t})$. In fact, $N(t) \leq \pi/\mu$ if $N(0) \leq \pi/\mu$. The domain $\mathcal{D}$ is thus positive-invariant.

If $N(0) > \pi/\mu$ is used, then the solution reaches $\mathcal{D}$ in finite time, or $N(t)$ tends π/μ asymptotically. The D area then attracts all solutions in $\mathbb{R}+^6$. □

Since the domain $\mathcal{D}$ is positive-invariant, it is possible to evaluate the dynamics of the flow model output (6.1) in $\mathcal{D}$, where the existence, uniqueness, continuity outcomes are preserved by the system.

6.2 Disease free equilibrium

The task is to perform stability analysis for the above system of ODEs. Let

$$\mathcal{E}_0 = (S^*, E^*, A^*, I^*, H^*, R^*) = \left(\frac{\pi}{\mu}, 0, 0, 0, 0, 0 \right) .$$

6.2.1 Local stability analysis

The local stability of $\mathcal{E}_0$ will be studied by means of the next generation operator method [164]. We obtain

$$F = \begin{pmatrix} 0 & \beta & 0 & \zeta\beta \\ 0 & 0 & 0 & 0 \\ 0 & 0 & 0 & 0 \\ 0 & 0 & 0 & 0 \end{pmatrix},$$

and

$$V = \begin{pmatrix} \kappa+\mu & 0 & 0 & 0 \\ -p\kappa & \gamma_2+\Phi+\mu+\delta_1 & 0 & 0 \\ -(1-p)\kappa & 0 & \gamma_1+\mu & 0 \\ 0 & -\Phi & 0 & \gamma_3+\mu+\delta_2 \end{pmatrix},$$

with inverse

$$V^{-1} = \begin{pmatrix} \frac{1}{\kappa+\mu} & 0 & 0 & 0 \\ \frac{\kappa p}{(\kappa+\mu)(\gamma_2+\delta_1+\mu+\Phi)} & \frac{1}{\gamma_2+\delta_1+\mu+\Phi} & 0 & 0 \\ -\frac{\kappa(p-1)}{(\alpha+\mu)(\kappa+\mu)} & 0 & \frac{1}{\gamma_1+\mu} & 0 \\ \frac{\kappa p\Phi}{(\kappa+\mu)(\gamma_3+\delta_2+\mu)(\gamma_2+\delta_1+\mu+\Phi)} & \frac{\Phi}{(\gamma_3+\delta_2+\mu)(\gamma_2+\delta_1+\mu+\Phi)} & 0 & \frac{1}{\gamma_3+\delta_2+\mu} \end{pmatrix}.$$

Recall that the control reproduction parameter is defined in terms of these matrices as follows:

$$\mathcal{R}_c = \rho\left(FV^{-1}\right) = \frac{\beta p\kappa(\gamma_3+\mu+\delta_2+\zeta\Phi)}{(\kappa+\mu)(\gamma_2+\Phi+\mu+\delta_1)(\gamma_3+\mu+\delta_2)}.$$

Then, the following assertion holds.

Theorem 6.2.1 ([164], Theorem 2)**.** *The disease free equilibrium of (6.1), $\mathcal{E}_0$, is locally-asymptotically stable if $\mathcal{R}_c < 1$, and unstable if $\mathcal{R}_c > 1$.*

The interpretation of $\mathcal{R}_c$ directly follows from its following term-wise representation:

$$\mathcal{R}_c = \frac{\beta p \kappa}{(\kappa+\mu)(\gamma_2+\Phi+\mu+\delta_1)} + \frac{\beta\zeta p\kappa\Phi}{(\kappa+\mu)(\gamma_2+\Phi+\mu+\delta_1)(\gamma_3+\mu+\delta_2)}.$$

In the above expression, the first term is the number of new infections induced by non-hospitalized infected persons, and the second term is the number of infections caused by hospitalized individuals.

6.2.2 Global stability analysis

In order to study the global stability of the disease free equilibrium $\mathcal{E}_0$, we are going to use the well-known Lyapunov function method.

Theorem 6.2.2. *The disease free equilibrium $\mathcal{E}_0$ of (6.1) is globally-asymptotically stable if $\mathcal{R}_c \leq 1$.*

Proof. Let us denote

$$r_1 = \kappa+\mu, \quad r_2 = \gamma_2+\Phi+\mu+\delta_1, \quad r_3 = \gamma_1+\mu, \quad r_4 = \gamma_3+\mu+\delta_2.$$

Then,

$$\mathcal{R}_c = \frac{\beta p\kappa(r_4+\zeta\Phi)}{r_1 r_2 r_4}.$$

Consider the following Lyapunov function

$$\mathcal{L} = \frac{r_4\mathcal{R}_c}{\zeta\beta}\cdot E + \frac{r_4+\zeta\Phi}{r_2\zeta}\cdot I + \frac{r_4}{r_3\zeta}\cdot A + H$$

with the first order time derivative

$$\begin{aligned}
\frac{\partial \mathcal{L}}{\partial t} &= \frac{r_4\mathcal{R}_c}{\zeta\beta}\cdot\frac{dE}{dt} + \frac{r_4+\zeta\Phi}{r_2\zeta}\cdot\frac{dI}{dt} + \frac{dH}{dt} + \frac{r_4}{r_3\zeta}\cdot\frac{dA}{dt} = \\
&= \frac{r_4\mathcal{R}_c}{\zeta\beta}\cdot\left(\beta\frac{A+I+\zeta H}{N}S - r_1E\right) + \frac{r_4+\zeta\Phi}{r_2\zeta}\cdot(p\kappa E - r_2 I) + \Phi I - \\
&- r_4 H + \frac{r_4}{r_3\zeta}(1-p)\kappa E - \frac{r_4}{\zeta}A \leq \\
&\leq \frac{r_4\mathcal{R}_c}{\zeta\beta}\cdot\left(\beta\left(A+I+\zeta H\right) - r_1E\right) + \frac{r_4+\zeta\Phi}{r_2\zeta}\cdot(p\kappa E - r_2 I) + \Phi I - \\
&- r_4 H + \frac{r_4}{r_3\zeta}(1-p)\kappa E - \frac{r_4}{\zeta}A \\
&= \frac{r_4\mathcal{R}_c}{\zeta}\cdot(A+I+\zeta H) - \frac{r_1 r_4\mathcal{R}_c}{\zeta\beta}\cdot E + \frac{r_4+\zeta\Phi}{r_2\zeta}p\kappa\cdot E - \frac{r_4+\zeta\Phi}{r_2\zeta}\cdot r_2 I + \Phi I - \\
&- r_4 H + \frac{r_4}{r_3\zeta}(1-p)\kappa E - \frac{r_4}{\zeta}A = \\
&= \frac{r_4\mathcal{R}_c}{\zeta}\cdot(A+I+\zeta H) + \left[-\frac{r_1 r_4\mathcal{R}_c}{\zeta\beta} + \frac{r_4+\zeta\Phi}{r_2\zeta}p\kappa + \frac{r_4}{r_3\zeta}(1-p)\kappa\right]\cdot E - \\
&- \frac{r_4+\zeta\Phi}{\zeta}\cdot I + \Phi I - r_4 H - \frac{r_4}{\zeta}A = \\
&= \frac{r_4\mathcal{R}_c}{\zeta}\cdot(A+I+\zeta H) + \left[-\frac{r_1 r_4\mathcal{R}_c}{\zeta\beta} + \frac{r_4+\zeta\Phi}{r_2\zeta}p\kappa + \frac{r_4}{r_3\zeta}(1-p)\kappa\right]\cdot E - \\
&- \frac{r_4}{\zeta}\cdot I - \Phi I + \Phi I - r_4 H - \frac{r_4}{\zeta}A = \\
&= \frac{r_4\mathcal{R}_c}{\zeta}\cdot(A+I+\zeta H) - \frac{r_4}{\zeta}\cdot(A+I+\zeta H) + \\
&+ \left[-\frac{r_1 r_4\mathcal{R}_c}{\zeta\beta} + \frac{r_4+\zeta\Phi}{r_2\zeta}p\kappa + \frac{r_4}{r_3\zeta}(1-p)\kappa\right]\cdot E = \\
&= -\frac{r_4}{\zeta}\cdot(1-\mathcal{R}_c)\left(A+I+\zeta H\right) \leq 0,
\end{aligned}$$

if and only if $1-\mathcal{R}_c \geq 0$. Here, we have taken into account that $S \leq N$.

Thus,

$$\frac{\partial \mathcal{L}}{\partial t} \leq 0 \quad \text{for} \quad \mathcal{R}_c \leq 1.$$

Then, it follows from the LaSalle invariance principle that

$$(E, I, A, H) \to (0, 0, 0, 0) \quad \text{as} \quad t \to \infty.$$

Now, let us consider other quantities of (6.1); such that, in view of positivity of μ, from the sixth equation of (6.1), we obtain that

$$\lim_{t\to\infty} R = 0.$$

Finally, from the first equation of (6.1), we similarly obtain

$$\lim_{t\to\infty} S = \frac{\pi}{\mu}.$$

This relation finalizes the proof. □

6.3 Existence and stability of endemic equilibria

6.3.1 Existence and Stability

We denote by

$$\mathcal{E}_1\left(\lambda^{**}\right) = \left(S^{**}\left(\lambda^{**}\right), E^{**}\left(\lambda^{**}\right), A^{**}\left(\lambda^{**}\right), I^{**}\left(\lambda^{**}\right), H^{**}\left(\lambda^{**}\right), R^{**}\left(\lambda^{**}\right)\right),$$

the endemic equilibrium of (6.1) such that

$$S^{**} + E^{**} + A^{**} + I^{**} + H^{**} + R^{**} = N^{**}.$$

At the steady-state, (6.1) provides

$$S^{**} = \frac{\pi}{\lambda^{**} + \mu}, \quad E^{**} = \frac{\lambda^{**} S^{**}}{r_1},$$

$$A^{**} = \frac{(1-p)\kappa}{\gamma_1 + \mu} E^{**} = \frac{(1-p)\kappa}{r_1(\gamma_1 + \mu)} \lambda^{**} S^{**} := c_1 \lambda^{**} S^{**},$$

$$I^{**} = \frac{p\kappa}{r_2} E^{**} = \frac{p\kappa}{r_2} \frac{(1-p)\kappa}{r_1(\gamma_1 + \mu)} \lambda^{**} S^{**} = \frac{(1-p)p\kappa^2}{r_1 r_2(\gamma_1 + \mu)} \lambda^{**} S^{**} := c_2 \lambda^{**} S^{**},$$

$$H^{**} = \frac{\Phi}{r_4} I^{**} = \frac{\Phi(1-p)p\kappa^2}{r_1 r_2 r_4(\gamma_1 + \mu)} \lambda^{**} S^{**} := c_3 \lambda^{**} S^{**},$$

$$R^{**} = \frac{\gamma_1}{\mu} A^{**} + \frac{\gamma_2}{\mu} I^{**} + \frac{\gamma_3}{\mu} H^{**} = \frac{\gamma_1 c_1}{\mu} \lambda^{**} S^{**} + \frac{\gamma_2 c_2}{\mu} \lambda^{**} S^{**} + \frac{\gamma_3 c_3}{\mu} \lambda^{**} S^{**} =$$
$$= \frac{\gamma_1 c_1 + \gamma_2 c_2 + \gamma_3 c_3}{\mu} \lambda^{**} S^{**} := c_4 \lambda^{**} S^{**},$$

where

$$\lambda^{**} = \beta \frac{A^{**} + I^{**} + \zeta H^{**}}{N^{**}}.$$

Therefore,

$$\lambda^{**} N^{**} = \beta(A^{**} + I^{**} + \zeta H^{**}).$$

or

$$\lambda^{**} S^{**} \left[1 + \left(\frac{1}{r_1} + c_1 + c_2 + c_3 + c_4\right) \lambda^{**}\right] = \beta \lambda^{**} S^{**}(c_1 + c_2 + \zeta c_3).$$

Since $\lambda^{**} S^{**} \neq 0$,

$$1 + c_5 \lambda^{**} = \beta(c_1 + c_2 + \zeta c_3) = \mathcal{R}_c,$$

where

$$c_5 = \frac{1}{r_1} + c_1 + c_2 + c_3 + c_4.$$

Therefore,

$$\lambda^{**} = \frac{\mathcal{R}_c - 1}{c_5},$$

and the endemic equilibrium is defined as

$$\mathcal{E}_1 = \left(\frac{\mathcal{R}_c - 1}{c_5}\right).$$

Thus, the following statement holds.

Lemma 6.3.1. *Main model (6.1) has a unique endemic equilibrium* $\left(\frac{\mathcal{R}_c-1}{c_5}\right)$ *if* $\mathcal{R}_c > 1$ *[169].*

6.3.2 Local stability

In this section, we are going to examine the local stability of $\mathcal{E}_1$. Then, the following holds.

Theorem 6.3.1. *The unique endemic equilibrium of (6.1) with* $N = N^*$ *is locally asymptotically stable if* $\mathcal{R}_c > 1$.

Proof. We start the proof by assuming that $\mathcal{R}_c > 1$, and that $N = N^*$ to ensure the existence of $\mathcal{E}_1$. Then, the substitution

$$S = N^* - E - A - I - H - R,$$

into (6.1), leads to

$$\begin{aligned}
\frac{dE}{dt} &= \beta\frac{A + I + \zeta H}{N^*}(N^* - E - A - I - H - R) - (\kappa + \mu)\, E,\\
\frac{dA}{dt} &= (1 - p)\, \kappa E - (\gamma_1 + \mu)\, A,\\
\frac{dI}{dt} &= p\kappa E - (\gamma_2 + \Phi + \mu + \delta_1)\, I,\\
\frac{dH}{dt} &= \Phi I - (\gamma_3 + \mu + \delta_2)\, H,\\
\frac{dR}{dt} &= \gamma_1 A + \gamma_2 I + \gamma_3 H - \mu R.
\end{aligned} \tag{6.5}$$

Linearizing the system (6.5) around the endemic equilibrium $\mathcal{E}_1$, gives

$$\begin{aligned}
\frac{dE}{dt} &= [-a_1 - (\kappa + \mu)]\, E + (a_2 - a_1)I - a_1 A + (\zeta a_2 - a_1)H - a_1 R \\
\frac{dA}{dt} &= (1-p)\,\kappa E - (\gamma_1 + \mu)\, A, \\
\frac{dI}{dt} &= p\kappa E - (\gamma_2 + \Phi + \mu + \delta_1)\, I, \\
\frac{dH}{dt} &= \Phi I - (\gamma_3 + \mu + \delta_2)\, H, \\
\frac{dR}{dt} &= \gamma_1 A + \gamma_2 I + \gamma_3 H - \mu R,
\end{aligned} \tag{6.6}$$

□

where

$$a_1 = \beta \frac{A^{**} + I^{**} + \zeta H^{**}}{N^*}, \quad a_2 = \beta \frac{S^{**}}{N^*}.$$

Then, the Jacobian of (6.6) evaluated at $\mathcal{E}_1$, will describe as

$$J(\mathcal{E}_1) = \begin{pmatrix}
-a_1 - r_1 & a_2 - a_1 & -a_1 & \zeta a_2 - a_1 & -a_1 \\
p\kappa & -r_2 & 0 & 0 & 0 \\
(1-p)\kappa & 0 & -r_3 & 0 & 0 \\
0 & \Phi & 0 & -r_4 & 0 \\
0 & \gamma_2 & \gamma_1 & \gamma_3 & \mu
\end{pmatrix}.$$

Due to linearity, (6.6) admits an exponential solution

$$\boldsymbol{x}(t) = \boldsymbol{x}(0) \exp(\omega t),$$

where $\boldsymbol{x} = (E \quad A \quad I \quad H \quad R)^T$ is the vector of unknowns, $\boldsymbol{x}(0)$ is the positive vector of initial conditions, ω is some complex (constant) frequency. Our aim is to show that under assumptions of Theorem 6.3.1, it holds Re $\omega < 0$.

Assume the opposite, i.e., Re $\omega \geq 0$ and split this into two distinct cases.

1) $\omega = 0$. Then, we have the constant solution

$$\boldsymbol{x}(t) = \boldsymbol{x}(0),$$

for all t. Obviously, it satisfies (6.6) if and only if $\boldsymbol{x}(0) = 0$ which is not always the case. Therefore, $\omega = 0$ does not make sense.

2) Re $\omega > 0$. Then,

$$\begin{aligned}\boldsymbol{x}(t) &= \boldsymbol{x}(0)\exp(\text{Re }\omega t)\exp(i\text{Im }\omega t) = \\ &= \boldsymbol{x}(0)\exp(\text{Re }\omega t)\cos(\text{Im }\omega t) + i\boldsymbol{x}(0)\exp(\text{Re }\omega t)\sin(\text{Im }\omega t).\end{aligned}$$

Since according to our assumption $\mathcal{R}_c > 1$, then Lemma 6.3.1 implies that

$$\lim_{t\to\infty} \boldsymbol{x}(t) = 0,$$

which is possible if and only if $\boldsymbol{x}(0) = 0$ leading to a trivial solution.

Therefore, indeed, Re $\omega < 0$ and the statement of the theorem holds.

6.3.3 Global stability for special case

Let us now examine the global asymptotic stability of (6.1) in the particular case when

1. Hospitalized people should not spread infection,

2. The related disease-induced death is negligible.

These assumptions are expressed in terms of parameters of (6.1) as follows:

$$\delta_1 = \delta_2 = \zeta = 0, \quad \lambda = \beta\frac{A+I}{N}.$$

Then, the model is reduced to

$$\begin{aligned}
\frac{dS}{dt} &= \pi - (\lambda + \mu)\, S, \\
\frac{dE}{dt} &= \lambda S - (\kappa + \mu)\, E, \\
\frac{dA}{dt} &= (1-p)\, \kappa E - (\gamma_1 + \mu)\, A, \\
\frac{dI}{dt} &= p\kappa E - (\gamma_2 + \Phi + \mu)\, I, \\
\frac{dH}{dt} &= \Phi I - (\gamma_3 + \mu)\, H \\
\frac{dR}{dt} &= \gamma_1 A + \gamma_2 I + \gamma_3 H - \mu R.
\end{aligned} \tag{6.7}$$

Add equations of (6.7) together to obtain

$$\frac{dN}{dt} = \pi - \mu N,$$

which implies

$$\lim_{t\to\infty} N = \frac{\pi}{\mu}.$$

Therefore, when $N(0) \leq \frac{\pi}{\mu}$ (or $> \frac{\pi}{\mu}$), then $\frac{\pi}{\mu}$ is an upper (resp. lower) bound for N. In the limiting case,

$$\lambda = \frac{\beta\mu}{\pi}(A + I),$$

and the reproduction number of (6.7) interprets as

$$\mathcal{R}_{cr} = \frac{\beta p \kappa}{c_1 c_2},$$

where

$$c_1 = \kappa + \mu, \quad c_2 = \gamma_2 + \Phi + \mu.$$

Repeating the steps of Section 6.3.1, we will obtain the following statement.

Lemma 6.3.2. *The reduced model (6.7) has an unique positive endemic equilibrium when* $\mathcal{R}cr > 1$.

Then, the following result is proved.

Theorem 6.3.2. *The unique endemic equilibrium of the reduced model (6.7) is globally-asymptotically stable in* $\mathcal{D} \setminus \mathcal{D}_0$ *if* $\mathcal{R}_{cr} > 1$. *Here,*

$$\mathcal{D}_0 = \{(S, E, A, I, H, R) \in \mathcal{D} : E = A = I = H = R = 0\}.$$

Proof. Assume that $\mathcal{R}_{cr} > 1$, so that by Lemma 6.3.2, (6.7) has a unique positive endemic equilibrium.

Further, considering the nonlinear Lyapunov function

$$\mathcal{L} = S - S^{**} - S^{**} \ln \frac{S}{S^{**}} + E - E^{**} - E^{**} \ln \frac{E}{E^{**}} + \frac{c_1}{p\kappa} \left[I - I^{**} - I^{**} \ln \frac{I}{I^{**}} \right] + \\ + \frac{c_1 c_2}{p\kappa c_3} \left[A - A^{**} - A^{**} \ln \frac{A}{A^{**}} \right],$$

where

$$c_3 = \gamma_1 + \mu,$$

and its Lyapunov derivative

$$\frac{\partial \mathcal{L}}{\partial t} = \frac{dS}{dt} - \frac{S^{**}}{S} \frac{dS}{dt} + \frac{dE}{dt} - \frac{E^{**}}{E} \frac{dE}{dt} + \frac{c_1}{p\kappa} \left[\frac{dI}{dt} - \frac{I^{**}}{I} \frac{dI}{dt} \right] + \frac{c_1 c_2}{p\kappa c_3} \left[\frac{dA}{dt} - \frac{A^{**}}{A} \frac{dA}{dt} \right] = \\ = \left[1 - \frac{S^{**}}{S} \right] \frac{dS}{dt} + \left[1 - \frac{E^{**}}{E} \right] \frac{dE}{dt} + \frac{c_1}{p\kappa} \left[1 - \frac{I^{**}}{I} \right] \frac{dI}{dt} + \frac{c_1 c_2}{p\kappa c_3} \left[1 - \frac{A^{**}}{A} \right] \frac{dA}{dt} = \\ = \left[1 - \frac{S^{**}}{S} \right] [\pi - (\lambda + \mu) S] + \left[1 - \frac{E^{**}}{E} \right] [\lambda S - c_1 E] + \\ + \frac{c_1}{p\kappa} \left[1 - \frac{I^{**}}{I} \right] [p\kappa E - c_2 I] + \frac{c_1 c_2}{p\kappa c_3} \left[1 - \frac{A^{**}}{A} \right] [(1-p)\kappa E - c_3 A].$$

After some simplifications, we obtain

$$\frac{\partial \mathcal{L}}{\partial t} = \pi\left[1-\frac{S^{**}}{S}\right] - \mu S\left[1-\frac{S^{**}}{S}\right] + c_1\alpha_1 E\left[1-\frac{A^{**}}{A}\right] + \left(\beta_1 S^{**} - \frac{c_1c_2}{p\kappa}\right)(A+I) -$$
$$- \beta_1\frac{E^{**}S(A+I)}{E} + c_1E^{**} - c_1\frac{EI^{**}}{I} + \frac{c_1c_2}{p\kappa}(A^{**}+I^{**}),$$

with

$$\alpha_1 = \frac{c_2(1-p)}{pc_3}.$$

Note that the endemic equilibrium $\mathcal{E}_1$,

$$\pi = \beta_1 S^{**}(A^{**}+I^{**}) + \mu S^{**},$$

$$\beta_1 S^{**} = \frac{c_1c_2}{p\kappa},$$

and

$$c_1E^{**} = \beta_1 S^{**}(A^{**}+I^{**}).$$

Therefore,

$$\frac{\partial \mathcal{L}}{\partial t} = \beta_1 S^{**}(A^{**}+I^{**}) - \beta_1 S^{**}\frac{S^{**}(A^{**}+I^{**})}{S} + \mu S^{**} - \mu S^{**}\frac{S^{**}}{S} - \mu S +$$
$$+ \mu S_1 - c_1\alpha_1 E\left[1-\frac{A^{**}}{A}\right] - \beta_1\frac{E^{**}S(A+I)}{E} + \beta_1 S^{**}(A^{**}+I^{**}) -$$
$$- c_1\frac{EI^{**}}{I} + \beta_1 S^{**}(A^{**}+I^{**}) =$$
$$= \mu S^{**}\left[2-\frac{S^{**}}{S}-\frac{S}{S^{**}}\right] +$$
$$+ \beta_1 S^{**}(A^{**}+I^{**})\left[3-\frac{S^{**}}{S}-\frac{EI^{**}}{E^{**}I}-\frac{E^{**}S(A+I)}{ES^{**}(A^{**}+I^{**})}-\alpha_1\frac{E}{E^{**}}\left[1-\frac{A^{**}}{A}\right]\right].$$

Now, taking into account that

$$2-\frac{S^{**}}{S}-\frac{S}{S^{**}} = -\frac{(S-S^{**})^2}{SS^{**}} \leq 0,$$

$$3 - \frac{S^{**}}{S} - \frac{EI^{**}}{E^{**}I} - \frac{E^{**}S(A+I)}{ES^{**}(A^{**}+I^{**})} \leq 0.$$

As all model parameters are non-negative, and the arithmetic mean exceeds the geometric mean,

$$\alpha_1 \frac{E}{E^{**}} \left[1 - \frac{A^{**}}{A}\right] \leq 0.$$

Hence,

$$\frac{\partial \mathcal{L}}{\partial t} \leq 0,$$

meaning that $\mathcal{L}$ is the Lyapunov function of the first three equations of the reduced model (6.7). Therefore, LaSalle's Invariance Principle provides

$$\lim_{t\to\infty}(S, E, A, I) = (S^{**}, E^{**}, A^{**}, I^{**}).$$

Then, since all parameters of (6.7) are positive, from its fifth equation, we obtain

$$\lim_{t\to\infty} H = \frac{\Phi I^{**}}{\gamma_3 + \mu} := H^{**}.$$

Similarly,

$$\lim_{t\to\infty} R = \frac{\gamma_1 A^{**} + \gamma_2 I^{**} + \gamma_3 H^{**}}{\mu} := R^{**}.$$

Thus,

$$\lim_{t\to\infty}(S, E, I, A, H, R) = (S^{**}, E^{**}, I^{**}, A^{**}, H^{**}, R^{**}),$$

proving the statement of the theorem. □

6.4 Discussion and Conclusion

The objective of this chapter is to conduct a thorough qualitative approach of a deterministic model for exclusion and segregation in order to gain a better understanding of the influence among these control measures on the propagation of MERS-CoV. This study utilizes a mathematical model to configure and examine the mechanisms of the MERS-CoV infection in Saudi Arabia . The goal of this model is to provide the health care sector and relevant authority with a predictive methodology to evaluate the various MERS-CoV circumstances and the efficiency of various intervention activities. Healthcare practitioners should be aware of the need to discover individuals who should be assessed for MERS-CoV infection. This needs clinical decision making as information on MERS-CoV transmission routes and clinical manifestations evolve.

We assessed the global stability of the disease free and endemic equilibria using the stability of the control reproduction number R_c.

First, we consider the impact of reduction in disease transmission by hospitalized individuals on $\mathcal{R}_c$. For this purpose, compute the derivative

$$\frac{\partial \mathcal{R}_c}{\partial \zeta} = \frac{\partial}{\partial \zeta}\left[\frac{\beta p\kappa}{(\kappa+\mu)(\gamma_2+\Phi+\mu+\delta_1)} + \frac{\beta\zeta p\kappa\Phi}{(\kappa+\mu)(\gamma_2+\Phi+\mu+\delta_1)(\gamma_3+\mu+\delta_2)}\right] = \\ = \frac{\beta p\kappa\Phi}{(\kappa+\mu)(\gamma_2+\Phi+\mu+\delta_1)(\gamma_3+\mu+\delta_2)}.$$

Evidently, for any set of values of model parameters,

$$\frac{\partial \mathcal{R}_c}{\partial \zeta} > 0,$$

i.e., $\mathcal{R}_c$ is an increasing function of ζ. This leads to the following result.

Lemma 6.4.1. *The use of isolation of the hospitalized individuals will always have positive (negative) population-level impact if* $\zeta < (>) b_1$, *where* $b_1 = \frac{\gamma_2+2\Phi+\mu+\delta_1}{\gamma_3+\mu+\delta_2}$.

Then, the impact of the isolation of infectious individuals is monitored by computing the partial derivative of $\mathcal{R}_c$ with respect to the parameter Φ given by

$$\begin{aligned}
\frac{\partial \mathcal{R}_C}{\partial \Phi} &= \frac{\partial}{\partial \Phi}\left[\frac{\beta p\kappa}{(\kappa+\mu)(\gamma_2+\Phi+\mu+\delta_1)} + \frac{\beta\zeta p\kappa\Phi}{(\kappa+\mu)(\gamma_2+\Phi+\mu+\delta_1)(\gamma_3+\mu+\delta_2)}\right] = \\
&= \frac{\beta p\kappa}{(\kappa+\mu)}\frac{\partial}{\partial \Phi}\left[\frac{1}{\gamma_2+\Phi+\mu+\delta_1}\right] + \\
&+ \frac{\beta\zeta p\kappa}{(\kappa+\mu)(\gamma_3+\mu+\delta_2)}\frac{\partial}{\partial \Phi}\left[\frac{\Phi}{(\gamma_2+\Phi+\mu+\delta_1)}\right] = \\
&= -\frac{\beta p\kappa}{(\kappa+\mu)}\frac{1}{(\gamma_2+\Phi+\mu+\delta_1)^2} + \\
&+ \frac{\beta\zeta p\kappa}{(\kappa+\mu)(\gamma_3+\mu+\delta_2)}\frac{\gamma_2+2\Phi+\mu+\delta_1}{(\gamma_2+\Phi+\mu+\delta_1)^2} = \\
&= \frac{\beta p\kappa}{(\gamma_2+\Phi+\mu+\delta_1)^2}\left[\frac{\zeta(\gamma_2+2\Phi+\mu+\delta_1)}{(\kappa+\mu)(\gamma_3+\mu+\delta_2)} - \frac{1}{\kappa+\mu}\right] := \\
&:= \frac{\beta p\kappa}{(\kappa+\mu)(\gamma_2+\Phi+\mu+\delta_1)^2}\left[b_1\zeta - 1\right],
\end{aligned}$$

where,

$$b_1 = \frac{\gamma_2+2\Phi+\mu+\delta_1}{\gamma_3+\mu+\delta_2} > 0.$$

Therefore,

$$\frac{\partial \mathcal{R}}{\partial \Phi} < 0 \quad (>0) \quad \text{iff} \quad b_1\zeta - 1 < 0 \quad (>0).$$

As a result, if the corresponding infectiousness of hospitalized patients ζ does not exceed the threshold b_1, the use of isolation of individuals with illness symptoms will be helpful to the community. The objective of this model is to offer the health-care industry and related authorities with a prediction approach for evaluating diverse MERS-CoV situations and the efficacy of various intervention efforts regard to the parameters above. For example, the hospital administration should guarantee that all staff working in the hospital get the appropriate personal protection against infection and are not exposed to infectious pathogens improperly. Employees who are infected or in a carrier condition must be managed properly

to prevent infection from spreading to patients, employees, or the environment. District management has to ensure that patients follow infection prevention and control policy and protocols, that they have access to adequate personal protection against infection, and that they follow protocols for infection notification and response in the hospital.

Isolated patient care is essential for infectious disease prevention in hospitals. There should exist protocols and measures dedicated to maximize the overall health and well-being of the patient while also reducing the spread of MERS-CoV. For instance, health-care professionals should make brief frequent visits to the patient rather than long ones as this method minimizes the potential spread of infectious bacteria and viruses. Health-care professionals should also close all doors behind them attentively and cautiously while entering and exiting the room to avoid creating adverse air circulation. Moreover, there are many considerations regarding the mental health of the patient. The potential decrease in the patient's mental health upon admission should not be consequent to isolation. Entertainments such as TV, radios, smartphones, and newspapers/magazines that are acceptable for the patient are excellent to maintain mental health during isolation. Large windows for appropriate daylight may also be a component for maintaining mental health during isolation. Furthermore, in addition to the health of the patient, it is necessary for the patient that they receive periodic updates and information with regards to their illness and general health.

The prevention of infectious spread of disease and bacteria is often a factor of hospital clothing attire. Replacing private uniforms to hospital owned ones that are used in hospital services can minimize the spread of cross contamination between patients and health-care professionals alike. In direct patient contact, for example, medical and personal protective equipment such as yellow infection gowns are often contaminated, and therefore should be frequently monitored, cleaned, and/or replaced. Moreover, hospital protocols regarding clothing attire for infectious disease prevention include the following: hospital shoes and socks should strictly be used in hospital settings, all forms of jewellery including wrist watches are

not permitted in work with patients or equipment , nails should be clean and short, synthetic nails are not permitted, long hair should be in a form that is controlled and secured since there can often be substantial amounts of bacteria in the hair, work clothing should be made of a strong and thick material that can withstand washing at 85 degrees celsius for at least 10 minutes, and work clothes/other textiles must be cleaned in hospital-approved laundries [173].

Chapter 7

General Mobility Process

7.1 Introduction

We are shifting to the influenza study now, so first focus on mobility processes. The classical SIR model with S: susceptible population, I: infected population and R: recovered population, satisfies the below differential equation:

$$\frac{dS}{dt} = -\beta SI, \tag{7.1a}$$

$$\frac{dI}{dt} = \beta SI - \gamma I, \tag{7.1b}$$

$$\frac{dR}{dt} = \gamma I. \tag{7.1c}$$

Here β is the infection rate of the disease and γ is the recovery rate. Usually β is assumed as equal to everybody in the population who is susceptible to the disease, and also does not vary along the time. An infected individual could contact and infect persons, where $N = S + I + R$, among which the percent of susceptible individuals is $\frac{S}{N}$. Hence the number of new infections in unit time per infective is $N\beta \times \frac{S}{N}$, resulting in the total new infections given by all infective are $N\beta \times \frac{S}{N} \times I = \beta SI$. It is noteworthy that, the whole population is

static without increase and decrease, i.e. the population birth and death and migrations are not considered in the model, implying that

$$\frac{dN}{dt} = \frac{dS}{dt} + \frac{dI}{dt} + \frac{dR}{dt} = 0. \tag{7.2}$$

Several contemporary models for the transmission of infectious diseases in human societies contain non-random patterns of mixing among subgroups, as well as a factor for interaction among group that is dependent on the home population groups of susceptible and infectious people [174, 175]. This parameter simply indicates the end result of the mixing process leaving the method by which contact happens between people from various subgroups implicit. Little thought has been given to the process through which the pathogen spreads over space. There might be heterogeneity in the frequencies at which transition individual interact, but there is homogeneity among people for any specific transition. Individual variations in the natural tendency to relocate to certain places cause the second type of population heterogeneity. Each individual in this population follows a Markov chain, however the chains differ between individuals.

Predicting the behaviour of the infection diseases with geographic discrete distance requires a mobility process model to study the spread of infectious diseases among regions, incorporating it with an SIR model to understand the global dynamics of diseases. Therefore, we applied SIR model incorporating with geographic mobility among regions to determine how the dynamics of diseases will be changed among individual classes (susceptible, infectious, and recovered) in specific time frame[81].

Millions of pilgrims gather annually to participate in religious rites at Saudi Arabia's Mecca. These pilgrims potentially carry diseases from diverse geographic regions. Saudi Arabia's government has tackled to control diseases that are spread during specific time frames. According to research, disease transmission results from epidemics by the mobility

process among geographic regions with population structures. This study incorporates a transmission model with a mobility process and applies SIR model to study the prevalence of diseases among mass gatherings in Hajj. Infectious diseases are transmitted among pilgrims at Mecca and also transported to their home countries.

7.2 Deterministic system of the General Mobility Process

Various factors, including involvement in the community, social activities, ethnic diversity, and social norms, impact the probability of interaction between susceptible and infected individuals. Now we introduce another model in the population migration. We modify the model for the geographic spread of the people that was created by Sattenspiel and Dietz [81]. Define N_{ij} the number of citizens of country i who are in country j at time t. Exclusively, N_{ii} is the population staying in the home country. Another two parameters, σ_i and ρ_i, are defined as the mobility rate of citizens in the country i leaving their home country, and as the proportion of people returning to their home country i from foreign country j separately. With these notations, a geographic mobility model may establish and it is accessible to be structured. The individual traveler among the regions is illustrated by

$$\frac{dN_{ii}}{dt} = \sum_{j=1} \rho_{ij} N_{ij} - \sigma_i N_{ii}, \tag{7.3}$$

$$\frac{dN_{ij}}{dt} = \sigma_i N_{ii} - \rho_{ij} N_{ij}. \tag{7.4}$$

To find equilibrium points, we set

$$\frac{dN_{ij}}{dt} = \sigma_i N_{ii} - \rho_{ij} N_{ij} = 0. \tag{7.5}$$

Then by re-ranging for N_{ii}, equation 7.5 yields

$$N_{ij} = \frac{\sigma_i}{\rho_{ij}} N_{ii}. \tag{7.6}$$

Adding sum in both side of equation when $i \neq j$ leads to

$$\sum_{j \neq i} N_{ij} = \sum_{j \neq i} \frac{\sigma_i}{\rho_{ij}} N_{ii}. \tag{7.7}$$

Since $\sigma_i N_{ii}$ is constant, then the term in right hand side in equation 7.7 yields,

$$\sum_{j \neq i} \frac{\sigma_i}{\rho_{ij}} N_{ii} = \sigma_i N_{ii} \sum_{j \neq i} \frac{1}{\rho_{ij}}. \tag{7.8}$$

Suppose N_i represent the number of citizens of country i, then

$$N_i = \sum_{s \neq i} N_{is} + N_{ii}, \tag{7.9}$$

where the index j from Equation 7.5 is replaced with s. Thus,

$$N_i = \sigma_i N_{ii} \sum_{s \neq i} \frac{1}{\rho_{is}} + N_{ii}, \tag{7.10a}$$

$$N_i = N_{ii}(1 + \sigma_i \sum_{s \neq i} \frac{1}{\rho_{is}}), \tag{7.10b}$$

and finally

$$N_{ii} = N_i(1 + \sigma_i \sum_{s \neq i} \frac{1}{\rho_{is}})^{-1}. \tag{7.10c}$$

The spread of a disease in the pilgrimage have a high probability with massive crowed

movement. The transmission term for the infection process is represented by:

$$\sum_{j=1}^{n}\sum_{k=1}^{n}\tau_k\kappa_k\beta_{ijk}\frac{I_{jk}S_{ik}}{N_k^*} \tag{7.11}$$

where,

τ_k is the probability of transmission per contact in region k.

κ_k is the average number of contacts per person in region k.

β_{ijk} is the proportion of the contacts in country k between susceptible individuals from country i and infected individuals from country j.

I_{jk} is the number of infected individuals currently in country k who are citizens of country j.

S_{ik} is the number susceptible individuals currently in country k who are citizens of country i.

Furthermore, the number of individuals currently in country k is represented by

$$N_k^* = \sum_m (S_{mk} + I_{mk} + R_{mk}). \tag{7.12}$$

Susceptible citizens of region i who are currently at that region given by:

$$\frac{ds_{ii}}{dt} = \text{Number of citizens returning home country}$$

$$\text{- Number of citizens leaving their home as travellers - transmission term,}$$

or,

$$\frac{dS_{ii}}{dt} = \sum_k \rho_{ik}S_{ik} - \sigma_i S_{ii} - \sum_j \tau_k\kappa_i\beta_{iji}\frac{S_{ii}I_{ji}}{N_i^*}. \tag{7.13}$$

The changing of susceptible citizens of region i who are travelling to other region is represented by

$$\frac{dS_{ik}}{dt} = \sigma_i S_{ii} - \rho_{ik}S_{ik} - \sum_j \tau_k\kappa_k\beta_{ijk}\frac{S_{ik}I_{jk}}{N_k^*}. \tag{7.14}$$

7.3 SIR Model:

The complete SIR epidemic model with the mobility process is given by:

$$\frac{dS_{ii}}{dt} = \sum_k \rho_{ik} S_{ik} - \sigma_i S_{ii} - \sum_j \tau_k \kappa_i \beta_{iji} \frac{S_{ii} I_{ji}}{N_i^*}, \tag{7.15a}$$

$$\frac{dS_{ik}}{dt} = \sigma_i S_{ii} - \rho_{ik} S_{ik} - \sum_j \tau_k \kappa_k \beta_{ijk} \frac{S_{ik} I_{jk}}{N_k^*}, \tag{7.15b}$$

$$\frac{dI_{ii}}{dt} = \sum_k \rho_{ik} I_{ik} - \sigma_i I_{ii} + \sum_j \tau_k \kappa_i \beta_{iji} \frac{S_{ii} I_{ji}}{N_i^*} - \gamma I_{ii}, \tag{7.15c}$$

$$\frac{dI_{ik}}{dt} = \sigma_i I_{ii} - \rho_{ik} I_{ik} + \sum_j \tau_k \kappa_k \beta_{ijk} \frac{S_{ik} I_{jk}}{N_k^*} - \gamma I_{ik}, \tag{7.15d}$$

$$\frac{dR_{ii}}{dt} = \sum_k \rho_{ik} R_{ik} - \sigma_i R_{ii} + \gamma I_{ii}, \tag{7.15e}$$

$$\frac{dR_{ik}}{dt} = \sigma_i R_{ii} - \rho_{ik} R_{ik} + \gamma I_{ik}. \tag{7.15f}$$

where γ is the recovery rate from the diseases.

We assume three countries, Saudi Arabia [Mecca] region(1), Egypt region(2), Iran region(3). These three are chosen since Saudi Arabia is the host country, Egypt and Iran have comparable populations with the largest number of pilgrims that attended. The model that represents the number of susceptible, infected, and recovered individuals in Mecca at Saudi Arabia is given by

$$\frac{dS_{11}}{dt} = \sum_k \rho_{ik} S_{1k} - \sigma_1 S_{11} - \sum_j \tau_k \kappa_1 \beta_{1j1} \frac{S_{11} I_{j1}}{N_1^*}, \tag{7.16a}$$

$$\frac{dS_{1k}}{dt} = \sigma_1 S_{11} - \rho_{1k} S_{1k} - \sum_j \tau_k \kappa_k \beta_{1jk} \frac{S_{1k} I_{jk}}{N_k^*}, \tag{7.16b}$$

$$\frac{dI_{11}}{dt} = \sum_k \rho_{1k} I_{1k} - \sigma_1 I_{11} + \sum_j \tau_k \kappa_1 \beta_{1j1} \frac{S_{11} I_{j1}}{N_1^*} - \gamma I_{11}, \tag{7.16c}$$

$$\frac{dI_{1k}}{dt} = \sigma_1 I_{11} - \rho_{1k} I_{1k} + \sum_j \tau_k \kappa_k \beta_{1jk} \frac{S_{1k} I_{jk}}{N_k^*} - \gamma I_{1k}, \tag{7.16d}$$

$$\frac{dR_{11}}{dt} = \sum_k \rho_{1k} R_{1k} - \sigma_1 R_{11} + \gamma I_{11}, \tag{7.16e}$$

$$\frac{dR_{1k}}{dt} = \sigma_i R_{11} - \rho_{1k} R_{1k} + \gamma I_{1k}. \tag{7.16f}$$

The model that represent the number of susceptible, infected, and recovered at Egypt is represented by

$$\frac{dS_{22}}{dt} = \sum_k \rho_{2k} S_{2k} - \sigma_2 S_{22} - \sum_j \tau_k \kappa_2 \beta_{2j2} \frac{S_{22} I_{j2}}{N_2^*}, \tag{7.17a}$$

$$\frac{dS_{2k}}{dt} = \sigma_2 S_{22} - \rho_{2k} S_{2k} - \sum_j \tau_k \kappa_k \beta_{2jk} \frac{S_{2k} I_{jk}}{N_k^*}, \tag{7.17b}$$

$$\frac{dI_{22}}{dt} = \sum_k \rho_{2k} I_{2k} - \sigma_2 I_{22} + \sum_j \tau_k \kappa_2 \beta_{2j2} \frac{S_{22} I_{j2}}{N_2^*} - \gamma I_{22}, \tag{7.17c}$$

$$\frac{dI_{2k}}{dt} = \sigma_2 I_{22} - \rho_{2k} I_{2k} + \sum_j \tau_k \kappa_k \beta_{2jk} \frac{S_{2k} I_{jk}}{N_k^*} - \gamma I_{2k}, \tag{7.17d}$$

$$\frac{dR_{22}}{dt} = \sum_k \rho_{2k} R_{2k} - \sigma_2 R_{22} + \gamma I_{22}, \tag{7.17e}$$

$$\frac{dR_{2k}}{dt} = \sigma_2 R_{22} - \rho_{2k} R_{2k} + \gamma I_{2k}. \tag{7.17f}$$

The model that represent the number of susceptible, infective, and recover individuals at Iran is represented by:

$$\frac{dS_{33}}{dt} = \sum_k \rho_{3k} S_{3k} - \sigma_3 S_{33} - \sum_j \tau_k \kappa_3 \beta_{3j3} \frac{S_{33} I_{j3}}{N_3^*}, \tag{7.18a}$$

$$\frac{dS_{3k}}{dt} = \sigma_3 S_{33} - \rho_{3k} S_{3k} - \sum_j \tau_k \kappa_k \beta_{3jk} \frac{S_{3k} I_{jk}}{N_k^*}, \tag{7.18b}$$

$$\frac{dI_{33}}{dt} = \sum_k \rho_{3k} I_{3k} - \sigma_3 I_{33} + \sum_j \tau_k \kappa_3 \beta_{3j3} \frac{S_{33} I_{j3}}{N_3^*} - \gamma I_{33}, \tag{7.18c}$$

$$\frac{dI_{3k}}{dt} = \sigma_3 I_{33} - \rho_{3k} I_{3k} + \sum_j \tau_k \kappa_k \beta_{3jk} \frac{S_{3k} I_{jk}}{N_k^*} - \gamma I_{3k}, \tag{7.18d}$$

$$\frac{dR_{33}}{dt} = \sum_k \rho_{3k} R_{3k} - \sigma_3 R_{33} + \gamma I_{33}, \tag{7.18e}$$

$$\frac{dR_{3k}}{dt} = \sigma_3 R_{33} - \rho_{3k} R_{3k} + \gamma I_{3k}. \tag{7.18f}$$

Table 7.1: Parameter values country 1 (Saudi Arabai)

Parameter values		
Parameters	Description	References
$\sigma_1 = 0$	people leaving the host country	[64]
$\rho_{12}, \rho_{13} = 0.001, 0.002$	people returning to the host country	[64]
$\beta = 0.32;$	contact rate	Assumed
$\tau_1 = 0.30$	probability transmission per contact	[58]

Table 7.2: Parameter values country 2 (Egypt)

Parameter Values		
Parameters	Description	References
$\sigma_2 = 0.001$	people leaving Egypt	[64]
$\rho_{21}, \rho_{23} = 0.009, 0.004$	people returning to Egypt	[64]
$\beta = 0.211$	contact rate	Assumed
$\tau_2 = 0.21$	probability transmission per contact	[176]

Table 7.3: Parameter values country 3 (Iran)

Parameter Values		
Parameters	Description	References
$\sigma_3 = 0.002$	people leaving Iran	[64]
$\rho_{31}, \rho_{32} = 0.019, 0.005$	people returning to Iran	[64]
$\beta = 0.311$	proportion of the contacts	Assumed
$\tau_3 = 0.15$	probability transmission per contact	[177]

7.4 Methods and Results

We solved the models numerically using ode45, and the results show; in Figure 7.1, the rate of susceptible people S_{11} at region (1) (Mecca) got very quick decreases and they finish within 5 days , so we see a decline in the results of the mass gatherings and pilgrims who became infected very quickly. However, the susceptible people S_{22}, and S_{33} at region (2) (Egypt) and region (3) (Iran) got slower decreases than the people at region (1) because of less contact. In addition, the people who were travelling from region (1) to region (2) S_{12} or region (3) S_{13} were at the same rate as in region (2) S_{22} and region (3) S_{33}. The pilgrims who were susceptible and travelled to region (1) rapidly became infected and we can realize the decreases of the rate of susceptibility; however, the visitors who were travelling between region (2) S_{23} and region (3) S_{32} became infected gradually.

In Figure 7.2, the infection rate increases promptly (see I_{11} which is the pilgrims in Mecca at the beginning); the peak of the infection occurred on the 5th day of the mass gathering with 1,700 cases, showing a sharp increase and then decreasing slowly after 6 days. This is due to fewer activities after the 5-to 6-day Hajj period, decreasing to 73 cases at the end of 30 days. Similarly, in infected pilgrims performing the Hajj from Egypt I_{21} and from Iran

I_{31}, the change of the rate of infection is the same as I_{11} since they are in the same scenario. In contrast, the visitors who were moved between Saudi Arabia, Egypt, and Iran, got slight infections and appear as normal distributions with the maximum number of infections being 1,250 cases. In the simulation, we estimated the initial condition of the susceptible class to be 2000 with infections in 10 people since we needed to start with a small aggregate of infectious numbers and investigate through the models how the dynamic of diseases changed between the different classes.

Finally, as we see in Figures 7.1, 7.2, and 7.3 , increasing the contact of people enables the growth of infection especially in region (1) with massive crowd movement and 5 persons per m^2 attendant decreasing of susceptibles. On the other hand, the recovery rate from the disease moved slowly in the first 5 days, but after that it increased sharply, particularly with R_{11}, R_{21}, and R_{31}; the recovery rate stayed at around 2000 cases which matches our initial guess for susceptibles. Increases and decreases of infection depend on how the dynamics of the infectious class spread among regions, so this hypothesis is clearly tested during the Hajj with more activity at the beginning of the month of the mass gathering and fewer activities after the period of the Hajj. Pilgrims may have less contact between them as compared to the first 4 days, the influenza immune system kicks in and they begin to recover regard to the parameter values in the tables 7.1, 7.2, and 7.3.

7.5 Discussion

Professional management of the Hajj is required to avoid health disasters. Collaboration between the saudi arabian health authorities and other national health organizations reduced the panic of an epidemic spread. In addition, new regulations from the Ministry of Health (MOH) helped to control a rapid outbreak of A (H1N1) during the 30 days of the Hajj [59]. In order to avoid infection, pilgrims were required to obtain vaccinations against the virus

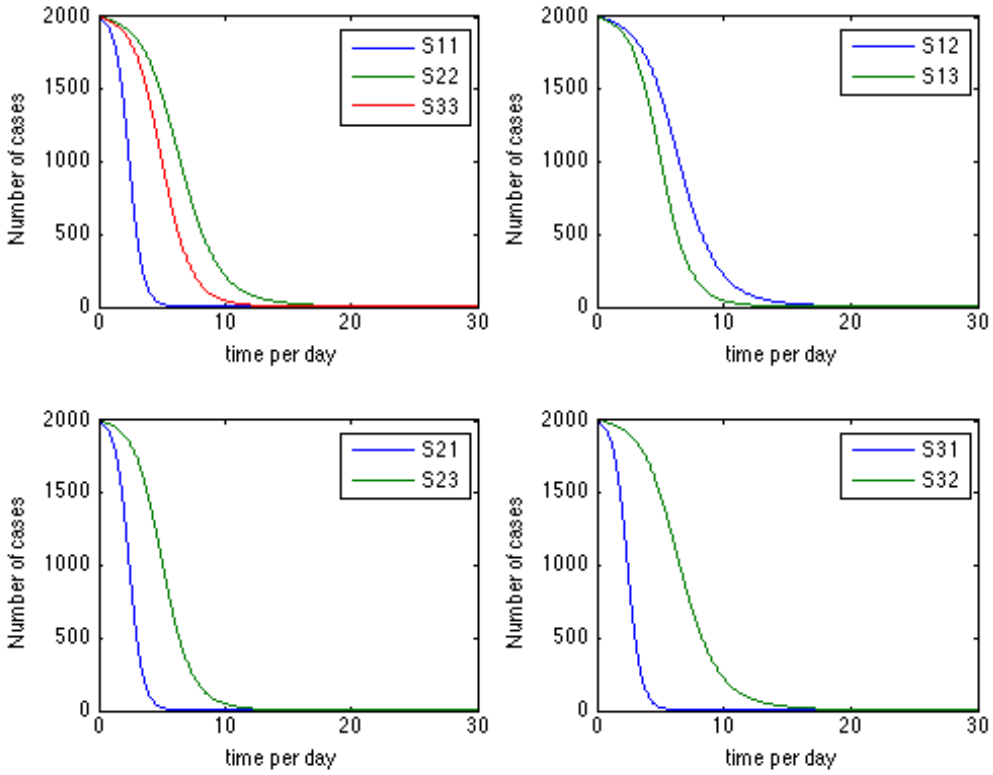

Figure 7.1: The number of susceptible individuals by H1N1 at different regions in 30 days

well in advance of performing the Hajj. However, pilgrims also had access to free medical and health care during that time, courtesy of the Saudi MOH. Health care professionals were faced with some confusion when attempting to differentiate between the symptoms of seasonal flu and A (H1N1); for example, headache, fever, cough, and sore throat are all symptoms of influenza, although they may not herald the onset of Swine flu. There makes difficulty to know the true number of cases of disease which lead to loss real data. Extreme weather conditions played a part, with temperatures rising to $45°C$. Also, it is challenging to check every patient when one is dealing with three million pilgrims, so we cannot get the exact count of the number of infected cases of A (H1N1). The real data that we found was that 80,000 pilgrims from Egypt performed the Hajj in 2009; we expect that 95% of them

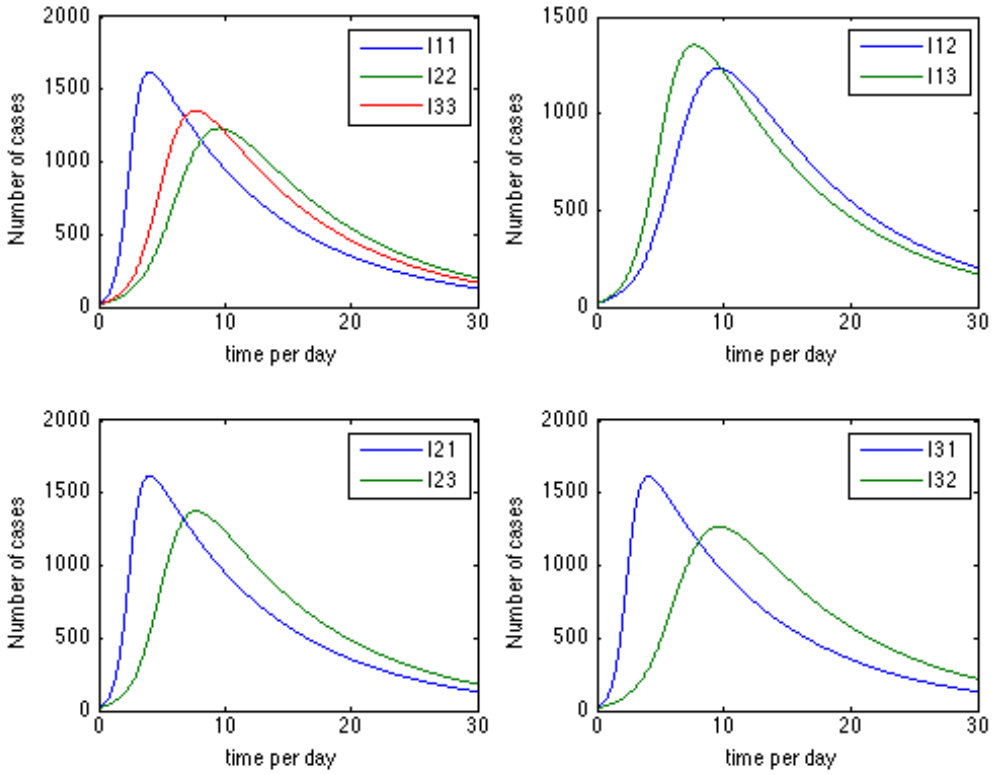

Figure 7.2: The number of infected individuals by H1N1 at different regions in 30 days

returned to their homes while the rest remained in Saudi Arabia. In addition, 65,000 were from Iran and 99% of them returned home since the agreement between Saudi Arabia and Iran concerning pilgrims leaving after the Hajj.

7.6 Conclusion

During the 2009 Hajj, 2.5 million pilgrims from 160 countries came to Mecca, coinciding with the outbreak of the worldwide Swine flu epidemic A(H1N1) [68]. A low incidence of the disease was unexpected during that time. However, the preventive measures that were taken prior to the pilgrims obtaining their visas, the thermal cameras they passed through at the

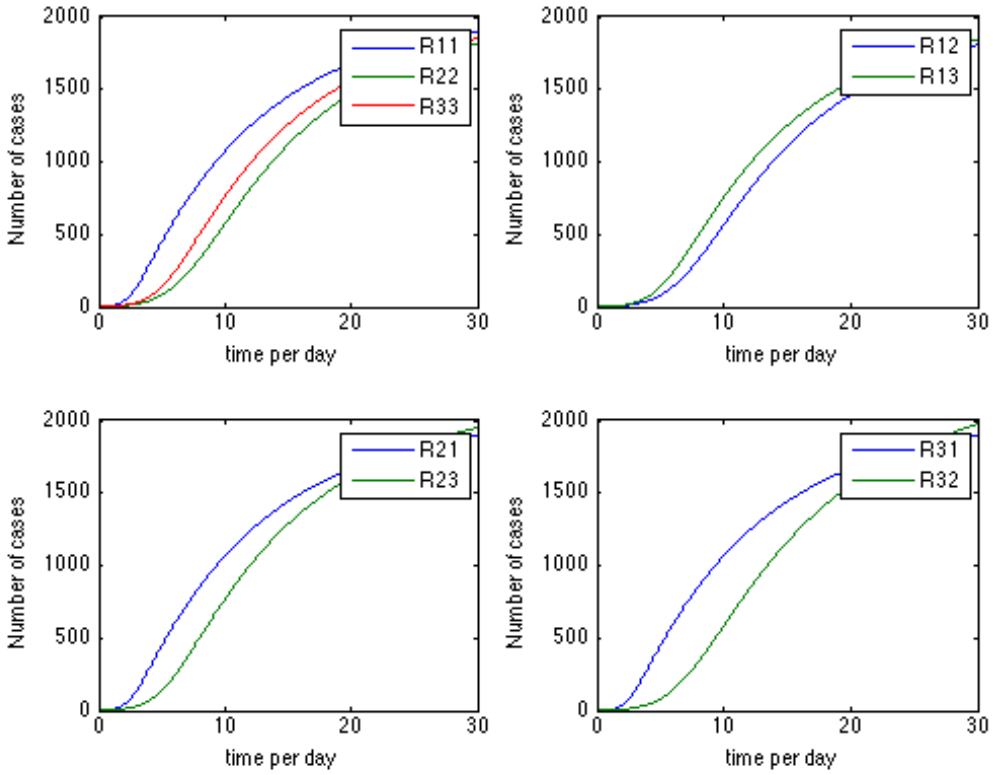

Figure 7.3: The number of recovered individuals by H1N1 at different regions in 30 days

point of entry, as well as temporary quarantines all contributed to the lack of an epidemic outbreak, especially at region (1). The short duration of the Hajj could also have contributed to the lower incidence of the disease though the reproductive number was 1.5. A survey of Egyptian pilgrims who returned home found that (98.1%) were vaccinated against A (H1N1) 2009, which was strongly recommended, and none of them returned with the pandemic H1N1 virus [176]. Likewise, in Iran, health authorities collected pharyngeal swabs of 305 pilgrims; 132 men (43.3%) and 173 women (56.7%) between the ages of 24 and 65. The result for A (H1N1) virus was positive in five pilgrims (1.6%) [177]. All of this evidence supports our findings. In addition, a mobility process model is a powerful tool to study the spread of infectious diseases among different geographic regions. Indeed, it becomes more useful

when an SIR model is incorporated to describe how contact occurs between individuals from different regions. Furthermore, simulation with non-constant parameters in the models can be used to better understand system dynamics not only with deterministic parameter profiles but also with stochastic parameters [69].

7.7 Stochastic Model of the General Mobility Process

7.7.1 Stochastic SIR Model:

It is very natural that we combine the deterministic and stochastic models to give an enhanced disease spread dynamic with population migration.

Suppose there is one host country and $M-1$ other home countries. For simplicity, populations can only migrate from their home countries to the host country (for host country, its citizen do not migrate) rather than other countries. hen we can show that the system of geographic mobility SIR system is static since there is no birth and death and population can only migrate within the system, i.e. the system is closed.

7.7.2 Methods: Probabilistic Solutions, Migration Probability

Obviously, the above geographic mobility SIR system (7.16) is an Ordinary Differential Equations (ODE) which can be solved in deterministic procedure. On the other hand, in the real world, the parameters, such as migration rate, infectious spread rate and recovery rate, are not constants, either varying along with the time, or affected by a noise. With the result that it is quite meaningful considering the stochastic behaviour in the parameters when solving the equation system. In the probabilistic problems, markov property is quite common and helpful for solving the stochastic systems [98]. Below we try to use markov property [101] to estimate the system evolution. Suppose one person in home country has such three statuses in migration: staying in home country, leaving for foreign country and returning home country. We use to define the migration, and 0, 1, 2 to present three different statuses at time t. Then the below probability equation is rational:

$$P(U_t = k \mid U_{t-1}, U_{t-2}, ...) = P(U_t = k \mid U_{t-1}), \tag{7.19}$$

where $k = 0, 1, 2$. Hence the migration randomness is said to have the markov property. The markov matrix for U_t is

$$\begin{pmatrix} \lambda_{11} & \lambda_{12} & 0 \\ 0 & \lambda_{22} & \lambda_{23} \\ 0 & 0 & 1 \end{pmatrix},$$

where

$$(P^{t,t-1})_{mn} = P(U_t = m \mid U_{t-1} = n).$$

The zero-element in the matrix is obvious. If a person is in the home country, then in the next moment he can only be either in the home country, or be in foreign country, but cannot be in returning status. Similarly, if a person is in the foreign country, he can never be in stay in home country any longer. Besides, if a person returns to his home country, his status can only be in returning in the future moments. One should note that, the migration status is independent of his SIR status, but only dependent on the time. To give the transition probability, we consider the transition in a small time interval :

$$P(U_{t+\Delta t} = k \mid U_{t+\Delta t} = j).$$

Here we suppose the probability of leaving for foreign country is 0.01 to the whole time span and uniformly distributed in every interval, which means within the whole time span (30 days, saying) the probability of leaving is 1%, and within 1 day, the probability is 0.033%.

While for the probability of returning home country from host country, we do not use uniform distribution on the time span. From the actual situation of Hajj, foreign people are more likely leave at the end of the Hajj period. Hence the uniform distribution is not suitable here and we need to use a "skewed"distribution. We find that a distribution having

the following format satisfies our requirement, which is skewed to the tail:

$$P(X < x) = \frac{\exp(ax + b)}{\exp(cx + d) + 1}. \tag{7.20}$$

That is the logistic function. However, in the logistic function the variable x can be positive and negative infinite, which is not the actual case in Hajj. Notwithstanding, we still apply the format by the following:

$$p = \frac{\exp((t - time_{span}/2)/20)}{\exp((t - time_{span}/2)/20) + 1}. \tag{7.21}$$

Here 20 is a scale factor used in our study, which determines the slope of the probability curve. Thus, we have completed the markov transition matrix used to determine the status of population geographic mobility in the below form:

$$P^{t+\Delta t,t} = \begin{pmatrix} 1 - \frac{0.01\times\Delta t}{T} & \frac{0.01\times\Delta t}{T} & 0 \\ 0 & 1 - \frac{\exp((t-time_{span}/2)/20)}{\exp((t-time_{span}/2)/20)+1} & \frac{\exp((t-time_{span}/2)/20)}{\exp((t-time_{span}/2)/20)+1} \\ 0 & 0 & 1 \end{pmatrix},$$

where 0.01 and 20 are adjustable.

Susceptible Status:

Similar to the markov matrix used in geographic mobility, we can also build a markov matrix for SIR movement. A gain we study the change in the time interval of $t, t + \Delta t$. The population may suffer a susceptible $\rightarrow$ infected $\rightarrow$ recovered process, which is not reversible.

Indeterminately, the desired markov matrix should have the below format:

$$Q^{t+\Delta t,t} = \begin{pmatrix} \omega_{11} & \omega_{12} & 0 \\ 0 & \omega_{22} & \omega_{23} \\ 0 & 0 & 1 \end{pmatrix},$$

where the 1^{st} column (row) stands for S, 2^{nd} column (row) for I and 3^{rd} column (row) for R. In the discretized-time problem, we need to determine the sequence of two or more occurrences, which would occur simultaneously in the real world. In our model, we conduct the migration status first and then classify the SIR status. Besides, at beginning of the model cycle, a person may be in S status or in I status. In our study, we assign a S or I status to a person randomly with probability:

$$P(W^0 = S) = 0.99,$$

and

$$P(W^0 = I) = 1 - P(W^0 = S) = 1 - 0.99 = 0.01.$$

Here W^t is the variable used for denote SIR status at moment of t. Again the initial probability 0.99 is adjustable to the actual position. In the program, for each person we generate a random variable rr following uniform distribution on [0,1]. If $rr < 0.99$, then the person is assigned with S status, else with I status [100].

From S to I:

After SIR status initialization, we should determine the infected process of a susceptible person. Without considering migration, the increase of I status is only due to the S person being infected, which is totally determined by the contact rate and infective density in a

person's environment. In our study, we assume that there is an inherent contact rate and a population migration growth rate jointly determining the contact rate, denoted as β_{ijk} in the above. Hence β_{ijk} can be calculates as

$$\beta_{ijk} = \beta_0 \times \frac{N_k^{t+\Delta t}}{N_k}, \tag{7.22}$$

where β_0 is a constant, playing a role of inherent contact rate, where $N_k^{t+\Delta t}$ is the population of country k in the moment $t + \Delta t$. Another factor in the $S - I$ process is the infective density in the country of a person, which is given by:

$$\text{Infective(density)} = \frac{I_k^{t+\Delta t}}{N_k^{t+\Delta t}}.$$

Hence the real contact rate and infective density will jointly determine the infected rate in a population. Here we try to map $\beta_{ijk} \times$ Infective(density) to the infected probability. Note that, if $\beta_{ijk} = 0$, meaning no contact among population or, Infective(density)=0, meaning no infective person in the population, will cause the extinction of the disease. On the contrary, if $\beta_{ijk} =$ is very large, or Infective(density) ≈ 1, a person is more likely to be infected. Based on this assumption, we try to build a probability function on $\beta_{ijk} \times$ Infective(density) , which is 0 when $\beta_{ijk} \times$ Infective(density) $= 0$ and is 1 when $\beta_{ijk} \times$ Infective(density) is very large. The below function satisfies the above requirement and is used in the model:

$$P(W^{t+\Delta t} = I \mid W^t = S) = \frac{\exp(\beta_{ijk} \times \text{Infective(density)}) - 1}{\exp(\beta_{ijk} \times \text{Infective(density)}) \times 10}. \tag{7.23}$$

Once again, 10 is a adjustable factor which ensures the probability of being infected a reasonable value [99, 101].

From I to R:

Now we are studying the probability that a infected person getting recovered. Therefore, we are looking for the probability $P(W^{t+\Delta t} = R \mid W^t = I)$; how it look like. In the classical SIR model, γ is the recovery rate, which means that the large γ will result a shorter time period of being infected. Hence, we believe that the days of being infected can be a random variable of which the distribution function is related to γ . Moreover, the days of being infective is non-negative and can be any positive number. Based on these assumptions, we find that the exponential distribution satisfies the requirement. Accordingly, we may assume the days of being infected follows an exponential distribution of $\frac{1}{\gamma}$. Once we fix the problem of days being infective, we can determine the probability $P(W^{t+\Delta t} = R \mid W^t = I)$, which has the below property:

$$P(W^{t+\Delta t} = R \mid W^t = I) = P(\Delta t \leq t_{exp}), \tag{7.24}$$

where t_{exp} follows the exponential distribution of parameter $\frac{1}{\gamma}$. In the programming, for each person we mark the moment that a person is infected (the moment is 0 if he is infected initially). With the time increase, we generate a random variable following the exponential distribution of parameter $\frac{1}{\gamma}$. If the increased time interval Δt is larger than t_{exp}, we regard the person is recovered. Now we have completed built the Markov matrix for SIR status transition. The matrix is:

$$Q^{t+\Delta t,t} = \begin{pmatrix} 1 - \frac{\exp\left(\beta_{ijk} \times \text{Infective(density)}\right) - 1}{\exp\left(\beta_{ijk} \times \text{Infective(density)}\right) \times 10} & \frac{\exp\left(\beta_{ijk} \times \text{Infective(density)}\right) - 1}{\exp\left(\beta_{ijk} \times \text{Infective(density)}\right) \times 10} & 0 \\ 0 & 1 - \exp\left(\frac{1}{\gamma}\right) & \exp\left(\frac{1}{\gamma}\right) \\ 0 & 0 & 1 \end{pmatrix}.$$

The meaning of $\exp\left(\frac{1}{\gamma}\right)$ is given as above. One should note that, the contact rate β_{ijk} and infective(density) reply on the country that a person is in, so the probability of

$$P(W^{t+\Delta t} = I \mid W^t = S),$$

depends on the geographic mobility, while the recovery probability

$$P(W^{t+\Delta t} = R \mid W^t = I),$$

does not [97, 98].

7.7.3 Results and Discussions

In this study we use Matlab as simulation platform to simulate Monte Carlo Method. As introduced in the above, some probability, such as recovery probability

$$P(W^{t+\Delta t} = R \mid W^t = I)$$

is decided from exponential distribution. So, we need to generate some random variables to determine status transition. Table 7.4 summarizes the generated random variables in the program and their usage.

Table 7.4: Generated random variables.

Table 1: Generate Random Variables		
Random Variables	Purpose	How to use
rr: uniform on [0,1]	Determine whether a person is susceptible at the beginning	If $rr \leq 0.99$ then the person is susceptible, otherwise infected at beginning
rr: exponential with $\frac{1}{\gamma}$	For an infected person, generate his expected recovery date	If the days of being infected is larger than rr, then he is recovered
rr: uniform on [0,1]	Determine whether a person would be migrate to foreign country	If $rr \leq \sigma$, then he is leaving for host country. Here σ is $0.01/N$, N is precision of simulation.
rr: uniform on [0,1]	Determine whether a person should leave foreign country and return	$p=\frac{\exp\left(\beta_{ijk}\times\text{Infective(density)}\right)-1}{\exp\left(\beta_{ijk}\times\text{Infective(density)}\right)\times 10}$

It is note that, in our simulation, each individual in every time unit is checked for their geographic mobility migration and SIR status, so the simulation involve huge steps, depending on time span (days of simulation times N) and population size of each country. Hence, if we assign a large population to a country, then the computation will be quite time consuming. We choose population sizes of the three countries, and choose time span as 4000 hours. The plot of Monte Carlo simulation is in Figures below. In all the three countries, the susceptible population decreases while the infected population increases rapidly, which means at the beginning, the epidemic explored. But after some time, the infected population slows down the increase and then decreases. Meanwhile, the recovered population grows.

Moreover, the infected population in country 2 decreases faster than that in other countries, and recovered population grow faster than other two countries, see figures 7.5 and 7.6. This may be caused by the larger recovery rate (0.02 v.s 0.01 and 0.005).

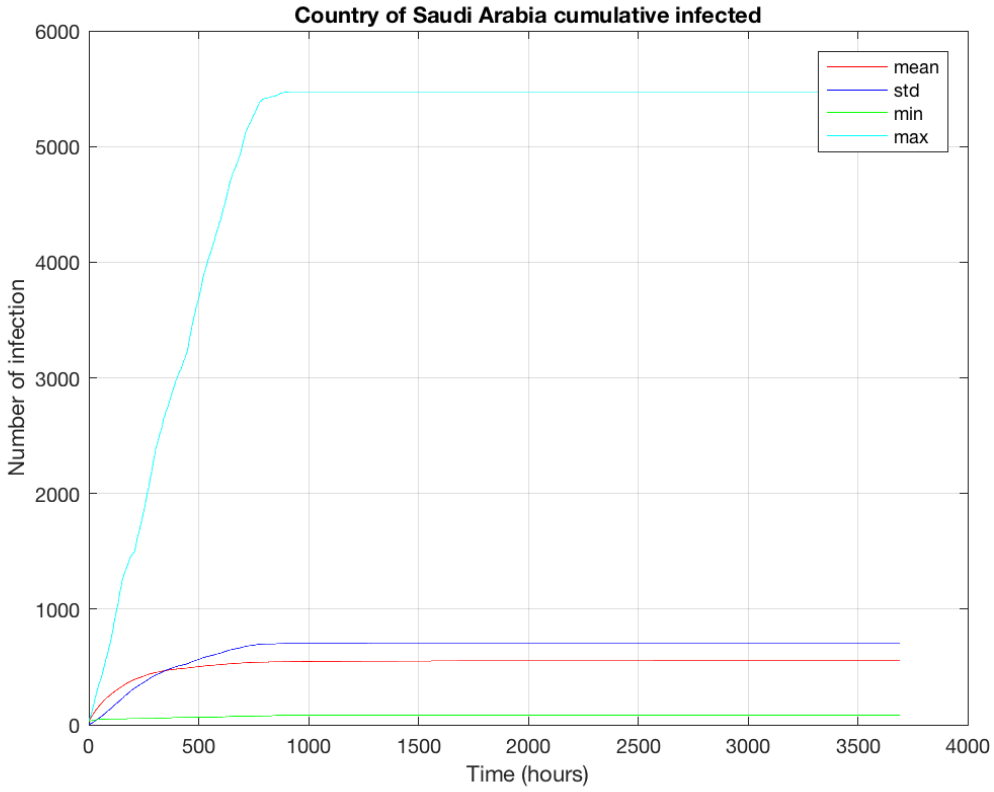

Figure 7.4: Stochastic SIR Model for country 1: Domestic Situation

If we think about Saudi Arabia as a host country for any diseases, then according to our simulation the infection rate increases promptly at the beginning of mass gathering among pilgrims since the contact rate is very high see figure 7.4; therefore, professional management during Hajj is required to avoid health disasters. The collaboration between health authorities in Saudi Arabia and other national health organizations worked effectively in reducing the panic of an epidemic spread. The new regulations from MoH (Ministry of Health; at Saudi Arabia) contributed to controlling the rapid outbreak of any disease for instance (H1N1)

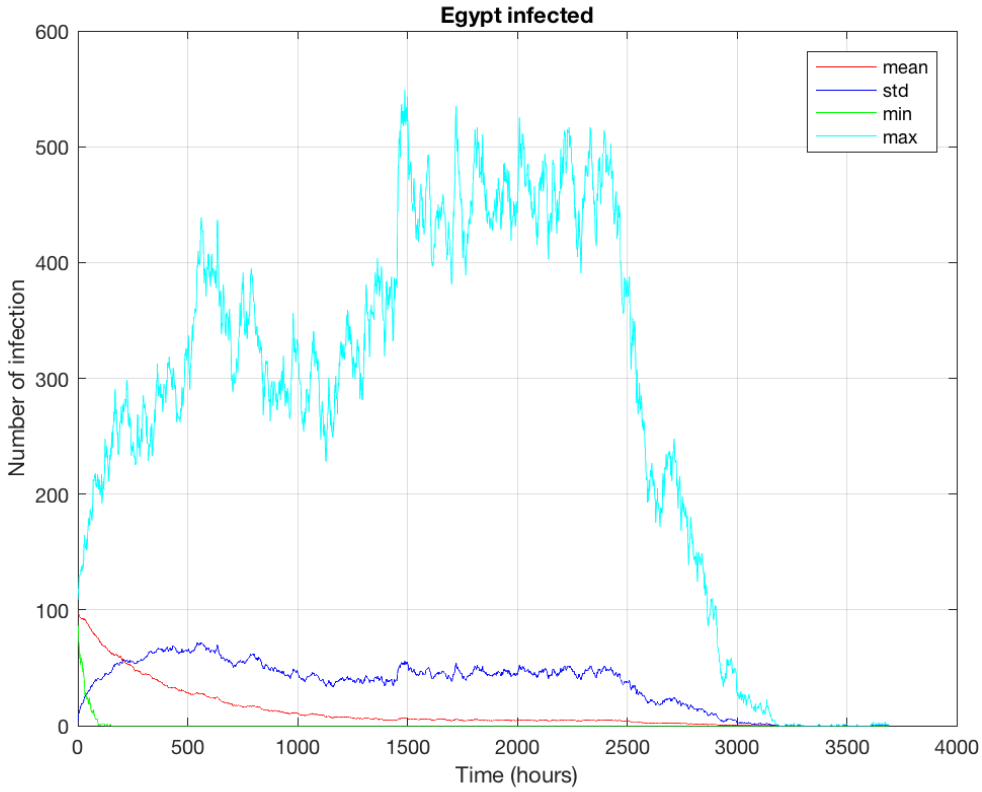

Figure 7.5: Stochastic SIR Model for country 2

during the period of Hajj or Umrah. The people who got infected up to now of (H1N1) are 299 resulting 87 death. During the period of Hajj or Umrah the number of infection will be high since large probability of contacts with massive crowd movement. Therefore, first, pilgrims should be vaccinated against the viruses well in advance of performing Hajj to avoid infection. Additionally, pilgrims have access to free medical and health care during the Hajj and Umrah time of MoH which would reduce the number of infectious. The pilgrims who get infected during Hajj and Umrah should stay there till get immune; otherwise, they will transfer diseases to their home country. Finally, we successfully combine the geographic mobility model and SIR model to derive the epidemic spread in connected countries, and use Monte Carlo simulation based on markov property of the model to simulate the spread. On

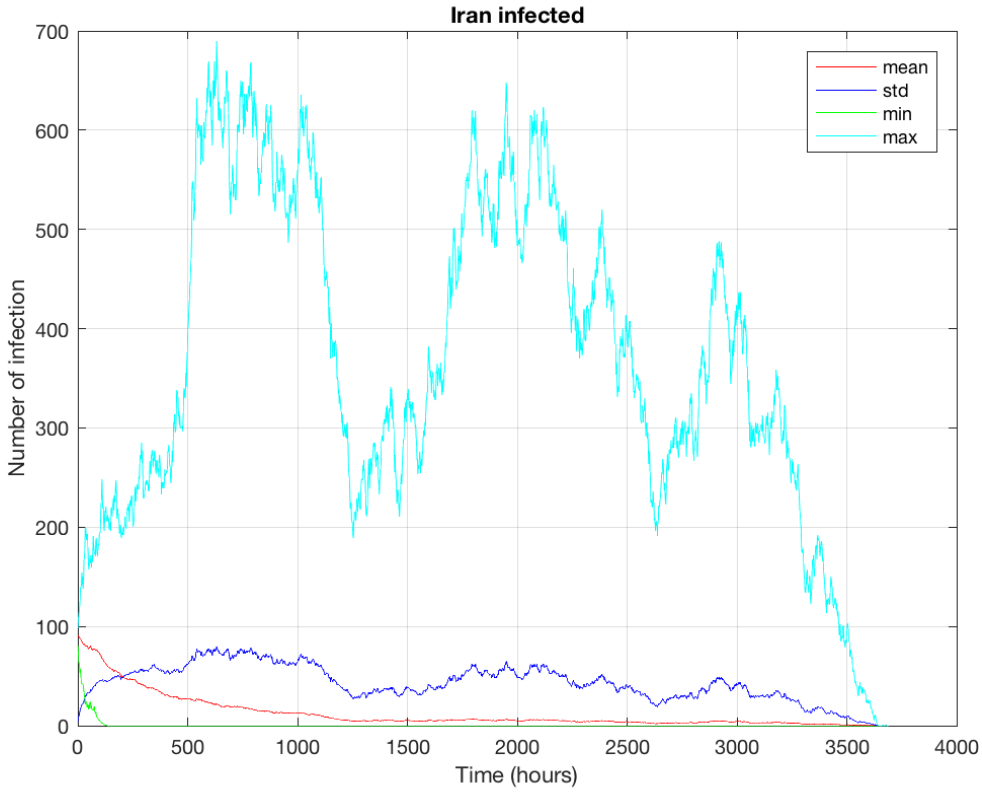

Figure 7.6: Stochastic SIR Model for country 3

the whole the simulated result is in line with what we expected before. The mobility process model is more capable of studying the transmission of infectious diseases across distinct geographic areas. Indeed, a mobility process model becomes more effective when used with the SIR model to describe how individuals from various places come into interact. However, simulation of non-constant parameters in the models may be utilized to better understand system dynamics with deterministic parameter characteristics as well as stochastic parameter features.

Chapter 8

General Discussion and Conclusion

8.1 Discussion and Conclusion

This thesis has focused on the development and analysis of mathematical models of issues affecting Saudi Arabia and the Middle East, specifically MERS-CoV and disease spread at the Hajj mass gathering. The models consider questions in public health, prevention, control of infection, health education, and transmission between humans and animal reservoirs.

Middle East Respiratory infection caused by Coronavirus (MERS-CoV) was reported in 2012 in Saudi Arabia [1, 3, 15, 90, 91, 153]. It has also been confirmed to have been transported to a variety of countries, 27 countries reported cases globally and 12 countries reported cases in the Eastern Mediterranean Region [23].

In Chapter 2, we formulated a mathematical model for two species to investigate the interactions between camel and human, and capture the dynamics of MERS epidemics by applying both deterministic and stochastic structure. Stability analysis has been done in the deterministic model; for example, global stability for the disease-free equilibrium and the endemic disease equilibrium using Lyapunov function. We discussed the probability of an outbreak as well as the number of deaths in the stochastic framework. Also, time to outbreak

and time to peak level of infection have been shown. We can conclude that the stochastic model simulations concede with the deterministic analytical results. The finding of our model agreed with the published results done by Allen et all. [178].

For further study in two species models as what was accomplished in chapter 3, we applied a network model in the previous model to have a better understanding of the epidemiological findings on superspreading scenarios. Probabilistic epidemic model and pairwise approximation examine the probability for all nodes and the prevalence of the disease. The findings showed that networks modelling address a significant role in influencing our comprehension of epidemic processes. For example, the confinement of contacts among individuals inside a network, rather than the overall population, slows and limits the spread of infection; hence, if we are seeking to predict species patterns from individual-level observations, network structure must be considered which is agreed with prior epidemiological studies by [116, 129].

Environmental infection transmission often plays a major role in transmission of infectious diseases. In Chapter 4, we formulated a mathematical model to understand the reflecting pathogen characteristics and the mechanisms of transmission through the environment. The framework provides a theoretical basis for understanding disease control for the environment. Here, we showed, non-negativity, boundedness, existence of the disease-free equilibrium, the local stability of the disease-free equilibrium, the existence and stability of equilibrium points of the model, the global stability of the disease-free equilibrium, and the existence of the endemic disease equilibrium. We also derived the basic reproduction number R_0 by two different methods, and showed how environmental transmission can contribute to disease spread.

In Chapter 5, the environmental model was followed by the mathematical modelling of the effects of public health education, to study the benefits of education and understanding

in disease control. The basic reproduction number R_0 and the effective reproduction number R_E were determined. We also showed the existence and local stability of the disease-free equilibrium, the global stability of the disease-free equilibrium, and the existence and global stability of the endemic equilibrium. The analytical results were supported by numerical simulations. Simultaneously, we investigated how different values of α influenced the overall density of MERS-infected individuals, concluding that public health education is an effective method of controlling the virus potential risk since it decreases the spreading of the threshold. The result supported the previous epidemiological findings by Rachel et al. 2018 [161].

In Chapter 6, we used a mathematical model to study disease control, including hospitalization and isolation/quarantine. Mathematical modelling of a single population was used to tackle questions surrounding respiratory diseases in Saudi Arabia. When the corresponding reproduction number of the model is smaller than one, the model (6.1) exhibited a globally stable disease-free equilibrium. When $R_c > 1$, the model possessed a unique endemic equilibrium. For special cases, the unique endemic equilibrium is proven to be locally asymptotically stable and globally asymptotically stable. The efficacy of isolation for symptomatic patients is proportional to the magnitude of the modification parameter for reducing infectiousness in hospitalized individuals ζ. Our model results of the study agree with previous findings of Mohammad et al. [169].

Mass gatherings can provide optimal environments for disease spread. Umrah and Hajj are two annual pious and religious festivals that are huge mass gatherings of more than 10 million travellers from different countries (approximately 184) to Saudi Arabia. Each year Hajj is considered as a chief pilgrimage and involves a mass crowd that continues for six days during the 12th month of the Islamic calendar, however Umrah is a minor pilgrimage which could be highly personalized that is made mostly during Ramadan, during the (9^{th} month of the Islamic calendar) period of 29 and 30 days. In Chapter 7, we formulated the deterministic system of the General Mobility Process, and we followed this work with a

stochastic model to investigate probabilities of transmission of infectious diseases at mass gathering events. In this regard we focused on influenza infection and spread, as this is a disease that organizers must consider every year. The model results suggested that human mixing and population movement, which were common in Umrah and Hajj, play a prominent role in disease transmission, and that the risk of exportation of infectious diseases back to pilgrim home countries can be reduced if mixing is controlled.

8.2 FutureWork

There are many important questions surrounding MERS-CoV and mass gatherings that remain. Therefore, I will extend the work to a study of MERS-CoV transmission in a hospital setting. This will include models of personal protective equipment use and procurement, and models of airborne transmission in closed environments. Finally, I am interested in adapting the model of the Hajj mass gathering to a study of COVID-19 transmission, and to other mass gatherings worldwide.

Bibliography

[1] Samy Kasem et al. "Cross-sectional study of MERS-CoV-specific RNA and antibodies in animals that have had contact with MERS patients in Saudi Arabia". In: *Journal of infection and public health* 11.3 (2018), pp. 331–338.

[2] Sebastiano Bruno Solerte et al. "Dipeptidyl peptidase-4 (DPP4) inhibition in COVID-19". In: *Acta diabetologica* 57 (2020), pp. 779–783.

[3] Anwar E Ahmed. "Diagnostic delays in 537 symptomatic cases of Middle East respiratory syndrome coronavirus infection in Saudi Arabia". In: *International Journal of Infectious Diseases* 62 (2017), pp. 47–51.

[4] Salim Baharoon and Ziad A Memish. "MERS-CoV as an emerging respiratory illness: a review of prevention methods". In: *Travel medicine and infectious disease* 32 (2019), p. 101520.

[5] Nianshuang Wang et al. "Structural definition of a neutralization-sensitive epitope on the MERS-CoV S1-NTD". In: *Cell reports* 28.13 (2019), pp. 3395–3405.

[6] Tridip Sardar et al. "A realistic two-strain model for MERS-CoV infection uncovers the high risk for epidemic propagation". In: *PLoS neglected tropical diseases* 14.2 (2020), e0008065.

[7] Ryan Aguanno et al. "MERS: Progress on the global response, remaining challenges and the way forward". In: *Antiviral research* 159 (2018), pp. 35–44.

[8] Chiara Poletto et al. "Assessment of the Middle East respiratory syndrome coronavirus (MERS-CoV) epidemic in the Middle East and risk of international spread using a novel maximum likelihood analysis approach". In: *Eurosurveillance* 19.23 (2014), p. 20824.

[9] Chiara Poletto, Vittoria Colizza, and Pierre-Yves Boëlle. "Quantifying spatiotemporal heterogeneity of MERS-CoV transmission in the Middle East region: a combined modelling approach". In: *Epidemics* 15 (2016), pp. 1–9.

[10] Karima A Al-Salihi and Jenan Mahmood Khalaf. "The emerging SARS-CoV, MERS-CoV, and SARS-CoV-2: An insight into the viruses zoonotic aspects". In: *Veterinary World* 14.1 (2021), p. 190.

[11] Maged G Hemida et al. "Dromedary camels and the transmission of Middle East respiratory syndrome coronavirus (MERS-CoV)". In: *Transboundary and emerging diseases* 64.2 (2017), pp. 344–353.

[12] Maged Gomaa Hemida et al. "Longitudinal study of Middle East respiratory syndrome coronavirus infection in dromedary camel herds in Saudi Arabia, 2014–2015". In: *Emerging microbes & infections* 6.1 (2017), pp. 1–7.

[13] Simon Cauchemez et al. "Middle East respiratory syndrome coronavirus: quantification of the extent of the epidemic, surveillance biases, and transmissibility". In: *The Lancet infectious diseases* 14.1 (2014), pp. 50–56.

[14] David S Hui et al. "Middle East respiratory syndrome coronavirus: risk factors and determinants of primary, household, and nosocomial transmission". In: *The Lancet Infectious Diseases* 18.8 (2018), e217–e227.

[15] Mohammad H Alyami, Hamad S Alyami, and Ansaar Warraich. "Middle East Respiratory Syndrome (MERS) and novel coronavirus disease-2019 (COVID-19): From causes to preventions in Saudi Arabia". In: *Saudi Pharmaceutical Journal: SPJ* (2020).

[16] *Middle East respiratory syndrome coronavirus (MERS-CoV)*. https://www.who.int/news-room/fact-sheets/detail/middle-east-respiratory-syndrome-coronavirus-(mers-cov). Accessed: 11 March 2019.

[17] Moran Ki. "2015 MERS outbreak in Korea: hospital-to-hospital transmission". In: *Epidemiology and health* 37 (2015).

[18] Esam I Azhar et al. "The Middle East respiratory syndrome coronavirus–a continuing risk to global health security". In: *Emerging and re-emerging viral infections*. Springer, 2016, pp. 49–60.

[19] Gerardo Chowell et al. "Synthesizing data and models for the spread of MERS-CoV, 2013: key role of index cases and hospital transmission". In: *Epidemics* 9 (2014), pp. 40–51.

[20] Hanaa Zakaria Nooh et al. "Public awareness of coronavirus in Al-Jouf region, Saudi Arabia". In: *Journal of Public Health* (2020), pp. 1–8.

[21] Alimuddin Zumla, David S Hui, and Stanley Perlman. "Middle East respiratory syndrome". In: *The Lancet* 386.9997 (2015), pp. 995–1007.

[22] Yaseen M Arabi et al. "Middle East respiratory syndrome". In: *New England Journal of Medicine* 376.6 (2017), pp. 584–594.

[23] Ziad A Memish et al. "Middle East respiratory syndrome". In: *The Lancet* 395.10229 (2020), pp. 1063–1077.

[24] Gerardo Chowell et al. "Transmission characteristics of MERS and SARS in the healthcare setting: a comparative study". In: *BMC medicine* 13.1 (2015), pp. 1–12.

[25] Romulus Breban, Julien Riou, and Arnaud Fontanet. "Interhuman transmissibility of Middle East respiratory syndrome coronavirus: estimation of pandemic risk". In: *The Lancet* 382.9893 (2013), pp. 694–699.

[26] AJ Kucharski and Christian L Althaus. "The role of superspreading in Middle East respiratory syndrome coronavirus (MERS-CoV) transmission". In: *Eurosurveillance* 20.25 (2015), p. 21167.

[27] Thamer H Alenazi et al. "Identified transmission dynamics of Middle East respiratory syndrome coronavirus infection during an outbreak: implications of an overcrowded emergency department". In: *Clinical Infectious Diseases* 65.4 (2017), pp. 675–679.

[28] Saleh A Eifan et al. "A pandemic risk assessment of Middle East respiratory syndrome coronavirus (MERS-CoV) in Saudi Arabia". In: *Saudi journal of biological sciences* 24.7 (2017), pp. 1631–1638.

[29] S Choi et al. "High reproduction number of Middle East respiratory syndrome coronavirus in nosocomial outbreaks: mathematical modelling in Saudi Arabia and South Korea". In: *Journal of Hospital Infection* 99.2 (2018), pp. 162–168.

[30] Yunhwan Kim et al. "The characteristics of Middle Eastern respiratory syndrome coronavirus transmission dynamics in South Korea". In: *Osong public health and research perspectives* 7.1 (2016), pp. 49–55.

[31] Xu-Sheng Zhang et al. "Estimating and modelling the transmissibility of Middle East Respiratory Syndrome CoronaVirus during the 2015 outbreak in the Republic of Korea". In: *Influenza and other respiratory viruses* 11.5 (2017), pp. 434–444.

[32] Hyuk-Jun Chang. "Estimation of basic reproduction number of the Middle East respiratory syndrome coronavirus (MERS-CoV) during the outbreak in South Korea, 2015". In: *Biomedical engineering online* 16.1 (2017), pp. 1–11.

[33] Zhi-Qiang Xia et al. "Modeling the transmission of Middle East respirator syndrome corona virus in the Republic of Korea". In: *PloS one* 10.12 (2015), e0144778.

[34] Hassan E El Bushra et al. "Outcome of strict implementation of infection prevention control measures during an outbreak of Middle East respiratory syndrome". In: *American journal of infection control* 45.5 (2017), pp. 502–507.

[35] Christian Drosten et al. "Transmission of MERS-coronavirus in household contacts". In: *New England Journal of Medicine* 371.9 (2014), pp. 828–835.

[36] Jung Wan Park et al. "Hospital outbreaks of middle east respiratory syndrome, Daejeon, South Korea, 2015". In: *Emerging infectious diseases* 23.6 (2017), p. 898.

[37] Sun Hee Park et al. "Outbreaks of Middle East respiratory syndrome in two hospitals initiated by a single patient in Daejeon, South Korea". In: *Infection & chemotherapy* 48.2 (2016), p. 99.

[38] Sun Young Cho et al. "MERS-CoV outbreak following a single patient exposure in an emergency room in South Korea: an epidemiological outbreak study". In: *The Lancet* 388.10048 (2016), pp. 994–1001.

[39] SW Kim et al. "Middle East respiratory syndrome coronavirus outbreak in the Republic of Korea, 2015". In: *Osong Public Health Res Perspect* 6.4 (2016), pp. 269–78.

[40] Victor Virlogeux et al. "Association between severity of MERS-CoV infection and incubation period". In: *Emerging infectious diseases* 22.3 (2016), p. 526.

[41] Benjamin J Cowling et al. "Preliminary epidemiological assessment of MERS-CoV outbreak in South Korea, May to June 2015". In: *Eurosurveillance* 20.25 (2015), p. 21163.

[42] Ji-Eun Park, Soyoung Jung, and Aeran Kim. "MERS transmission and risk factors: a systematic review". In: *BMC public health* 18.1 (2018), p. 574.

[43] HY Park et al. "Epidemiological investigation of MERS-CoV spread in a single hospital in South Korea, May to June 2015". In: *Eurosurveillance* 20.25 (2015), p. 21169.

[44] Abdullah Assiri et al. "Epidemiological, demographic, and clinical characteristics of 47 cases of Middle East respiratory syndrome coronavirus disease from Saudi Arabia: a descriptive study". In: *The Lancet infectious diseases* 13.9 (2013), pp. 752–761.

[45] Jianping Sha et al. "Fatality risks for nosocomial outbreaks of Middle East respiratory syndrome coronavirus in the Middle East and South Korea". In: *Archives of virology* 162.1 (2017), pp. 33–44.

[46] Mengxue Liu et al. "Middle East respiratory syndrome and medical students: letter from China". In: *International journal of environmental research and public health* 12.10 (2015), pp. 13289–13294.

[47] Amy Dighe et al. "A systematic review of MERS-CoV seroprevalence and RNA prevalence in dromedary camels: Implications for animal vaccination". In: *Epidemics* 29 (2019), p. 100350.

[48] Siming Tang, Wanbiao Ma, and Peifan Bai. "A novel dynamic model describing the spread of the MERS-CoV and the expression of dipeptidyl peptidase 4". In: *Computational and mathematical methods in medicine* 2017 (2017).

[49] David N Fisman. "Seasonality of infectious diseases". In: *Annu. Rev. Public Health* 28 (2007), pp. 127–143.

[50] Maimuna S Majumder et al. "Estimation of MERS-coronavirus reproductive number and case fatality rate for the spring 2014 Saudi Arabia outbreak: insights from publicly available data". In: *PLoS currents* 6 (2014).

[51] Khalid Al-Ahmadi, Sabah Alahmadi, and Ali Al-Zahrani. "Spatiotemporal clustering of Middle East respiratory syndrome coronavirus (MERS-CoV) incidence in Saudi Arabia, 2012–2019". In: *International journal of environmental research and public health* 16.14 (2019), p. 2520.

[52] Daniel C Payne et al. "Multihospital outbreak of a Middle East respiratory syndrome coronavirus deletion variant, Jordan: a molecular, serologic, and epidemiologic investigation". In: *Open forum infectious diseases*. Vol. 5. 5. Oxford University Press US. 2018, ofy095.

[53] Zhao Zhang, Libing Shen, and Xun Gu. "Evolutionary dynamics of MERS-CoV: potential recombination, positive selection and transmission". In: *Scientific reports* 6.1 (2016), pp. 1–10.

[54] World Health Organization et al. *Middle East respiratory syndrome coronavirus (MERS-CoV): summary of current situation, literature update and risk assessment*. Tech. rep. World Health Organization, 2015.

[55] Dipo Aldila et al. "Analyzing the MERS disease control strategy through an optimal control problem". In: *International Journal of Applied Mathematics and Computer Science* 28 (2018).

[56] Jonggul Lee, Gerardo Chowell, and Eunok Jung. "A dynamic compartmental model for the Middle East respiratory syndrome outbreak in the Republic of Korea: a retrospective analysis on control interventions and superspreading events". In: *Journal of theoretical biology* 408 (2016), pp. 118–126.

[57] World Health Organization et al. *WHO. Communicable disease alert and response for mass gatherings: technical workshop. Geneva, 29–30 April 2008*. Tech. rep. WHO/HSE/EPR, 2008.

[58] Kamran Khan et al. "Global public health implications of a mass gathering in Mecca, Saudi Arabia during the midst of an influenza pandemic". In: *Journal of travel medicine* 17.2 (2010), pp. 75–81.

[59] Qanta A Ahmed, Maurizio Barbeschi, and Ziad A Memish. "The quest for public health security at Hajj: the WHO guidelines on communicable disease alert and response during mass gatherings". In: *Travel medicine and infectious disease* 7.4 (2009), pp. 226–230.

[60] A Rashid Gatrad et al. *Hajj and the risk of influenza*. 2006.

[61] Qanta A Ahmed, Yaseen M Arabi, and Ziad A Memish. "Health risks at the Hajj". In: *The Lancet* 367.9515 (2006), pp. 1008–1015.

[62] Abdul Rashid Gatrad and Aziz Sheikh. "Hajj: journey of a lifetime". In: *Bmj* 330.7483 (2005), pp. 133–137.

[63] Andrew Petersen. "The archaeology of the Syrian and Iraqi Hajj routes". In: *World Archaeology* 26.1 (1994), pp. 47–56.

[64] Liliana Menjivar. "A metapopulation model for mass gatherings Application: global travel, Hajj and the spread of measles". In: (2013).

[65] Wayne H Bowen. "The History of Saudi Arabia". In: (2014).

[66] Steven Stalinsky. "The Islamic Affairs Department of the Saudi Embassy in Washington, DC". In: *Middle East Media Research Institute (MEMRI) Special Dispatch* 23 (2003).

[67] Hani Jokhdar et al. "COVID-19 mitigation plans during Hajj 2020: a success story of zero cases". In: *Health security* (2020).

[68] ZA Memish et al. "Establishment of public health security in Saudi Arabia for the 2009 Hajj in response to pandemic influenza A H1N1". In: *The Lancet* 374.9703 (2009), pp. 1786–1791.

[69] Ziad A Memish et al. "Hajj: infectious disease surveillance and control". In: *The Lancet* 383.9934 (2014), pp. 2073–2082.

[70] Ashraf Farahat et al. "Air quality over major cities of Saudi Arabia during Hajj periods of 2019 and 2020". In: *Earth Systems and Environment* 5.1 (2021), pp. 101–114.

[71] Saber Yezli et al. "Umrah. An opportunity for mass gatherings health research". In: *Saudi Medical Journal* 38 (Aug. 2017), pp. 868–871. DOI: 10.15537/smj.2017.8.20124.

[72] Jean Maguire Van Seventer and Natasha S Hochberg. "Principles of infectious diseases: transmission, diagnosis, prevention, and control". In: *International Encyclopedia of Public Health* (2017), p. 22.

[73] Cheng Ding, Xiaoxiao Liu, and Shigui Yang. "The value of infectious disease modeling and trend assessment: a public health perspective". In: *Expert Review of Anti-infective Therapy* (2021), pp. 1–11.

[74] William Ogilvy Kermack and Anderson G McKendrick. "A contribution to the mathematical theory of epidemics". In: *Proceedings of the royal society of london. Series A, Containing papers of a mathematical and physical character* 115.772 (1927), pp. 700–721.

[75] Daniel T Gillespie. "Exact stochastic simulation of coupled chemical reactions". In: *The journal of physical chemistry* 81.25 (1977), pp. 2340–2361.

[76] Geoff P Garnett et al. "The transmission dynamics of gonorrhoea: modelling the reported behaviour of infected patients from Newark, New Jersey". In: *Philosophical Transactions of the Royal Society of London. Series B: Biological Sciences* 354.1384 (1999), pp. 787–797.

[77] David N Fisman, Amy L Greer, and Ashleigh R Tuite. "Bidirectional impact of imperfect mask use on reproduction number of COVID-19: A next generation matrix approach". In: *Infectious Disease Modelling* 5 (2020), pp. 405–408.

[78] MJ Keeling, DA Rand, and AJ Morris. "Correlation models for childhood epidemics". In: *Proceedings of the Royal Society of London. Series B: Biological Sciences* 264.1385 (1997), pp. 1149–1156.

[79] James Dunyak, Murat Guven, and Donald Wunsch. "Training fuzzy number neural networks using constrained backpropagation". In: *1998 IEEE International Conference on Fuzzy Systems Proceedings. IEEE World Congress on Computational Intelligence (Cat. No. 98CH36228)*. Vol. 2. IEEE. 1998, pp. 1142–1146.

[80] John J Potterat, Richard B Rothenberg, and Steven Q Muth. "Network structural dynamics and infectious disease propagation". In: *International journal of STD & AIDS* 10.3 (1999), pp. 182–185.

[81] Lisa Sattenspiel and Klaus Dietz. "A structured epidemic model incorporating geographic mobility among regions". In: *Mathematical biosciences* 128.1-2 (1995), pp. 71–91.

[82] Michael Y Li. *An introduction to mathematical modeling of infectious diseases*. Vol. 2. Springer, 2018.

[83] Fred Brauer, Carlos Castillo-Chavez, and Zhilan Feng. *Mathematical models in epidemiology*. Vol. 32. Springer, 2019.

[84] Roy M Anderson and Robert M May. *Infectious diseases of humans: dynamics and control*. Oxford university press, 1992.

[85] BT Grenfell. "Chance and chaos in measles dynamics". In: *Journal of the Royal Statistical Society: Series B (Methodological)* 54.2 (1992), pp. 383–398.

[86] David JD Earn et al. "A simple model for complex dynamical transitions in epidemics". In: *science* 287.5453 (2000), pp. 667–670.

[87] Carlos Castillo-Chavez et al. "Epidemiological models with age structure, proportionate mixing, and cross-immunity". In: *Journal of mathematical biology* 27.3 (1989), pp. 233–258.

[88] Odo Diekmann, Johan Andre Peter Heesterbeek, and Johan AJ Metz. "On the definition and the computation of the basic reproduction ratio R_0 in models for infectious diseases in heterogeneous populations". In: *Journal of mathematical biology* 28.4 (1990), pp. 365–382.

[89] Geoffrey P Garnett and Edward C Holmes. "The ecology of emergent infectious disease". In: *Bioscience* 46.2 (1996), pp. 127–135.

[90] Qianying Lin et al. "Modeling the spread of Middle East respiratory syndrome coronavirus in Saudi Arabia". In: *Statistical methods in medical research* 27.7 (2018), pp. 1968–1978.

[91] Nofe Al-Asuoad and Meir Shillor. "Modeling, analysis and simulations of MERS outbreak in Saudi Arabia". In: *BIOMATH* 7.1 (2018), p. 1802277.

[92] Nofe Al-Asuoad et al. "Mathematical model and simulations of MERS outbreak: predictions and implications for control measures". In: *Biomath* 5.2, article 1612141 (2016).

[93] AG M'Kendrick. "Applications of mathematics to medical problems". In: *Proceedings of the Edinburgh Mathematical Society* 44 (1925), pp. 98–130.

[94] Daryl J Daley and Joe Gani. *Epidemic modelling: an introduction*. 15. Cambridge University Press, 2001.

[95] Peter Whittle. "On the use of the normal approximation in the treatment of stochastic processes". In: *Journal of the Royal Statistical Society: Series B (Methodological)* 19.2 (1957), pp. 268–281.

[96] Norman TJ Bailey et al. *The mathematical theory of infectious diseases and its applications*. Charles Griffin and Company Ltd, 5a Crendon Street, High Wycombe, Bucks HP13 6LE., 1975.

[97] Priscilla E Greenwood and Luis F Gordillo. *Mathematical and Statistical Estimation Approaches in Epidemiology*. 2009.

[98] L. J. S. Allen. *An Introduction to Stochastic Processes with Applications to Biology, Second Edition*. CRC Press, 2010. ISBN: 978-1-4398-1882-4.

[99] L. J. S. Allen and G.E. Jr. Lahodny. "Extinction thresholds in deterministic and stochastic epidemic models". In: *Journal of Biological Dynamics* 6 (2013), pp. 590–611.

[100] L. J. S. Allen and P. van den Driessche. "Relations between deterministic and stochastic thresholds for disease extinction in continuous and discrete time infectious disease models." In: *Mathematical Biosciences* 243 (2013), pp. 99–108.

[101] L. J. S. Allen. *Stochastic Population and Epidemic Models*. Springer, 2015. ISBN: 978-3-319-21553-2.

[102] Alfred James Lotka. *Elements of physical biology*. Williams and Wilkins, 1925.

[103] Vito Volterra. *Variazioni e fluttuazioni del numero d'individui in specie animali conviventi*. 1927.

[104] V Volterra. "Variazioni e fluttuazioni del numero dindividui in specie animali conviventi, Memorie Della R". In: *Accademia Nazionale dei Lincei* 423 (1926), pp. 1–110.

[105] Michael L Rosenzweig and Robert H MacArthur. "Graphical representation and stability conditions of predator-prey interactions". In: *The American Naturalist* 97.895 (1963), pp. 209–223.

[106] Crawford Stanley Holling. "The functional response of predators to prey density and its role in mimicry and population regulation". In: *The Memoirs of the Entomological Society of Canada* 97.S45 (1965), pp. 5–60.

[107] HI Freedman and Paul Waltman. "Persistence in models of three interacting predator-prey populations". In: *Mathematical biosciences* 68.2 (1984), pp. 213–231.

[108] Alden S Klovdahl et al. "Networks and tuberculosis: an undetected community outbreak involving public places". In: *Social science & medicine* 52.5 (2001), pp. 681–694.

[109] M Elizabeth Halloran et al. "Community interventions and the epidemic prevention potential". In: *Vaccine* 20.27-28 (2002), pp. 3254–3262.

[110] Nayeem Islam, Amitabh Dave, and Roy H Campbell. "Communication compilation for unreliable networks". In: *Proceedings of 16th International Conference on Distributed Computing Systems*. IEEE. 1996, pp. 188–195.

[111] Jesper LR Andersson et al. "Brain networks affected by synchronized sleep visualized by positron emission tomography". In: *Journal of Cerebral Blood Flow & Metabolism* 18.7 (1998), pp. 701–715.

[112] Odo Diekmann, MCM De Jong, and Johan Anton Jacob Metz. "A deterministic epidemic model taking account of repeated contacts between the same individuals". In: *Journal of Applied Probability* (1998), pp. 448–462.

[113] Mark EJ Newman. "Spread of epidemic disease on networks". In: *Physical review E* 66.1 (2002), p. 016128.

[114] Mark Neal. "Meta-stable memory in an artificial immune network". In: *International Conference on Artificial Immune Systems*. Springer. 2003, pp. 168–180.

[115] Matthew J Keeling. "Correlation equations for endemic diseases: externally imposed and internally generated heterogeneity". In: *Proceedings of the Royal Society of London. Series B: Biological Sciences* 266.1422 (1999), pp. 953–960.

[116] Matt J Keeling and Ken TD Eames. "Networks and epidemic models". In: *Journal of the Royal Society Interface* 2.4 (2005), pp. 295–307.

[117] CJ Rhodes and Roy M Anderson. "Epidemic thresholds and vaccination in a lattice model of disease spread". In: *Theoretical Population Biology* 52.2 (1997), pp. 101–118.

[118] Duncan J Watts and Steven H Strogatz. "Collective dynamics of small world networks". In: *nature* 393.6684 (1998), pp. 440–442.

[119] Jari Saramaki and Kimmo Kaski. "Modelling development of epidemics with dynamic small-world networks". In: *Journal of Theoretical Biology* 234.3 (2005), pp. 413–421.

[120] Cristopher Moore and Mark EJ Newman. "Epidemics and percolation in small world networks". In: *Physical Review E* 61.5 (2000), p. 5678.

[121] Michael Boots and Akira Sasaki. "Small worlds and the evolution of virulence: infection occurs locally and at a distance". In: *Proceedings of the Royal Society of London. Series B: Biological Sciences* 266.1432 (1999), pp. 1933–1938.

[122] Marcelo Kupennan et al. "Small world effect in an epidemiological model". In: *The Structure and Dynamics of Networks*. Princeton University Press, 2011, pp. 489–492.

[123] Luis J Gilarranz and Jordi Bascompte. "Spatial network structure and metapopulation persistence". In: *Journal of Theoretical Biology* 297 (2012), pp. 11–16.

[124] Matt Keeling. "The implications of network structure for epidemic dynamics". In: *Theoretical population biology* 67.1 (2005), pp. 1–8.

[125] Qinghua Chen and Dinghua Shi. "The modeling of scale-free networks". In: *Physica A: Statistical Mechanics and its Applications* 335.1-2 (2004), pp. 240–248.

[126] Albert-Laszlo Barabasi, Reka Albert, and Hawoong Jeong. "Mean-field theory for scale-free random networks". In: *Physica A: Statistical Mechanics and its Applications* 272.1-2 (1999), pp. 173–187.

[127] Albert-Laszlo Barabasi, Reka Albert, and Hawoong Jeong. "Scale-free characteristics of random networks: the topology of the world-wide web". In: *Physica A: statistical mechanics and its applications* 281.1-4 (2000), pp. 69–77.

[128] Istvan Z Kiss, Darren M Green, and Rowland R Kao. "Infectious disease control using contact tracing in random and scale-free networks". In: *Journal of The Royal Society Interface* 3.6 (2006), pp. 55–62.

[129] Miller J.C. Kiss I.Z. and P.L. Simon. "Mathematics of epidemics on networks". In: *Cham: Springer* 598 (2017).

[130] Matt J Keeling and Pejman Rohani. *Modeling infectious diseases in humans and animals*. Princeton university press, 2011.

[131] James O Lloyd-Smith et al. "Superspreading and the effect of individual variation on disease emergence". In: *Nature* 438.7066 (2005), pp. 355–359.

[132] Amy S Collins. "Preventing health care–associated infections". In: *Patient safety and quality: an evidence-based handbook for nurses* (2008).

[133] Michael Small, Chi Kong Tse, and David M Walker. "Super-spreaders and the rate of transmission of the SARS virus". In: *Physica D: Nonlinear Phenomena* 215.2 (2006), pp. 146–158.

[134] Wayne M Getz et al. "Modeling the invasion and spread of contagious diseases in heterogeneous populations". In: *Disease evolution: models, concepts, and data analyses* 71 (2006), pp. 113–144.

[135] Mohammad A Safi and Abba B Gumel. "Mathematical analysis of a disease transmission model with quarantine, isolation and an imperfect vaccine". In: *Computers & Mathematics with Applications* 61.10 (2011), pp. 3044–3070.

[136] Chiara Poletto, Pierre-Yves Boëlle, and Vittoria Colizza. "Risk of MERS importation and onward transmission: a systematic review and analysis of cases reported to WHO". In: *BMC infectious diseases* 16.1 (2016), pp. 1–13.

[137] Jaffar A Al-Tawfiq and Ziad A Memish. "Middle East respiratory syndrome coronavirus: epidemiology and disease control measures". In: *Infection and drug resistance* 7 (2014), p. 281.

[138] Woohyun Yoo, Doo-Hun Choi, and Keeho Park. "The effects of SNS communication: how expressing and receiving information predict MERS-preventive behavioral intentions in South Korea". In: *Computers in Human Behavior* 62 (2016), pp. 34–43.

[139] Pyoeng Gyun Choe et al. "MERS-CoV antibody responses 1 year after symptom onset, South Korea, 2015". In: *Emerging infectious diseases* 23.7 (2017), p. 1079.

[140] Joseph P LaSalle. "Stability theory for ordinary differential equations". In: *Journal of Differential Equations* 4.1 (1968), pp. 57–65.

[141] Joseph P La Salle. *The stability of dynamical systems*. SIAM, 1976.

[142] Mohammad A Safi and Salisu M Garba. "Global stability analysis of SEIR model with holling type II incidence function". In: *Computational and mathematical methods in medicine* 2012 (2012).

[143] JP LaSalle. "The stability of dynamical systems, regional conference series in appl". In: *Math, SIAM, Philadelphia* (1976).

[144] Michael D McKay, Richard J Beckman, and William J Conover. "A comparison of three methods for selecting values of input variables in the analysis of output from a computer code". In: *Technometrics* 42.1 (2000), pp. 55–61.

[145] Mark EJ Newman. "The structure and function of networks". In: *Computer Physics Communications* 147.1-2 (2002), pp. 40–45.

[146] G Witten and G Poulter. "Simulations of infectious diseases on networks". In: *Computers in Biology and Medicine* 37.2 (2007), pp. 195–205.

[147] Marcelo Kuperman and Guillermo Abramson. "Small world effect in an epidemiological model". In: *Physical Review Letters* 86.13 (2001), p. 2909.

[148] Jonathan M Read and Matt J Keeling. "Disease evolution on networks: the role of contact structure". In: *Proceedings of the Royal Society of London. Series B: Biological Sciences* 270.1516 (2003), pp. 699–708.

[149] Nan Zhang et al. "Close contact behavior in indoor environment and transmission of respiratory infection". In: *Indoor air* 30.4 (2020), pp. 645–661.

[150] Andrew F Brouwer et al. "Dose-response relationships for environmentally mediated infectious disease transmission models". In: *PLoS computational biology* 13.4 (2017), e1005481.

[151] Lawrence Perko. *Differential equations and dynamical systems*. Vol. 7. Springer Science & Business Media, 2013.

[152] Walter G Kelley and Allan C Peterson. *The theory of differential equations: classical and qualitative*. Springer Science & Business Media, 2010.

[153] Mohammed Al Ghamdi et al. "Treatment outcomes for patients with Middle Eastern Respiratory Syndrome Coronavirus (MERS CoV) infection at a coronavirus referral

center in the Kingdom of Saudi Arabia". In: *BMC infectious diseases* 16.1 (2016), pp. 1–7.

[154] Brian Rha et al. "Update on the epidemiology of Middle East respiratory syndrome coronavirus (MERS-CoV) infection, and guidance for the public, clinicians, and public health authorities-January 2015". In: *MMWR. Morbidity and mortality weekly report* 64.3 (2015), p. 61.

[155] Abdelmalik I Khalafalla. "Emerging infectious diseases in camelids". In: *Emerging and Re-emerging Infectious Diseases of Livestock*. Springer, 2017, pp. 425–441.

[156] Christopher M Coleman and Matthew B Frieman. "Coronaviruses: important emerging human pathogens". In: *Journal of virology* 88.10 (2014), pp. 5209–5212.

[157] Mustafa Saad et al. "Clinical aspects and outcomes of 70 patients with Middle East respiratory syndrome coronavirus infection: a single-center experience in Saudi Arabia". In: *International Journal of Infectious Diseases* 29 (2014), pp. 301–306.

[158] Jean M Tchuenche et al. "The impact of media coverage on the transmission dynamics of human influenza". In: *BMC public health* 11.1 (2011), pp. 1–14.

[159] R Liu, J Wu, and H Zhu. *Media/psychological impact on multiple outbreaks of emerging infectious diseases. Comput Math Methods Med 8 (3): 153–164*. 2007.

[160] Jaffar A Al-Tawfiq et al. "A multi-faceted approach of a nursing led education in response to MERS-CoV infection". In: *Journal of infection and public health* 11.2 (2018), pp. 260–264.

[161] Rachel A Nyang'inja et al. "Mathematical modeling of the effects of public health education on tungiasis-a neglected disease with many challenges in endemic communities". In: *Advances in Difference Equations* 2018.1 (2018), pp. 1–19.

[162] Vangipuram Lakshmikantham, Srinivasa Leela, and Anatoly A Martynyuk. *Stability analysis of nonlinear systems*. Springer, 1989.

[163] Herbert W Hethcote. "The mathematics of infectious diseases". In: *SIAM review* 42.4 (2000), pp. 599–653.

[164] Pauline Van den Driessche and James Watmough. "Reproduction numbers and subthreshold endemic equilibria for compartmental models of disease transmission". In: *Mathematical biosciences* 180.1-2 (2002), pp. 29–48.

[165] Carlos Castillo-Chavez et al. *Mathematical approaches for emerging and reemerging infectious diseases: models, methods, and theory*. Vol. 126. Springer Science & Business Media, 2002.

[166] Carlos Castillo-Chavez and Baojun Song. "Dynamical models of tuberculosis and their applications". In: *Mathematical Biosciences & Engineering* 1.2 (2004), p. 361.

[167] Zoraida I Velasco-Salas et al. "Dengue seroprevalence and risk factors for past and recent viral transmission in Venezuela: a comprehensive community-based study". In: *The American journal of tropical medicine and hygiene* 91.5 (2014), pp. 1039–1048.

[168] Jaffar A Al-Tawfiq and Ziad A Memish. "Lack of seasonal variation of Middle East respiratory syndrome coronavirus (MERS-CoV)". In: *Travel medicine and infectious disease* 27 (2019), p. 125.

[169] Mohammad A Safi and Abba B Gumel. "Global asymptotic dynamics of a model for quarantine and isolation". In: *Discrete & Continuous Dynamical Systems-B* 14.1 (2010), p. 209.

[170] Tariq A Madani, Abdulhakeem O Althaqafi, and Basem M Alraddadi. "Infection prevention and control guidelines for patients with Middle East respiratory syndrome coronavirus (MERS-CoV) infection". In: *Saudi Med J* 35.8 (2014), pp. 897–913.

[171] World Health Organization et al. *Infection prevention and control during health care for probable or confirmed cases of Middle East respiratory syndrome coronavirus (ââ MERS-CoV)ââ infection: interim guidance: updated October 2019*. Tech. rep. World Health Organization, 2019.

[172] Yudong Yin and Richard G Wunderink. "MERS, SARS and other coronaviruses as causes of pneumonia". In: *Respirology* 23.2 (2018), pp. 130–137.

[173] Richard Putnam Wenzel, Timothy F Brewer, and Jean-Paul Butzler. *A guide to infection control in the hospital*. PMPH-USA, 2002.

[174] Ira M Longini Jr. "A mathematical model for predicting the geographic spread of new infectious agents". In: *Mathematical Biosciences* 90.1-2 (1988), pp. 367–383.

[175] Leonid A Rvachev and Ira M Longini Jr. "A mathematical model for the global spread of influenza". In: *Mathematical biosciences* 75.1 (1985), pp. 3–22.

[176] Amr Kandeel et al. "Pandemic (H1N1) 2009 and Hajj pilgrims who received predeparture vaccination, Egypt". In: *Emerging infectious diseases* 17.7 (2011), p. 1266.

[177] Mazyar Ziyaeyan et al. "Pandemic 2009 influenza A (H1N1) infection among 2009 Hajj Pilgrims from Southern Iran: a real-time RT-PCR-based study". In: *Influenza and other respiratory viruses* 6.6 (2012), e80–e84.

[178] Christina J Edholm et al. "Searching for superspreaders: Identifying epidemic patterns associated with superspreading events in stochastic models". In: (2018), pp. 1–29.